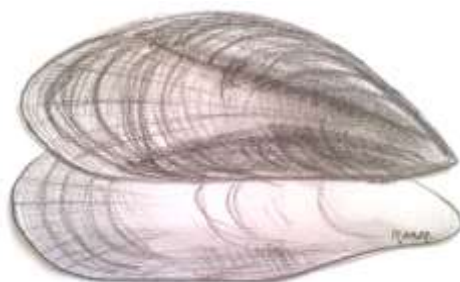


**UNIVERSIDADE DO ALGARVE
FACULDADE DE CIÊNCIAS E TECNOLOGIA**

**MULTIBIOMARKER ASSESSMENT OF
CADMIUM-BASED QUANTUM DOTS
EFFECTS IN THE MARINE MUSSEL
*MYTILUS GALLOPROVINCIALIS***

Thiago Lopes Rocha



Dissertação apresentada na Universidade do Algarve

Doutoramento em Ciências do Mar, Terra e Ambiente

Ramo de Ciências e Tecnologias do Ambiente

Especialidade Ecotoxicologia

Trabalho efetuado sobre a orientação da

Professora Doutora Maria João da Anunciação Franco Bebianno

2016

**Multibiomarker assessment of cadmium-based quantum dots effects in the
marine mussel *Mytilus galloprovincialis***

Declaração de autoria de trabalho

Declaro ser o autor deste trabalho, que é original e inédito. Autores e trabalhos consultados estão devidamente citados no texto e constam da listagem de referências incluída.

©Thiago Lopes Rocha

A Universidade do Algarve tem o direito perpétuo e sem limites geográficos, de arquivar e publicitar este trabalho através de exemplares impressos reproduzidos em papel ou de forma digital, ou por qualquer outro meio conhecido ou que venha a ser inventado, de o divulgar através de repositórios científicos e de admitir a sua cópia e distribuição com objetivos educacionais ou de investigação, não comerciais, desde que seja dado crédito ao autor e editor.

This thesis was supported by

- National Council for Scientific and Technological Development (CNPq) through the Brazil's Science Without Borders Program (239524/2012-8)



- Foundation of Science and Technology (FCT) through the project NANOECOTOX (PTDC/AAC-AMB/121650/2010) and project NANO NF (PTDC/ECM/102244/200)



ACKNOWLEDGEMENTS

I wish to thank all the people and institutions that helped me to carry out this Ph.D. Without their support none of this would have been possible.

Professor Maria João Bebianno (Centre for Marine and Environmental Research – CIMA, Faculty of Science and Technology – FCT, University of Algarve - UAlg), supervisor of my Ph.D. thesis, for giving me the opportunity to perform this research work within the “Ecotoxicology and Environmental Chemistry” research group, and for all her support, scientific advice, cordiality and encouragement during these three years.

Professor Margarida Ribau and Vânia Sousa (Center for Environmental and Sustainability Research - CENSE, FCT, CIMA, UAlg) for giving me the opportunity and assistance to perform the nanoparticle characterization.

Professor José Paulo Pinheiro (Observatoire Terre et Environnement de Lorraine - OTELo, University of Lorraine) and Luciana Sarabando Rocha (FCT, UAlg) for helping to understand the electrochemical methods and its importance in a nanoecotoxicology context.

Professor Luís Miguel Nunes (Civil Engineering Research and Innovation for Sustainability – CERIS, Instituto Superior Técnico - IST, UAlg) for his support with the statistical analyses and assessment of kinetics models.

Professor Simone Maria Teixeira Sabóia-Morais (Laboratory of Cellular Behavior, Federal University of Goiás - UFG) for giving me the opportunity and assistance to perform the histopathological analysis.

Paulo Zaragoza Pedro (CIMA, UAlg) for this support with the chemical analysis. A special thanks to all the technical and scientific support of UAlg, especially Filomena, João Quintela, Miguel and Zélia, for the daily support.

My friend Tânia Gomes for all the precious support, friendship and encouragement during these years. I would like to thank especially her scientific support in the experimental design and analysis of written articles.

All my friends from the Ecotoxicology and Environmental Chemistry Group (Ambra, Bruna, Cátia, Chiara, Emerson, Francisca, Julie, Luís, Manon, Matilde, Mustafa, Nélia, Tainá) for all assistance, friendship, endearment and laughter during these years.

All my friends from the UAlg, especially Amanda, Catarina, Cris, Flá, Lica, Luciana and Natalyia for all precious moments shared together. A special thanks for all my friends from the “Zumba family” for the affection, healthy and happy times spent together.

My best friend and companion of every day (“neggão”) and my family, especially my parents (João e Rosimeire), brothers (Amanda, Raquel, Renata, Rodrigo, Roger and Taynara), to whom I dedicate this thesis.

GENERAL ABSTRACT

Nanotechnology and use of engineered nanomaterials (ENMs) may improve life quality, economic growth and environmental quality, but their environmental risk in the marine environment is scarce. Properties of quantum dots (QDs), namely small size, unique optical and biofunctional properties, allow their use in nanomedicine, biology and electronics, but also confer different toxicity compared to its dissolved counterparts. Accordingly, this thesis assessed the toxicokinetics (TK), mode of action (MoA) and toxicity of CdTe QDs ($10 \mu\text{g Cd L}^{-1}$) in the marine mussel *Mytilus galloprovincialis*, compared to dissolved Cd for 21 days followed by 50 days depuration. For this purpose, Cd distribution in different mussel tissues, subcellular fractions and biodeposits were analysed, TK parameters estimated (accumulation and elimination rates, bioconcentration factor and half-life time) and multibiomarkers assessed: immunotoxicity (density, viability and differential cell count of hemocytes), cytotoxicity (lysosomal membrane stability - LMS), genotoxicity (DNA damage and nuclear anomalies), oxidative stress (superoxide dismutase - SOD, catalase - CAT, glutathione peroxidase - GPx and glutathione-S-Transferase - GST), metal exposure (metallothionein - MT), oxidative damage (lipid peroxidation - LPO), tissue-level biomarkers (17 histomorphometric parameters of digestive tubules, inflammatory and histopathological conditions indices) and proteomic responses. Results showed that the digestive gland plays an important role in storage, metabolism and detoxification of QDs, while gills have similar functions for dissolved Cd and the hemolymph in transport, distribution and regulation of QDs. Tissue specific metabolism patterns and nano-specific effects were identified, wherein the MoA and toxicity of QDs in mussels is time dependent and involve oxidative stress, immune response, DNA damage and differential protein expression. Mussels were unable to completely eliminate the QDs ($t_{1/2} > 50$ days), highlighting their potential source of toxicity for human health and environment. *M. galloprovincialis* is a significant target of QDs ecotoxicity and represent a suitable biomonitor for assess their environment risk.

Keywords: Nanoecotoxicity, nanomaterials, CdTe quantum dots, cadmium, biomarkers, oxidative stress, bivalve, *Mytilus galloprovincialis*.

RESUMO GERAL

A nanotecnologia e o uso de nanomateriais manufaturados (NMs) podem melhorar a qualidade de vida, o crescimento económico e a qualidade ambiental. Contudo, o rápido desenvolvimento e uso dos NMs em vários produtos levantam preocupações sobre a sua libertação no ambiente, em especial em águas residuais e no ambiente marinho, ao mesmo tempo em que o conhecimento sobre seu risco ambiental permanece escasso. Dentre os NMs, os pontos quânticos (“*quantum dots*” - QDs) são nanocristais semicondutores com ampla aplicação na nanomedicina, biologia e eletrónica devido às suas propriedades físico-químicas, tais como tamanho (1 - 10 nm), propriedades ópticas e eletrónicas e capacidade de bioconjugação. Entretanto, as propriedades nano-específicas dos QDs podem também induzir toxicidade diferente da comparada com a sua contraparte dissolvida. Por conseguinte, esta dissertação avaliou a toxicocinética (TK), o modo de ação (MoA) e a toxicidade dos CdTe QDs no mexilhão marinho *Mytilus galloprovincialis*, em comparação com o Cd dissolvido.

Inicialmente, as características dos QDs, seu comportamento e destino na água do mar foram analisados em termos de forma, tamanho, diâmetro hidrodinâmico, carga superficial (potencial zeta), índice de poli-dispersão, ponto isoelétrico, cinética de agregação/aglomeração, estabilização com diferentes tipos matéria orgânica natural (NOM), taxa de sedimentação e taxa de dissolução. Para análise da toxicocinética dos QDs em comparação com sua parte dissolvida, os mexilhões *M. galloprovincialis* foram expostos (a uma mesma concentração ambientalmente relevante de Cd, 10 µg Cd L⁻¹) a QDs e a Cd dissolvido durante 21 dias, seguido de um período de depuração de 50 dias, juntamente com um grupo controlo. A cinética de acumulação e eliminação do Cd foi analisada em diferentes tecidos (brânquias, glândula digestiva, hemolinfa e resto), frações subcelulares (fração insolúvel, fração das proteínas de elevado peso molecular e fração das proteínas de baixo peso molecular) e biodepósitos dos mexilhões (fezes e pseudofezes) por espectrometria de absorção atómica com forno de grafite, seguido da estimativa dos parâmetros toxicocinéticos (taxas de acumulação e eliminação, fator de bioconcentração e tempo de meia-vida - $t_{1/2}$). Para o estudo comparativo do MoA e toxicidade dos QDs e sua contraparte dissolvida, os mexilhões foram expostos a QDs e a Cd dissolvido (10 µg Cd L⁻¹) durante 14 dias e uma bateria de biomarcadores foi analisada: imunotoxicidade (densidade, viabilidade e contagem diferencial de hemócitos), citotoxicidade (estabilidade da membrana lisossomal - LMS),

genotoxicidade (danos no ADN e anomalias nucleares), estresse oxidativo (superóxido dismutase - SOD, catalase - CAT, glutathione peroxidase - GPx e glutathione-S-transferase - GST), exposição a Cd (metalotioneína - MT), dano oxidativo (peroxidação lipídica - LPO) e biomarcadores a nível tecidual (17 parâmetros histomorfométricos dos túbulos digestivos, condição inflamatória e os índices de condição histopatológica). Além disso, um estudo exploratório para identificar possíveis novos biomarcadores foi realizado na glândula digestiva dos mexilhões expostos a ambas formas de Cd (QDs e Cd dissolvido) ($10 \mu\text{gCd L}^{-1}$) durante 14 dias através de análise proteômica.

Os CdTe QDs usados neste estudo foram nanopartículas esféricas cobertas com grupos carboxílicos (-COOH) e com tamanho primário de 6 ± 1 nm. Em água do mar, os QDs tendem a formar agregados/aglomerados com diâmetro hidrodinâmico de 1014 ± 187 nm e carga superficial negativa (potencial zeta = -9.4 ± 1.2 mV), reduzindo a sua área superficial total em contato com o meio circundante. A taxa de dissolução dos QDs na água do mar foi de 27.6 % e a sua taxa de sedimentação rápida e lenta foi de $0.88 \pm 5 \times 10^{-4}$ e $0.009 \pm 8.45 \times 10^{-4}$, respectivamente, confirmando a sua tendência de agregar/aglomerar e sedimentar nos tanques de exposição, enquanto a estabilização com diferentes tipos de NOM (ácidos húmicos, ácido tânico, ácido salicílico) não foi observada. Uma visão geral dos resultados indica que a especiação do Cd na água do mar durante a exposição dos mexilhões aos CdTe QDs corresponde a 72 % são pequenos e grandes homo-agregados de QDs, 27.6 % são Cd iônico livre (Cd^{2+}) e complexos orgânicos e/ou inorgânicos de Cd devido à libertação de Cd dissolvido dos QDs.

Ambas as formas de Cd estão disponíveis para o mexilhão *M. galloprovincialis* e são acumuladas dependendo dos tecidos e tempo de exposição. Detectaram-se uma distribuição tecidual semelhante nos mexilhões expostos aos QDs e ao Cd dissolvido (glândula digestiva > brânquias > resto > hemolinfa), mas a cinética de acumulação foi dependente da forma de Cd. Nos mexilhões expostos aos QDs, foi detectada uma acumulação de Cd nas frações contendo mitocôndrias, núcleo e lisossomas, indicando potenciais alvos sub-celulares para a toxicidade dos QDs. Embora os níveis de MTs estejam diretamente associados com ambas as formas de Cd, a distribuição subcelular dos QDs está relacionada ao metal na sua forma biologicamente ativa (BAM), mas sem indução de LPO, enquanto que o Cd dissolvido foi detectado na forma biologicamente detoxificado (BDM), indicando efeitos nano específicos. Os resultados mostraram ainda que a glândula digestiva desempenha um papel fundamental no armazenamento,

metabolismo e desintoxicação dos QDs, enquanto as brânquias têm funções semelhantes nos mexilhões expostos ao Cd dissolvido e a hemolinfa atua no transporte, distribuição e regulação dos QDs. Padrões específicos de metabolismo foram observados para ambas as formas de Cd de acordo com os tecidos analisados.

O MoA e a toxicidade dos QDs nos mexilhões são dependentes do tecido e do tempo de exposição e envolvem mudanças na atividade das enzimas antioxidantes, estresse oxidativo, resposta imune e danos no ADN. As brânquias são o principal órgão afetado pelo estresse oxidativo induzido pelos QDs com efeitos associados ao aumento da atividade da SOD, GST e GPx, enquanto que os efeitos do Cd dissolvido estão relacionados com o aumento da atividade da CAT. Os efeitos dos QDs nos mexilhões classificam-se como imunocitotóxicos e genotóxicos, mas não citogenotóxicos. A imunotoxicidade dos QDs nos mexilhões é mediada pela redução da LMS, mudanças na frequência dos tipos de hemócitos e danos no ADN, enquanto os efeitos na densidade e viabilidade dos hemócitos e alterações cromossômicas não foram observados, em oposição aos efeitos observados para o Cd dissolvido.

Os resultados da análise proteômica indicam que os QDs e o Cd dissolvido induzem mudanças na expressão de proteínas na glândula digestiva dos mexilhões de modo dependente da forma de Cd. Foram observadas diferenças significativas (≥ 2 vezes) em 304 proteínas entre os mexilhões expostos a ambas as formas de Cd e aos não expostos, em que 32 e 123 proteínas são específicas para os QDs e o Cd dissolvido, respectivamente, enquanto alterações em 28 proteínas foram observadas somente após a exposição a ambas as formas de Cd. Esses resultados indicam que o MoA e a toxicidade dos QDs não são devidos somente à dissolução dos QDs e liberação de Cd dissolvido (Cd^{2+}), mas também estão relacionados com as suas propriedades nano específicas.

Durante o período de depuração, as brânquias dos mexilhões possuem baixa capacidade de eliminação dos QDs, enquanto a glândula digestiva é o principal órgão de acumulação, metabolismo e eliminação de ambas as formas de Cd. Os mexilhões não foram capazes de eliminar completamente os QDs acumulados ($t_{1/2} > 50$ dias), destacando a sua fonte potencial de toxicidade para a saúde humana e ambiental. Além disso, o mexilhão marinho *M. galloprovincialis* é alvo significativo da ecotoxicidade dos QDs e representa um biomonitor adequado para avaliar o seu risco ambiental.

Palavras-chave: Nanoecotoxicologia, nanomateriais, CdTe quantum dots, cádmio, biomarcadores, estresse oxidativo, bivalve, *Mytilus galloprovincialis*.

INDEX

Acknowledgements.....	I
General abstract.....	II
Resumo geral.....	III
Index.....	i
Figure index.....	viii
Table index.....	xvi
Abbreviations.....	xix
Chapter 1. General introduction.....	1
1.1. Nanotechnology and nanomaterial.....	3
1.2. ENMs properties and characterization.....	4
1.3. Behaviour and fate of ENMs in the aquatic environment.....	7
1.4. Bivalve molluscs as a target group of ENMs toxicity.....	9
1.4.1. Types of ENMs.....	10
1.4.2. ENMs ecotoxicity studies with bivalve molluscs.....	19
1.4.3. Bivalve species.....	19
1.4.4. Experimental design of nanotoxicological studies.....	20
1.4.5. Bioaccumulation and tissue distribution.....	20
1.4.6. Subcellular localization.....	23
1.4.7. Mode of action (MoA).....	25
1.4.7.1. Oxidative stress.....	25
1.4.7.2. Immunotoxicity.....	27
1.4.7.3. Genotoxicity.....	28
1.4.7.4. Behavioural changes and neurotoxicity.....	29
1.4.7.5. Embryotoxicity.....	30
1.4.8. Interactive effect of ENMs and other stressors.....	31
1.5. Proteomic research and identification of new biomarkers.....	35
1.6. Ecotoxicity of quantum dots at various trophic levels.....	37
1.6.1. Quantum dots.....	37
1.6.2. QDs applications and properties.....	38
1.6.2.1. Morphology and composition.....	39
1.6.3. Behaviour, transformation and fate of QDs in the aquatic environment.....	41

1.6.3.1. Physicochemical transformations.....	42
1.6.3.2. Macromolecular interactions.....	43
1.6.3.3. Biological mediated reactions.....	43
1.6.4. Ecotoxic effects of QDs at various trophic levels.....	44
1.6.4.1. Micro-organisms.....	44
1.6.4.1.1. Bacteria.....	44
1.6.4.1.2. Algae.....	46
1.6.4.1.3. Protozoa.....	50
1.6.4.1.4. Fungi.....	51
1.6.4.2. Invertebrates.....	55
1.6.4.2.1. Annelida and platyhelminths.....	55
1.6.4.2.2. Nematoda.....	55
1.6.4.2.3. Bivalvia.....	56
1.6.4.3. Aquatic vertebrates.....	57
1.6.4.3.1. Fish.....	57
1.6.5. Trophic transfer and biomagnification.....	66
1.7. Objectives and outline.....	68
1.7.1. General structure of thesis.....	71
 Chapter 2. Toxicokinetics and tissue distribution of cadmium-based quantum dots in the marine mussel <i>Mytilus galloprovincialis</i>.....	75
Graphical abstract 1.....	75
Abstract.....	77
2.1. Introduction.....	78
2.2. Materials and methods.....	49
2.2.1. QDs characterization.....	49
2.2.2. Aggregation of QDs with NOM.....	49
2.2.3. Cd speciation.....	80
2.2.4. Experimental design.....	80
2.2.5. Cd concentrations in seawater and mussel tissues.....	81
2.2.6. Condition index.....	81
2.2.7. Kinetic models.....	81
2.2.8. Biodeposits.....	82

2.2.9. Statistical analysis.....	82
2.3. Results.....	82
2.3.1. QDs characterization.....	82
2.3.2. Aggregation of QDs with NOM.....	83
2.3.3. QDs dissolution and Cd speciation.....	83
2.3.4. Condition Index (CI).....	84
2.3.5. Cd accumulation.....	85
2.3.6. Cd elimination.....	88
2.3.7. Production and Cd concentration of biodeposits.....	88
2.4. Discussion.....	89
2.5. Conclusions.....	94

Chapter 3. Subcellular partitioning kinetics, metallothionein response and oxidative damage in the marine mussel <i>Mytilus galloprovincialis</i> exposed to cadmium-based quantum dots.....	95
-----------------------------------------------------------------------------------------------------------------------------------------------------------------------------------------------------	-----------

Graphical abstract 2.....	95
----------------------------------	-----------

Abstract.....	97
----------------------	-----------

3.1. Introduction.....	98
-------------------------------	-----------

3.2. Materials and methods.....	100
----------------------------------------	------------

3.2.1. Experimental design.....	100
---------------------------------	-----

3.2.2. Subcellular partitioning.....	100
--------------------------------------	-----

3.2.3. Cd concentration.....	101
------------------------------	-----

3.2.4. Subcellular kinetic models.....	102
----------------------------------------	-----

3.2.5. Net accumulation rates.....	103
------------------------------------	-----

3.2.6. Metallothioneins.....	103
------------------------------	-----

3.2.7. Lipid peroxidation.....	103
--------------------------------	-----

3.2.8. Total protein concentration.....	104
-----------------------------------------	-----

3.2.9. Statistical analysis.....	104
----------------------------------	-----

3.3. Results and discussion.....	104
-----------------------------------------	------------

3.3.1. Cd accumulation.....	104
-----------------------------	-----

3.3.2. Subcellular partitioning strategy.....	105
-----------------------------------------------	-----

3.3.2.1. Gills response.....	106
------------------------------	-----

3.3.2.2. Digestive gland response.....	108
----------------------------------------	-----

3.3.3. Net accumulation rates.....	111
3.3.4. Cd elimination.....	111
3.3.5. MTs response.....	114
3.3.6. Oxidative damage.....	118
3.3.7. Tissue specific metabolism patterns.....	120
3.4. Conclusions.....	121

Chapter 4. Immunocytotoxicity, cytogenotoxicity and genotoxicity of cadmium-

based quantum dots in the marine mussel <i>Mytilus galloprovincialis</i>.....	125
Graphical abstract 3.....	125
Abstract.....	127
4.1. Introduction.....	128
4.2. Materials and methods.....	130
4.2.1. QDs characterization.....	130
4.2.1.1. Stock solution.....	130
4.2.1.2. Morphology, size, surface charge and aggregation kinetics.....	130
4.2.1.3. Sedimentation rate (SR).....	130
4.2.1.4. Spectral properties.....	131
4.2.2. Exposure experiments.....	131
4.2.3. Cd concentration.....	131
4.2.4. Immunocytotoxicity assessments.....	132
4.2.4.1. Cell viability and hemocyte density.....	132
4.2.4.2. Lysosomal Membrane Stability.....	132
4.2.4.3. Differential Cell Count, Micronucleus test and Nuclear	
Abnormalities assay.....	132
4.2.4.4. Comet assay.....	133
4.2.5. Statistical analysis.....	134
4.3. Results.....	134
4.3.1. QDs characterization.....	134
4.3.2. Cd concentration.....	137
4.3.3. Immunocytotoxicity.....	138
4.3.3.1. Hemocyte viability and density.....	138
4.3.3.2. LMS.....	138

4.3.3.3. DCC.....	139
4.3.4. Cytogenotoxicity.....	140
4.3.4.1. Micronucleus Assay and Nuclear Abnormalities.....	140
4.3.5. Genotoxicity.....	142
4.3.5.2. Comet assay.....	142
4.4. Discussion.....	145
4.5. Conclusions.....	149

Chapter 5. Tissue specific toxicity of cadmium-based quantum dots in the marine mussel <i>Mytilus galloprovincialis</i>.....	151
Graphical abstract 4.....	151
Abstract.....	153
5.1. Introduction.....	154
5.2. Materials and methods.....	156
5.2.1. QDs characterization.....	156
5.2.2. Experimental design.....	156
5.2.3. Cd concentration.....	157
5.2.4. Antioxidant enzymes.....	157
5.2.5. Total protein concentration.....	158
5.2.6. Statistical analysis.....	158
5.3. Results and discussion.....	159
5.3.1. Characterization and behaviour of QDs in seawater.....	159
5.3.2. Cd accumulation.....	159
5.3.3. Antioxidant responses.....	160
5.3.4. Tissue specific antioxidant patterns.....	165
5.4. Conclusions.....	168

Chapter 6. Histopathological assessment and inflammatory response in the digestive gland of marine mussel <i>Mytilus galloprovincialis</i> exposed to cadmium-based quantum dots.....	171
Graphical abstract 5.....	171
Abstract.....	173
6.1. Introduction.....	174

6.2. Materials and methods.....	176
6.2.1. Experimental design.....	176
6.2.2. Cd concentrations.....	177
6.2.3. Histopathological assessment.....	177
6.2.3.1. Histomorphometry.....	178
6.2.4. Inflammatory response.....	178
6.2.5. Histopathological condition indices.....	178
6.2.6. Statistical analysis.....	179
6.3. Results and discussion.....	180
6.3.1. Characterization of QDs in seawater and bioaccumulation.....	180
6.3.2. Histomorphometry.....	181
6.3.2.1. Morphological phases of digestive tubules.....	181
6.3.2.2. Digestive tubule status.....	183
6.3.2.3. Cell-type replacement.....	184
6.3.3. Inflammatory response.....	187
6.3.4. Histopathological condition indices.....	189
6.3.5. Principal component analysis.....	190
6.4. Conclusions.....	193
 Chapter 7. Differential proteomic response to cadmium-based quantum dots in the marine mussel <i>Mytilus galloprovincialis</i>.....	 194
Graphical abstract 6.....	194
Abstract.....	196
7.1. Introduction.....	197
7.2. Materials and methods.....	199
7.2.1. QDs characterization.....	199
7.2.2. Experimental design.....	199
7.2.3. Cd accumulation.....	200
7.2.4. Protein extraction and two-dimensional electrophoresis (2-DE).....	200
7.2.5. Image analysis.....	201
7.3. Results and discussion.....	201
7.3.1. QDs behaviour in seawater and bioaccumulation.....	201
7.3.2. Protein expression profiles (PEPs).....	202

7.4. Conclusions.....	208
 Chapter 8. General discussion, conclusions and future perspectives.....	 217
8.1. General discussion.....	218
8.1.1. Nanomaterials.....	218
8.1.2. Nanoecotoxicology.....	218
8.1.3. Behaviour and fate of QDs in the aquatic environment.....	219
8.1.4. Uptake, accumulation and tissue distribution.....	221
8.1.5. Subcellular partitioning and metabolism.....	222
8.1.6. Mode of action and toxicity.....	223
8.2. Conclusions.....	227
8.3. Future perspectives.....	229
References.....	230

FIGURE INDEX

Chapter 1 General Introduction

Figure 1.1.	Scheme illustrating the potential behaviour and fate of engineered nanomaterials (ENMs) in the aquatic environment and associated biological processes with bivalve molluscs.....	7
Figure 1.2.	Timeline of the number (■) and cumulative number (□) of papers published <i>per</i> year related to ecotoxicity of engineered nanomaterials (ENMs) in bivalve molluscs until December, 2014.....	11
Figure 1.3.	Number of papers <i>per</i> year related to type of engineered nanomaterials (ENMs) until December, 2014.....	12
Figure 1.4.	Number of papers related to ecotoxicity of engineered nanomaterials (ENMs) according to species of bivalve molluscs until December, 2014...	12
Figure 1.5.	General scheme illustrating the potential toxicokinetics of engineered nanomaterials (ENMs) in bivalve molluscs (e. g. clams).....	22
Figure 1.6.	General scheme of subcellular localization of engineered nanomaterials (ENMs) in the bivalve mollusc cells.....	24
Figure 1.7.	General scheme illustrating the mode of action (MoA) of metal-based ENMs in bivalve molluscs.....	26
Figure 1.8.	Anatomy and optical properties of quantum dots (QDs).....	40
Figure 1.9.	General scheme illustrating the behaviour and transformation of quantum dots (QDs) in the aquatic environment.....	41
Figure 1.10.	General scheme illustrating the mode of action (MoA) of quantum dots (QDs) in bacteria, using the gram-negative bacteria <i>Escherichia coli</i> as model system.....	45
Figure 1.11	Representative scheme of different approaches used to study the toxicity of quantum dots (QDs) in fish species, using zebrafish <i>Danio rerio</i> as model system.....	62
Figure 1.12.	Scheme illustrating the trophic transfer of quantum dots (QDs).....	67
Figure 1.13.	Analytical techniques used for characterization of CdTe quantum dots (QDs).....	71
Figure 1.14.	Multibiomarker approaches used to assess the MoA and toxicity of quantum dots (QDs) in the marine mussel <i>M. galloprovincialis</i>	72
Figure 1.15.	The marine mussel <i>Mytilus galloprovincialis</i> used in this study. A. The	

	shell as seen from the right site B. The internal structure of mussels: posterior retractor muscle (1), byssus (2), gills (3), digestive gland (4), foot (5) and shell (6).....	73
Figure 1.16.	Map showing the collection site (red circle), located in the Ria Formosa Lagoon, Southeast of Portugal (37°06'59.4"N, 7°37'45.0"W).....	74
Chapter 2	Toxicokinetics and tissue distribution of cadmium-based quantum dots in the marine mussel <i>Mytilus galloprovincialis</i>	
Figure 2.1.	Transmission Electron Microscopy (TEM) image of CdTe quantum dots (QDs) (A) and hydrodynamic diameter histogram of QDs suspended in seawater at pH 8.0 (B).....	83
Figure 2.2.	Hydrodynamic diameter (mean \pm std nm) (A) and zeta potential (mean \pm std mV) (B) of CdTe quantum dots (QDs) suspended in Milli-Q water (MQ) and seawater (SW) with three types of natural organic matter (NOM): salicylic acid (SA), tannic acid (TA) and humic acid (HA) at pH 8.0.....	84
Figure 2.3.	Cd concentration (mean \pm std M) in water after exposure to CdTe quantum dots (QDs) and to dissolved cadmium (Cd) for 24 h (A) during accumulation (21 days) and depuration (50 days) periods (B).....	85
Figure 2.4.	Cd concentration (mean \pm std $\mu\text{g g}^{-1}$ d. w. tissue) and first-order kinetic model (K_m) of Cd accumulation (A-E) and elimination (F-J) in the whole soft tissues (A,F), gills (B,G), hemolymph (C,H), digestive gland (D,I) and remaining tissues (E,J) of mussels <i>M. galloprovincialis</i> from controls (C), exposed to CdTe quantum dots (QDs) and to dissolved cadmium (Cd) during the accumulation period (21 days) (A-E) and the depuration period (50 days) (F-J).....	87
Chapter 3	Effects of cadmium-based quantum dots on subcellular partitioning, metallothionein response and oxidative damage on the marine mussel <i>Mytilus galloprovincialis</i>	
Figure 3.1.	Analytical procedure for subcellular fractionation of mussel tissues by differential centrifugation.....	102
Figure 3.2.	Cd distribution (%) in the subcellular fractions of the gills (A-C) and	

	digestive gland (D-F) of mussels <i>M. galloprovincialis</i> from control (A,D), exposed to CdTe quantum dots (QDs) (B,E) and to dissolved Cd (C,F) during the exposure period (21 days). Cd concentration was analysed in the total homogenate (Ht) and in three subcellular fractions: insoluble (IF), high-molecular-weight proteins (HMW) and low-molecular-weight proteins (LMW) fractions.....	107
Figure 3.3.	Cd concentration (mean \pm std $\mu\text{g g}^{-1}$ d. w.) and first-order kinetic model (K_M) of the Cd accumulated in the biologically active (BAM) and detoxified (BDM) form in the gills (A) and digestive gland (B) from mussels <i>M. galloprovincialis</i> exposed to CdTe quantum dots (QDs) and to dissolved Cd during the exposure period (21 days).....	110
Figure 3.4.	Net accumulation rates for total accumulated Cd (Cd-total), biologically active metal (BAM) or biologically detoxified metal (BDM) in the gills (A-C) and digestive gland (D-E) from mussels <i>M. galloprovincialis</i> exposed to CdTe quantum dots (QDs) and to dissolved Cd during the exposure period (21 days).....	112
Figure 3.5.	Cd concentration (mean \pm std $\mu\text{g g}^{-1}$ d. w. tissue) and first-order kinetic model (K_M) of the Cd accumulated in the biologically active (BAM) and detoxified (BDM) forms in the gills (A) and digestive gland (B) from mussels <i>M. galloprovincialis</i> exposed to CdTe quantum dots (QDs) and to dissolved Cd during the depuration periods (50 days).....	113
Figure 3.6.	Cd distribution (%) in the subcellular fractions of the gills (A-C) and digestive gland (D-F) of mussels <i>M. galloprovincialis</i> from control (A,D), exposed to CdTe quantum dots (QDs) (B,E) and to dissolved Cd (C,F) during the depuration period (50 days). Cd concentration was analysed in the total homogenate (Ht) and three subcellular fractions: insoluble (IF), high-molecular-weight protein (HMW) and low-molecular-weight protein fractions (LMW).....	114
Figure 3.7.	MTs concentration (mean \pm std $\mu\text{g g}^{-1}$ w. w. tissue) in the gills (A,B) and digestive gland (C,D) of mussel <i>M. galloprovincialis</i> from controls (C), exposed to CdTe quantum dots (QDs) and to dissolved Cd (Cd) during the exposure period (21 days) (A,C) and depuration (50 days) periods (B,D).....	115

Figure 3.8.	LPO levels (mean \pm std MDA + 4-HNE nmol g ⁻¹ w. w. tissue) in the gills (A,B) and digestive gland (C,D) of mussel <i>M. galloprovincialis</i> from controls (C), exposed to CdTe quantum dots (QDs) and to dissolved Cd (Cd) during the exposure period (21 days) (A,C) and depuration periods (50 days) (B,D).....	120
Figure 3.9.	PCA analysis between total Cd concentration and in different subcellular fractions (IF, HMW, LMW), MTs and LPO levels in the gills (A-B) and digestive gland (C-D) of mussels <i>M. galloprovincialis</i> from controls (C), exposed to CdTe quantum dots (QDs) and to dissolved cadmium (Cd) during 21 days of exposure (A-D) and after 50 days of depuration (E-H)..	123
Chapter 4	Immunocytotoxicity, cytogenotoxicity and genotoxicity of cadmium-based quantum dots in the marine mussel <i>Mytilus galloprovincialis</i>	
Figure 4.1.	Transmission Electron Microscopy (TEM) image of CdTe quantum dots (QDs) in Milli-Q water (A) and particle size histogram of QDs obtained from TEM images (B).....	135
Figure 4.2.	ζ -potential (A) and hydrodynamic diameter (B) of CdTe quantum dots (QDs) suspended in Milli-Q water and natural seawater at pH between 1.7 and 12.....	136
Figure 4.3.	Hydrodynamic diameter (A), polydispersity index (B), turbidity (C) and sedimentation rate (D) of CdTe quantum dots (QDs) suspended in Milli-Q water and natural seawater at pH 8.0 over time.....	137
Figure 4.4.	Cd accumulation in whole soft tissue (A) and hemolymph (B) of mussels <i>M. galloprovincialis</i> ($\mu\text{g g}^{-1}$ d. w. tissue) from controls (C), exposed to CdTe quantum dots (QDs) and dissolved Cd (Cd ²⁺) for 14 days (mean \pm std).....	138
Figure 4.5.	Lysosomal membrane stability (LMS) (mean \pm std) in mussels <i>M. galloprovincialis</i> from controls (C), exposed to CdTe quantum dots (QDs) and dissolved Cd (Cd ²⁺) for 14 days.....	140
Figure 4.6.	Light microscopic image of hemocytes in mussels <i>M. galloprovincialis</i> from controls (C), exposed to CdTe quantum dots (QDs) and dissolved Cd (Cd ²⁺) and for 14 days.....	141
Figure 4.7.	Frequency of hemocytes types (mean \pm std) of mussels	

	<i>M. galloprovincialis</i> from controls (C), exposed to CdTe quantum dots (QDs) and dissolved cadmium (Cd^{2+}) at 14 days expressed as Eosinophils % (A), Basophils % (B), Hyalinocytes % (C) and hemocytes aggregates % (D).....	142
Figure 4.8.	Genotoxic effects of CdTe quantum dots (QDs) and dissolved Cd (Cd^{2+}) in mussels <i>M. galloprovincialis</i> exposed for 14 days. (A). Frequency of nuclear abnormalities (mean \pm std) expressed as frequency of binucleated cells (BN), micronucleus (MN) and Bud. (B). DNA damage (mean \pm SEM) expressed as tail DNA %.....	143
Figure 4.9.	Comet assay images of hemocytes in mussels <i>M. galloprovincialis</i> from controls (C), exposed to CdTe quantum dots (QDs) and dissolved Cd (Cd^{2+}) and for 14 days (total magnification 400x). H_2O_2 was the positive control.....	144
Chapter 5	Tissue specific toxicity of cadmium-based quantum dots in the marine mussel <i>Mytilus galloprovincialis</i>	
Figure 5.1.	Superoxide dismutase (SOD) (A-B), catalase (CAT) (C-D), total glutathione peroxidase (Total GPx) (E-F) and glutathione-S-transferase (GST) (G-H) activities in the gills and digestive gland of mussels <i>M. galloprovincialis</i> from controls (C), exposed to CdTe quantum dots (QDs) and to dissolved cadmium (Cd) for 14 days (mean \pm std).....	162
Figure 5.2.	Se-independent glutathione peroxidase (Se-I GPx) (A-B) and Se-dependent glutathione peroxidase (Se-D GPx) (C-D) activities in the gills (A, C) and digestive gland (B, D) of mussels <i>M. galloprovincialis</i> from controls (C), exposed to CdTe quantum dots (QDs) and to dissolved cadmium (Cd) for 14 days (mean \pm std).....	164
Figure 5.3.	Principal component analysis (PCA) of Cd accumulation and of a battery of biomarkers (SOD, CAT, total GPx, Se-I GPx, Se-D GPx and GST activities) in the gills (A-B) and digestive gland (C-D) of mussels <i>M. galloprovincialis</i> from controls (C), exposed to CdTe quantum dots (QDs) and to dissolved cadmium (Cd) for 14 days.....	167
Figure 5.4.	General scheme illustrating the tissue specific response in the gills (A) and digestive gland (B) of mussel <i>M. galloprovincialis</i> exposed to CdTe	

	quantum dots (QDs) and to dissolved cadmium (Cd) for 14 days.....	169
Chapter 6	Histopathological assessment and inflammatory response in the digestive gland of marine mussel <i>Mytilus galloprovincialis</i> exposed to cadmium-based quantum dots	
Figure 6.1.	Scheme of the procedure used to measure the histomorphometric parameters of digestive tubules in mussels <i>M. galloprovincialis</i> (adapted from Marigómez et al. 1990).....	179
Figure 6.2.	Digestive tubule types (%) in mussels <i>M. galloprovincialis</i> from control (C), exposed to CdTe quantum dots (QDs) and to dissolved Cd (Cd) for 14 days.....	182
Figure 6.3.	Photomicrographs of the digestive gland of mussels <i>M. galloprovincialis</i> from control (A-B), exposed to CdTe quantum dots (QDs) (C-D) and to dissolved Cd (E-F) for 14 days.....	183
Figure 6.4.	Histomorphometric parameters (mean \pm std) of digestive tubules in mussels <i>M. galloprovincialis</i> from control (C), exposed to CdTe quantum dots (QDs) and to dissolved Cd (Cd) for 14 days: tubule perimeter (P_0) (A), lumen perimeter (P_i) (B), epithelial layer area (S_0) (C), lumen area (S_i) (D), mean epithelial thickness (h) (E) and circularity (F).....	185
Figure 6.5.	Cell type composition (mean \pm std) of the digestive tubule epithelium in mussels <i>M. galloprovincialis</i> from control (C), exposed to CdTe quantum dots (QDs) and to dissolved Cd (Cd) for 14 days: basophilic cell frequency (%) (A), digestive cell frequency (%) (B), rate between both digestive tubule cell types ($R_{Bas/Dig}$) (C), hemocyte frequency (%) (D), total cell number <i>per</i> digestive tubule (E) and <i>per</i> epithelial layer area (S_0) (F).....	188
Figure 6.6.	Inflammatory response (mean \pm std) in the digestive gland of mussels <i>M. galloprovincialis</i> from control (C), exposed to CdTe quantum dots (QDs) and to dissolved Cd (Cd) for 14 days: intensity of the haemocytic infiltration (A) and haemocytic aggregates (B).....	189
Figure 6.7.	Frequency of the haemocytic infiltration (%) (A - C) and haemocytic aggregates (%) (D - F) distributed by grade of the inflammatory response in the digestive gland of mussels <i>M. galloprovincialis</i> from control (C)	

	(A and D), exposed to CdTe quantum dots (QDs) (B and E) and to dissolved Cd (Cd) (C and F) for 14 days.....	190
Figure 6.8.	Histopathological condition indices (I_h) (mean \pm std) of the digestive gland in mussels <i>M. galloprovincialis</i> from control (C), exposed to CdTe quantum dots (QDs) and to dissolved Cd (Cd) for 14 days: tubular alteration index (I_{h1}) (A), intertubular alteration index (I_{h2}) (B) and total histopathological index ($I_{h_{total}}$) (C).....	192
Figure 6.9.	Principal component analysis (PCA) of Cd concentration and of a battery of tissue-level biomarkers (histomorphometric parameters of the digestive tubule epithelium and lumen, digestive tubule cell type composition and histopathological indices) and inflammatory response (haemocytic infiltration and aggregation intensities) in the digestive gland of mussels <i>M. galloprovincialis</i> from controls (C), exposed to CdTe quantum dots (QDs) and to dissolved cadmium (Cd) during 14 days of exposure (A-B).....	193
Chapter 7	Differential proteomic response to cadmium-based quantum dots in the marine mussel <i>Mytilus galloprovincialis</i>	
Figure 7.1.	Master gel (A) constructed combining the information from the 2-DE gels of the digestive gland of <i>M. galloprovincialis</i> from control (B), exposed to CdTe quantum dots (QDs) (C) and to dissolved cadmium (Cd) (D) for 14 days.....	203
Figure 7.2.	Venn diagrams comparing the number of differential expressed proteins in the digestive gland of unexposed mussels and exposed to CdTe quantum dot (QDs) and dissolved Cd.....	204
Figure 7.3.	Sets of protein spots differently expressed in the digestive gland of mussels exposed to CdTe quantum dot (QDs) and dissolved Cd compared to unexposed ones.....	206
Figure 7.4.	Sets of protein spots observed only in the digestive gland of mussels exposed to both Cd forms (QDs vs dissolved Cd) compared to unexposed ones.....	207
Figure 7.5.	Sets of protein spots differently expressed only in the digestive gland of mussels exposed to both Cd form (QDs and dissolved Cd) compared to	

unexposed ones.....	208
---------------------	-----

Chapter 8 General discussion, conclusions and future perspectives

Figure 8.1.	General scheme illustrating routes for uptake, tissue distribution and elimination of quantum dots (QDs) and its dissolved counterpart in the marine mussel <i>M. galloprovincialis</i>	222
Figure 8.2.	General scheme illustrating the mode of action (MoA) and toxicity of quantum dots QDs in marine mussels <i>M. galloprovincialis</i>	226

TABLE INDEX

Chapter 1 General Introduction

Table 1.1.	Ecotoxicological impact of engineered nanomaterials (ENMs) in marine and freshwater bivalve molluscs.....	13
Table 1.2.	Interactive effects of nanomaterials (NMs) with other pollutants in marine organisms.....	33
Table 1.3.	Ecotoxicity of quantum dots (QDs) to bacteria.....	47
Table 1.4.	Ecotoxicity of quantum dots (QDs) to different micro-organisms (algae, protozoa, rotifera and fungi).....	52
Table 1.5.	Ecotoxicity of quantum dots (QDs) to different invertebrates (crustacean, annelid, platyhelminths, nematode and bivalve).....	58
Table 1.6.	Ecotoxicity of quantum dots (QDs) to different fish species.....	63

Chapter 2 Toxicokinetics and tissue distribution of cadmium-based quantum dots in the marine mussel *Mytilus galloprovincialis*

Table 2.1.	Accumulation rate (Ka), loss rate (Kl), elimination rate (Ke), half-life ($t_{1/2}$) and bioconcentration factor (BCF) in <i>M. galloprovincialis</i> tissues from controls (C), exposed to CdTe quantum dots (QDs) and to dissolved cadmium (Cd) during the accumulation (21 days) and depuration (50 days) periods.....	88
Table 2.2.	Production rate (mean \pm std mg g ⁻¹ d. w. tissue <i>per</i> day) and Cd concentration in biodeposits (mean \pm std μ g g ⁻¹ d. w.) of mussel <i>M. galloprovincialis</i> from controls (C), exposed to CdTe quantum dots (QDs) and to dissolved cadmium (Cd) during the accumulation (21 days) and depuration periods (50 days).....	89

Chapter 3 Effects of cadmium-based quantum dots on subcellular partitioning, metallothionein response and oxidative damage on the marine mussel *Mytilus galloprovincialis*

Table 3.1.	Characterization of CdTe quantum dots (QDs) in aqueous medium using different analytical techniques.....	105
Table 3.2.	Accumulation rate (Ka), loss rate (Kl), elimination rate (Ke), half-life ($t_{1/2}$) and bioconcentration factor (BCF) in the gills and digestive gland of	

	mussels <i>M. galloprovincialis</i> from controls (C), exposed to CdTe quantum dots (QDs) and to dissolved Cd (Cd) during the exposure (21 days) and the depuration (50 days) periods.....	109
Table 3.3.	Accumulation rate (<i>Ka</i>), loss rate (<i>Kl</i>), elimination rate (<i>Ke</i>) and half-life (<i>t</i> _{1/2}) of MTs and LPO in the gills and digestive gland of mussels <i>M. galloprovincialis</i> from controls (C), exposed to CdTe quantum dots (QDs) and to dissolved Cd (Cd) during the exposure (21 days) and the depuration (50 days) periods.....	117
Chapter 4	Immunocytotoxicity, cytogenotoxicity and genotoxicity of cadmium-based quantum dots in the marine mussel <i>Mytilus galloprovincialis</i>	
Table 4.1.	Cell viability and hemocyte density in mussels <i>M. galloprovincialis</i> from controls (C), exposed to CdTe quantum dots (QDs) and dissolved cadmium (Cd ²⁺) for 14 days (mean ± std).....	139
Table 4.2.	Frequency of hemocytes (%) distributed by grade of DNA damage in <i>M. galloprovincialis</i> from controls (C), exposed to CdTe quantum dots (QDs) and dissolved cadmium (Cd ²⁺) for 14 days.....	144
Chapter 5	Tissue specific toxicity of cadmium-based quantum dots in the marine mussel <i>Mytilus galloprovincialis</i>	
Table 5.1	Characterization of CdTe quantum dots (QDs) in aqueous medium using different analytical techniques.....	160
Chapter 6	Histopathological assessment and inflammatory response in the digestive gland of marine mussel <i>Mytilus galloprovincialis</i> exposed to cadmium-based quantum dots	
Table 6.1.	Histopathologies in the digestive gland of mussel <i>M. galloprovincialis</i> and their importance weight (<i>w</i>).....	180
Chapter 7	Differential proteomic response to cadmium-based quantum dots in the marine mussel <i>Mytilus galloprovincialis</i>	
Table 7.1.	Number of differentially expressed proteins (≥ 2 fold) in the digestive gland of mussels <i>Mytilus galloprovincialis</i> exposed to quantum dots (QDs)	

	and dissolved Cd (Cd) compared with unexposed mussels (C).....	206
Table 7.2.	List of protein spots observed in the digestive gland of mussels exposed only to quantum dots (QDs).....	210
Table 7.3.	List of protein spots differently expressed in the digestive gland of mussels exposed to quantum dot (QDs) compared to controls and dissolved Cd-exposed mussels.....	211
Table 7.4.	List of protein spots observed in the digestive gland of mussels exposed to dissolved Cd.....	211
Table 7.5.	List of protein spots differently expressed only in the digestive gland of mussels exposed to dissolved Cd compared to controls and QDs-exposed mussels.....	214
Table 7.6.	List of protein spots observed only in the digestive gland of mussels exposed to both Cd forms (QDs and dissolved Cd).....	215
Table 7.7.	List of protein spots differently expressed only in the digestive gland of mussels exposed to both Cd form (QDs and dissolved Cd).....	216
Table 7.8.	List of spots only observed in the digestive gland of unexposed mussels (C).....	218

ABBREVIATIONS

1-DE	One dimension electrophoresis,
2-DE	Two-dimensional gel electrophoresis
2D-PAGE	Two-dimensional polyacrylamide gel electrophoresis
4-HNE	4-hydroxyalkenals
AAS	Atomic absorption spectrometry
AChE	Acetylcholinesterase
ACP	Acid phosphatase
AFM	Atomic force microscopy
AGNES	Absence of gradients and Nernstian equilibrium stripping
AMP	Adenosine monophosphate
APP	Amphiphilic polymers like modified polyacrylic acid
BAM	Biologically active metal
BCF	Bioconcentration factor
BDM	Biologically detoxified metal
BDs	Biodeposits
BMs	Biomarkers
BN	Binucleated cell
BSA	Bovine serum albumin
CAS	Caspase
CAT	Catalase
Cb	Carbonylation
c_b	Conduction band
C_B	Cd concentration in the subcellular fraction
C_{B0}	Initial Cd concentration
Cd	Cadmium
CDNB	1-chloro 2,4 dinitrobenzene
CFU	Colony-forming unit
CI	Condition index
CNPq	National council for scientific and technological development
CNT	Carbon nanotubes
Co-NC	Co^{2+} -containing nanoscale polymeric complex
CP	Consumer products

C _w	Cd concentration in seawater
DAPI	4,6-diamidino-2-phenylindole
DCC	Differential cell counts
DG	Digestive gland
<i>dh</i>	Hydrodynamic diameter
DHLA	Dihydrolipoic acid
DIGE	Difference gel electrophoresis
DLS	Dynamic light scattering
DNA	Deoxyribonucleic acid
DOC	Dissolved organic carbon
DOPC	1,2-DiOleoyl-sn-glycéro-3-PhosphoCholine
E2	17β-estradiol
EC ₅₀	Half maximal effective concentration
EDTA	Ethylenediaminetetraacetic acid
ELS	Electrophoretic light scattering
ENMs	Engineered nanomaterials
ENPs	Engineered nanoparticles
EPA	US Environmental Protection Agency
EPF	Extrapallial fluid
EPS	Extracellular polymeric substances
ERKs	Extracellular signal regulating kinase
FTIR	Fourier transform infrared spectroscopy
FW	Freshwater
Go	Gonad
GPx	Glutathione peroxidase
GR	Glutathione reductase
GSH	Glutathione
GSH-t	Total glutathione
GSSG	Glutathione disulphide
GSSH	Oxidized glutathione
GST	Glutathione-S-transferase
<i>h</i>	Mean epithelial thickness
HA	Humic acid

HMW	High molecular weight
HRG	Histidine-rich glycoprotein
HSA	Human serum albumin
HSP	Heat shock proteins
Ht	Whole tissue homogenate
IARC	International agency for research on cancer
IC ₅₀	Half maximal inhibitory concentration
IEF	Isoelectric focusing
IF	Insoluble fraction
I_h	Histopathological condition indices
iTRAQ	Isobaric tags for relative and absolute quantitation
K_a	Accumulation rate
K_e	Elimination rate
K_l	Loss rate
LC ₅₀	Median lethal concentration
LDH	Lactate dehydrogenase
LMA	Low melting point agarose
LMS	Lysosomal membrane stability
LMW	Low molecular weight
LPO	Lipid peroxidation
LOD	Limit of detection limit
LOQ	Limit of quantification
MAA	Mercaptoacetic acid
MAPKs	Mitogen-activated protein kinase
MAS	Mercaptosuccinic acid
MDA	Malondialdehyde
MEA	2-mercaptoethylamine
MN	Micronucleus
MoA	Modes of action
MPA	Mercaptopropionic acid
MPEG-SH	Thiol-terminated methyl polyethylene glycol
MQ	Milli-Q water
MS	Mass spectrometry

MT	Metallothionein
MT-SH	Metallothionein related thiols
MxR	Multixenobiotic resistance
NAC	N-acetyl-L-cysteine
NCB	Nano-sized carbon Black
NER	Nucleotide excision repair
NMA	Normal melting point agarose
NO	Nitric oxide
NOM	Natural organic matter
NPs	Nanoparticles
n-Ps	Nanopolystyrene
NR	Neutral red
NRRT	Neutral red retention time
NTA	Nanoparticle tracking analysis
OECD	Organization for economic co-operation and development
Ox	Oxidation
P_0	Tubule perimeter
PAHs	Polycyclic aromatic hydrocarbons
PAA	Poly(acrylic acid)-octylamine copolymer
PC	Phytochelatins
PCA	Principal component analysis
PEG	Polyethylene glycol
PEPs	Protein expression profiles
Pf	Pseudofeces
Phe	Phenanthrene
P_i	Lumen perimeter
P_k	Proportion of each digestive tubule type
PMF	Peptide mass fingerprinting
PO	Phenoloxidase
PSH	Protein thiol
PSMA	Amphiphilic polymer poly(styrene-co-maleic anhydride) terminated with cumene
QDs	Quantum dots

$R_{Bas/Dig}$	Rate between number of basophilic and digestive cells
RNS	Reactive nitrogen species
ROS	Reactive oxygen species
RT	Remaining tissues
S_0	Epithelial layer area
SA	Salicylic acid
SAA	Sulfhydryl acetic acid
SCP	Stripping chronopotentiometry
Se-D GPx	Se-dependent glutathione peroxidase
Se-I GPx	Se-independent glutathione peroxidase
SEM	Scanning electron microscopy
S_i	Digestive tubule lumen area
SOD	Superoxide dismutase
SPM	Suspended particulate matter
SR	Sedimentation rate
SW	Seawater
SWCNHs	Single walled carbon nanohorns
$t_{1/2}$	Half-life time
TA	Tannic acid
TBARS	Tiobarbituric acid reactive substances
TCA	Trichloroacetic acid
TCDD	2,3,7,8-tetrachlorodibenzo- <i>p</i> -dioxins
TEM	Transmission electron microscopy
TGA	Thioglycolic acid
THR	Turbidimeter of high resolution
TK	Toxicokinetics
TLR	Toll-like receptor
TOPO	Tri- <i>n</i> -octylphosphine
TrxR	Thioredoxin reductase
TTF	Trophic transfer factor
Ub	Ubiquitination
v_b	Valence band
VTG	Vitellogenin

V_{BAS}	Basophilic cell volume density
w	Importance weight
WAF	Water accommodated fraction
WGA	Wheat germ agglutinin
XRD	X-ray diffraction
ZFL	Zebrafish liver
ZVI	Zero-valent nanoiron
ζ -potential	Zeta potential

CHAPTER I

General Introduction

Part of this Chapter was published in:

- Rocha, T.L., Gomes, T., Sousa, V.S., Mestre, N.C., Bebianno, M.J., 2015a. Ecotoxicological impact of engineered nanomaterials in bivalve molluscs: an overview. Marine Environmental Research. 111, 74-88. doi:10.1016/j.marenvres.2015.06.013

Part of this Chapter is being prepared for submission to:

- Rocha, T.L., Mestre, N.C., Bebianno, M.J. Ecotoxicity of quantum dots at various trophic levels: an overview. Science of the Total Environment.

1.1. Nanotechnology and nanomaterial

Nanotechnology is a key enabling technology (KET) and provides the basis for innovation in a wide range of products across all industrial sectors. This technology is defined by the European Committee for standardization (CEN) as “*design, characterization, production, and application of structures, devices, and systems by controlling shape and size at the atomic scale*” (CEN, 2016). Additionally, the Environmental Protection Agency (EPA) defines nanotechnology as “*research and technology development at the atomic, molecular, or macromolecular levels using a length scale of approximately one to one hundred nanometers in any dimension; the creation and use of structures, devices and systems that have novel properties and functions because of their small size; and the ability to control or manipulate matter on an atomic scale*” (EPA100/B-07/001:2007), while the U.S. National Nanotechnology Initiative (NNI) describes nanotechnology as “*the understanding and control of matter at dimensions between approximately 1 and 100 nm, where this unique phenomena enable novel applications*” (NNI, 2010). Nanotechnology has been considered as research priority in several countries, including member states of the European Union, USA, Japan, China and Russia, wherein nanotechnological innovations may improve the quality of life, economic growth and competitiveness of the industry (Savolainen et al., 2015), as well as environmental quality. In the Latin America, Brazil has been recognized as a leader in nanotechnology research, where started in the early 1990s, but its impacts on health and environment risks are still in its infancy (Kay and Shapira, 2009).

Nanoparticles (NPs) occur naturally in the environment (e. g. colloids, volcanic eruptions, forest fires). However the rapid development of nanotechnology has led to the production of engineered nanomaterials (ENMs) designed with specific characteristics to be used in a broad range of consumer products. Global production of ENMs are projected to grow to half a million tons with the number of ENMs-containing consumer products reaching 3400 by 2020 (www.nanoproject.org). This fast expansion will inevitably drive the release of ENMs into the aquatic environment directly (sewage, effluents, river influx) or indirectly (aerial deposition, dumping and run-off) (Moore, 2006; Baker et al., 2014) and reach different compartments (water, sediments, etc.). However, data about the concentration range at which different ENMs can actually be

detected in the environment is limited, especially due to methodological restrictions and scarce information about their fate in the aquatic environment (Minetto et al., 2014).

ENMs released into the aquatic systems may interact with aquatic organisms and induce toxic effects at different levels of biological organization. These potential ecotoxicological risks of ENMs to aquatic organisms have recently been reviewed (Lapresta-Fernández et al., 2012; Matranga and Corsi, 2012; Misra et al., 2012; Ma and Lin, 2013; Maurer-Jones et al., 2013; Baker et al., 2014; Corsi et al., 2014; Minetto et al., 2014; Grillo et al., 2015) but their mode of action (MoA) and biological risk remain unclear. Despite the emerging literature on the toxicity of ENMs in bivalve molluscs in recent years, their MoA and specific biomarkers for monitoring water pollution needs further clarification.

1.2. ENMs properties and characterization

ENMs can be classified as organic and inorganic. Fullerenes and carbon nanotubes (CNT) are carbon-based ENMs, while metals and metals oxides NPs, quantum dots (QDs) and SiO₂ NPs are defined as inorganic (Fadeel and Garcia-Bennett, 2010). ENMs exhibit specific physico-chemical properties that differ from their bulk material, which can be tailored due to the amount of atoms lying on the surface of the material (Casals et al., 2008). In bulk material there is a very low ratio between the number of atoms on the surface and those in the bulk, while at the nanoscale range the ratio between the surface area and volume is higher (Cupaioli et al., 2014). These properties are affected by ENMs small size and determine their behaviour, biological effects and consequently their toxicity. In addition, some ENMs are coated or capped with slight amounts of oxides or other chemical compounds to increase several chemical properties such as dispersibility and conductivity, as well as to prevent aggregation/agglomeration (Peralta-Videa et al., 2011).

In order to determine ENMs intrinsic properties it is critical to perform an appropriate physical and chemical characterization. Particle size, surface chemistry and charge, crystallinity, phase purity, solubility and shape are essential to explain the homogeneity, stability, reactivity, bioavailability and application potential of ENMs in different media (Kahru and Dubourguier, 2010). Particle size is one of the most important physico-chemical properties of ENMs which can be related with their

behaviour. It is also one of the main factors that affect bioavailability, distribution and retention of the ENMs in target tissues (Peralta-Videa et al., 2011; Cho et al., 2013).

Microscopic techniques provide an accurate assessment of the size and shape of ENMs, creating surface images by scanning the ENMs using a physical probe (López-Serrano et al., 2014). Scanning and Transmission Electron Microscopy (SEM and TEM) also allow the identification of structure and morphology of ENMs (Karlsson et al., 2009). However, it often requires complicated sample preparation, which could lead to imaging artefacts due to previous sample treatment and also to vacuum conditions. Atomic Force Microscopy (AFM) provides quantitative and qualitative data on physical properties such as size, morphology, surface texture and roughness (López-Serrano et al., 2014). This technique is based on van der Waals forces and could be applied in liquid media (Ju-Nam and Lead, 2008). However ENMs dimensions could be overestimated in some conditions.

Dynamic Light Scattering (DLS) is commonly used for ENMs size determination since it provides a simple and fast estimate of particle size. It is also very valuable to determine the size and aggregation/agglomeration conditions in nanotoxicological tests. According to their size, ENMs and aggregates acquire different mobility, which is referred as hydrodynamic diameter (d_h). In DLS, the Brownian movement of ENMs suspended in a liquid is measured (Pelley and Tufenkji, 2008). Despite DLS being frequently used to establish the size and d_h of ENMs in solution (Karlsson et al., 2009), several studies suggest inherent limitations of this technique, often associated with signal loss by smaller particles due to the signal intensity of bigger ones, i. e., the scattering intensity of small particles tends to be masked by the larger ones (Hoo et al., 2008).

Other technique widely used for ENMs size determination is X-ray diffraction (XRD), which also provides information on surface properties and coatings, crystallographic structure or elemental composition (Ju-Nam and Lead, 2008). XRD applies the Scherrer method to calculate particle size, but the accuracy of such method is poor (Calvin et al., 2005). An innovative system for ENMs sizing is nanoparticle tracking analysis (NTA), a single particle tracking technique based on dark field or fluorescence microscopy and automatic imaging analysis. NTA is an advantageous method since it tracks individual ENMs and provides a high resolution for multimodal samples and aggregation/agglomeration (Saveyn et al., 2010).

Electrophoretic light scattering (ELS) is a common technique in surface charge determination, expressed as zeta potential (ζ -potential). Applying an electric field, the electrophoretic mobility of suspended ENMs in the medium is evaluated (Ju-Nam and Lead, 2008). Generally, if the ζ -potential is more positive than +30 mV or more negative than -30 mV the ENMs have colloidal stability maintained by electrostatic repulsion. Similar to DLS, in bimodal samples ζ -potential of larger particles dominates the scattering signal of smaller ones (Murdock et al., 2008). ζ -potential of different ENMs is affected by ionic strength and pH of solutions, as for example, variations according to pH of ENMs suspended in freshwater in comparison to seawater, as seen for CdTe QDs (Rocha et al., 2014).

Techniques like UV-Vis and Fourier transform infrared spectroscopy (FTIR) are spectroscopic methods usually employed in fullerenes and derivatives characterization particularly in aquatic environments (Pérez et al., 2009). Elemental composition and chemical state of ENMs can be assessed by X-ray photoelectron spectroscopy (Chae et al., 2009). Secondary ion mass spectroscopy is another technique used to verify ENMs elemental composition by ionization and sputtering of the surface atoms (Putnam et al. 2008). It is well known that an appropriate characterization is needed. The most applied and useful techniques for characterizing ENMs were described, however a detailed explanation about each one is beyond the scope of this review.

Since all these techniques depend on different sample preparation and physical principles, the results of ENMs characterization in ecotoxicological tests differ according to the method used (Mahl et al., 2011). For example, based on different methods and types of reports, namely intensity, number or volume, silver (70 nm) and gold (15 nm) NPs were measured in the range of 40 - 124 nm and 11 - 52 nm, respectively (Mahl et al., 2011). In addition, even applying the same method, size determination depends on sample preparation. Bath sonication or vortex mixing is normally used to ensure ENMs dispersion for DLS measurements. Therefore, it is often observed that increasing sonication duration ultimately promotes agglomeration after initial dispersion (Murdock et al., 2008). In this context, no standardized methods for preparation of ENMs are used in ecotoxicological tests with marine and freshwater species, making a direct comparison between studies difficult. This concern was also raised recently in the experimental conditions with n-TiO₂ using different taxa of seawater organisms (Minetto et al., 2014).

1.3. Behaviour and fate of ENMs in the aquatic environment

Once released into the environment, ENMs will interact with each other and with their surrounding environment (Wiesner et al. 2009). In Figure 1.1 the possible interactions of ENMs in the aquatic environment are described. In the aquatic environment, ENMs behaviour and fate is dependent on nano-specific properties such as size, shape, chemical composition, surface charge, coating and particles state (free or matrix incorporated).

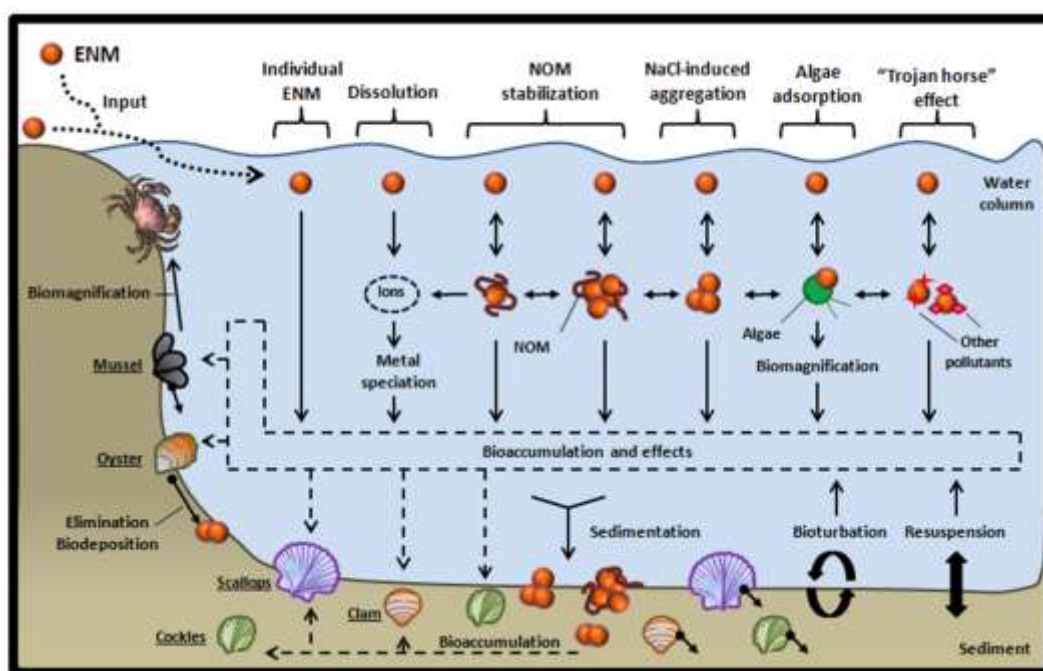


Figure 1.1. Scheme illustrating the potential behaviour and fate of engineered nanomaterials (ENMs) in the aquatic environment and associated biological processes with bivalve molluscs. NOM: Natural Organic Matter.

Environmental conditions, such as pH, temperature, ionic strength, composition and concentration of natural organic matter (NOM) and suspended particulate matter (SPM) also play an important role on ENMs behaviour, interacting to affect their aggregation/agglomeration or stabilisation (Fabrega et al., 2011; Sousa and Teixeira, 2013; Corsi et al., 2014). Identifying ENMs interactions under different conditions is essential to predict their fate and behaviour in the aquatic environment and thus estimate exposure scenarios as well as their potential ecotoxicity (Blinova et al., 2010; Keller et al., 2010). Accordingly, species can interact with different states of ENMs in the aquatic environment: (i) individual; (ii) small and larger homo-aggregates (NaCl-induced

aggregation/agglomeration); (iii) individual ENMs stabilized by NOM or SPM; (iv) small and larger hetero-aggregates (NOM-stabilization); (v) ion metal released from ENMs; (vi) metal-complex formed after metal release from ENMs; (vii) ENMs adsorbed to algae; (viii) ENMs adsorbed to other pollutants (*Trojan horse* effect) (Fig. 1.1).

Environmental impact is determined by the extent of aggregation/agglomeration, stabilisation and settling of ENMs when entering aquatic systems, as well as by the characteristics of the environmental matrix itself (Maurer-Jones et al., 2013; Sousa and Teixeira, 2013; Rocha et al., 2014). However, individual or small aggregates of ENMs may remain dispersed as colloids in solution (Brar et al., 2010). The rate of ENMs aggregation/agglomeration and sedimentation depend upon concentration, surface area and forces involved in collision, but variations in NOM, pH, ionic strength and surfactant present in fresh and marine waters will have a substantial influence on these phenomena (Peralta-Videa et al., 2011). On the other hand, when ENMs mobility increase, prolonged suspension in aquatic systems could lead to the horizontal transport of these materials over substantial distances (Baalousha et al., 2008). In the case of ENMs sedimentation, horizontal transport in the water column is reduced while local exposure to ENMs can increase. After sedimentation, benthic bivalve species are important targets for accumulation and toxicity of ENMs, as observed for the clam *Scrobicularia plana* exposed to CuO (10 - 100 nm; 10 g L⁻¹; 16 d), ⁶⁷ZnO (21 - 34 nm; 3 mg Kg⁻¹ sediment; 16 d) and Ag NPs (40 - 50 nm; 10 µg L⁻¹; 14 h) (Buffet et al., 2012, 2013b; Mouneyrac et al., 2014). Furthermore, bioturbation and resuspension in the sediment can lead to an increase of ENMs concentration in the sediment-water interface, promoting particle exchange between the sediment and water column, potentially enhancing the bioaccumulation and impact of ENMs (Fig. 1.1).

The marine environment is generally more alkaline and has high ionic strength. Therefore, seawater has a more pronounced effect in the surface charge of ENMs causing more particle collisions and consequently more aggregation/agglomeration and further sedimentation, than freshwater. NOM can increase ENMs stability extending their residence time in the water column and consequently increasing the exposure of aquatic biota, including benthic organisms (Mohd Omar et al., 2014). NOM can stabilize ENMs by the formation of a coating, which can involve a complex combination of electrostatic forces and steric effects between NOM and ENMs surface (Baalousha and Lead, 2013). The majority of authors reported that NOM increase

ENMs stability even in the presence of high concentrations of salts such as NaCl. However, this was not often observed in the presence of divalent ions at levels exceeding the critical coagulation concentration (Mashayekhi et al., 2012). Divalent species can assist in the formation of complexes between humic substances and ENMs promoting aggregation/agglomeration (Chen and Elimelech, 2007). Several authors demonstrated that the presence of NOM resulted in lower toxicity to the majority of the organisms, as shown by Grillo et al. (2015), although these findings have not been fully explained. However, a recent study where humic acids were combined with TiO₂ NPs to assess the toxicity to zebrafish show that humic acids stabilized ENMs and therefore increased the toxicity to fish following ingestion (Yang et al., 2013). In addition, polymeric substances secreted by aquatic microorganisms and bivalve molluscs, such as extracellular polymeric substances (EPS), polysaccharides and proteins, may induce aggregation/agglomeration, acting as chelating agents to bind and stabilize ENMs dispersion (Miao et al., 2009). Further studies of ENMs aggregation/agglomeration, deposition and mobilization with different experimental conditions (e. g. presence of different NOM or SPM) will help to better predict their fate and stability in aquatic environments.

1.4. Bivalve molluscs as a target group of ENMs toxicity

Sentinel species have widely been used worldwide to assess the current status and the long-term changes in environmental quality in freshwater, estuarine and coastal waters due to stressors. Several characteristics make bivalves particularly important and extensively used as sentinel organisms (Viarengo and Canesi, 1991; Livingstone, 1993; Kimbrough et al., 2008; Canesi et al., 2012; Falfushynska et al., 2012):

(i) they are sessile, filter-feeders and accumulate particles from water enabling the measurement of stressor levels in their tissues what in turn is a good indicator of the health of the surrounding environment;

(ii) they are relatively resistant to a wide variety of contaminants and environmental stressors (e. g. salinity, temperature), thus, being able to survive in stressed environments;

(iii) they are easily collected and maintained under well defined laboratory conditions;

(iv) they are found in high densities in quite stable populations, allowing repeated sampling and time-integrated indication of environmental contamination throughout a sampling area;

(v) they are distributed worldwide (both in fresh and marine environments), allowing data comparison from different areas;

(vi) many bivalve species are used commercially as food worldwide;

(vii) extensive background information exists about their biology and response to a wide range of environmental conditions.

For the above reasons, bivalves are therefore useful for characterizing the environmental impact of new and emerging contaminants in the aquatic environment, such as ENMs.

The first paper concerning the possible hazards associated with ENMs and their toxic effects for aquatic organisms was published by Moore in 2006, after which bivalve molluscs were recognized as a unique target group for nanotoxicology (Canesi et al., 2012). Publications increased rapidly, especially after 2008, as shown in Figure 1.2. A 14.6-fold increase in number of papers concerning nanotoxicity using bivalve species was observed by 2014 (Fig. 1.2). Similarly, Kahru and Ivask (2013) reported gradual growth in scientific production with other aquatic species (algae, bacteria, protozoa and daphnids) and reaffirmed the ecotoxicological risks of ENMs in the aquatic environment.

1.4.1. Types of ENMs

The nanotechnology sector is extremely diverse given its potential to synthesize, manipulate and create a wide range of products/materials with varied technological applications. Given the necessity for innovation, a wide range of ENMs with different composition, shape and size are currently being created and commercialized. Of the available information on nanotoxicological studies using bivalve species, 85% were performed using inorganic ENMs, while the remaining 15% used organic ones. Within the inorganic ENMs, metal oxides (36 %) and metals (35 %) are highlighted, followed by QDs (9 %) and SiO₂ NPs (5 %) (Fig. 1.3).

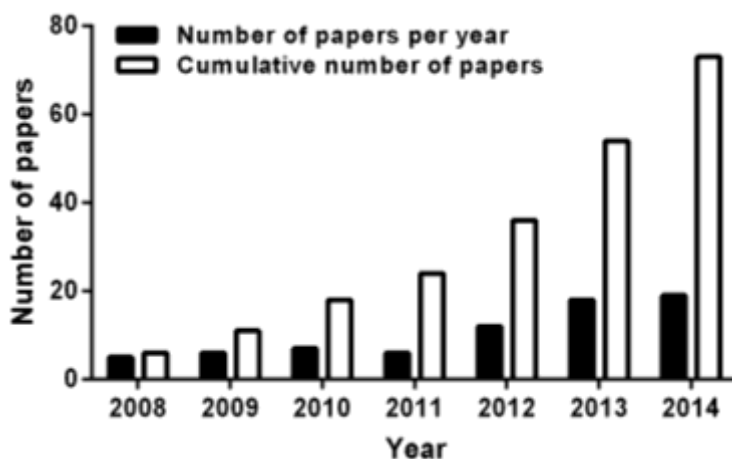


Figure 1.2. Timeline of the number (■) and cumulative number (□) of papers published *per year* related to ecotoxicity of engineered nanomaterials (ENMs) in bivalve molluscs until December, 2014. This scheme was organized based on data from Table 1.1.

Metal-containing ENMs have received considerable attention as they have been massively produced over the last years and extensively used in food, new materials development, chemicals and biological areas (www.nanoproject.org). This is the case of n-TiO₂ (16 %), Ag NPs (16 %), Au NPs (13 %), CuO NPs (9 %) and n-ZnO (8 %) (Fig. 1.3). n-TiO₂ is widely used in cosmetic and sunscreens, dye solar cells, paints and self-sterilizing surfaces and an increase in its production to more than 201000 t is expected (Markets Ra, 2011). Similarly, Ag NPs are extensively used in textiles, personal care products and food storage due to its antibacterial activity, while Au NPs and QDs are used in a wide variety of biomedical applications and biological research (www.nanoproject.org). QDs represent 9 % of these studies, but different toxic effects were identified, mostly due to a wide range of cores, shell and binding properties (Gagné et al., 2008; Peyrot et al., 2009; Bruneau et al., 2013; Katsumiti et al., 2014a; Munari et al., 2014). Surprisingly, only 5 % of toxicity studies using bivalves were conducted with n-SiO₂, the most used and produced ENMs (Piccinno et al., 2012).

The OECD priority list of manufactured nanomaterials for testing includes all previously described ENMs, except n-CuO (OECD, 2010). However, information about the toxic effects of other ENMs listed by OECD, such as dendrimers and nanoclays, is not available for bivalves (Table 1.1, Fig. 1.3). Furthermore, only two studies evaluated the toxicity of metallic nanoscaled polymeric complexes (Cleveland et al., 2012; Falfushynska et al., 2012).

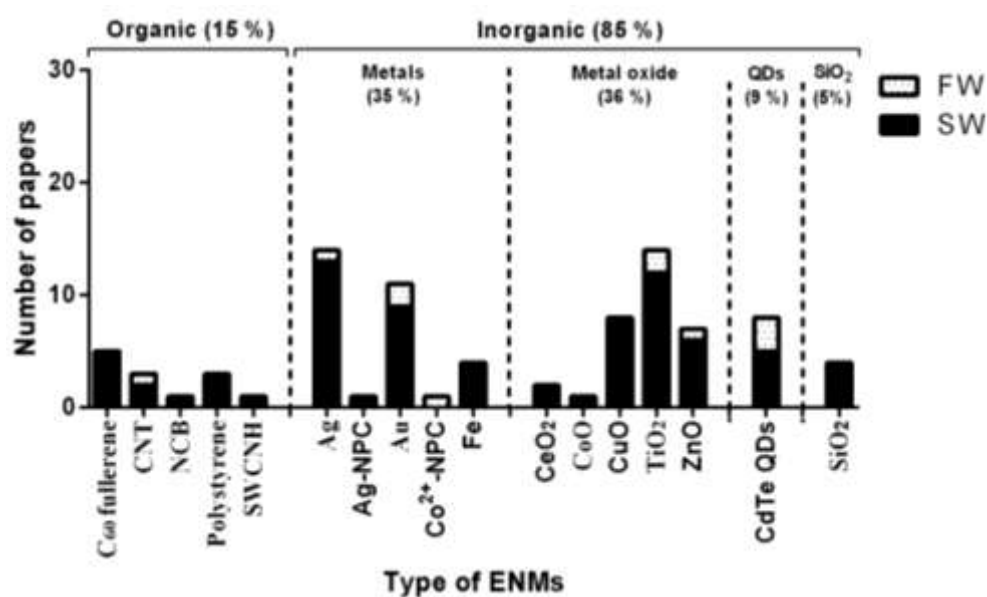


Figure 1.3. Number of papers *per year* related to the type of engineered nanomaterials (ENMs) until December, 2014.

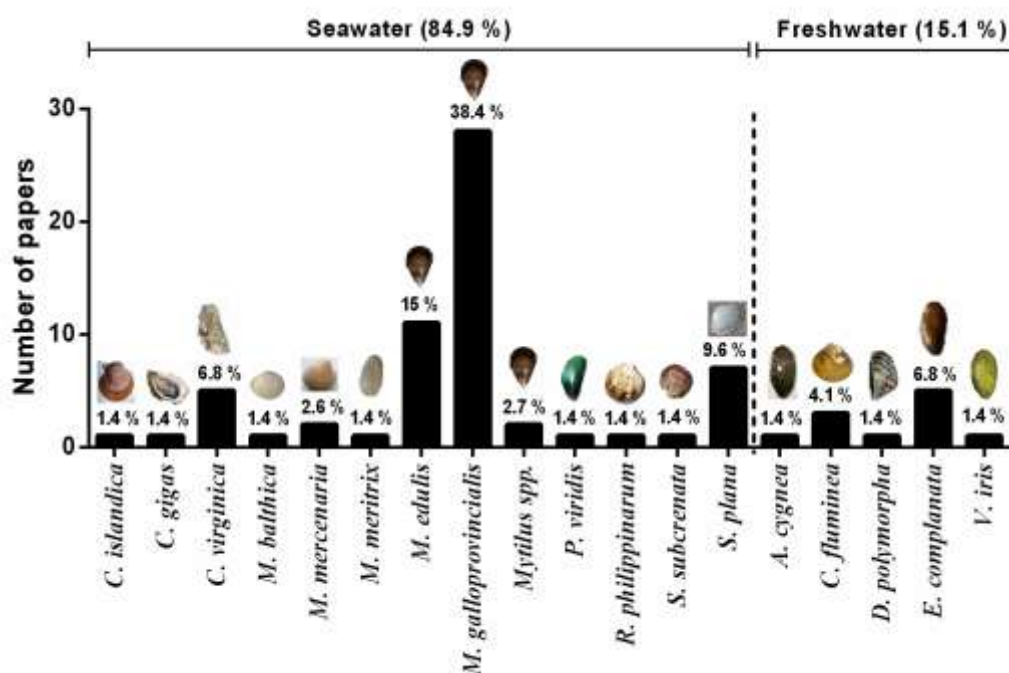


Figure 1.4. Number of papers related to ecotoxicity of engineered nanomaterials (ENMs) according to species of bivalve molluscs until December, 2014. The numbers above each bar represent the percentage of papers.

Table 1.1. Ecotoxicological impact of engineered nanomaterials (ENMs) in marine and freshwater bivalve molluscs.

Specie	ENMs		Exposure		Tissue ^c	Uptake/ Accumul ation	Effects ^d	Ref.
	Type ^a	Size (nm)	Conc. (µg L ⁻¹)	Time (h) ^b				
<i>M. galloprovincialis</i>	Seawater species							
	Ag, CuO	42, 31	10	15 d	H	-	Genotoxicity mediated by oxidative stress (NPs > bulk).	Gomes et al., 2013a
	Ag	42	10	15 d	DG, G	DG > G	↑Oxidative stress; Proteomic analysis show classical (HSP70, GST, actin) and new BMs (Major vault protein, Ras parcial, Precollagen-P).	Gomes et al., 2013b
	Ag	42	10	15 d	DG, G	G > DG	↑SOD, ↑CAT, ↑GPx, ↑MTs, ↑LPO (G). ↑Oxidative stress (G > DG).	Gomes et al., 2014b
	Au	14	0.1-1 nM	24	DG, G	x	No oxidative stress or morphological alterations. Biomagnification across algae and mussels.	Larguinho et al., 2014
	C ₆₀ , CNT	n.d.	10 ⁻² -10 µg mL ⁻¹	1	H*	-	C ₆₀ : immunocytotoxic (↓LMS damage). CNT: no LMS damage.	Moore et al., 2009
	C ₆₀ , SiO ₂ , TiO ₂	0.7, 12, 22	1-10	4	H*	-	Lysozyme release; ↑extracellular oxyradical and NO production; no LMS; hemocytes are a significant target for NPs.	Canesi et al., 2010a
	C ₆₀ , SiO ₂ , TiO ₂ , NCB	0.7, 12, 22, 30	0.05-5 mg L ⁻¹	24	DG, G, H	-	↓LMS (H, DG); lysosomal lipofuscin, ↑CAT (DG); oxidative stress; NCB and TiO ₂ : ↑GST; DG lysosomal system is a significant target for NPs <i>in vivo</i> .	Canesi et al., 2010b
	CdSe/ZnS, FeO	12 x 6, 50	185 µg, 1 mg, 0.48 nM	E: 24; Dep: 5 d	C, DG, H	DG	NPs stability and bioavailability are dependent of surface properties. Humic acid increase Fe NPs bioavailability.	Hull et al., 2013
	CdS	5	10 ⁻⁴ -10 ² mgCd L ⁻¹	24	G*, H*	x	↑MxR (potential detoxification). Cytotoxicity and genotoxicity (bulk > NPs). Nano-specific effect on phagocytosis and no changes on cytoskeleton (H).	Katsumiti et al., 2014a
	CdTe	6	10	14 d	H, O	x	↑DNA damage (H); immunocytotoxic (↓LMS, changes types of hemocytes). Hemocytes are targets for <i>in vivo</i> toxicity.	Rocha et al., 2014
	CeO ₂ , SiO ₂ , TiO ₂ , ZnO	15-30, 20, 21, 42	1-10	4	H*		↓LMS; ↑total extracellular oxyradical; ZnO: mitochondrial damage, cardiolipin oxidation. TiO ₂ and ZnO in the endossomes (30 min); TiO ₂ in the nucleus (60 min); ZnO: ↑pre-apoptotic processes.	Ciacci et al., 2012
	CeO ₂ , ZnO	24, 67	1-10 mg L ⁻¹	96	O, Pf	x	Excretion in Pf.	Montes et al., 2012
	CeO ₂	67 x 8	1-30 mg L ⁻¹	37 d	O, Pf	x	Dietary and direct exposure induces similar accumulation time dependent; ↑Pf production; ↑clearance rates.	Conway et al., 2014
	CuO	31	10	15 d	G	x	↑Oxidative stress; ↑LPO; ↓AChE; ↑MT.	Gomes et al., 2011

<i>M. edulis</i>	CuO	31	10	15 d	DG	x	↑Oxidative stress; ↑MT; ↑SOD, ↑CAT, ↑GPx, ↑LPO (7d).	Gomes et al., 2012
	CuO	31	10	15 d	DG,G	DG > G	↑Oxidative stress; proteomic analysis show classical (HSPs, actin, GST, ATP synthase) and new BMs (caspase 3/7-1, catL, Zn-finger).	Gomes et al. 2014a
	CNT	1.2-2 x 10 ² -10 ³ μm	1-3 mg L ⁻¹	4 w	DG, F, G, Mt,Pf	x	↓Clearance rate; no change in growth. Excretion in biodeposits (F and Pf).	Hanna et al., 2014
	NCB	35	1-10	4	H*	-	Hydrolytic enzymes release; oxidative burst; ↑NO production, inflammatory effects (rapid activation/phosphorylation of stress-activated MAPKs; ↑mitochondrial damage; no LMS damage.	Canesi et al., 2008
	SWCNHs	70	1-10 mg L ⁻¹	48	DG, H	-	↑Oxidative stress; ↓GPx; ↓LMS.	Mochino et al., 2014
	TiO ₂	15-60	1-100	96	DG, H	-	↓LMS; ↑antioxidant and immune-related gene (DG); ↓phagocytosis, ↑extracellular O ²⁻ production, ↑nitrite, ↑transcription of antimicrobial peptides (H).	Barmo et al., 2013
	TiO ₂	24	10 mgL ⁻¹	96	DG, G	-	Toxicity (NPs < bulk): histopathological and histochemical changes. Genotoxicity (bulk = “fresh” = “aged” NPs).	D’Agata et al., 2013
	TiO ₂	24	0-64 mg L ⁻¹	48	E	-	Light exposure ↑embryotoxicity.	Libralato et al., 2013
	TiO ₂	27	100	96	DG, E, H	x	Co-exposure (NPs + Cd ²⁺). No effects in Cd ²⁺ accumulation. ↓LMS; ↓phagocytosis; ↑NO production, lysozyme release (H). ↑MT; Synergistic effects on lysozyme and TLR-i genes.	Balbi et al., 2014
	TiO ₂	27	100	96	DG, G*, H	x	Co-exposure (NPs + TCDD): ↑TCDD accumulation, synergistic and antagonistic effects time dependent, cell/tissue and BMs. <i>Trojan horse</i> effects.	Canesi et al., 2014
	TiO ₂	10, - 100	0.1-100 mg L ⁻¹	24	G*, H*	-	Toxicity (small NPs > large NPs; NPs > bulk). No relationship between crystal structure and cytotoxicity. Similar sensitivity between H and G cells.	Katsumiti et al., 2014b
	ZnO	20	0.1-2 mg L ⁻¹	E: 84 d; Dep: 14 d	O	x	Changes in energy budgets (↓feeding capacity, ↑maintenance requirements; ↓life time for gametogenesis. Maintenance was a primary target of toxicant action.	Muller et al., 2014
	ZnO	20-30	0.1-2 mg.L ⁻¹	12 w	Go, O	x	Toxicity (small mussel > larger mussel); ↓Growth; ↓survival; ↑respiration rate.	Hanna et al., 2013
	ZVI	50	0.1-10 μg mL ⁻¹	2	E*,Sp*	-	Toxicity (stabilized NPs > no stabilized NPs); Spermiotoxic; genotoxic (S); ↓sperm fecundity; developmental impairments.	et al., 2011
	Ag	20 - 35	0.7	3.5	EPF, O	x	Transport of Ag to EPF is not form dependent. Complexation by organic molecules in the EPF. Hemocytes play an important role in Ag translocation to extrapallial cavity.	Zuykov et al., 2011a
	Ag	<40	0.7	3.5	S	-	Change shell calcification mechanism; shell nacre showed doughnut shape structures.	Zuykov et al., 2011b

	Ag ₂ S, CdS	13, 4	0.01-10 mg L ⁻¹	4	H*	-	Both NPs and capping agent (MPEG-SH) are genotoxic only at 10 mg.L ⁻¹ .	Munari et al., 2014
	Au	13	750	24	DG, G, H, M	-	↑Oxidative stress (DG); ↑ubiquitination (G, DG), ↑CAT induction (DG); ↑carbonylation (G). No LMS damage.	Tedesco et al., 2008
	Au	15.6	750	24	DG, G, M	DG > G	Larger NPs induce modest oxidative stress (DG): ↓GSH/GSSG ratio, ↓protein thiol group; no LPO; no changes TrxR.	Tedesco et al., 2010a
	Au	5.3	750	24	DG, G, H, M	DG	Oxidative stress and cytotoxicity (Small NPs >larger NPs); ↓Thiol-containing proteins; ↓LMS (H).	Tedesco et al., 2010b
	CdS-CdTe	1-10	0-2.7	21	H*	-	Toxicity (NP aggregates > bulk). Small NPs ↓phagocytosis while larger ones ↑. Mussel hemocytes are less sensitive to NPs than <i>O. mykiss</i> and <i>E. complanata</i> hemocytes.	Bruneau et al., 2013
	CuO	50	400-10 ³	1	DG, G, H*, Mt	G > DG	↑Oxidation and carbonylation of cytoskeleton and enzyme proteins. ↑ pigmented brown cells (DG, G, Mt); ↓LMS.	Hu et al., 2014
	n-Ps	30	0.1-0.3 g L ⁻¹	8	O	-	Excretion in Pf; behavioural impairments (↓feeding rate).	Wegner et al., 2012
	n-Ps	100	1.3 x 10 ⁴ NP mL ⁻¹	72	DG, F	x	↑Gut retention time; ↑egestion with time. Mussels ingested more NPs than oysters (<i>C. virginica</i>).	Ward & Kach, 2009
	SiO ₂	3-7 x 0.1-1 μm	n.d.	16 d	DG, G	x	↑Oxidative stress; sub-cellular distribution: endocytotic vesicles/lysosomes (<5-9 nm or >60 fibres), mitochondria (5-10 nm) and nuclei (<7 nm); ↓LMS; ↑lipofuscin.	Koehler et al., 2008
<i>Mytilus</i> spp.	C ₆₀	100 - 200	0.1, 1 mg L ⁻¹	3 d	DG, G, H, M	DG	Co-exposure (C ₆₀ + fluoranthene). ↑DNA damage; no DNA adducts, ↑tissue damage (M, G, DG). Co-exposure ↑damage with additive rather than synergistic effects.	Al-Subiai et al., 2012
	Fe ₂ O ₃	5 - 90	1 mg L ⁻¹	12	G*, H*	x	↓LMS; no LPO; no AChE inhibition.	Kádár et al., 2010
<i>P. viridis</i>	TiO ₂	20	2.5, 10 mg L ⁻¹	9 d	H	-	Co-exposure (NPs + hypoxia). Hypoxia ↑nanotoxicity; Synergistic effects.	Wang et al., 2014
<i>S. plana</i>	Ag	40 - 50	10	14 h	O	x	Toxicity (NPs = soluble form); ↑SOD, ↑CAT, ↑GST, ↓clearance rates (dietary exposure); no changes in TBARS, LDH, CAS 3-like and burrowing test; no MT induction; no neurotoxicity.	Buffet et al., 2013a
	Ag	40	10	21 d	DG, G, O	x	Mesocosms. Oxidative stress (TBARS), detoxification, apoptosis (CAS-3 like) and immunomodulation (lysozyme) (NP = soluble form); genotoxicity (DG; NPs > soluble form); ↑PO; no MT induction; no neurotoxicity; no changes in LDH, ACP and behaviour.	Buffet et al., 2014
	Au	5, 15, 40	100	16 d	O	x	No oxidative damage; ↑MT (5, 40 nm); ↑CAT (15, 40 nm), ↑SOD (40 nm), ↑GST (all sizes); ↑AChE; ↓burrowing speed; no changes in LDH.	Pan et al., 2012

	Au	5, 15, 40	100	16 d	DG, G	x	Sub-cellular distribution: G has fewer NPs (free in the cytoplasm or associated with vesicles) than DG (associated with chromatin); association with microtubules (15 nm); ↑perinuclear space, ↑swollen nuclei; ↓heterochromatin; nuclear localization size dependent.	Joubert et al., 2013
	CuO	10 - 100	10 g L ⁻¹	16 d	O	-	No oxidative stress. ↑GST, ↑CAT, ↑SOD; behavioural impairments (burrowing and feeding behaviour); no neurotoxicity;	Buffet et al., 2011
	CuO	29.5	10	21 d	H, O	x	Mesocosms. No oxidative stress. ↑DNA damage; behavior changes; ↑MT; ↑CAS3-like; ↑CAT, ↑GST. No effects in SOD and LDH;	Buffet et al., 2013b
	ZnO	20 - 34	3 mg Kg ⁻¹ sed.	16 d	O	x	No oxidative stress. ↑CAT; ↑LDH; ↓feeding rate; no change in GST, SOD and MT; no neurotoxicity.	Buffet et al., 2012
<i>M. mercenaria</i>	Ag CP	20, 80	24-300 mg	60 d	O	x	Mesocosms. Ag accumulation in biota, especially clams, via processes of adsorption and trophic transfer.	Cleveland et al., 2012
	Au	65 x 15	7.08 x 10 ⁸ NP mL ⁻¹	12 d	O	x	Mesocosms. Clam and biofilm accumulate more NPs than mud snails, fish, grass shrimp and vascular plant.	Ferry et al., 2009
<i>M. balthica</i>	Ag, CuO	20, 80, <100	200 µg g ⁻¹ sed.	E: 35 d; Dep: 15 d	H, O	x	Toxicokinetics is form dependent (ionic > NPs > micron). No effects on mortality, CI, burrowing behavior; no genotoxicity.	Dai et al., 2013
<i>M. meritrix</i>	CoO	n.d.	0.2, 2 mg mL ⁻¹	7 d	G*	-	↑Tissue damage (irregular cells, pyknotic nucleus and cells shrinkage); ↓cell density; ↑LDH; ↑ACP release; Lysosomal mediated cell injury; ↑necrosis.	Rebello et al., 2010
<i>R. philippinarum</i>	Au	21.5	6, 30	28 d	DG, G	G > DG	Sub-cellular distribution: heterolysosomes (DG).	García-Negrete et al., 2013
<i>C. virginica</i>	Ag	15	0.0016 - 16	48	E, DG	-	↑Embryotoxicity (1.6 µg.L ⁻¹); ↓LMS (0.16-16 µg.L ⁻¹); ↑MT (embryos > adults).	Ringwood et al., 2010
	Ag, TiO ₂	26, 70	1-400	2	H*	-	Toxicity (NPs = ionic form). ↓Phagocytosis.	Chalew et al. 2012
	Ag	20-30	0.02-20	48	G, DG	-	Toxicity (DG > G): ↓LMS, ↑LPO, ↑GSH.	McCarthy et al., 2013

	C ₆₀	10 - 100	1-500	4 h*, 4 d	E, DG*, O	x	↓LMS (adults, DG cells); ↑embryotoxicity (10-100 µg.L ⁻¹); no LPO; Endocytotic and lysosomal pathways are major targets.	Ringwood et al., 2009
	n-Ps	100	1.3 x 10 ⁴ NP mL ⁻¹	72	DG, F	x	Oysters <i>C. virginica</i> ingested less NPs than mussels <i>M. edulis</i> .	Ward and Kach, 2009
<i>C. gigas</i>	ZnO	31.7	50 µg L ⁻¹ - 50 mg L ⁻¹	96	DG, G, H	G (24h), DG (48h)	LC ₅₀ = 37.2 mg.L ⁻¹ ; ↓GR activity (G, DG), ↓PSH (G); ↑LPO (G); mitochondrial damage (G, DG). No effects in immunological functions and biochemical BMs (GSH-t, GSSG, CAT, TrxR).	Trevisan et al., 2014
<i>C. islandica</i>	Ag	10-20, 70-80	110, 151 ng L ⁻¹	E: 12; Dep: 8 w	O	DG > other organs	Toxicokinetics and tissue distribution is size dependent. Anal excretion route dominate over renal excretion.	Al-Sid-Cheikh et al., 2013
<i>S. subcrenata</i>	TiO ₂	≤ 10	500	E: 35 d; Dep: 30 d	G, M, Pf	G	Co-exposure (NPs + Phe). NPs as the carrier to facilitate Phe bioaccumulation. No NPs accumulation in M and G.	Tian et al., 2014
Freshwater species								
<i>E. complanata</i>	Ag	20, 80	0.8-20	48	DG, G, Go	-	↑Oxidative stress; ↑MT; ↑protein-ubiquitin; ↑DNA damage. Part of NPs toxicity attributed to release of Ag ⁺ .	Gagné et al., 2013b
	CdS-CdTe	1-10	0.05-2.7	21	H*	-	Toxicity (immunoactivity and immunoefficiency): larger NPs > smaller NPs.	Bruneau et al., 2013
	CdTe	n.d.	1.6-8 mg L ⁻¹	24	DG, G, H	x	↑Immunotoxicity (↓phagocytosis); ↑cytotoxicity (H); ↑oxidative stress (G); ↑DNA damage (G, DG).	Gagné et al., 2008
	CdTe	n.d.	1.6-8 mg L ⁻¹	24	DG, G, Go, H	x	↑MT (DG); ↓MT related to oxidative stress (G).	Peyrot et al., 2009
	ZnO	35	2	21 d	DG, G, Go	-	Co-exposure (NPs + municipal effluent). ↑oxidative stress; ↑Zn, ↑Fe, ↑Ni, ↑As, ↑Mo, ↑Cd (DG); Co-exposure change NPs effects on metallome.	Gagné et al., 2013a
<i>A. cygnea</i>	Co-NC	10-100	50	14 d	DG, Go, H	-	Toxicity [Co-NC < separate compounds (Co ²⁺ and polymeric substance)]. ↑MT-SH, low oxyradical formation; No changes in protein carbonylation and VTG-like protein. MT-SH involving in successful antioxidant defence.	Falfushynska et al., 2012

<i>D. polymorpha</i>	TiO ₂	25	0.1-25 mg L ⁻¹	24	H	x	↓Phagocytosis; ↑ERK1/2, ↑p38 phosphorylation (5 and 25 mg.L ⁻¹).	Couleau et al., 2012
<i>V. iris</i>	CNT	2 - 20	1 mg L ⁻¹	14 d	O	-	↓Survival. Dissolved metals contributed to ENMs toxicity. Nitric acid removes soluble metals from CNT and ↓toxicity.	Mwangi et al., 2012
<i>C. fluminea</i>	Au	10	1.6x10 ³ - 1.6x10 ⁵ NP cell ⁻¹	7d	DG, G, Vm	x	↑Oxidative stress; ↑MT; gene expression changes of CAT, SOD, GST and cytochrome C oxidase subunit-1 (G and Vm).	Renault et al., 2008
	Au	7.8, 15, 46	2-8 mgL ⁻¹	12 - 180	O, Pf	x	NPs undergoing extracellular digestion process. Faeces with nanoscale aggregates and free NPs.	Hull et al., 2011
	TiO ₂	20, 5	0.1-1 mg L ⁻¹	10 d	DG, O	x	Co-exposure (n-TiO ₂ + Cd ²⁺): ↓free Cd levels (FW); ↑CAT; ↑oxidative stress (O); ↑tissue damage (DG). No effects in SOD, GST and Cd accumulation.	Vale et al., 2014

^a CNT (Carbon Nanotubes), Co-NC (Co²⁺-containing nanoscale polymeric complex), CP (Consumer Products), NCB (Nano-sized Carbon Black), n-Ps (Nanopolystyrene), SWCNHs (Single walled carbon nanohorns), ZVI (Zero-valent nanoiron).

^b E (exposure period), Dep (depuration period).

^c E (embryos), C (carcass), EPF (extrapallial fluid), DG (digestive gland), F (feces), G (gill), Go (gonad), H (hemolymph/hemocyste), M (muscle), Mt (mantle), O (whole organism), Pf (pseudofeces), S (shell), Sp (sperm), Vm (visceral mass). *In vitro* exposure (*).

^d AChE (Acetylcholinesterase), ACP (Acid phosphatase), BMs (Biomarkers), CAT (Catalase), CI (Condition index), CAS (Caspase), DG (Digestive gland), DNA (Deoxyribonucleic acid), EPF (Extrapallial fluid), ENMs (Engineered nanomaterials), ERKs (Extracellular signal regulating kinase), F (Feces), FW (Freshwater), G (Gill), GPx (Glutathione peroxidase), GR (Glutathione reductase), GSH (Glutathione), GSH-t (Total glutathione), GSSG (Glutathione disulphide), GST (Glutathione s-transferase), HSP (Heat shock proteins), LC₅₀ (Median lethal concentration), LDH (Lactate dehydrogenase), LMS (Lysosomal membrane stability), LPO (Lipid peroxidation), MAPKs (Mitogen-activated protein kinase), MPEG-SH (Thiol-terminated methyl polyethylene glycol), MT (Metallothionein), MT-SH (MT related thiols), MxR (Multixenobiotic resistance), NPs (Nanoparticles), NO (Nitric oxide), PEG (Polyethylene glycol), Pf (Pseudofeces), Phe (Phenanthrene), PO (Phenoloxidase), PSH (Protein thiol), SOD (Superoxide dismutase), SW (Seawater), TBARS (Tiobarbituric acid reactive substances), TCDD (2,3,7,8-Tetrachlorodibenzo-*p*-dioxins), TLR (Toll-like receptor), TrxR (Thioredoxin reductase), VTG (Vitellogenin), Vm (Visceral mass).

1.4.2. ENMs ecotoxicity studies with bivalve molluscs

Table 1.1 describes the biological effects of ENMs in bivalve species. The first paper on bivalve molluscs described *in vitro* immunotoxicity of nanosized carbon black (NCB, 35 nm; 1 - 10 $\mu\text{g L}^{-1}$; 0.5 - 4 h) in the marine mussel *Mytilus galloprovincialis* (Canesi et al., 2008) followed by others whose effects are described in Table 1.1. They mainly focused on immunotoxicity, oxidative stress, DNA damage, subcellular accumulation and lysosomal damage in bivalve tissues, protein ubiquitination/carbonylation and protein expression changes (e. g. Gagné et al., 2008; Koehler et al., 2008; Renault et al., 2008; Tedesco et al., 2008; Gomes et al., 2013b) (Table 1.1). As the number of studies on ENMs-induced toxicity on bivalves under laboratory conditions progresses and several other nanotoxicological questions are raised, the research focus changed to a more environmentally realistic point of view, the interaction of ENMs with other contaminants.

1.4.3. Bivalve species

Figure 1.4 describes the different bivalve species used in nanotoxicology studies. ENMs toxicity tests (*in vitro* and *in vivo*) using different bivalve species were conducted mainly with seawater species (84.9 %) when compared to freshwater ones (15.1 %; Fig. 1.4). However, when considering other taxonomic groups (bacteria, algae, rotifers, annelids, crustaceans, echinoderms and fishes), studies are more abundant with freshwater species than with seawater ones (Matranga and Corsi, 2012; Libralato et al., 2013; Baker et al., 2014). Hence, this data emphasizes the importance of bivalve species as a significant group for understanding the mode of action of ENMs in marine and freshwater organisms and its application in monitoring programs.

Mussels are the main model group used (68 %), followed by clams (22 %), oysters (8 %), cockles (1 %) and scallops (1 %) (Table 1.1). Among the mussels, the genus *Mytilus* is the most studied taxa (56.1 %), especially *M. galloprovincialis* (38.4 %). Regarding freshwater bivalves, the mussel *Elliptio complanata* and the clam *Corbicula fluminea* represent 6.8 and 4.1 % of the studied species, respectively (Fig. 1.4). In contrast, there is no available data for economically important species, such as clams *Anadara granosa*, *Paphia undulate*, *Ruditapes decussatus*, *Sinonovacula constricta*, oysters *Ostrea edulis* and *Crassostrea angulata*, scallop *Argopecten gibbus* or mussels *Perna perna* and *Perna viridis*. Because there is the potential for

contamination by human consumption of molluscs contaminated with ENMs, further studies are still required.

1.4.4. Experimental design of nanotoxicological studies

Given the enormous expansion of nanotoxicological studies, difficulty arises in interpreting results and in drawing conclusions on ENMs ecotoxicity due to a lack of standardization in experimental conditions, e. g., *in vivo* versus *in vitro* testing, exposure routes (seawater, freshwater, dietary, sediments), concentrations (majority environmentally irrelevant) and time of exposure (normally short-term) (e. g. Baun et al., 2008; Canesi et al., 2012; Baker et al., 2014; Minetto et al., 2014).

The majority of the ecotoxicity studies of ENMs on bivalves is focused on *in vivo* testing (78 %) compared to *in vitro* (22 %), namely through waterborne exposure, followed by dietary and sediment routes (Table 1.1). This could be mainly due to the limited information about environmental factors that can modify the dietary ENMs uptake in bivalve species, sediment complexity as testing matrices and technical limitations on the analysis of ENMs behaviour in sediments.

Most of the tests published with bivalves were conducted under continuous exposure systems and no comparative data between intermittent and continuous exposure is available (Table 1.1). In relation to exposure time, data were mainly on short time of exposure (≤ 24 h: 38 %; 24 - 96 h: 16 %; 96 h - 7 d: 8 %) when compared to long-time exposure (7 d - 14 d: 9 %; 14 d - 1 m: 19 %; ≥ 1 m: 9 %) (Table 1.1), indicating that the long-term effects of ENMs in the bivalves deserve further attention.

Marine mesocosms are an exception, since experiments can be conducted with more realistic and relevant environmental conditions, thus allowing the study of bioaccumulation and trophic transfer in complex food webs and natural systems (Mouneyrac et al., 2014). This information is essential to study the fate, accumulation and toxicity of ENMs as was the case of CuO, Ag and Au NPs in the endobenthic species *S. plana* and *Mercenaria mercenaria* (Ferry et al., 2009; Buffet et al., 2012, 2013a; Cleveland et al., 2012).

1.4.5. Bioaccumulation and tissue distribution

Bivalve molluscs accumulate ENMs and are target of their toxicity mainly due to feeding habits. As filter-feeders, they can remove ENMs from the water column independently of their forms: individual, homo-aggregates (NaCl-induced

aggregation/agglomeration) and/or hetero-aggregates (e. g. algae-ENMs complex, NOM-ENMs complex and ENMs absorbed to other pollutants) (Fig. 1.1). Bioavailability and accumulation of ENMs in bivalves are dependent on nano-specific properties, behaviour and fate, as well as on the surrounding media and presence of NOM and/or SPM (Lowry et al., 2012; Misra et al., 2012; Sousa and Teixeira, 2013; Corsi et al., 2014; Grillo et al., 2015). Bivalves accumulate ENMs in their tissues to a higher extent than other aquatic organisms, such as the clam *M. mercenaria* versus snails, shrimp, fish and biofilm in estuarine mesocosms (Ferry et al., 2009; Cleveland et al., 2012).

The high ionic strength in the marine environment induces homo-aggregation/agglomeration of ENMs (NaCl-induced agglomeration) and this behaviour is a key factor for accumulation and tissue distribution of ENMs in bivalves. Aggregates interfere with the uptake route of inorganic nanoparticles, since they enter the organism mainly by endocytosis in the digestive system, while gills uptake individual ENMs or dissolved metal forms (Canesi et al., 2010a, 2010b; Gomes et al., 2011, 2012). The accumulation of ENMs according to size and hydrodynamic diameter remains controversial. The preferential accumulation of larger/aggregates than small/free ENMs was initially proposed (Ward and Kach, 2009) and confirmed (Hull et al., 2011; García-Negrete et al., 2013). However, recent studies indicate that dissolved metal (Ag and Cu) and NPs (Ag and Cu NPs) are more accumulated than micrometer-sized particles ones (Dai et al., 2013).

Based on data available from literature, a possible toxicokinetics scenario of ENMs in bivalves is suggested in Figure 1.5. During waterborne exposure, ENMs aggregates/agglomerates can be broken by cilia action in the gills or microvillus border in the digestive gland (Joubert et al., 2013), and under an intracellular digestion process inside lysosomes, at acidic pH, the metal-based ENMs release free metal ions in the digestive system. However there is a gap between ENM aggregates/agglomerates breaking down and their reaching the lysosomal system. In the clam *S. plana* exposed to Au NPs (5 - 40 nm; 100 $\mu\text{g L}^{-1}$; 16 d), ingestion was achieved through the inhalant siphon, transported to the mouth, then to the digestive tract and the digestive gland for intracellular digestion (Joubert et al., 2013). Similarly, the scallop *Chamys islandica* exposed to Ag NPs (10 - 80 nm; 110 - 151 ng L^{-1} ; 12 h) accumulated more ENMs in the digestive system (digestive gland, intestine, crystalline style and anus) than in other tissues (gills, mantle, gonads, kidney and muscle) (Al-Sid-Cheikh et al., 2013). Several

of the available studies confirm that the digestive gland is the main organ for ENMs accumulation in bivalve molluscs (e. g. Moore, 2006; Hull et al., 2011; Gomes et al., 2012) (Table 1.1).

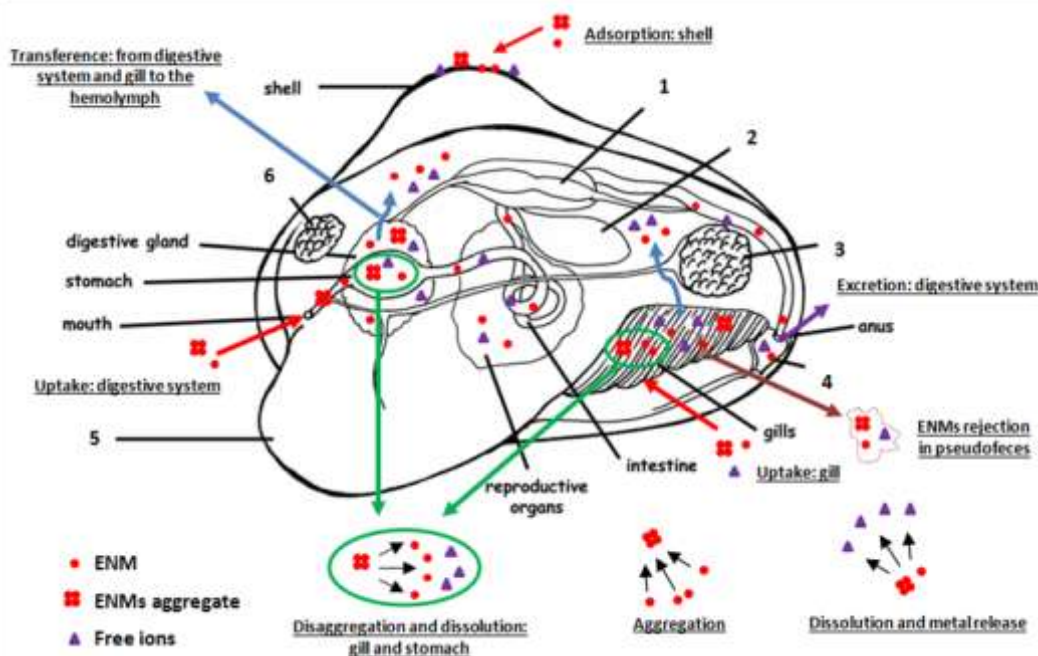


Figure 1.5. General scheme illustrating the potential toxicokinetics of engineered nanomaterials (ENMs) in bivalve molluscs (e. g. clams). Red arrow: Uptake of ENMs in the gill and digestive system; Brown arrow: ENMs rejection in pseudofeces; Green arrow: Deagglomeration and dissolution of ENMs in the gill and stomach; Blue arrow: Transfer of ENMs from digestive system and gill to the hemolymph; Purple arrow: Excretion of ENMs in the digestive system; 1: Heart; 2: Kidney; 3: Posterior shell muscle; 4: Siphon out (excurrent); 5: Foot; 6: Anterior shell muscle.

Different types of ENMs, such as nanopolystyrene, Ag NPs and BSA-Au NPs, accumulate preferentially in the digestive system of bivalves (Ward and Kach, 2009; Hull et al., 2011; Zuykov et al., 2011a; Wegner et al., 2012; Al-Sid-Cheikh et al., 2013). The longer gut retention time usually indicates that the ENMs undergo extensive extracellular digestion or are transported to the digestive gland for complete intracellular digestion (Ward and Kach, 2009; Hull et al., 2011; Al-Sid-Cheikh et al., 2013). However, ENMs in the gut may induce digestive system disorders such as blockage of food passage, leading to reduced growth or death (Mwangi et al., 2012). During ingestion and digestion, the state of dissolution and aggregation/agglomeration, size, shape and charge of the ENMs can be altered, and these modifications facilitate the

dispersion, coating degradation, aggregation/agglomeration or distribution of ENMs in tissues (Fig. 1.5).

After uptake, ENMs can also be transferred from the digestive system to the hemolymph and circulating hemocytes (Canesi et al., 2010a, 2010b; Ma and Lin, 2013). However, hemocytes will only uptake ENMs after they have crossed the epithelium of the digestive gland tubules (Moore et al., 2009). Therefore, bivalve hemocytes represent a good target for *in vitro* and *in vivo* effects of ENMs (Canesi et al., 2010a, 2010b; Katsumiti et al., 2014a; Katsumiti et al., 2014b; Rocha et al., 2014; Chapter 4) and their role in assessing the impact of ENMs in bivalve molluscs is described in the following sections.

1.4.6. Subcellular localization

ENMs can enter cells and alter the cytophysiology of target organs depending on its subcellular localization. The subcellular fate of ENMs in mollusc cells is one of the key properties in their MoA, but this aspect remains controversial and depends on the nano-specific properties, route and time of exposure, target organ, bivalve species and stage of development (Fig. 1.6; Table 1.1). They can be freely dispersed in the cytoplasm, be associated to the cytoskeleton or be inside endocytic vesicles, lysosomes, mitochondria or the nucleus (Fig. 1.6) (Koehler et al., 2008; Kádár et al., 2010; Ciacci et al., 2012; Couleau et al., 2012; García-Negrete et al., 2013; Joubert et al., 2013; Katsumiti et al., 2014a; Trevisan et al., 2014). Koehler et al. (2008) showed different subcellular localization of SiO₂ NPs (3 - 7 nm; 12 h - 16 d) in *M. edulis* according to size: endocytotic vesicles/lysosomes (< 5 - 9 nm or > 60 fibres), mitochondria (5 - 10 nm) and nucleus (< 7 nm). On the other hand, in the clam *S. plana* exposed to Au NPs (100 µg L⁻¹; 16 d), individual (5 and 15 nm) or small aggregates (40 nm) passed through the nuclear pore and were localized in the nucleus, but were also free in the cytoplasm or associated with vesicles in gill cells (Joubert et al., 2013).

The endocytic and lysosomal pathways are the major subcellular fate of ENMs in bivalve species (Kádár et al., 2010; Ciacci et al., 2012; García-Negrete et al., 2013; Joubert et al., 2013; Katsumiti et al., 2014a; Fig. 1.6). For example, C₆₀-fullerenes (10 - 100 nm; 10 - 500 µg L⁻¹; 4 day) tend to localize and concentrate in lysosomes of the oyster *C. virginica* (Ringwood et al., 2009), while CdS QDs (5 nm; 5 mgCd L⁻¹) accumulate inside vesicles of the endocytic-lysosomal system in *M. galloprovincialis* hemocytes after 1 h of exposure (Katsumiti et al., 2014a). Furthermore, the important

toxic mechanism of metal ENMs, oxide metal ENMs and QDs in bivalves is through dissolution inside the acidic environment of lysosomes (pH \pm 5) (Katsumiti et al., 2014a; Trevisan et al., 2014). Due to distinct lysosomal functions, as defence, intracellular digestion, tissue repair, protein turnover, autophagy and nutrition, ENMs damaging effects in the lysosomal system may induce disease processes, cell injury and death, as well as adverse effects on the development of bivalve embryos (Moore et al., 2009; Ringwood et al., 2009).

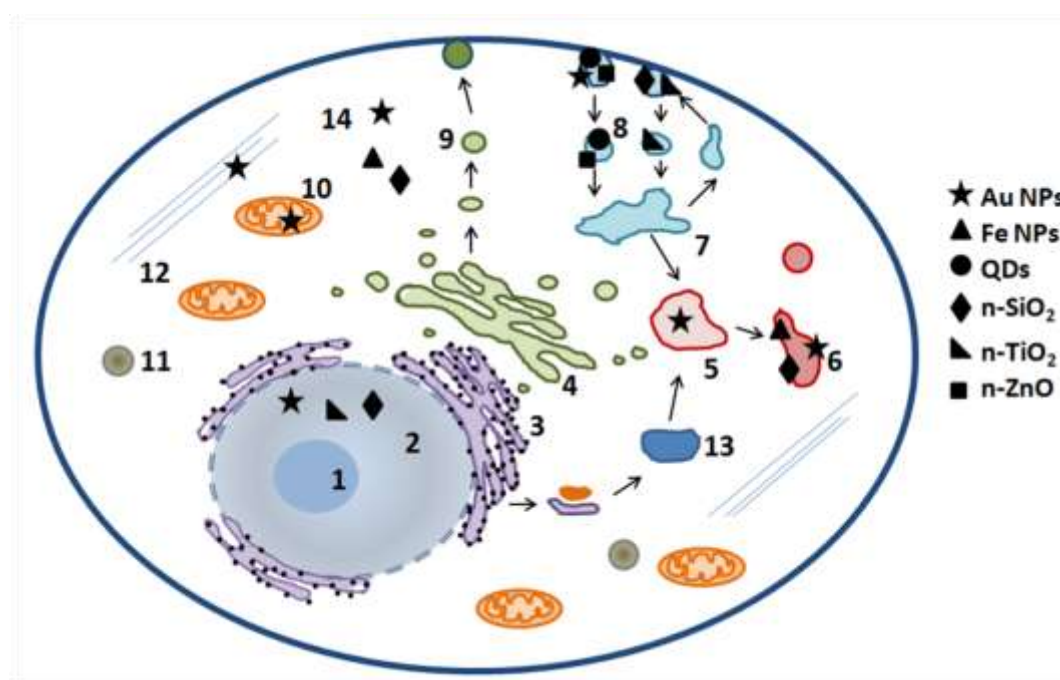


Figure 1.6. General scheme of subcellular localization of engineered nanomaterials (ENMs) in the bivalve mollusc cells. The numbers indicate the nucleus (1), nucleolus (2), endoplasmic reticulum (3), Golgi apparatus (4), late endosome (5), lysosome (6), early endosome (7), endocytic vesicles (8), secretory route (9), mitochondria (10), peroxisome (11), cytoskeleton (12), autophagosome (13) and cytoplasm (14). This scheme was organized from previous data of Au nanoparticles (NPs) (García-Negrete et al., 2013; Joubert et al., 2013), Fe NPs (Kádár et al., 2010), n-SiO₂ (Ciacci et al., 2012), n-TiO₂ (Ciacci et al., 2012; Couleau et al., 2012), n-ZnO (Ciacci et al., 2012; Trevisan et al., 2014) and QDs (Katsumiti et al., 2014).

Bivalve mitochondria are also an important target for ENMs toxicity. *M. galloprovincialis* hemocytes after *in vitro* exposure to NCB (35 nm; 1 - 10 μ g L⁻¹; 4 h) or to n-ZnO (42 nm; 1 - 10 μ g L⁻¹; 4 h) display mitochondrial impairment in terms of mass/number and membrane potential (Canesi et al., 2008; Ciacci et al., 2012). Oysters

C. gigas exposed to n-ZnO (31.7 nm; 4 mg L⁻¹; 48 h) show mitochondrial damage (loss of mitochondrial cristae, disruption of membranes and swollen morphology) in gills and digestive cells (Trevisan et al., 2014) similar to that of mammalian cells (Lin et al., 2012), confirming that mitochondria are early targets of ENM-stress (Lovrić et al., 2005). On the other hand, the effects of the ENMs in the synthetic-secretory pathway and other organelles of bivalves such as the Golgi apparatus, the endoplasmic reticulum and the peroxisome are unknown.

1.4.7. Modes of action (MoA)

Figure 1.7 describes the MoA of ENMs in bivalve cells. Overall, the data indicate that dissolution and release of ions from the particles, oxidative stress and cell injury in proteins, membrane and DNA damage are the major MoA of ENMs in bivalves (Table 1.1). The best developed paradigm to explain most of the cytotoxic effects exerted by ENMs in mussels is directly or indirectly mediated by reactive oxygen species (ROS) and free radicals production (Canesi et al., 2010a; Gomes et al., 2013a).

1.4.7.1. Oxidative stress

Among the oxidative damage induced by ENMs in bivalves breakdown of the antioxidant defence system [superoxide dismutase (SOD), catalase (CAT), glutathione peroxidase (GPx), glutathione s-transferase (GST)] (Gomes et al., 2011, 2012, 2014b; Zhu et al., 2011; Ali et al., 2012; Barmo et al., 2013), cytoskeleton disorganization (down and up-regulation of cytoskeleton protein) (Gomes et al., 2013b, 2014a), lipid peroxidation (LPO), protein oxidation (increase protein carbonylation or decrease of thiol-containing protein) (Tedesco et al., 2010a, 2010b), mitochondrial disruption (Trevisan et al., 2014) and DNA damage (DNA strand breaks) stands out (Ali et al., 2012; Gomes et al., 2013a; Katsumiti et al., 2014a; Munari et al., 2014; Rocha et al., 2014; Fig. 1.7).

Oxidative damage induced by ENMs in bivalves depends on the size, composition and concentration, mode and time of exposure, bivalve species and target organ analysed (Table 1.1). The ENMs size is a key factor in the induction of oxidative stress and is associated with its high surface area. For example, small Au NPs (5.3 nm; 750 µg L⁻¹) induce greater oxidative stress than larger ones (13 nm; 750 µg L⁻¹) in *M. edulis* after 24 h of exposure (Tedesco et al., 2010a, 2008). However, the relationship

between the hydrodynamic diameter and morphology of ENMs aggregates and oxidative stress in bivalves is still uncertain.

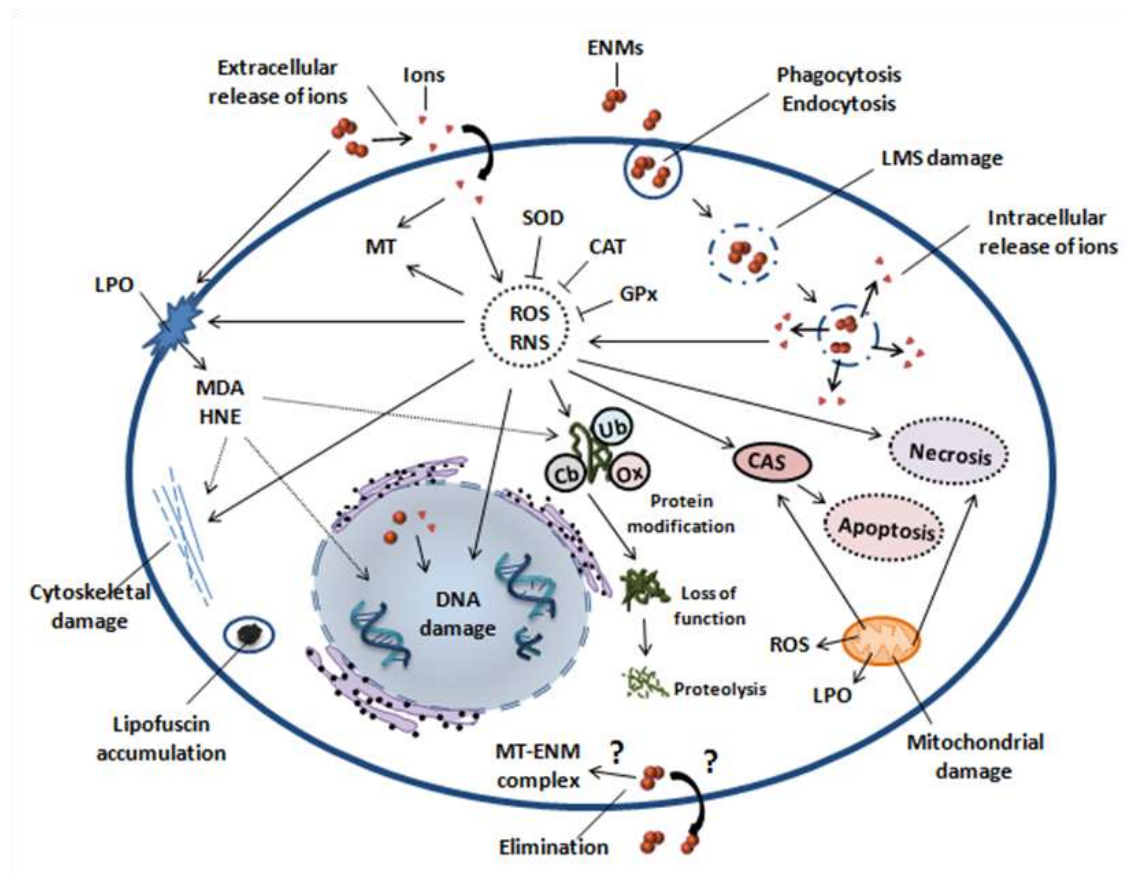


Figure 1.7. General scheme illustrating the mode of action (MoA) of metal-based ENMs in bivalve molluscs. Inorganic ENMs release extracellular metal ions, which penetrate the cell and induce oxidative stress by free radicals or reactive oxygen species (ROS) and reactive nitrogen species (RNS) production and/or metallothionein (MT) induction. ENMs uptake *via* phagocytosis and endocytosis, induction of lysosomal membrane stability (LMS) damage and/or release metal ions induction of oxidative stress, inhibited by the induction of superoxide dismutase (SOD), catalase (CAT) and glutathione peroxidase (GPx) activity. Both nano and dissolved forms induce membrane lipid peroxidation (LPO) resulting in malondialdehyde (MDA) and 4-hydroxyalkenals (HNE) production. Oxidative stress increase protein modification (Ub: ubiquitination; Cb: carbonylation, Ox: oxidation) resulting in loss of protein function and proteolysis, DNA damage induction and cellular death, apoptosis via caspase (CAS) cascade or necrosis. Detoxification pathways of ENMs in bivalve remain unclear. The mechanisms described are based on the revised data in the present work (Table 1.1).

Moreover, oxidative stress induced by ENMs also depends on bivalve tissue and cell types. The gills of *M. galloprovincialis* are more susceptible to oxidative stress induced by CuO NPs (< 50 nm; 10 $\mu\text{g L}^{-1}$; 7 - 15 d) than digestive gland (Gomes et al., 2011). On the other hand, Au NPs (15.6 nm; 750 $\mu\text{g L}^{-1}$) induced LPO only in digestive gland and no effects were observed in the gills or mantle of *M. edulis* after 24 h exposure (Tedesco et al., 2010a). Furthermore, no oxidative damage was observed in digestive gland cells of the oyster *C. virginica* exposed to C₆₀ fullerene (10 - 100 nm; 1 - 500 $\mu\text{g L}^{-1}$; 4 d) (Ringwood et al., 2009), in excised gills of *Mytilus spp.* after *in vitro* exposure to Fe₂O₃ NPs (5 - 90 nm; 1 mg L^{-1} ; 5 - 12 h) (Kádár et al., 2010) and in *S. plana* exposed to Au NPs (5, 15 and 40 nm; 100 $\mu\text{g L}^{-1}$; 16 d) (Pan et al., 2012). In a mesocosm study, no significant effects on LPO levels were observed in *S. plana* exposed to CuO NPs (29.5 nm; 10 $\mu\text{g L}^{-1}$; 21 d) (Buffet et al., 2013a). ROS production and oxidative stress were also observed in mussel hemocytes after *in vitro* and *in vivo* exposure to ENMs, such as NCB, C₆₀ fullerenes, n-TiO₂, n-SiO₂, n-ZnO and n-CeO₂ (Canesi et al., 2008; Canesi et al., 2010a, 2010b; Ciacchi et al., 2012; Barmo et al., 2013) and promote a decrease of immunological function and induce inflammatory conditions (Gagné et al., 2008).

1.4.7.2. Immunotoxicity

The immune system of bivalves is a sensitive target of ENMs toxicity. Among the analysed species, *Mytilus* hemocyte is the cell type most investigated in both *in vitro* and *in vivo* exposure (Table 1.1). Upon exposure and after crossing the epithelium of digestive gland tubules, bivalve hemocytes can uptake ENMs through endocytic pathways or via cell-surface lipid raft associated domains named caveolae (Moore, 2006; Moore et al., 2009). The immunocytotoxicity, immunoactivity and immunoefficiency are size, composition and concentration of ENMs, as well as bivalve species dependent. For example, small CdS/CdTe QDs (1 - 4.6 nm; 0.05 - 2.7 $\mu\text{g.L}^{-1}$) tend to reduce the phagocytic activity of *M. edulis* hemocytes while the opposite occurs with larger particles (4.6 - 10 nm; 0.05 - 2.7 $\mu\text{g.L}^{-1}$) after 21h of *in vitro* exposure (Bruneau et al., 2013). Furthermore, larger QDs (4.6 - 10 nm) are more toxic than small ones (1 - 4.6 nm) in *E. complanata* hemocytes after *in vitro* exposure to CdS/CdTe QDs (0.05 - 2.7 $\mu\text{g.L}^{-1}$; 21 h) (Bruneau et al., 2013), confirming that immunotoxicity of ENMs in bivalves is size-dependent. The cytotoxicity of n-TiO₂ to mussels also varied

according to the mode of synthesis, size, crystalline structure (anatase or rutile forms) and presence of additives in experimental medium (Katsumiti et al., 2014b).

Changes in phagocytosis activity, cell viability/density, stimulation of lysosomal enzyme release, ROS production, LMS damage, mitochondrial damage, DNA damage and pre-apoptotic processes were observed in bivalve hemocytes after exposure to different ENMs, such as NCB, C₆₀ fullerene, different metal oxides NPs (n-TiO₂, n-SiO₂, n-ZnO, n-CeO₂) and QDs (CdTe, CdS/CdTe) (Canesi et al., 2008; Gagné et al., 2008; Moore et al., 2009; Canesi et al., 2010a, 2010b; Ciacci et al., 2012; Couleau et al., 2012; Barmo et al., 2013; Gomes et al., 2013a; Katsumiti et al., 2014a, 2014b; Rocha et al., 2014). Generally, ENMs induce ROS production that lead to changes in the immune system due to inflammatory processes (reduction in phagocytic activity and hemocyte viability). The hemocytes response after *in vitro* exposure are not necessarily equivalent to that of *in vivo* exposure, making the specific cellular response of each types of hemocytes an emerging issue in the immunotoxicity of ENMs in bivalve molluscs.

1.4.5.3. Genotoxicity

DNA is a key cellular component highly susceptible to oxidative damage induced by ENMs in bivalve cells. The assessment of DNA damage after exposure to ENMs is of extreme relevance in nanotoxicological assessment due to the importance of DNA in maintaining cellular homeostasis and transmission of genetic information between generations. DNA damage induced by ENMs in bivalves is frequently assessed by the alkaline comet assay, using hemocytes or gill cells (Table 1.1). The association between the comet assay and cytogenotoxic tests (micronucleus test - MN and nuclear abnormalities assay) is indicated as a more realistic analysis of the nano-genotoxic effects in bivalves (Canesi et al., 2014; Rocha et al., 2014) since the alkaline comet assay enables the identification of DNA strand breaks (single and double), while the MN assay determines chromosomal damage induced by clastogenic (DNA breakage) or aneugenic (abnormal segregation) effects (Almeida et al., 2011; Bolognesi and Fenech, 2012).

Genotoxicity of Ag NPs (42 nm; 10 µg L⁻¹) and CuO (31 nm; 10 µg L⁻¹) are mediated by oxidative stress and both NPs show lower genotoxic effects than their soluble forms in *M. galloprovincialis* after 15 days of exposure (Gomes et al., 2013a). On the other hand, no genotoxic effects were observed in *M. balthica* after exposure to sediment spiked with Ag NPs (20, 80 nm) and CuO NPs (< 100 nm) (200 µg g⁻¹ d. w.

sed.; 35 days) (Dai et al., 2013). In a mesocosm study, similar genotoxicity of CuO NPs (29.5 nm) and soluble Cu was observed in the *S. plana* after 21 days of exposure at 10 $\mu\text{g L}^{-1}$ (Buffet et al., 2013a). DNA damage induced by Cd-based QDs was observed in marine mussels hemocytes after *in vitro* exposure to CdS QDs (4 nm; 10 mg L^{-1} ; 4 h) (Munari et al., 2014) and CdS QDs (5 nm; 0.001 - 100 mg L^{-1} ; 24 h) (Katsumiti et al., 2014a), and *in vivo* exposure to CdTe QDs (6 nm; 10 $\mu\text{g L}^{-1}$; 14 d) (Rocha et al., 2014). Furthermore, similar genotoxicity was observed in the freshwater mussel *E. complanata* exposed to CdTe QDs (1.6 - 8 mg L^{-1} ; 24 h) (Gagné et al., 2008). ENMs can also alter their genotoxic potential when adsorbed to other pollutants, as shown by Al-Subiai et al. (2012) in *Mytilus* hemocytes exposed to C₆₀ (100 - 200 nm; 0.1 - 1 mg L^{-1}) and polycyclic aromatic hydrocarbons (PAHs) where an additive effect was observed after 3 days exposure.

The nano-specific mechanism of genotoxicity in bivalve cells remains unknown. However, ENMs can penetrate the nucleus *via* nuclear pore complexes due to their small size (1 - 100 nm) (Fig. 1.5) and promote DNA damage by direct interaction with DNA or nuclear proteins due to high reactivity and surface charge, or by intracellular release of ionic metal or *via* overproduction of ROS which lead to oxidative damage (Gagné et al., 2008; Aye et al., 2013; Gomes et al., 2013a; Rocha et al., 2014; Fig. 1.7). Among these mechanisms, oxidative stress is indicated as the key factor of genotoxicity induced by ENMs in bivalve species and ENMs accumulation associated with exposure time is also an important factor in nano-genotoxicity (Gomes et al., 2013a; Rocha et al., 2014).

1.4.7.4. Behavioural changes and neurotoxicity

Behavioural biomarkers, such as burrowing, feeding rate and valve opening, are indicated as important tools to assess the ENMs toxicity in bivalves (Buffet et al., 2011; Pan et al., 2012; Wegner et al., 2012). The behaviour of bivalves exposed to ENMs depends on size, composition and concentration of ENMs, mode and time of exposure and species (Table 1.1). Data for this type of biomarkers mainly exists for the clam *S. plana* (Table 1.1). Large Au NPs (40 nm) induce stronger inhibition of burrowing kinetics of *S. plana* when compared to smaller ones (5 - 15 nm; 100 $\mu\text{g L}^{-1}$; 7 d) (Pan et al., 2012). Burrowing of *S. plana* is also modified after exposure to CuO (10 - 100 nm; 10 g L^{-1} ; 16 d) and ⁶⁷ZnO NPs (21 - 34 nm; 3 mg Kg^{-1} sediment; 16 d) (Buffet et al.,

2011, 2012). Furthermore, the exposure route is an important approach to assay the behavioural responses in bivalves exposed to ENMs. Dietary exposure reduces the clearance rate in *S. plana* more than the waterborne exposure to Ag NPs (40 - 50 nm; 10 $\mu\text{g L}^{-1}$; 14 h) (Buffet et al., 2013b). In addition, the mussel *M. edulis* also reduces their filtering activity after exposure to nanopolystyrene (30 nm; 0.1 - 0.3 g L^{-1} ; 8 h) (Wegner et al., 2012). In general, these behavioural changes indicate the potential ecological risk of ENMs towards energy acquisition necessary for survival, growth and reproduction, as well as their impact on ecological relationships by increasing the susceptibility to predation and impairment on inter- and intra-specific competition.

The association between behavioural changes and neurotoxicity effects [acetylcholinesterase (AChE) inhibition] is still controversial for bivalves exposed to ENMs. Exposure to CuO (10 - 100 nm; 10 g L^{-1} ; 16 d), ^{67}ZnO (21 - 34 nm; 3 mg Kg^{-1} sediment; 16 d) and Ag NPs (40 - 50 nm; 10 $\mu\text{g L}^{-1}$; 14 h) did not change AChE activity in *S. plana* (Buffet et al., 2011, 2012, 2013), and no obvious neurotoxic effects in *Mytilus* sp. after *in vitro* exposure to nano-Fe (50 nm; 1000 $\mu\text{g L}^{-1}$; 1 - 12 h) were observed (Kádar et al., 2010). On the other hand, Au NPs increased AChE activity in the clam *S. plana* (5 - 40 nm; 100 $\mu\text{g L}^{-1}$; 16 d) (Pan et al., 2012), which was associated with a phenomenon of overcompensation. Only Gomes et al. (2011) showed the applicability of using AChE activity as a specific biomarker for neurotoxic effects by ENMs after a significant inhibition of this enzyme in *M. galloprovincialis* exposed to CuO NPs (31 nm; 10 $\mu\text{g L}^{-1}$; 15 days).

1.4.7.5. Embryotoxicity

The developmental toxicity induced by ENMs was only investigated for n-TiO₂ and zero-valent nanoiron (n-ZVI) in *M. galloprovincialis* (Kadar et al., 2011; Libralato et al., 2013; Balbi et al., 2014). Exposure to natural light increases the embryotoxicity of n-TiO₂ by increasing the frequency of retarded larvae (pre-D shell stage) compared to malformed ones (24 nm; 0 - 64 mg L^{-1} ; 48 h) (Libralato et al., 2013). On the other hand, n-TiO₂ (alone or in combination with Cd^{2+}) did not affect mussel larval development at 100 $\mu\text{g L}^{-1}$ (Balbi et al., 2014). As bivalves reproduce by direct release of their gametes into the water column, the increase of sperm DNA damage decreases the gamete viability and fertilization success and consequently the frequency of normal D-shelled larvae. In *M. galloprovincialis* exposed to n-ZVI (50 nm; 0.1 - 10 $\mu\text{g mL}^{-1}$; 2 h) (Kadar

et al., 2011) the gametes and early developmental stages of bivalves are potentially more susceptible to toxic effects of ENMs when compared to later development or adult stages.

1.4.8. Interactive effects of ENMs and other stressors

Ecosafety and risk assessment of NMs in the marine environment should not only consider their inherent nanotoxicity, but also include the potential interaction of NMs with others pre-existing pollutants (Baun et al., 2008). According to the *Trojan horse* concept, NMs can act as a carrier for other pollutants, which can change their accumulation and toxicity (Limbach et al., 2007). Although the physico-chemical interactions of NMs with several pollutants have been widely investigated, interactive effects of NMs with other pollutants in marine organisms are scarce and were only available for n-TiO₂ (71.4 %), Au NPs (14.3 %), C₆₀ (7.1 %) and single-walled carbon nanotubes (SWCNT) (7.1 %), while Cd²⁺ (28.6 %) and 2,3,7,8-tetrachlorodibenzo-p-dioxins (TCDD; 28.6 %) were pollutants whose interactions with NMs were the most investigated, following by polycyclic aromatic hydrocarbons (PAHs: benzo(a)pyrene, fluoranthene and phenanthrene), pro-oxidant compound menadione and two emergent pollutants (1 - 5 µm microplastics and 15 nm Ag NPs) (Table 1.2), indicating that more studies are required concerning the interactive effect of NMs with other types of NMs and other traditional and emerging pollutants, such as pharmaceutical and personal care products.

Bivalve molluscs are the most studied group (64.3 %) for investigated interactive effects of ENMs with other stressors, while fish and sea urchin represent 28.6 and 7.1 %, respectively. Among the species studied, the mussel *M. galloprovincialis* is as already pointed out (Fig. 1.4) the main biological model (50 %), followed by the marine fish *Dicentrarchus labrax* (21.4 %) (Table 1.2). In light of this, further studies are needed on interactive effects of NPs with other pollutants in phytoplankton, zooplankton, macroalgae, marine vertebrates and marine mammals, as well as in sediment dwelling species.

In the marine environment, the interaction of NMs with others pollutants can alter the behaviour and fate of NMs and consequently change the bioavailability, uptake, accumulation and toxicity of both NMs and pollutants in marine organisms. The increase of TCDD accumulation was observed in mussel *M. galloprovincialis* whole soft tissues exposed to a mixture of n-TiO₂ (27 nm; 100 µg L⁻¹) and TCDD (0.25 µg L⁻¹)

for 96 h (Canesi et al., 2014), but a decrease in TCDD accumulation occurred in the digestive gland (Banni et al., 2016), indicating that the *Trojan horse* effect in marine mussels is tissue dependent, such as observed for exposure to NMs alone (Gomes et al., 2014; Rocha et al., 2015b). On the other hand, no effect on Cd accumulation was observed in the digestive gland of *M. galloprovincialis* after the co-exposure to n-TiO₂ (27 nm; 100 µg L⁻¹) and Cd²⁺ (100 µg L⁻¹) (Balbi et al., 2014) but increased n-TiO₂ in the gills (Della Torre et al., 2015), while reduced C₆₀ accumulation was observed in *M. galloprovincialis* after the co-exposure to C₆₀ (100 - 200 nm; 0.1 - 1 mg L⁻¹) and fluoranthene (32 µg L⁻¹) for 72 h (Al-Subiai et al., 2012).

Several studies showed that more antagonistic effects occur in marine organisms after co-exposure to NMs and other pollutants (Table 1.2). Furthermore, lower NPs-induced chromosomal damage and partial recovery of genome template stability in the marine fish *D. labrax* and mussel *M. galloprovincialis* after co-exposure to n-TiO₂ (24 nm; 100 µg L⁻¹) and Cd (100 µg L⁻¹) (Della Torre et al., 2015; Nigro et al., 2015), indicating that changes in the NMs behaviour during co-exposure can lead to a decrease on nano-specific toxicity. However, further studies about the ability of NMs to act as a carrier of other contaminants are further are needed using different types, size and surface coating NMs with other traditional and emerging contaminants.

Table 1.2. Interactive effects of nanomaterials (NMs) with other pollutants in marine organisms.

Species	NM			Pollutant		Exposure time (h)	Cell/ Tissue ^b	Effects ^c	References
	Type ^a	Size (nm)	Concentration (µg L ⁻¹)	Type ^a	Concentration (µg L ⁻¹)				
Bivalve molluscs									
<i>Mytilus edulis</i>	TiO ₂	62	200, 2000	B(a)P	20	96	DG, H, W	B(a)P accumulation ↓. SOD and GPx =. Chromosomal damage and CAT ↑.	Farkas et al., 2015
<i>Mytilus galloprovincialis</i>	Au	15.6	750	Menadione	1 mM	24	DG	Au accumulation ↓. TrxR; GSH/GSSG ratio; protein thiol group =.	Tedesco et al., 2010
	C ₆₀	100-200	100, 1000	Fluo	32	72	DG, G, H, M	C ₆₀ accumulation ↓. Additive (DNA damage) and synergic effects (GSH content).	Al-Subiai et al., 2012
	TiO ₂	27	100	Cd	100	96	DG, E, H	Cd accumulation =. Synergic effects (lysozyme, TLR-i genes). Decreased retarded development induced by Cd ²⁺ .	Balbi et al., 2014
	TiO ₂	27	100	TCDD	0.25	96	DG, G, H	TCDD accumulation ↑. Antagonistic (hemocyte phagocytosis, ABC transport) more than synergic effects (neutral lipid content and lysosome/cytoplasm volume ratio, transcription of estrogens receptors)	Canesi et al., 2014
	TiO ₂	24	100	Cd	100	96	G	Cd accumulation ↓. Antagonistic (<i>abcb</i> 1 gene, GST, DNA damage) more than additive effects (NO production).	Della Torre et al., 2015a
	TiO ₂	24	100	Cd	100	96		Chromosomal damage =. Partial recovery of genome template stability.	Rocco et al., 2015
	TiO ₂	27	100	TCDD	0.25	96	DG	TCDD accumulation ↓. 28 DEGs ↑ and 34 DEGs ↓. Tissue damage ↓.	Banni et al., 2016
<i>Scapharca subcrenata</i>	TiO ₂	≤ 10	500	Phen	20.9 ng	840	G, M, Pf	Phen accumulation ↑.	Tian et al., 2014
Fish									
<i>Dicentrarchus labrax</i>	TiO ₂	27	1000	TCDD	46 pg L ⁻¹	168	L, G, Er, S,	TCDD accumulation =.	Della Torre et al., 2015b

	TiO ₂	24	1000	Cd	100	168	M Er, M	NPs induced chromosomal damage ↓. Partial recovery of genome template stability.	Nigro et al., 2015
	TiO ₂	27	1000	TCDD	46 pg L ⁻¹	168	L	<i>ahrr</i> , <i>erβ2</i> , <i>Abcb1</i> , <i>Abcb2</i> genes ↓. <i>Cyp1a</i> , <i>gst</i> , <i>elmod2</i> genes =.	Vannuccini et al., 2016
<i>Pomatoschistus microps</i> Sea urchin	Au	5	200	Microplastic (1-5μm)	184	96	He, O	NPs accumulation and NP-induced toxic effects .	Ferreira et al., 2016
<i>Strongylocentrotus droebachiensis</i>	COOH-SWCNT	1.4 μm x 2-20 nm	200-5000	PAAm-Ag NPs (15 nm)	20-500	96	E	Toxic effects on early development stages ↓.	Magesky and Pelletier, 2015

^a 2,3,7,8-tetrachlorodibenzo-p-dioxins (TCDD); benzo(a)pyrene [B(a)P]; Fluoranthene (Fluo); Phenanthrene (Phen); poly(allylamine)-coated silver nanoparticles (PAAm-AgNps); single-walled carbon nanotubes (SWCNT).

^b Digestive gland (DG); embryo (E); erythrocytes (Er); gills (G); head (He); hemolymph/hemocyte (H); liver (L); muscle (M); pseudofeces (Pf); skin (S); whole tissues (W).

^c Benzo(a)pyrene [B(a)P]; catalase (CAT); differentially expressed genes (DEGs); glutathione (GSH); glutathione disulphide (GSSG); glutathione peroxidase (GPx); glutathione s-transferase (GST); nitric oxide (NO); superoxide dismutase (SOD); thioredoxin reductase (TrxR) toll-like receptor (TLR).

1.5. Proteomic research and identification of new biomarkers

As seen in the previous sections, conventional biomarkers have been extensively used to assess ENMs toxicity with bivalve species; nevertheless, many of these toxic responses (e. g. oxidative stress, LPO, enzymatic activation/inhibition, genotoxicity) are common to conventional contaminants, including NPs, dissolved and/or bulk forms (Handy et al., 2012). For this reason, there is a pressing need to develop nano-specific biological measurements to differentiate nano-specific responses and MoA from their similar dissolved/bulk counterparts, as well as other contaminants. With this in mind, proteomics-based methods have been applied to nanotoxicology in the last few years to complement the information given by traditional biomarkers, help identify protein pathways affected by these particles and possibly yielding greater insights into their toxic molecular mechanisms.

Tedesco et al. (2008) first reported the applicability of redox proteomics in *M. edulis* tissues exposed to Au NPs-citrate (13 nm; 750 $\mu\text{g L}^{-1}$; 24 h). Proteomic separations (1 dimension electrophoresis, 1-DE) showed higher protein carbonylation in the gills compared to the digestive gland, where higher ubiquitination occurred. The effects of the same Au NPs (~15 nm) were further explored by both 1-DE and two-dimensional gel electrophoresis (2-DE) in the digestive gland of *M. edulis*, showing a reduction in protein thiol oxidation as a response to targeting of protein thiols by ROS (Tedesco et al., 2010a). When using a smaller Au NPs particle size (5.3 ± 1 nm), the same authors showed changes in spot patterns in the sub-proteome of thiol-containing proteins consistent with greater oxidation (Tedesco et al., 2010b). Changes in carbonyls and protein thiols were also reported in *M. edulis* in response to CuO NPs (50 nm, 400 - 1000 mg L^{-1} , 1 h), where a decrease in reduced protein thiols and an increase in protein carbonyls were observed in gill extracts (Hu et al., 2014). Peptide mass fingerprinting (PMF) combined with Mass Spectrometry (MS) analysis identified six proteins: alpha- and beta-tubulin, actin, tropomyosin, triosephosphate isomerase and Cu-Zn superoxide dismutase, indicative of significant protein oxidation of cytoskeleton and key enzymes in response to CuO NPs.

CuO NPs toxicity (31 ± 10 nm, 10 $\mu\text{g L}^{-1}$, 15 d) was also investigated in *M. galloprovincialis* tissues (gills and digestive gland) and compared to that of Cu^{2+} . Alterations in the proteome of exposed mussels were detected with specific protein expression signatures to CuO NPs compared to Cu^{2+} . Identified proteins further

indicated that the biochemical pathways of cytoskeleton and cell structure, stress response, transcription regulation, energy metabolism, oxidative stress, apoptosis and proteolysis were altered during CuO NPs exposure, playing a putative role in cellular toxicity and consequent cell death in mussels. Apart from the traditional molecular targets of CuO NPs exposure in mussel tissues (e. g. ATP synthase, GST and HSPs), potential novel targets were identified (caspase 3/7-1, cathepsin L, Zn-finger protein and precollagen-D) and considered as putative new biomarkers for the CuO NPs exposure (Gomes et al., 2014a).

A similar technique was employed to characterize the effects of Ag NPs in *M. galloprovincialis* tissues (42 ± 10 nm, $10 \mu\text{g L}^{-1}$, 15 days), also in comparison to its ionic form by analysing variations in the gill and digestive gland proteomes by 2-DE. Tissue-specific protein expression profiles to Ag NPs and Ag^+ were reported, which reflect differences in uptake, tissue-specific functions, redox requirements and modes of action. Proteins analysis by PMF combined with MS analysis led to the identification of 15 proteins: catchin, myosin heavy chain, HSP70, GST, nuclear receptor subfamily 1G, precollagen-P, ATP synthase F0 subunit 6, NADH dehydrogenase subunit 2, putative C1q domain containing protein, actin, α -tubulin, major vault protein, paramyosin and ras, partial. The exclusive identification of the major vault protein, paramyosin and ras, partial to Ag NPs exposure lead the authors to suggest their use as new putative candidate molecular biomarkers to assess Ag NPs toxicity (Gomes et al., 2013b).

Overall, the redox proteomics revealed more specific effects than more traditional biomarkers of oxidative stress in sentinel species. Furthermore, 2-DE approach also proved to be a valuable tool for the identification of proteins altered by ENMs, allowing a global view of their MoA at the molecular level, the differentiation of their toxic mechanisms in comparison to its dissolved counterparts and even provide novel and unbiased biomarkers of exposure and effect. Nonetheless, as highlighted by Gomes et al. (2014a), due to the exploratory nature of the proteomics approach applied in these studies, additional work is required to confirm and validate the usefulness of the identified proteins as novel biomarkers of ENMs exposure and effect in a more realistic environmental exposure and risk perspective/scenario. Furthermore, proteomic research using bivalve species still do not benefit from the application of more high throughput sensitive techniques, such as difference gel electrophoresis (DIGE) and isobaric tags for relative and absolute quantitation (iTRAQ) coupled to MS that could provide a deep understanding of the molecular mechanisms of ENMs-induced stress syndrome in

organisms. The main reason for this limitation is the lack of complete genome sequencing of bivalve species, that except for oyster *C. gigas* whose full genome is already available, prevent the identification of proteins that might be relevant to clarify the MoA of ENMs in bivalve species (Campos et al., 2012).

Other OMICS technologies (transcriptomics, metabolomics) applied to the nanotoxicological field may also provide researchers with new tools for the high throughput identification of molecular markers that may be sensitive to ENMs. However, similarly to the proteomics approach, these techniques are also biased by the lack of information from only partly sequenced genomes of bivalve species and no studies exist at the present on the effects of ENMs in the transcriptome and metabolome of bivalve species. Although, proteomic analysis represents a powerful tool to understand the cell/tissue nano-specific response transcriptomics and metabolomics data are needed to complement this approach.

1.6. Ecotoxicity of quantum dots at various trophic levels

1.6.1. Quantum dots

QDs are a class of ENPs with nanometer diameters (2 – 10 nm) firstly discovered by Ekimov and Onushchenko (1982). The terminology “quantum dots” was first used by Reed et al. (1988) when referring to heterostructures with quantum confinement to zero dimensions and is related to the quantum confinement effect in which nanocrystals with size smaller than the Bohr radius ($a_0 = \approx 5.29 \times 10^{-11}$ m) have quantized energy levels with values directly related to size (Reed et al., 1988; Michalet et al, 2005).

QDs were first used in biological imaging in 1998 and its global production was estimated to be between 0.6 and 55 t year⁻¹ in 2012 (Piccinno et al., 2012), with an expected annual increase of 55 % in the period between 2012 - 2022 (Market Research Report, 2012). Most of QDs produced are for light-emitting diode (LED) or organic light-emitting diode (OLED) (90 %) and 10 % is used in laboratories for imaging purposes (Piccinno et al., 2012). The increasing production and use of QDs will inevitably lead to its release into the wastewater, freshwater and marine environment, where potential sources of toxicity might result in their interaction and uptake by organisms at different trophic levels.

Although the concentration of QDs in the aquatic environment are unknown, the ecotoxicological impact of QDs is an emerging problem, especially because of their nano-specific and biofunctional properties, physic-chemical transformation in the

environment (i. e. photo-activation and ROS generation) in aqueous solutions under exposure to ultraviolet or visible electromagnetic radiation) and release of toxic metals, such as Cd (Ipe et al., 2005; Ribeiro et al., 2012; Katsumiti et al., 2014; Santana et al., 2015; Rocha et al., 2015a) (Chapter 2). Although the toxicity of QDs to mammal cells have been previously revised by Hardman (2006) and Pelley et al. (2009), the knowledge of their behaviour and fate in the aquatic environment and their toxic effects to different trophic levels are required in the environmental health context.

1.6.2. QDs applications and properties

QDs have many applications, such as electronics (e. g. LED, OLED, photovoltaic and lasers), solar panels, photo-chemistry (e. g. photoelectrodes), analytical chemistry, pharmacy, molecular and cell biology (e. g. live-cell imaging, co-localization of genes/proteins, multicolour staining and flow cytometry) and nanomedicine (e. g. molecular profiling of cancer, antimicrobial agents, *in vivo* tumor imaging and photodynamic therapy) (Michalet et al., 2005; Deerinck et al., 2008; Tholouli et al., 2008; Kosaka et al., 2009; Rizvi et al., 2010; Byers and Hitchman, 2011; Zhang et al., 2012). In addition, some authors highlighted the potential application of QDs in personalized medicine, especially in the early stage of diagnosis and on the development of disease- and patient-specific therapies (Zhang et al., 2012). These varieties of QDs applications are strongly related to their physical, chemical and biological properties such as:

- strong fluorescence at narrow and size-tunable wavelengths ranging from visible to near-infrared wavelengths (Deerinck et al., 2008; Loginova et al., 2012) and high fluorescence at low concentrations (Feswick et al., 2013);
- the emission spectrum that can be controlled by modification of size, composition and surface coating (Rizvi et al., 2010);
- resistance to photobleaching (highly photostable) (Feswick et al., 2013) and maintenance of fluorescence after the excitation long periods (slow excited-state decay rates) (Loginova et al., 2012);
- specific bio-activity and identification of specific cellular targets when coated and linked to functional groups, such as avidin, biotin, oligonucleotides, peptides, antibodies, DNA or albumin (Michalet et al., 2005; Rizvi et al., 2010; Aye et al., 2013).

Furthermore, QDs can be used simultaneously with standard dyes (Michalet et al., 2005) and in confocal microscopy to perform nanometer-resolution colocalization of multiple-colour individual QDs (Kosaka et al., 2009).

1.6.2.1. Morphology and composition

The typical structure of QDs is referred to as “core-shell-conjugate” (Fig. 1.8A). Usually, the QD is spherical or oblong (Fig. 1.8B) and their morphology can be easily analyzed by TEM due to their metalloid composition and electron dense nature (Deerinck, 2008; Rocha et al., 2014, 2015a). The QD core can be made of a variety of metal complexes, such as group II-IV series (CdSe, CdTe, CdSeS, ZnS, ZnSe and PbSe) or group III-V series (InP, InAs, GaAs and GaN) (Zhang et al., 2013) and determines their colour, while the inorganic shell or ligand(s) can enhance stability, brightness, water solubility and conjugation capacity (Michalet et al., 2005; Nguyen et al., 2013). The most common QDs core used for biological and medical applications is CdSe and CdTe (Smith et al., 2008), which can be coated with shell and additional capping layer or ligands (Fig. 1.8A)

The QD shell consists mainly of a second semiconductor material (e. g. ZnS) and protects the core from oxidation and degradation, while surface ligands can be hydrophilic, hydrophobic or amphiphilic polymer, such as mercaptoacetic acid (MAA), mercaptosuccinic acid (MAS), thioglycolic acid (TGA), dihydrolipoic acid (DHLLA) and amphiphilic polymers like modified polyacrylic acid (APP) (Fig. 1.8A) and increase the QDs water solubility and compatibility for applications in biological systems (Maysinger et al., 2007). Furthermore, QDs can also be conjugated with biomolecules (e. g. peptides and oligonucleotides), antibodies and/or drugs for identification and action in specific biological targets (Smith et al., 2008; Rizvi et al., 2010) (Fig. 1.8A).

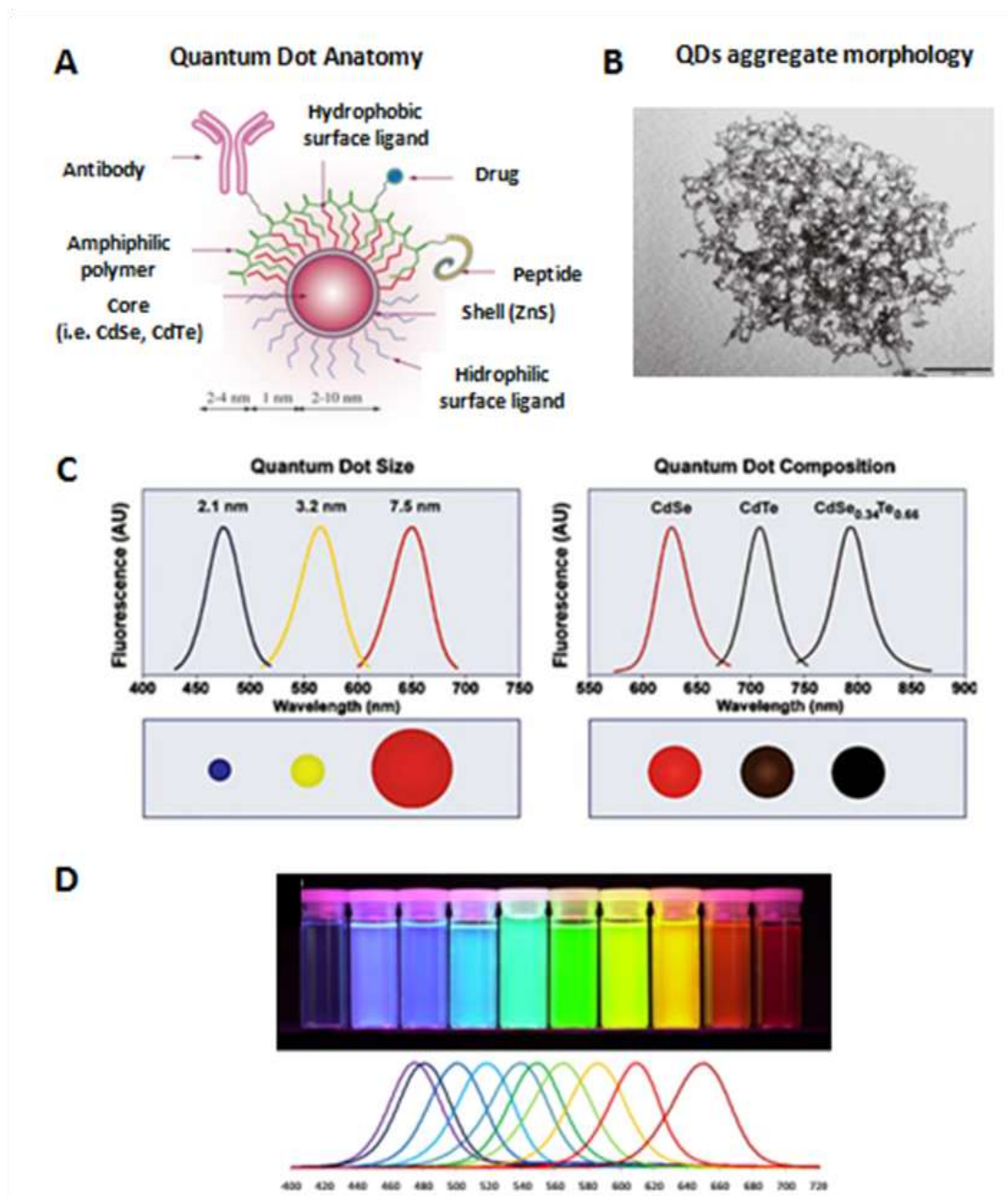


Figure 1.8. Anatomy and optical properties of quantum dots (QDs). **A.** Schematic anatomy of QDs referred as “core-shell-conjugate” (modified from Maysinger et al., 2007). **B.** Morphology of QDs aggregates in aqueous solution analyzed by transmission electron microscopy (TEM) (Rocha et al., 2014; Chapter 4). **C.** Fluorescence emission spectrum of QDs according to their size and composition (Smith and Gao, 2004). **D.** QDs fluorescence under UV light at different colours depending on their size (Zrazhevskiy and Gao, 2009).

1.6.3. Behaviour, transformation and fate of QDs in the aquatic environment

In the aquatic environment, different processes influence the behaviour and environmental fate of ENPs, such as surface coating changes (e. g. degradation and charge changes), homo- and hetero-aggregation/agglomeration, disaggregation/deagglomeration, diffusion, advection, oxidation, sulfidation, settling, bioturbation, resuspension, NOM stabilization, absorption with SPM, interaction with macromolecules and/or organisms and biological transformation (Fabrega et al., 2011; Sousa and Teixeira, 2013; Corsi et al., 2014; Dale et al., 2015). In this section, different processes that influence the behaviour and environmental fate of QDs are classified as proposed by Dwivedi et al. (2015) namely physicochemical transformation, macromolecular interaction and biologically mediated reactions (Fig. 1.9).

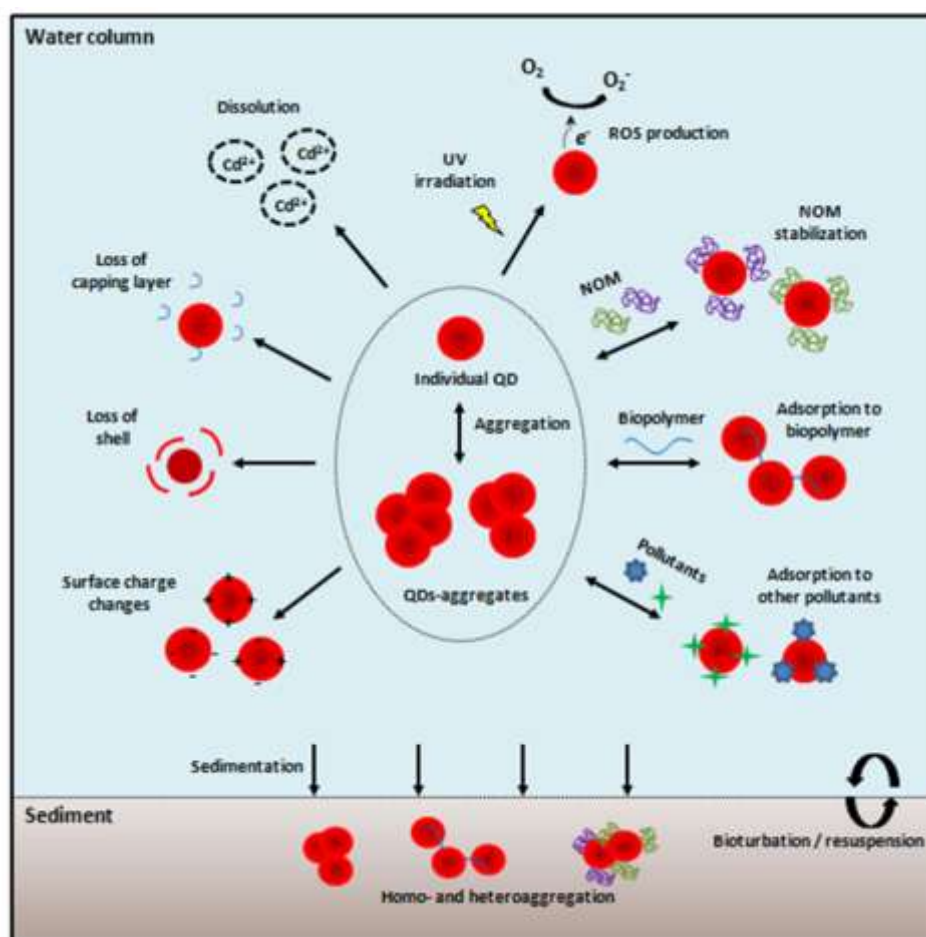


Figure 1.9. General scheme illustrating the behaviour and transformation of quantum dots (QDs) in the aquatic environment. Size and colour are not representative and should not be compared. NOM: natural organic matter (NOM); ROS: reactive oxygen species; UV radiation: ultraviolet radiation.

1.6.3.1. Physicochemical transformations

Abiotic characteristics of the surrounding media, such as ionic strength, pH, visible and ultraviolet electromagnetic radiation, promote different physicochemical transformations in the QD surface and change their behaviour and fate in the aquatic environment. The main physicochemical transformation of QDs in the aqueous medium is aggregation/agglomeration (Fig. 1.9), which can be classified as homo- or hetero-aggregation. QDs-homoaggregates are formed by the interaction between similar QDs, while the QDs-heteroaggregates are the result of the interaction between dissimilar QDs, macromolecules (e. g. NOM, SPM or biopolymers from the aquatic biota), other ENPs or pollutants. These processes depend on the collision frequency, attractive and repulsive forces at the QDs surface (e. g. van der Waals forces and electrostatic repulsion), as described by Derjaguin, Landau, Verwey and Overbeek (DLVO) theory (Grasso et al., 2002).

In seawater, QDs are highly aggregated and sediment more easily than in Milli-Q water (Morelli et al., 2012; Rocha et al., 2014; Chapter 4). For example, carboxyl-coated CdTe QDs (6 nm, 40 mg L⁻¹) form QDs-aggregates with negative surface charge in seawater (-9.37 ± 1.16 mV) and in Milli-Q water (-42.64 ± 0.55 mV) at pH 8.0, while the ionic strength changes the isoelectric point of QDs (z-potential is near to zero at pH 10-12 for seawater and at pH 1.7 for Milli-Q water) (Rocha et al., 2014; Chapter 4). Furthermore, there is a tendency of QDs to aggregate in different exposure medium, such as freshwater, seawater and culture medium (Tables 1.3 - 1.6) and indicate that further studies about the QDs behaviour in the soil/sediment and in environment relevant conditions (e. g. mesocosms) are need.

QDs are efficient energy donors and under ultraviolet or visible electromagnetic radiation can reduce O₂ and oxidize H₂O molecules to produce ROS, such as superoxide radical (O₂^{-•}) and hydroxyl radical (OH[•]) (Ipe et al., 2005; Ribeiro et al., 2012; Santana et al., 2015). The photo-induction of ROS produced by QDs is size dependent and not only promotes changes in the stability and dissolution of QDs, but is probably one source of toxicity of QDs, which can induce changes in antioxidant enzymes activities and oxidative damage in QDs-exposure organisms (Tables 1.3 - 1.6).

The QDs dissolution is dependent on nanoparticle type, coatings, ligands, concentration, size, aggregate state, presence of ligands and surrounding environment factors, such as pH and salinity (Domingos et al., 2011, 2013; Rocha et al., 2015b; Chapter 2). The surface charge and total surface area, more than size and chemical

composition of the core, has an important role in the QDs dissolution. In general, the increasing ionic strength induces higher aggregation/agglomeration of QDs, reduces their total surface area in contact with the surrounding environment, and consequently decreases their dissolution. Moreover, the presence of complexing ligands (e. g. citric acid, glycine and histidine) can also increase the QDs dissolution by chelating the dissolved metal and increasing the driving force for dissolution (Domingos et al., 2011, 2013).

1.6.3.2. Macromolecular interactions

The interaction, aggregation and stabilization of QDs with NOM, SPM and/or biopolymers are important process that interferes in the behaviour and fate of QDs. Both processes depend on QDs properties (e. g. size, composition, shell/capping layer and surface charge), abiotic parameters of medium and composition of NOM, SPM and biomolecules. For example, interaction between CdSe/ZnS QDs coated by carboxyl-polyethylene-glycol-(PEG) (2.1 nm, 20 nM) and linear alginate chains (5 or 50 mgC L⁻¹) induce high QDs aggregates (Slaveykova et al., 2009). On the other hand, there is no complexation between carboxyl-coated CdTe QDs (6 nm, 40 mg L⁻¹) and different NOM (humic acid, tannic acid and salicylic acid) at 2 - 10 mg C L⁻¹ pH 8, indicating that the ionizable carboxylic groups confers negative surface charge and repulsive forces between QDs surface and NOM (Rocha et al., 2015a) (Chapter 2). The interaction between QDs and biopolymers from algae (e. g. proteins and extracellular polymeric substances - EPS) indicated that the macromolecular interaction changes the bioavailability and toxicity of QDs (Zhang et al., 2012; Worms et al., 2012).

1.6.3.3. Biological mediated reactions

The biological production of CdS QDs by fungi cells was firstly described in two yeast species, *Schizosaccharomyces pombe* and *Candida glabrata*, as the interaction with phytochelatins and intracellular detoxification mechanism under sub-lethal metal concentrations (Dameron et al., 1989). Biosynthesis of metal sulfide NPs was optimized in other bacteria, fungi and yeast species (e. g. Williams et al., 1996; Duran and Seabra, 2012; Mala and Rose, 2014).

The uptake, toxicokinetics and biotransformation of QDs by organisms change their environmental fate. In the aquatic environment, under acidic conditions in the digestive system or inside to lysosomes from bivalve mollusc and fish species, there is a

potential of QDs dissolution and release of Cd^{2+} ions in the extra- and intercellular medium (Tables 1.3 - 1.6), promoting different exposure scenarios after interaction with organisms.

1.6.4. Ecotoxic effects of QDs at various trophic levels

Tables 1.3 - 1.6 show data about the ecotoxicity of QDs at various trophic levels, such as micro-organisms [bacteria (Table 1.3), algae, protozoa, rotifers and fungi (Table 1.4)], invertebrates (annelids, platyhelminths, nematodes and bivalves) (Table 1.5) and aquatic vertebrates (fish) (Table 1.6). More information on QDs ecotoxicity is available for freshwater species than for seawater ones. Similar discrepancies in the scientific production concerning the ecotoxicity of ENPs on marine organisms were also observed for TiO_2 NPs (Minetto et al., 2014), metal and metal oxide NPs (Baker et al., 2014) and other ENPs (Matranga and Corsi, 2012; Lapresta-Fernández et al., 2012), emphasizing the need of future studies about the nanoecotoxicity on estuarine and marine species, especially in sediment dwelling ones.

1.6.4.1. Micro-organisms

1.6.4.1.1. Bacteria

Bacteria are unicellular prokaryotic organisms with highly important role in the terrestrial and aquatic ecosystems and their responses can be an important tool to assess the environmental risk of ENPs (Lyon and Adams, 2006). In contrast to the uptake of uncoated QDs by endocytose in eukaryote cells, bacteria lack of endocytosis mechanisms cannot uptake uncoated QDs (Dwarakanath et al., 2004; Sweeney et al., 2004; Lai et al., 2013). On the other hand, the gram-negative bacteria *Escherichia coli* treated with Ca^{2+} showed increase in membrane permeability, likely through the holes in the membrane (50 - 300 nm in diameter), and develops competence to QDs (bacteria are capable of taking up QDs from their environment), which cannot enter cells normally due to their greater diameter (Wenhua et al., 2004). Other studies indicate that the functionalization of QDs with specific biomolecules allows its uptake by bacteria and subsequent detection on different fluorescence channels (Hirschey et al., 2006). QDs uptake was observed in *E. coli* and in gram-positive bacteria *Bacillus subtilis* exposed to adenosine monophosphate (AMP)-coated CdSe/ZnS QDs (3.6 - 6.5 nm; 10 - 40 nM; 5 h) (Kloepfer et al., 2005) and in *E. coli* exposed to different organic-acid-stabilized (citrate, isocitrate, succinate and malate) CdSe/CdS QDs (3.8 - 6 nm; 24 h)

(Hirschey et al., 2006). Given their size-dependent fluorescence and narrow-emission spectra, functionalized QDs can be used simultaneously for labelling and detection of different bacteria species, allowing studies of the bacterial community architecture and interactions between bacterial species (Yang and Li, 2006; Chalmers et al., 2007).

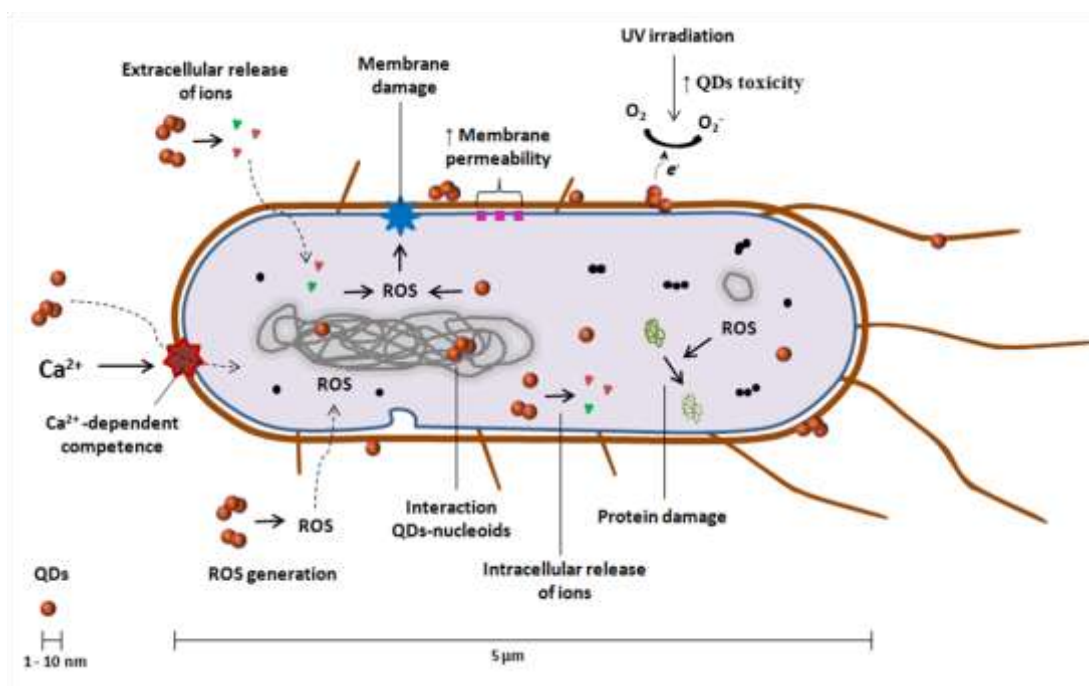


Figure 1.10. General scheme illustrating the mode of action (MoA) of quantum dots (QDs) in bacteria, using the gram-negative bacteria *E. coli* as model system. Size and colour are not represented and should not be compared. The mechanisms described are based on the revised data in Table 1.3. ROS: reactive oxygen species.

Despite its wide use for bacterial labeling and detection, the MoA of different QDs for prokaryotic cells remains unknown (Table 1.3; Fig. 1.10). QDs exposure can inhibit bacterial growth rate in a dose-dependent manner, while the UV irradiation dramatically increase its toxicity (Xiao et al., 2013). Generally, gram-positive strains are more vulnerable to exposure to QDs than the gram-negative ones and this differential toxicity is associated with electron transfer between QDs and gram positive strains (Dumas et al. 2010) (Table 1.3).

Antimicrobial activity of QDs was associated to binding on the bacterial surface, decrease in antioxidant response related genes encoding for endonuclease IV (*nfo*), manganese-superoxide dismutase (*sod A*) and glucose-6-phosphate dehydrogenase (*zwf*), changes in antioxidant enzyme activities (e. g. SOD and peroxidase), ROS

production and oxidative damage by protein carbonylation and LPO (Fig. 1.10, Table 1.3). In QDs-exposed bacteria, proteins were more sensitive to oxidative damage compared to lipids (Lu et al., 2008), while the genotoxicity of QDs was associated to its co-localization with nucleoids in *E. coli* exposed to CdSe/CdS QDs (3.8 - 6 nm; 24 h) (Hirschey et al., 2006) and to filamentation process in *B. subtilis* exposed to TGA-CdTe QDs (2.7 - 4.2 nm; 1 - 100 nM; 6.7 h) (Schneider et al., 2009).

1.6.4.1.2. Algae

Algae form the basis of the aquatic food web and knowledge on uptake, accumulation and toxicity of QDs in this primary producer is fundamental to assess their environmental effects at different trophic levels. The algae cell wall is the primary site for interaction with QDs and acts as barrier to prevent their uptake (Table 1.4). As the pore size of algae cell walls is around 5 - 20 nm in diameter and although individual QDs have between 2 and 10 nm in diameter, it is common that they aggregate/agglomerate in the aqueous medium and this behaviour affect their interaction and absorption by algae cells. Thus, as a result of the higher aggregation/agglomeration of QDs in seawater than in freshwater, QDs internalization by marine algae is potentially lower when compared to freshwater algae species (Table 1.4).

The interaction and adsorption of QDs on algae surface were observed in the freshwater microalgae *Chlamydomonas reinhardtii* exposed to carboxyl-coated CdSe/ZnS QDs (13 - 16 nm; 20 nmol L⁻¹; 1 h) (Worms et al., 2012), in *Chlamydomonas* sp. exposed to MPA-coated CdSe/ZnS QDs (5 - 9 nm; 0.05 - 5 ppm; 2 h) (Lin et al., 2009), in the marine green alga *Dunaliella tertiolecta* and in the marine diatom *Phaeodactylum tricornutum* exposed to CdSe/ZnS QDs encapsulated with the amphiphilic polymer poly(styrene-co-maleic anhydride) terminated with cumene (PSMA) and ethanolamine (8.5 nm; 0.5 - 2.5 nM ; 4 d) (Morelli et al., 2013). The interaction and effects of QDs depend on nano-specific properties, physicochemical characteristics of the exposure medium, composition and structure of cell walls and on the presence of molecules excreted by algae, such as proteins and EPS (Table 1.4). EPS excreted by algae modulate the interaction algae-QDs and affect the behaviour and stability of QDs (Zhang et al., 2012; Worms et al., 2012).

Table 1.3. Ecotoxicity of quantum dots (QDs) to bacteria.

Bacteria		QDs			Exposure conditions		Absorpt	Uptake	Detectio	Effects ^b	Ref.
Species	Strain	Core/ Shell	Capping layer ^a	Size (nm)	Concentration (μM)	Time (h)					
Gram-positive bacteria											
<i>Bacillus megaterium</i>	ATCC 14581	CdSe	MAA, WGA, transferin	-	0.25	8	x	-	-	-	Kloepfer et al., 2003
<i>Bacillus subtilis</i>	ATCC 9372	CdSe	MAA, WGA, transferin	-	0.25	8	x	-	x	-	Kloepfer et al., 2003
	Wild-type	CdSe, CdSe/ZnS	AMP, WGA	3.6 - 6.5	10 - 40 nM	5	x	x	x	↓growth	Kloepfer et al., 2005
	ATCC 31578	CdSe/ZnS	Carboxyl	18	10 - 1000 mg L ⁻¹	48	-	-	-	↓growth; weathered QDs toxicity > coated QDs toxicity	Mahendra et al., 2008
	ATCC23857	CdTe	Carboxyl	3.6	40 - 500 nM	0.5	x	-	-	↓fluorescence; EC _{50, 2.5h} : 11.1 ± 1 mM; electron transfer between QDs and gram+ bacteria; membrane depolarization	Dumas et al., 2010
	LMG 7135	CdTe	TGA	2.7 - 4.2	1 - 1000 nM	6.7	x	-	-	↓growth; filamentation; genotoxic effects	Schneider et al., 2009
<i>Micrococcus luteus</i>	ATCC 14581	CdSe	MAA, WGA, transferin	-	0.25	8 h	x	-	x	-	Kloepfer et al., 2003
<i>Staphylococcus aureus</i>	ATCC 29213	CdSe	MAA, WGA, transferin	-	0.25	8	x	-	x	-	Kloepfer et al., 2003
	Clinical isolate	CdTe	Carboxyl	3.6	40 - 500 nM	0.5	x	-	-	↓fluorescence; EC _{50, 2.5h} : 11.6 ± 1.1 mM; electron transfer between QDs and Gram+ bacteria; weak noncovalent interaction; membrane depolarization	Dumas et al., 2010
	CCTCC AB910393	CdSe, CdSe/ZnS	MAA, CA	2.77 - 2.93	1.1x10 ⁻⁷ - 4x10 ⁻⁶ M	12.5	x	-	-	↑growth (MAA-QDs); ↓growth (CA-QDs); UV irradiation ↑ toxicity.	Xiao et al., 2013
<i>Staphylococcus epidermidis</i>	ATCC 12228	CdSe	MAA, WGA, transferin	-	0.25	8	x	-	x	-	Kloepfer et al., 2003
<i>Staphylococcus saprophyticus</i>	ATCC 15305	CdSe	MAA, WGA, transferin	-	0.25	8	x	-	x	-	Kloepfer et al., 2003
<i>Staphylococcus warneri</i>	ATCC 17917	CdSe	MAA, WGA, transferin	-	0.25	8	x	-	x	-	Kloepfer et al., 2003

<i>Streptococcus gordonii</i>	DL1	-	Antibody	10 - 20	10 - 30 nM	0.4	x	-	x	-	Chalmer s et al., 2007
<i>Streptococcus mutans</i>	ATCC 700610	-	Antibody	10 - 20	10 - 30 nM	0.4	x	-	x	QD-based immunofluorescence not affected by EPS in biofilm; simultaneous detection of <i>S. mutans</i> and <i>Veillonella</i> <i>spp.</i>	Chalmer s et al., 2007
Gram-negative bacteria											
<i>Cupriavidus metallidurans</i>	CH34, AE104	CdTe	TGA	2.7 - 4.2	1 - 10 nM	5	x	-	-	↓growth; = effects between resistant and sensitive strains	Schneide r et al., 2009
<i>Escherichia coli</i>	ATCC 25922	CdSe	MAA, WGA, transferin	-	0.25 µM	8 h	x	-	-	-	Kloepfer et al., 2003
	ATCC 25922, ATCC 23804	CdSe, CdSe/ZnS	AMP, WGA	3.6 - 6.5	10 - 40 nM	5	x	x	-	↓growth; toxicity in <i>E. coli</i> < than in <i>B. subtilis</i> ; QDs elimination	Kloepfer et al., 2005
	O111:B 4	CdSe/ZnS , CdSe/ZnS	Antibody, aptamer, amine, carboxyl	4.3, 6.3	-	1	x	-	x	↓fluorescence	Dwaraka nath et al., 2004
	HB101	CdSe/CdS	SAA	3 - 4	-	0.75	x	x	x	Ca ²⁺ -induced competence results in QDs uptake	Wenhua et al., 2004
	K12 wild- type, XL10	CdSe/CdS	Citrate, isocitrate, succinate, malate	3.8 - 6	-	24	x	x	x	interaction between QDs and nucleoids; potential genotoxic effects	Hirschey et al., 2006
	ATCC 43888	CdTe/ZnS	Antibody, streptavidin	10 x 20	10 nM	0.67	x	-	x	simultaneous detection of <i>E. coli</i> and <i>S. Typhimurium</i>	Yang and Li, 2006
	O111:B 4	CdSe/ZnS , CdSe/ZnS	Antibody, aptamer, amine, carboxyl	-	4 - 200 µg mL ⁻¹	0.5	x	-	-	↓CFU; antibody-QDs toxicity > unconjugated QDs toxicity	Dwaraka nath et al., 2007
	ATCC 29181	CdTe	MAS	-	40 - 200 nM	12	x	-	x	↓CFU; ↑ROS in culture medium; ↓gene expression (<i>nfo</i> , <i>sod</i> <i>A</i> , <i>zwf</i>); ↓SOD; ↓peroxidase; ↑LPO; ↑protein carbonyl	Lu et al. 2008
	ATCC 25404	CdSe/ZnS	Carboxyl	18	10 - 1000 mg L ⁻¹	48	x	-	-	↓growth; toxicity in <i>E. coli</i> > than in <i>P. aeruginosa</i>	Mahendr a et al., 2008
	MG165 5	CdTe	TGA, GSH, CdO	2.7 - 4.2	1 - 100 nM	6.7	x	-	-	↓growth; UV irradiation ↑toxicity; CdO-QDs more toxic	Schneide r et al., 2009

	ATCC 11775	CdTe	Carboxyl	3.6	4 - 100 nM	0.5	x	-	-	↓fluorescence; EC _{50, 2.5h} : 21.2 ± 1 mM; no electron transfer between QDs and Gram- bacteria; noncovalent interaction	Dumas et al., 2010
	HB101	CdTe	MPA	-	4x10 ⁻⁸ , 12x10 ⁻⁸ mol L ⁻¹	120	x	-	-	↓growth; ↓viability; IC ₅₀ : 7.4x10 ⁻⁸ to 8.8x10 ⁻⁸ ; protein conformational changes; outer membrane damage; small QDs more toxic than bigger ones; QDs toxicity > Cd ²⁺ toxicity	Fang et al., 2012
	ATCC25922	CdTe	MPA, NAC, GSH	4	0.1 - 3.2	10	x	-	x	↓growth; ↓membrane fluidity; ↑membrane permeability; toxicity order: MPA-QDs > GSH-QDs > NAC-QDs.	Lai et al., 2013
	CCTCC AB91112	CdSe, CdSe/ZnS	MAA, CA	2.77 - 2.93	1.1x10 ⁻⁷ - 4x10 ⁻⁶ mol L ⁻¹	12.5	x	-	-	↓growth; UV irradiation ↑ toxicity; MAA-CdSe toxicity > MAA-CdSe/ZnS toxicity	Xiao et al., 2013
<i>Pseudomonas aeruginosa</i>	ATCC 10145U	CdSe	MAA, WGA, transferin	-	0.25	8	x	-	-	-	Kloepfer et al., 2003
	-	CdSe/ZnS	Carboxyl	18	10 - 1000 mg L ⁻¹	48	x	-	-	↓growth	Slaveykova et al., 2009
	ATCCBAA-47	CdTe	Carboxyl	3.6	40 - 500 nM	0.5	x	-	-	↓fluorescence; EC _{50, 2.5h} : 17.4 ± 1.1 mM; no electron transfer between QDs and Gram- bacteria	Dumas et al., 2010
<i>Salmonella typhimurium</i>	ATCC 14028	CdTe/ZnS	Antibody, streptavidin	10 x 20	10 nM	40 min	x	-	x	simultaneous detection of <i>S. Typhimurium</i> and <i>E. coli</i>	Yang and Li, 2006
<i>Salmonella enterica</i>	-	CdSe/ZnS	Antibody, amine, carboxyl	-	10, 25 µg	48	x	-	-	antibody-QDs toxicity > unconjugated QDs	Dwarakath et al., 2007
<i>Shewanella oneidensis</i>	MR-1A	CdTe	TGA	2.7 - 4.2	1 - 1000 nM	6.7	x	-	-	↓growth	Schneider et al., 2009
<i>Veillonella spp.</i>	R1	-	Antibody	10 - 20	10 - 30 nM	0.4	x	-	x	simultaneous detection of <i>S. mutans</i> and <i>Veillonella spp.</i>	Chalmers et al., 2007

^a Adenosine monophosphate (AMP); cysteamine (CA); glutathione (GSH); mercaptoacetic acid (MAA); mercaptopropionic acid (MPA); mercaptosuccinic acid (MAS); n-acetyl-L-cysteine (NAC); sulfhydryl acetic acid (SAA); thioglycolic acid (TGA); wheat germ agglutinin (WGA).

^b Colony-forming units (CFUs); extracellular polymeric substances (EPS); glutathione (GSH); half maximal effective concentration (EC₅₀); half maximal inhibitory concentration (IC₅₀); lipid peroxidation (LPO); reactive oxygen species (ROS); superoxide dismutase (SOD).

QDs can induce different effects on algae, such as growth rate inhibition (Wang et al., 2008), decrease in the photosynthetic activity (Lin et al., 2009), changes in antioxidant system by alteration in gene expression (e. g. *sod1*, *gpx*, *cat*) (Wang et al., 2008; Morelli et al., 2015) and/or enzyme activities (e. g. SOD and CAT activities) (Morelli et al., 2012, 2013), induction of oxidative damage (LPO) and changes in proteomic profile (Morelli et al., 2015, 2016a,b) (Table 1.4).

The trophic transfer of QDs from the algae to primary consumers was detected for freshwater and marine species (Table 1.4). The transfer of carboxyl-CdSe QDs occurred from the freshwater algae *Pseudokirchneriella subcapitata* to the daphnia *Ceriodaphnia dubia* (10 - 25 nm; 32.2 - 330 $\mu\text{g L}^{-1}$; 48 - 96 h) (Bouldin et al., 2008), while the transfer of carboxyl-CdSe/ZnS QDs was reported from the marine algae *Isochrysis galbana* to the amphipod *Leptocheirus plumulosus* (15 - 20 nm; 3.6 mg L^{-1} ; 96 h) (Jackson et al., 2012).

1.6.4.1.3. Protozoa

Protozoa are unicellular eukaryotic organisms abundant in the aquatic environment and represent valuable model for assessment of trophic transfer of QDs (Werlin et al., 2011; Xiao et al., 2012; Lee and An, 2014). Studies about the QDs ecotoxicity using protozoa exist only for two species, the ciliated protozoa *Tetrahymena thermophila* and the flagellate protozoa *Astasia longa* (Table 1.4).

QDs uptake by protozoa cells is mediated principally by endocytotic and phagocytotic pathways (Werlin et al., 2011; Lee and An, 2014). However, a potential alternative QDs uptake pathway was suggested in *T. thermophila* exposed to carboxyl-coated CdSe/ZnS QDs (12 nm; 0.625 - 10 nM, 24 h) (Mortimer et al., 2014). Accumulation, trophic transfer and biomagnification of QDs were reported in protozoa (Table 1.4). Citrate-coated CdSe QDs (5 nm; 75 mg L^{-1} ; 16 h) was accumulated in the bacteria *P. aeruginosa* and was transferred and biomagnified in *T. thermophila* with a high trophic transfer factor (TTF = ~5.4) when compared to dissolved Cd (TTF = 3.5) (Werlin et al., 2011). This biomagnification of QDs in the protozoa was related to elevated phagocytosis rate and inhibition of the bacteria digestion by QDs (Werlin et al., 2011). A three-level trophic transfer of carboxyl-coated CdSe/ZnS QDs (4.6 nm, 5 nM) was assessed in the protozoa *A. longa*, the cladoceran *Moina macrocopa* and the fish *Danio rerio*, but no biomagnification was observed (BMF = 0.01 L g^{-1}) (Lee and An, 2014).

1.6.4.1.4. Fungi

Fungi were also used as a model eukaryotic organism for analysis of the QDs toxicity (Table 1.4). QDs can interact and adsorb on the fungi cell surface and induce different toxic effects, such as decrease in the growth rate and cell viability, changes in EPS layer, cell wall damage (i. e. decrease in the thickness and density of cell wall) and changes in mitochondrial membrane potential (Manikandan and Wu, 2013; Mei et al., 2014). However, no consensus exist about the MoA and differential toxicity of QDs compared to dissolved Cd (Table 1.4), probably due to the higher diversity of QDs type, shells/capping layer, culture medium and exposure conditions. Similar toxic mechanism of n-acetylcysteine (NAC)-coated CdTe QDs and dissolved Cd was observed in *S. cerevisiae* (4.1 - 5.8 nm; 4.9 - 209.4 nmol L⁻¹; 12 h) (Han et al., 2012), while the *S. cerevisiae* response to CdS QDs (5 nm; 40 - 100 mg L⁻¹; 72 h) was associated to nano-specific effects on gene expression changes (abiotic stress response, metabolic processes, mitochondrial organization, transport and DNA repair) (Marmiroli et al., 2015).

Table 1.4. Ecotoxicity of quantum dots (QDs) to different micro-organisms (algae, protozoa, rotifera and fungi).

Species	QDs		Exposure conditions			Accu- mula- tion	Effects ^b	Ref.
	Core/ Shell	Capping layer ^a	Size (nm)	Concentration (nM)	Time (h)			
Algae								
<i>Chlamydomon- as reinhardtii</i>	CdTe	TGA	3.5 - 4.5	0.01 - 100 mg L ⁻¹	72	-	↓growth; EC ₅₀ = 5 mg L ⁻¹ ; ↑LPO; ↑gene expression (<i>sod1</i> , <i>gpx</i> , <i>cat</i> , <i>ptox2</i>); QDs toxicity > n-TiO ₂ toxicity	Wang et al., 2008
	CdTe/CdS	Carboxyl	4.2 - 5.7	2x10 ⁻⁷ - 4x10 ⁻⁶ M	0.4 - 0.5	x	Intracellular QDs dissolution; ↑gene expression (transmembrane activity, proteolysis, ubiquitin-mediated processes)	Domingo s et al., 2011
	CdSe/ZnS QDs	Carboxyl-	13 - 16	20	1	-	co-exposure (QDs + Pb; QDs + Cu): adsorption on surface; ↑intracellular Pb and Cu levels	Worms et al., 2012
<i>Chlamydomon- as sp.</i>	CdSe/ZnS	MUA	5 - 9	0.05-5 ppm	2	-	absorption only on surface; ↓QDs fluorescence; ↓O ₂ production; ↓CO ₂ depletion;	Lin et al., 2009
<i>Chlorella kesslerii</i>	CdSe/ZnS	Carboxyl- PEG	2.1	20	1	-	↓QDs fluorescence	Slaveyko va and Startchev, 2009
	CdSe/ZnS	Carboxyl	13 - 16	20	1	-	co-exposure (QDs + Pb; QDs + Cu): ↓intracellular Pb and Cu levels; absorption on surface	Worms et al., 2012
<i>Dunaliella tertiolecta</i>	CdSe/ZnS	APP	8.5	0.5 - 2.5	96	-	adsorption only on surface; ↑growth; no oxidative stress	Morelli et al., 2013
<i>Phaeodactylum tricornutum</i>	CdSe, CdSe/ZnS	-	3.2, 3.5	20 - 480	5 - 72	-	CdSe QDs: ↑phytochelatins. CdSe/ZnS QDs: ↓growth rate; ↑ROS; ↑SOD; ↑CAT	Morelli et al., 2012
	CdSe/ZnS	APP	8.5	0.5 - 2.5	96	-	adsorption only on surface; ↓growth; ↑SOD; ↑CAT; ↑ROS; ↑LPO	Morelli et al., 2013
	CdSe/ZnS	APP	8.5	0.5 - 2.5	12 d	-	↑glutathione; ↑PC; ↑gene expression (<i>hsp101</i> , <i>cat</i> , <i>gsr2</i>); no change in <i>vit1</i> ; proteomic profile changes	Morelli et al., 2015
	CdSe/ZnS	APP	8.5	2.5	4 – 8 d	-	Proteomic profile changes	Scebba et al., 2016
<i>Pseudokirchne- riella subcapitata</i>	CdSe	Carboxyl	10 - 25	32.2 - 330 µg L ⁻¹	48, 96	x	LC _{50,96h} = 37.1 ppb; trophic transfer (algae to daphnids); change in algae shape	Bouldin et al., 2008
<i>Thalassiosira pseudonana</i>	CdSe/ZnS	Amine, carboxyl	20 - 25	18.5, 10.1	0.5 - 5	-	no effects on growth; ↑extracellular protein production; QDs aggregation with EPS	Zhang et al., 2013

Protozoa								
<i>Astasia longa</i>	CdSe/ZnS	Carboxyl	4.6	5	48	x	three-level trophic transfer (protozoa - cladoceran - fish); no growth inhibition; BCF = 0.01 L.g ⁻¹	Lee and An, 2014
<i>Tetrahymena thermophila</i>	CdSe	Citrate	5	75 mg L ⁻¹	16	x	trophic transfer (bacteria - protozoa); biomagnification (TTF = ~5.4); ↑protein carbonylation; ↓digestion	Werlin et al., 2011
	CdSe; CdSe/ZnS	MAA, BSA, HSA, PEG, nucleotide	2.77, 2.93	0.14 - 9.04 µM	100	x	↓growth; IC ₅₀ : CdSe QDs = 1.14 x 10 ⁻⁶ mol L ⁻¹ ; CdSe/ZnS QDs = 1.33 x 10 ⁻⁶ mol.L ⁻¹ ; cell morphology changes; QDs toxicity depend on surface ligands	Xiao et al., 2012
	CdSe/ZnS	Carboxyl	12	0.625 - 10	E: 24; D: 24	x	no effects on growth; uptake by alternative endocytotic pathways; QDs elimination as large extracellular agglomerates; no completely elimination (24 h)	Mortimer et al., 2014
Fungi								
<i>Candida utilis</i>	CdS	-	1 - 7	10 - 30 mg L ⁻¹	27	-	↓growth; QDs interact with EPS; ↓EPS layer; ↑number of protein peaks	Manikandan and Wu, 2013
<i>Kluyveromyces bulgaricus</i>	CdTe	TGA-Man, Gal, Glu	2.5 - 2.9	-	0.25	x	labelling with galactose-TGA QDs	Coulon et al. 2010
<i>Penicillium chrysogenum</i>	CdSe	MAA, WGA, transferin	-	0.25 µM	8	-	labelling with both QDs; ↓survival	Kloepfer et al., 2003
<i>Saccharomyces cerevisiae</i>	CdTe	TGA-Man, Gal, Glu	2.5 - 2.9	-	0.25	x	labelling with mannose-TGA QDs	Coulon et al. 2010
	CdTe	NAC	4.1, 5.8	4.9 - 209.4 nM	12	x	↓growth; toxicity: larger QDs (IC ₅₀ = 17.07 nmol L ⁻¹) > smaller QDs (IC ₅₀ = 80.81 nmol L ⁻¹); ↓cell viability; morphologic changes; nuclear localization; ↓QDs fluorescence; similar toxic mechanism of QDs and dissolved Cd	Han et al., 2012
	CdS	-	1 - 7	10 - 30 mg L ⁻¹	27	-	↓growth; QDs interact with EPS; ↓EPS layer; ↑number of protein peaks	Manikandan and Wu, 2013
	CdS	-	5	40 - 100 mg L ⁻¹	72	-	↓growth; 112 sensitivity and 114 tolerance phenotypes; sensitivity to QDs not related to the release of dissolved Cd; genes response related to QDs toxicity: abiotic stress response, metabolic processes, mitochondrial organization, transport and DNA repair; role of stress oxidative	Marmioli et al., 2015
<i>Schizosaccharo</i>	CdSe	MAA,	-	0.25 µM	8	-	no labelling	Kloepfer et al., 2003

<i>myces pombe</i>	WGA, transferin						adsorption on cell surface; CdSe: ↓growth; ↓cell viability; ↓thickness and density of cell wall; ↓mitochondrial membrane potential; ↓QDs fluorescence; ZnS and EDTA ↓QDs toxicity; toxicity: CdSe (IC ₅₀ = 304 nM) > CdSe/ZnS	Mei et al., 2014
	CdSe; CdSe/ZnS	OPA	4	33 - 1319.5 nM	0.5 - 24	-		

^a Amphiphilic polymer poly(styrene-co-maleic anhydride) (APP); bovine serum albumin (BSA); human serum albumin (HSA); mercaptoacetic acid (MAA); mercaptoundecanoic acid (MUA); methoxy-polyethylene glycol (PEG); thioglycolic acid (TGA); wheat germ agglutinin (WGA).

^b Bioconcentration factor (BCF); catalase (CAT); ethylenediaminetetraacetic acid (EDTA); extracellular polymeric substances (EPS); half maximal effective concentration (EC₅₀); half maximal inhibitory concentration (IC₅₀); lipid peroxidation (LPO); phytochelatins (PC); reactive oxygen species (ROS); superoxide dismutase (SOD); trophic transfer factor (TTF).

1.6.4.2. Invertebrates

1.6.4.2.1. Annelida and platyhelminths

Sediment dwelling species are particularly vulnerable to ENPs, especially due to agglomeration/aggregation and precipitation of ENPs from the water column into the sediments. In this context, accumulation and toxicity of QDs in the *Hediste diversicolor* depend on the type of QDs and the route of exposure (waterborne, sediment or dietary) (Table 1.5). *H. diversicolor* after waterborne exposure to CdS QDs showed higher Cd accumulation, oxidative stress and behavioural impairments when compared to dietary exposure (5 - 10 nm; 10 $\mu\text{g L}^{-1}$; 14 d) and to its dissolved counterpart (Buffet et al., 2014; Saez et al., 2014). The immunotoxic and genotoxic effects of QDs were also investigated in *H. diversicolor* coelomocytes, which were more sensitive cells when compared to those from the terrestrial worm *Eisenia fetida* after intracoelomic injection of TOPO-DOPC/DOTAU-coated CdSe/ZnS QDs for 2 h (5.9 nm; 0.001 - 1 ng g^{-1} tissue weight) (Saez et al., 2014). However, despite the growing concern over the potential impact of ENPs in benthic species, there is no ecotoxicological information available for polychaete exposed to QDs-contaminated sediments and future works are required to understand the trophic transfer of QDs from polychaetes to higher trophic levels (Table 1.5).

1.6.4.2.2. Nematoda

In vivo imaging of *Caenorhabditis elegans* exposed to QDs contributed to the understanding of their tissue- and cell-specific distribution in invertebrate organisms (Table 1.5). QDs are principally distributed into the digestive lumen of the *C. elegans* during feeding, but these ENPs can also attach to the pharyngeal inter surface, what is followed by their localization into lysosomes (Qu et al., 2011). Although the body surface of a nematode (cuticle) is in direct contact with the environment, no QDs internalization by dermal route in *C. elegans* occurred (Table 1.5). Probably the presence of negative glycoproteins layer in the cuticle of *C. elegans* (Gonzalez-Moragas et al., 2015) provides a barrier against interaction and internalization of QDs, especially via electrostatic interactions. QDs can be transferred from the digestive system to gonads and motor neurons, indicating potential reproductive and neurotoxic effects (Qu et al., 2011; Zhao et al., 2015), while the anal and vulvar pathway was indicated as mainly routes for elimination/excretion of QDs in *C. elegans*.

Autophagy was described as a defensive strategy to clear and recycle QDs-damaged organelles in *C. elegans* exposed to CdTe and CdTe/CdS/ZnS QDs (6.1 - 6.7 nm; 1×10^{-5} mol L⁻¹; 3 h - 15 d) (Zhou et al., 2015). In addition, the mechanism of QDs-induced neurotoxicity on RME motor neurons was reported for *C. elegans* exposed to CdTe QDs and CdTe/ZnS QDs (3.6 - 4; 0.1 - 1 µg L⁻¹; 3.5 d) (Zhao et al., 2015), indicating that the long-term exposure to QDs induce neurotoxic effects on the development and function of motor neurons in nematodes. In both studies, QDs toxicity was not related to QDs dissolution and release of dissolved Cd, while the ZnS shell reduced their toxicity (Zhao et al., 2015; Zhou et al., 2015).

C. elegans has also been used as a model to assess the multigenerational effects of QDs, especially due to its short life cycle (3 days) and lifespan (2 - 3 weeks). Contreras et al. (2013) investigated the multigenerational acclimation and tolerance in *C. elegans* exposed to CdTe and CdTe/ZnS QDs (3.4 - 4.1; 10 - 300 mg L⁻¹; 72 h). Uncoated CdTe QDs exposure induced similar acute effects on *C. elegans* fitness compared to dissolved Cd exposure, such as decrease in lifespan and brood size, while no CdTe/ZnS effects were observed (Contreras et al., 2013), indicating their usefulness in regulatory tests for screening the ENPs toxicity.

1.6.4.2.3. Bivalvia

Bivalve molluscs have been considered as a target group of the ENMs toxicity (Canesi et al., 2012, 2016; Rocha et al., 2015a) and have higher capacity to accumulate different QDs from the water column (Table 1.4.). Toxic effects of Cd-based QDs on cell-mediated immunity and gills functions were associated with extra- and intracellular release of dissolved Cd and oxidative stress in *M. galloprovincialis* cells (hemocytes and gills) after *in vitro* exposure to CdS QDs (5 nm; 10^{-4} to 10^2 mgCd L⁻¹; 24 h) (Katsumiti et al., 2014). Genotoxic effects (DNA damage) induced by Cd-based QDs were observed in *M. edulis* hemocytes after *in vitro* exposure to MPEG-SH coated CdS (4 nm; 0.001 - 10 mg L⁻¹; 4 h) (Munari et al., 2014), indicating that the use of *in vitro* approaches provide a suitable tool for the screening of QDs toxicity.

Changes in the antioxidant capacity, oxidative stress and behaviour impairments were also observed in the marine clam *S. plana* after *in vivo* exposure to CdS QDs (5 - 6 nm; 10 µgCd L⁻¹; 14 d), indicating that CAT and GST are the most sensitive biomarkers in response to CdS QDs (Buffet et al., 2014a). Similar QDs-related oxidative stress were reported in freshwater species, wherein immunosuppressive and inflammatory

effects were associated to ROS production, oxidative stress and DNA damage, while distinct MT responses and LPO levels were observed in the gills and digestive gland in the freshwater mussel *E. complanata* exposed to CdTe QDs (1.6 - 8 mg L⁻¹; 24 h) (Gagné et al., 2008a; Peyrot et al., 2009).

1.6.4.3. Aquatic vertebrates

1.6.4.3.1. Fish

Fish was used to assess QDs toxicity with three different approaches: embryotoxicity assessment; adult fish exposed to QDs via waterborne and dietary exposure or via intraperitoneal injection; *in vitro* cytotoxicity assessment (Fig. 1.11 A-C). Among the fish species, the zebrafish *D. rerio* is a model species, followed by the rainbow trout *Oncorhynchus mykiss*. The early development stages (embryos and larvae) of *D. rerio* are more susceptible to QDs toxicity when compared to mature stage (King-Heiden et al., 2009; Zhang et al., 2012a, b; Zolotarev et al., 2012; Zhang et al., 2013). On the other hand, the zebrafish liver (ZFL) cell line was used to study the MoA of QDs and its dissolved counterpart (Table 1.6; Fig 1.11 A-C).

The endocytosis is the main route for QDs uptake by fish cells (Table 1.6), such as observed for other ENPs (Handy et al., 2008; Shaw and Handy, 2011). QDs and its degradation products are taken up via diet or through the gills epithelium, being distributed and accumulated in different organs, such as intestine, liver and muscle. Intestine was reported as the major organ for QDs localization in adult *D. rerio* fed with zooplankton contaminated with poly(acrylic acid)-octylamine copolymer (PAA)-coated CdSe/ZnS QDs (10 QDs-artemia fish⁻¹; 14 d) (Lewinski et al., 2011), in embryos exposed to glutathione (GSH)-cysteine-coated CdTe QDs (18.1 nm; 35 - 185 µM; 7 d) (Duan et al., 2013) and in estuarine fish *Fundulus heteroclitus* exposed to lecithin-coated CdSe/ZnS QDs (1 - 10 µg d⁻¹; 85 d) (Blickley et al., 2014). The lower tissue distribution of QDs in *D. rerio* after dietary exposure was associated to its small chemical degradation due to the lack of a stomach and no acid phase digestion in this species (Lewinski et al., 2011). On the other hand, gradual Si/SiO₂ QDs accumulation was observed by fluorescence microscopy in the liver and muscle of freshwater carp *Carassius auratus gibelio* after intraperitoneal injection (5 nm; 2 mg Kg⁻¹; 7 d) (Stanca et al., 2012, 2013).

Table 1.5. Ecotoxicity of quantum dots (QDs) to different invertebrates (crustacean, annelid, platyhelminths, nematode and bivalve).

Species	QDs			Exposure conditions		Cell/ tissue ^b	Accumulation	Effects ^c	Ref.
	Core/ Shell	Capping layer ^a	Size (nm)	Concentration (nM)	Time (h)				
Crustaceans									
<i>Leptocheirus plumulosus</i>	CdSe/ZnS	Carboxyl	15 - 20	3.6 mg L ⁻¹	96	O	x	trophic transfer (algae - crustacean); biomagnification; mortality: dietary exposure > waterborne exposure	Jackson et al., 2012
<i>Ceriodaphnia dubia</i>	CdSe	Carboxyl	10 - 25	32.2 - 330 µg L ⁻¹	48, 96	O	x	trophic transfer (algae - daphnids); LC _{50,96h} > 110 ppb	Bouldin et al., 2008
<i>Moina macrocopa</i>	CdSe/ZnS	Carboxyl	4.6	5	48	O	x	three-level trophic transfer (protozoa - cladoceran - fish); BAF = 2.9	Lee and An, 2014
Annelida									
<i>Eisenia fetida</i>	CdSe/ZnS	TOPO-DOPC/DO TAU	5.9	0.001 - 1 ng g ⁻¹ w.	2	Co	-	no mortality; ↑DNA damage (QDs < dissolved Cd); <i>E. fetida</i> less sensitive than <i>H. diversicolor</i> ; no change in SOD and LPO	Saez et al., 2014
<i>Hediste diversicolor</i>	CdS	-	5 - 10	10 µg L ⁻¹	14	O	x	↑Cd accumulation (QDs > dissolved Cd; waterborne exposure > dietary exposure); ↑CAT; ↑GST; ↑CAS-3; ↓body undulation; no changes in the LPO, SOD, LDH and AChE	Buffet et al., 2014
	CdSe/ZnS	TOPO-DOPC/DO TAU	5.9	0.001 - 1 ng g ⁻¹ w.	2	Co	-	↑DNA damage (QDs > dissolved Cd); <i>H. diversicolor</i> more sensitive than <i>E. fetida</i> ; ↑SOD; ↑LPO (QDs > dissolved Cd)	Saez et al., 2014
Platyhelminths									
<i>Mesostoma lingua</i>	CdSe/ZnS	TOPO-DOPC/DO TAU	8.69 - 9.96	0.25 - 1000 µg L ⁻¹	96	O	x	QDs accumulation in cytoplasm, nucleus and organelles; QDs transfer from adult to offspring	De Jong et al., 2013
Nematoda									
<i>Caenorhabditis elegans</i>	CdTe	BSA	-	6.5 x 10 ⁻⁴ M	12	O	x	labelling with CdTe QDs and BSA-coated CdTe QDs	Hui-lian et al., 2006
	CdSe/ZnS	MPA,	5 - 6	20 - 200	72	O	x	QDs accumulation in digestive lumen and reproductive system;	Qu et al., 2011

, CdTe	MEA		nM				elimination <i>via</i> anus and vulva; co-localization with lysosomes; changes in Ca and K distribution; no effects in self-fertilization and male mating; ↓body length; ↓brood size; toxicity: (+)QDs > (-)QDs; shell ↓QDs toxicity	
CdSe/ZnS	MSA	5.8	0.01 - 1 μM	6 d	O	x	no mortality; no changes in body length; ↑egg production; ↑embryonic mortality; ↑egg-laying defect; ↓life span; disruption of motor neurons during the reproductive process	Hsu et al., 2012
CdSe, CdSe/ZnS	PMAO- PEG	3.4 - 4.1	10 - 300 mg L ⁻¹	72	O	x	QDs distribution: digestive lumen; ↑Cd levels (CdSe > CdSe/ZnS); ↓life span; ↓brood size; shell ↓QDs toxicity; no multigenerational effects	Contreras et al., 2013
CdTe, CdTe/ZnS	MPA	3.6 - 4	0.1 - 1 μg L ⁻¹	3.5 d	O	x	QDs transfer from intestinal barrier and accumulation in RMEs motor neurons; neurotoxicity; ↑abnormal foraging behavior; ↑gene expression (Mn-SOD, <i>unc-30</i>); shell ↓neurotoxicity; toxicity not related to dissolved Cd	Zhao et al., 2015
CdTe, CdTe/CdS /ZnS	MPA	6.1 - 6.7	1 x 10 ⁻⁵ M	3 h - 15 d	O	x	Autophagy induced by endocytosis disorder; ↑autophagosome number; ↑autophagy related gene (<i>lgg-1</i> ; <i>bec-1</i> ; <i>atg-18</i>); QDs-induced autophagy not related to dissolved Cd; no QDs degradation by autophagosome; autophagy is a defensive strategy to clear and recycle QDs-damaged organelles	Zhou et al., 2015

Bivalvia

<i>Mytilus galloprovincialis</i>	CdSe/ZnS	PEG	12 x 6	0.48 nM	E: 24; D: 72	C, DG, H	x	↑Cd accumulation (DG > H); depuration period: ↓Cd levels in H	Hull et al., 2013
	CdS	GSH	5	10 ⁻⁴ - 10 ² mg L ⁻¹	24	G*, H*	x	↓cell viability; ↑ROS; ↑DNA damage; ↑AcP; ↑MXR transport; ↑phagocytosis; no changes on cytoskeleton; cytotoxicity: dissolved Cd > QDs > bulk CdS	Katsumiti et al., 2014a
	CdTe	Carboxyl	6	10 μg L ⁻¹	14 d	H, O	x	↑DNA damage; ↓LMS; changes types of hemocytes; no cytogenotoxicity	Rocha et al., 2014
	CdTe	Carboxyl	6	10 μg L ⁻¹	E: 21 d; D: 50 d	G, DG, H	x	↑Cd accumulation (DG > G > H); no QDs aggregation with NOM; t _{1/2} > 50 d	Rocha et al., 2015a
<i>Mytilus edulis</i>	CdS	MPEG-SH	4	0.01 - 10 mg L ⁻¹	4	H*	-	QDs and MPEG-SH: ↑DNA damage at 10 mg.L ⁻¹	Munari et al., 2014
	CdTe/ CdS	Carboxyl	1 - 10	0.05 - 2.7	21	H*	-	toxicity: QDs > bulk; small QDs ↓phagocytosis while larger ones ↑	Bruneau et al., 2013
<i>Elliptio</i>	CdTe/	Carboxyl	1 -	0.05 - 2.7	21	H*	-	toxicity: larger QDs > smaller ones; ↓cell viability	Bruneau et al.,

<i>complanata</i>	CdS		10	$\mu\text{g L}^{-1}$						2013	
	CdTe	-	-	1.6 - 8 mg L^{-1}	24	DG, G, H	x	↓phagocytosis; ↓cell viability; ↑oxidative stress; ↑DNA damage; LPO: ↑G and ↓DG			Gagné et al., 2008
	CdTe	-	-	1.6 - 8 mg L^{-1}	24	DG, G, Go, H	x	↑Cd accumulation (G > DG); MT: ↑DG and ↓G			Peyrot et al., 2009

^a 1,2-DiOleoyl-sn-glycéro-3-PhosphoCholine (DOPC); 2-mercaptoethylamine (MEA); amphiphilic copolymer poly(maleic anhydride- alt-1-octadecene (PMAO); Glutathione (GSH); mercaptopropionic acid (MPA); mercaptosuccinic acid (MSA); methoxy-polyethylene glycol (PEG); methyl polyethylene glycol (MPEG); N-[5'-(2',3'-DiOleoyl) Uridine]-N',N',N'-TriméthylAmmon ium Tosylate (DOTAU); bovine serum albumin (BSA); tri-n-octylphosphine (TOPO).

^b All organism (O); carcass (C); digestive gland (DG); gill (G); hemocyte (H).

^c Acetylcholinesterase (AChE); acid phosphatase (AcP); bioaccumulation factor (BAF); caspase (CAS); catalase (CAT); Glutathione-S-transferase (GST); half-life time ($t_{1/2}$); lactate dehydrogenase (LDH); lysosomal membrane stability (LMS); median lethal concentration (LC_{50}); metallothionein (MT); multixenobiotic resistance (MXR); natural organic matter (NOM); reactive oxygen species (ROS); superoxide dismutase (SOD).

Studies on the metabolism and mode of action of QDs in fish species are limited and no consensus exist about the comparative toxicity between QDs and its dissolved counterpart (Table 1.6). QDs can induce changes in gene expression and in antioxidant enzyme activities (e. g. SOD, CAT, GPx, GR) and promote ROS generation and oxidative damage, such as LPO and protein oxidation (Stanca et al., 2012, 2013; Tang et al., 2013a, b), changes in vitellogenin (VTG) profile (HongCheng et al., 2009; Blickley et al., 2014; Petushkova et al., 2015) and induction of immunotoxic and genotoxic effects in fish species (Gagné et al., 2008, 2010; Sanders et al., 2008; Tang et al., 2013a). Similar gene expression pattern was observed in *D. rerio* hepatocytes after *in vitro* exposure to MPA-coated CdTe QDs (3.4 nm) and dissolved Cd, while differential response was identified for MPA-coated CdSe/ZnS (3.4 - 4.4 nm) and MPA-coated InP/ZnS (3 nm) QDs when compared to dissolved Cd (50 - 500 nM; 24 h) (Tang et al., 2013a,b), confirming that the shells/capping layer and particle size alter the cytotoxicity of QDs (King-Heiden et al., 2009). Furthermore, the maternal transfer of QDs or its degradation products was reported in *F. heteroclitus* after dietary exposure to lecithin-coated CdSe/ZnS QDs (1 and 10 $\mu\text{g d}^{-1}$; 85 d) (Blickley et al., 2014), indicating the potential risk to progeny through maternal transfer and/or possible endocrine disrupting effects. Limited data about QDs toxicity is available for estuarine, seawater and neotropical fish species (Table 1.6), indicating that the impact of QDs in these species deserve further attention.

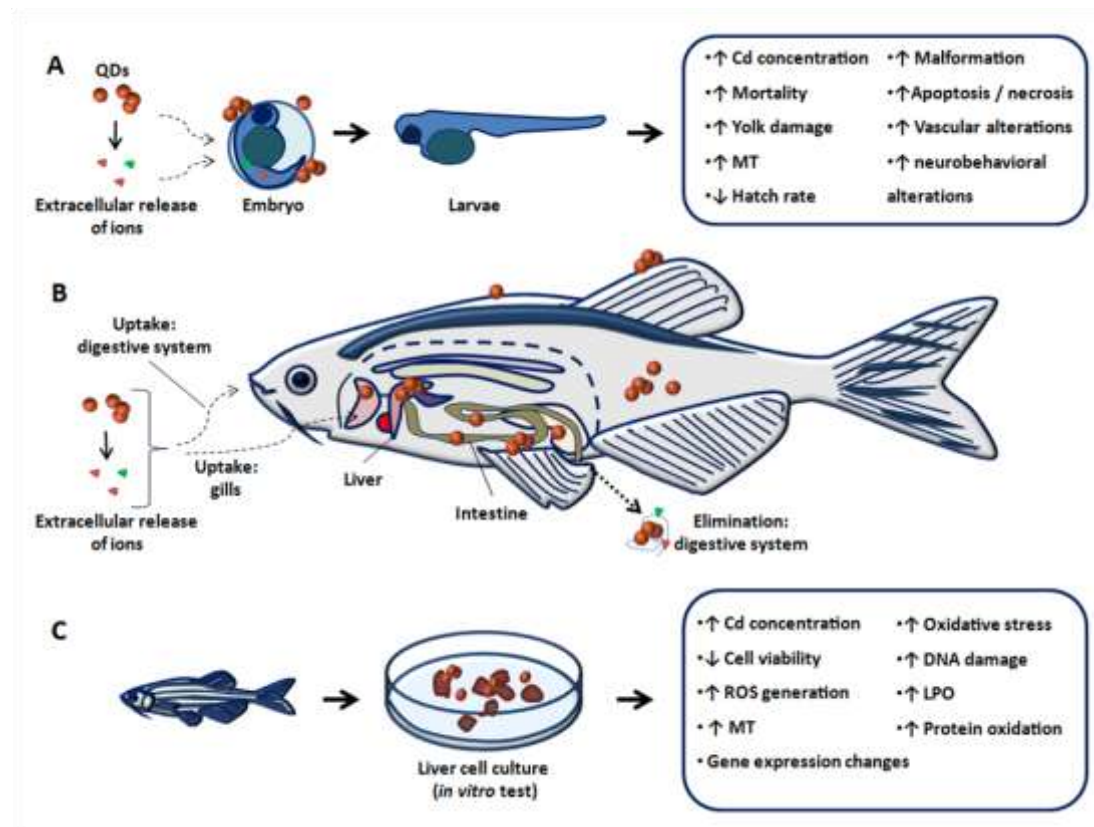


Figure 1.11. Representative scheme of different approaches used to study the toxicity of quantum dots (QDs) in fish species, using zebrafish *D. rerio* as model system. Embryotoxicity assessment (A); adult fish exposed to QDs via waterborne and dietary exposure or via intraperitoneal injection (B); *in vitro* cytotoxicity assessment (C). Size and colour are not representative and should not be compared. The scheme is based on the revised data present work Table 1.6. LPO: lipid peroxidation; MT: metallothionein; ROS: reactive oxygen species.

Table 1.6. Ecotoxicity of quantum dots (QDs) to different fish species.

Fish species	QDs		Exposure conditions			Cell/tissue ^b	Accumulation	Effects ^c	Ref.
	Core/Shell	Capping layer ^a	Size (nm)	Concentration (nM)	Time (h)				
<i>Carassius gibelio</i>	Si/SiO ₂	-	5	2 mg Kg ⁻¹	7 d	M	x	↑SOD; ↑CAT; ↑GR; ↑GSH; ↑protein oxidation; ↓protein thiol; ↑G6PDH; ↑LPO; ↑tissue damage	Stanca et al., 2012
	Si/SiO ₂	-	5	2 mg Kg ⁻¹	7 d	L	x	↑SOD; ↑CAT; ↑GPx; ↓GST; ↓GSH; ↓protein thiol; ↓G6PDH; ↑LPO; ↑protein oxidation; no protein carbonylation; ↑tissue damage	Stanca et al., 2013
<i>Danio rerio</i>	CdSe/ZnS	PLL, PEG-thiol, PEG-carboxylate, PEG-methoxy, PEG-amine	-	0.2 - 200 μM	120	E	x	↑mortality; LC _{50, 120h} = 7 - 42 μM; ↑necrosis; ↑yolk damage; ↑malformed tail; ↑MT	King-Heiden et al., 2009
	CdSe/ZnS	PAA	-	10 QDs-artemia fish ⁻¹	E: 14 d; D: 7 d	L, I, C	I	no mortality; no growth inhibition; no biomagnification (BMF < 1); t _{1/2} = 26 - 38 h	Lewinski et al., 2011
	CdSe	MPA	3.5	0.05 - 31.25 mg L ⁻¹	6 - 120	E, La	-	LC _{50, 120 hpf} = 1.98 mg.L ⁻¹ ; ↓hatch rate; ↑malformation; ↑apoptosis; ↑abnormal vascular; ↑neurobehavioral alterations	Zhang et al., 2012a
	CdTe	TGA	3.5	1 - 400	6 - 120	E, La	-	LC _{50, 120 hpf} = 185.9 nM; ↓hatch rate; ↓body length; ↓heart beat; ↑malformation; ↑abnormal vascular; ↓reduce swimming speed	Zhang et al., 2012b
	CdSe/CdS/ZnS	SSDAPA	18.1	35, 185 μM	7 d	E, La	-	no embryotoxicity; ↓larvae survival; LC _{50, 120h} = 7 - 42 μM	Zolotarev et al., 2012
	CdTe	GSH-cysteine	4	2.5 - 20	144	O, I	I	↑mortality; ↓hatching rate; ↓heart rate; embryonic malformations; ↓swimming; larval behavior changes	Duan et al., 2013
	CdTe	MPA	3.4	50 - 500	24	H*	x	↓cell viability; IC _{50, 24h} = 465.8 nM; ↑ROS; ↑DNA damage; similar gene expression changes by dissolved Cd and QDs (↓p53; ↑sod-1; ↑oggl; ↑xpc, ↑xpa); no effect in NER	Tang et al., 2013a
	CdSe/Zn; CdTe;	MPA	3 - 4.4	5 - 3000	24	H*	x	↓cell viability; toxicity order: CdTe > InP/ZnS > CdSe/ZnS; small QDs more toxic than larger ones; similar gene expression change by dissolved Cd and CdTe QDs (↑mt1; ↑mt2; ↑mtf-1; dmt-1; zip-1);	Tang et al., 2013b

InP/ZnS		different response to CdSe/ZnS or InP/ZnS QDs							
	CdTe	TGA	3.5	6 mg L ⁻¹	6 - 120	E, La	-	co-exposure (QDs + Cu ²⁺): ↑mortality; ↑vascular damage; ↑malformation; synergy effects	Zhang et al., 2013
	CdSe/ZnS	Carboxyl	4.6	5	48	O	x	three-level trophic transfer (protozoa - cladoceran - fish); no toxic effects; no biomagnification in fish (BMF = 0.1)	Lee and An, 2014
	CdSe/ZnS	DHLA	9.5	2 µM	48	E	-	changes in the VTG profile; no embryotoxicity	Petushkova et al., 2015
<i>Fundulus heteroclitus</i>	CdSe/ZnS	Lecithin	-	1, 10 µg d ⁻¹	85 d	L, I, Eg	x	↑VTG (male); ↓fecundity; no changes in GSH, LPO or in expression genes (<i>β-actin</i> , <i>mt</i> , <i>gstmu</i> , <i>gpx</i> , <i>sod1</i> , <i>sod2</i> , <i>vtg</i>); gender specific response; maternal transfer	Blinckley et al., 2014
<i>Gasterosteus aculeatus</i>	CdS	MPEG	4.2	5 - 500 µg L ⁻¹	21 d	Li, O	x	↓male reproductive fitness; ↓male building nests; ↑hepatocellular nuclear pleomorphism; no change in VTG and GSH/GSSG	Sanders et al., 2008
<i>Misgurnus anguillicaudatus</i>	CdTe/ZnS	PEG, TGA	-	35 µg Kg ⁻¹	7	K, L, P, T, B	x	co-exposure (QDs + E2); QDs ↓VTG induced by E2; no morphological damage in the testes; t _{1/2} > 7 d; no changes in GSH and SOD	HongCheng et al., 2009
<i>Oncorhynchus mykiss</i>	CdTe	Cysteamine	-	0.4 - 250 µg.mL ⁻¹	48	H*	x	↓cell viability; ↑MT; ↑DNA damage; ↑HSP70; ↓LPO	Gagné et al., 2008
	CdS/CdTe	Carboxyl	-	1 - 6 µg L ⁻¹	96	H, K*	-	↓leukocyte counts; ↓cell viability; ↑phagocytosis; ↑gene expression (<i>mt</i> , <i>cp2k1</i>); 25 specific genes related to immune endpoints	Gagné et al., 2010
	CdTe/CdS	Carboxyl	1 - 10	0 - 2.7 µg mL ⁻¹	21	Ly, Ma*	-	↓cell viability; no changes in phagocytosis; ↓lymphoblastic transformation	Bruneau et al., 2013a
	CdTe/CdS	Sodium polyacrylate	1 - 10	0 - 2.7 µg mL ⁻¹	21	Ly, Ma*	-	↓cell viability; larger aggregates ↑ phagocytosis while no effect in smaller ones	Bruneau et al., 2013b

^a Dihydrolipoic acid (DHLA); glutathione (GSH); mercaptopropionic acid (MPA); methoxy-polyethylene glycol (PEG); methyl polyethylene glycol (MPEG); poly(acrylic acid)-octylamine copolymer (PAA); poly-L-lysine (PLL); S,S-dihydrolipoic acid/polyacrylic acid (SSDAPA); thioglycolic acid (TGA).

^b All organism (O); bone (B); carcass (C); eggs (Eg); embryo (E); hepatocyte (H); intestine (I); *in vitro* test (*); kidney (K); larvae (La); liver (L); lymphocytes (Ly); macrophage (Ma); muscle (M); plasma (P); testes (T).

^c 17 β -estradiol (E2); biomagnification factor (BMF); catalase (CAT); glucose 6-phosphate dehydrogenase (G6PDH); glutathione (GSH); glutathione peroxidase (GPx); Glutathione reductase (GR); glutathione-S-transferase (GST); half maximal inhibitory concentration (IC₅₀); half-life time ($t_{1/2}$); heat-sensitive proteins (HSP); lipid peroxidation (LPO); metallothionein (MT); nucleotide excision repair (NER); oxidized glutathione (GSSH); reactive oxygen species (ROS); superoxide dismutase (SOD); vitellogenin (VTG).

1.6.5. Trophic transfer and biomagnification

Trophic transfer and biomagnification of QDs were assessed in experiments with reconstructed trophic chains, where living organisms were exposed to QDs and then used as food to other species of a next trophic level (Fig. 1.12). In freshwater, two-level trophic transfer of QDs was observed from the bacteria (*E. coli*) to the protozoan (*Tetrahymena pyriformis*) (TTF = ~5.4) (Werlin et al. 2011); from the algae (*P. subcapitata*) to the daphnia (*C. dubia*) (Bouldin et al., 2008); from the zooplankton (*D. magna* and *Artemia franciscana*) to the fish (*D. rerio*) (BMF = 0.04 and 0.004 for adult and juvenile zebrafish) (Lewinski et al., 2011). Three-level trophic transfer of QDs was observed from the freshwater protozoa (*Astasia longa*) to the zooplankton (*Moina macrocopa*) and to the fish (*D. rerio*) (BMF = 0.1) (Lee and An, 2014). In seawater, two-level trophic transfer of QDs was reported from the marine algae (*I. galbana*) to the marine amphipod (*L. plumulosus*) (Jackson et al. 2012) (Fig. 1.12). Despite the QDs accumulation and trophic transfer reported, limited biomagnification was confirmed, since generally the biomagnification factor (BMF) was less than 1 (BMF < 1). Furthermore, no data is available from environmentally relevant approaches, such as multispecies exposures, mesocosms and systems with tidal cycles (Tables 1.3 - 1.6).

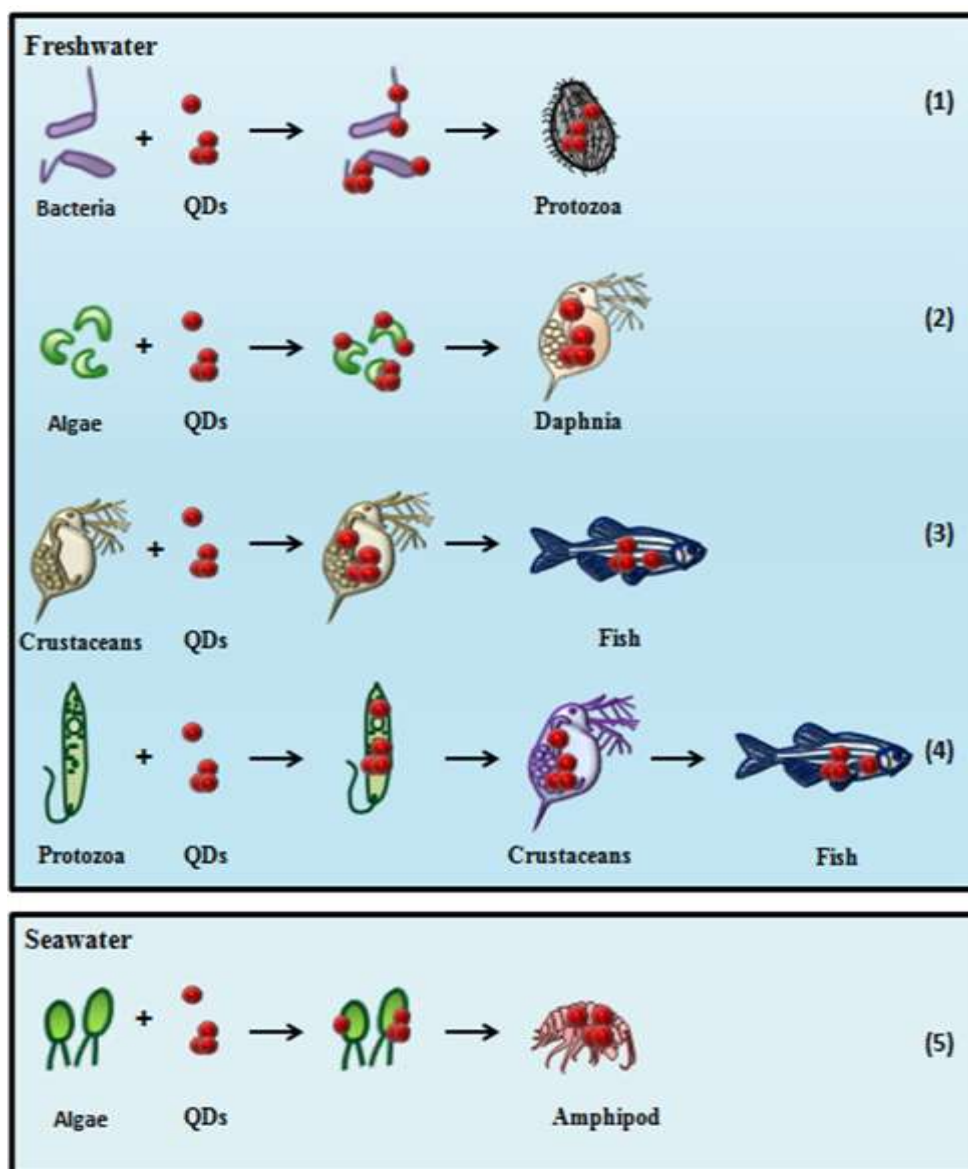


Figure 1.12. Scheme illustrating the trophic transfer of quantum dots (QDs). In freshwater, two-level trophic transfer of QDs was reported from the bacteria (*E. coli*) to the protozoan (*T. pyriformis*) (Werlin et al. 2011) (1), from the algae (*P. subcapitata*) to the daphnia (*C. dubia*) (Bouldin et al., 2008) (2) and from the zooplankton (*D. magna* and *A. franciscana*) to the fish (*D. rerio*) (Lewinski et al., 2011) (3). In freshwater, three-level trophic transfer of QDs was observed from protozoa (*A. longa*) to zooplankton (*M. macrocopa*) to fish (*D. rerio*) (Lee and An, 2014) (4). In seawater, trophic transfer of QDs was observed from the algae (*I. galbana*) to the amphipod (*L. plumulosus*) (Jackson et al. 2012) (5). Size and colour are not representative and should not be compared.

1.7. Objectives and outline

The aquatic environment represents the ultimate sink for ENMs, which will potentially affect the environment quality and human health. Although the marine mussel *Mytilus* spp. is the most utilized marine organism to assess the ecotoxic effects of ENMs in the marine environment, the knowledge regarding potential hazardous effects of Cd-based QDs on mussels *M. galloprovincialis* after *in vivo* exposure remains scarce. The behaviour and fate of QDs in the marine environment and their MoA and toxicity in biomonitor species must be clarified to be able to develop ecotoxicological tools suitable for a better environmental assessment of ENMs and development of sustainable nanotechnologies. Accordingly, the main objective of this thesis was to assess the toxicokinetics, MoA and toxicity of CdTe QDs in the marine mussel *M. galloprovincialis* using a multibiomarker approach associated with differential protein expression and compared with their effects to dissolved Cd. To achieve this purpose, this thesis is divided in eight Chapters outlined as follows:

Chapter 1. The first part of this Chapter reviews the data available from the literature on behaviour and fate of different ENM types in the aquatic environment and their ecotoxicological impact in marine and freshwater bivalve species. The toxicokinetics (TK), tissue and subcellular distribution, and MoA (oxidative stress, genotoxicity, immunotoxicity, behavioural changes, neurotoxicity, embryotoxicity and changes in protein expression) of different ENMs in bivalve species are discussed. The second part of this Chapter reviews the data regarding properties and applications of QDs, their behaviour, transformation and fate in the aquatic environment and their ecotoxicity at various trophic levels (micro-organisms, invertebrates and fish).

Chapter 2. The aim of this Chapter was to address the bioavailability, uptake, tissue distribution, accumulation and elimination kinetics in the mussel *M. galloprovincialis* exposed to CdTe QDs and their dissolved counterpart at the same concentration ($10 \mu\text{gCd L}^{-1}$) for 21 days (accumulation period) followed by a 50 days depuration period. The condition index was determined, accumulation and depuration models and TK parameters were estimated to predict and understand the TK of QDs in different

tissues of *M. galloprovincialis*. In this Chapter, QDs are characterized in terms of individual size, hydrodynamic diameter, surface charge, NOM stabilization, dissolution and Cd speciation in seawater because the behaviour, fate and ecotoxicity of QDs are dependent on their primary characteristics and components of the surrounding environment.

Chapter 3. The Cd subcellular partitioning in different tissues (gills and digestive gland) of the marine mussel *M. galloprovincialis* exposed to CdTe QDs and their dissolved counterpart during a 21 days exposure period followed by a 50 days depuration period was analyzed in this Chapter. Furthermore, the relationships between Cd subcellular partitioning, metallothioneins (MTs) response and oxidative damage (lipid peroxidation - LPO) in mussels exposed to both Cd forms were examined to identify potential subcellular targets and which subcellular fraction was more important in the accumulation, metabolism and detoxification of Cd-based QDs.

Chapter 4. The potential immunocytotoxic, cytogenotoxic and genotoxic effects of CdTe QDs on *M. galloprovincialis* hemocytes were analysed and compared to their dissolved counterpart after exposure for 14 days. Immunocytotoxicity was evaluated in terms of hemocyte density, cell viability, lysosomal membrane stability (LMS) and differential cell counts (DCC) of circulating hemocytes, while cytogenotoxicity and genotoxicity were analyzed by the micronucleus (MN) test and nuclear abnormalities (chromosomal damage) and comet assay (DNA damage). In this Chapter, QDs were characterized in terms of shape, individual size, optical properties, hydrodynamic diameter, surface charge, aggregation kinetics, polydispersity index and sedimentation rate in seawater.

Chapter 5. In this Chapter, the antioxidant response in different tissues (gills and digestive gland) of mussels *M. galloprovincialis* exposed to CdTe QDs and dissolved Cd for 14 days was investigated. The antioxidant capacity was analyzed in terms of activities of antioxidant enzymes, such as superoxide dismutase (SOD), catalase (CAT), glutathione-S-transferase (GST), total glutathione peroxidase (total GPx), Se-

independent GPx (Se-I GPx) and Se-dependent (Se-D GPx) along with Cd accumulation in both tissues. Furthermore, the tissue specific toxicity of CdTe QDs was compared to their dissolved counterpart.

Chapter 6. Different tissue-level biomarkers were measured in the digestive gland of mussels *M. galloprovincialis* to assess histopathological alterations and inflammatory responses induced by CdTe QDs, in comparison with its dissolved counterpart during 14 days of exposure. The histopathological assessment was performed by evaluating the epithelium and tubular lumen modification of digestive tubules (histomorphometry) and semi-quantitative histopathological condition indices, while inflammatory responses were analyzed through microscopy examination of infiltrates and haemocytic aggregates, followed by classification of inflammatory response.

Chapter 7. Protein expression profiles were analyzed in the digestive gland of mussels *M. galloprovincialis* exposed to CdTe QDs for 14 days, in comparison with their dissolved counterpart. The differential protein expression was performed by 2D-PAGE associated to image analysis in order to identify putative/new biomarkers of Cd-based QDs exposure.

Chapter 8. Finally, this last Chapter includes the general discussion of the results obtained in the previous Chapters, wherein overall conclusions were summarized and future research proposed.

1.7.1. General structure of thesis

The analytical techniques used for the characterization of QDs are summarized in Fig. 1.13, while methodological approaches for assessment of the MoA and toxicity of QDs in mussels *M. galloprovincialis* are summarized in the Fig. 1.14.

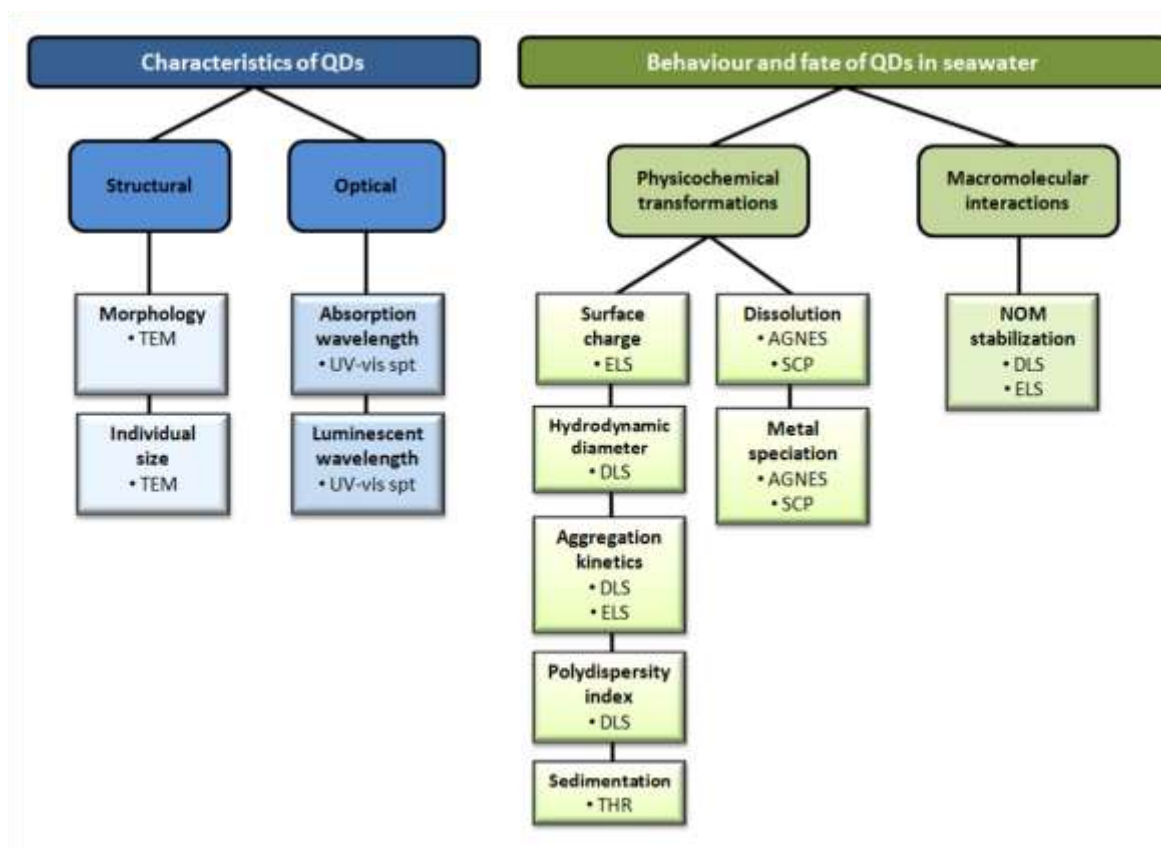


Figure 1.13. Analytical techniques used for characterization of CdTe QDs. AGNES: Absence of Gradients and Nernstian Equilibrium Stripping; DLS: Dynamic Light Scattering; ELS: Electrophoretic Light Scattering; SCP: Stripping Chronopotentiometry; TEM: Transmission Electron Microscopy; THR: Turbidimeter of high resolution.

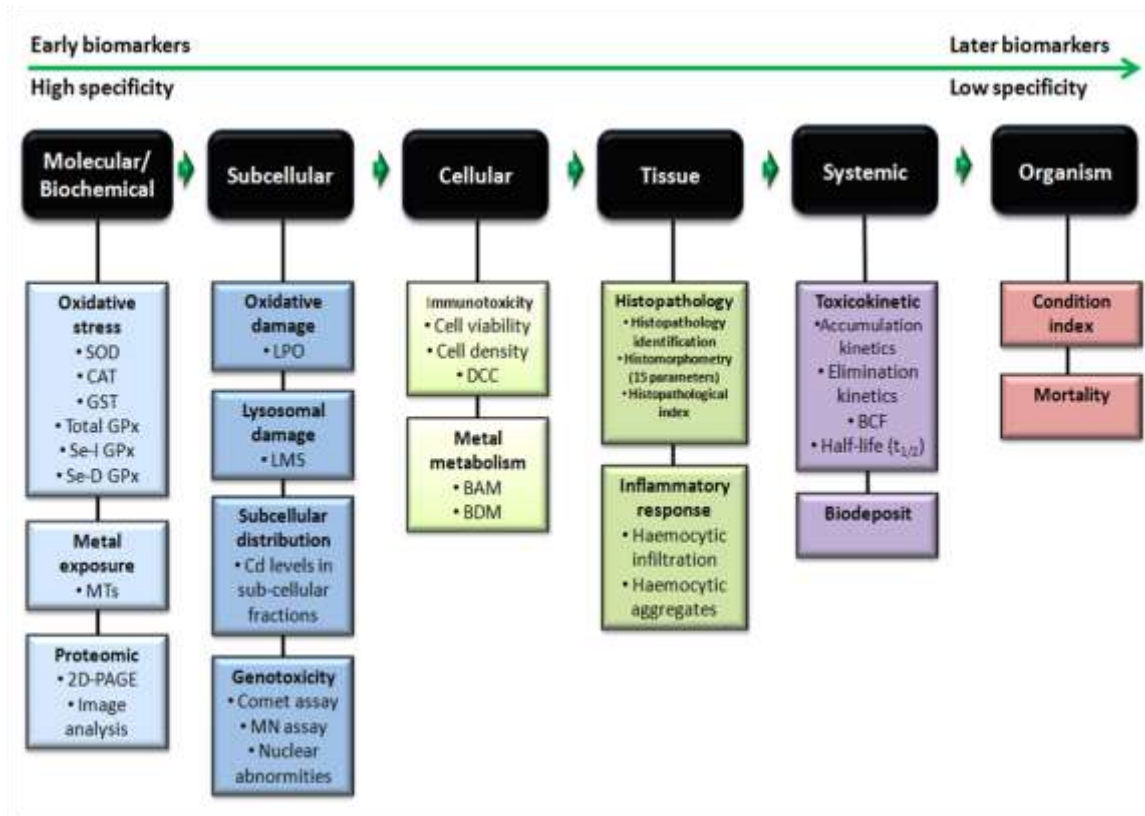


Figure 1.14. Multibiomarker approaches used for assess the MoA and toxicity of QDs in the marine mussel *M. galloprovincialis*. 2D-PAGE: two-dimensional gel electrophoresis; BAM: biologically active metal; BCF: bioconcentration factor; BDM: biologically detoxified metal; CAT: catalase, DCC: differential cell counts; GST: glutathione-S-transferase; LPO: lipid peroxidation; MN: micronucleus; MTs: metallothioneins; Se-D GPx: Se-dependent; Se-I GPx: Se-independent GPx; SOD: superoxide dismutase; $t_{1/2}$: half-life time; total GPx: total glutathione peroxidase.

1.7.2. Selected model-system: *Mytilus galloprovincialis*

In this thesis, the marine mussel *M. galloprovincialis* (Lamarck, 1819) (Fig. 1.16), commonly known as “mediterranean mussel” or “blue mussel”, was selected as model-system to assess the MoA and toxicity of CdTe QDs. Bivalve molluscs were recognized as a unique target group for nanoparticle toxicity and represent the most used group in nanoecotoxicological studies (Canesi et al., 2012; 2016). Among the bivalves, mussels and genus *Mytilus* is the main group and taxa studied, respectively, wherein the *M. galloprovincialis* is the most studied species (Table 1.1; reviewed in Rocha et al., 2015a). The genus *Mytilus* has been used worldwide in several

biomonitoring programs (e. g. “Mussel Watch Programs”) and in ecotoxicological studies (Viarengo and Canesi, 1991; Bolognesi et al., 2004; Cravo et al., 2009; Dagnino et al., 2007; Marigómez et al., 2013).

The mussel *M. galloprovincialis* is an economically valuable species, used in aquaculture in several countries, mainly in coastal waters from some southern Mediterranean countries, Galicia (Spain), Russian Federation, Ukraine, South Africa and China. In 2013, the worldwide annual aquaculture production of *M. galloprovincialis* was estimated to be around 116 574 tonnes (FAO, 2016). This species is native to the Mediterranean coast and the Black and Adriatic Seas, but was classified as one of 100 of the “World’s Worst” invaders by the global invasive species database (GISD, 2012), especially due to their high tolerance to air exposure and faster growth than other native species. It is a filter feeder that feed mainly on phytoplankton and organic matter and when the size is 5 cm in length can filter 5 L of seawater *per* hour. It lives attached to substrates (rocks and piers) by byssal threads, which are secreted by the foot, and have external fertilization and gonochoristic reproduction, where males and females spawn simultaneously and fertilised eggs developing into free swimming larvae (Bayne, 1976; Picker & Griffiths 2011; FAO, 2012).

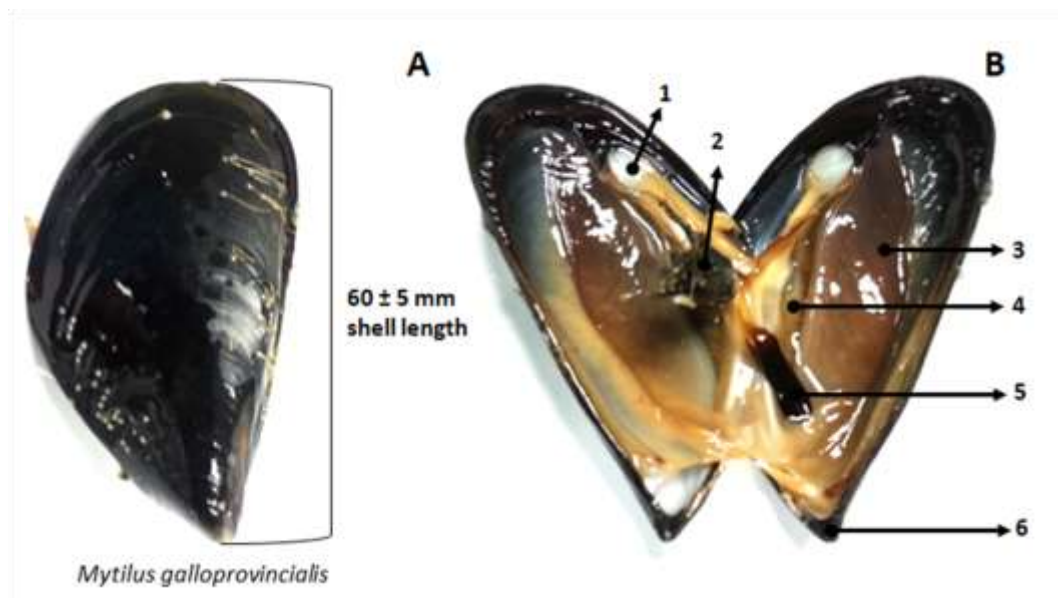


Figure 1.15. The marine mussel *Mytilus galloprovincialis* used in this study. **A.** The shell as seen from the right site. **B.** The internal structure of mussels: posterior retractor muscle (1), byssus (2), gills (3), digestive gland (4), foot (5) and shell (6).

In this study, specimens of mussels *M. galloprovincialis* (60 ± 5 mm shell length) were collected in the Ria Formosa Lagoon, Southeast of Portugal ($37^{\circ}06'59.4''\text{N}$, $7^{\circ}37'45.0''\text{W}$) (Figure 1.14).

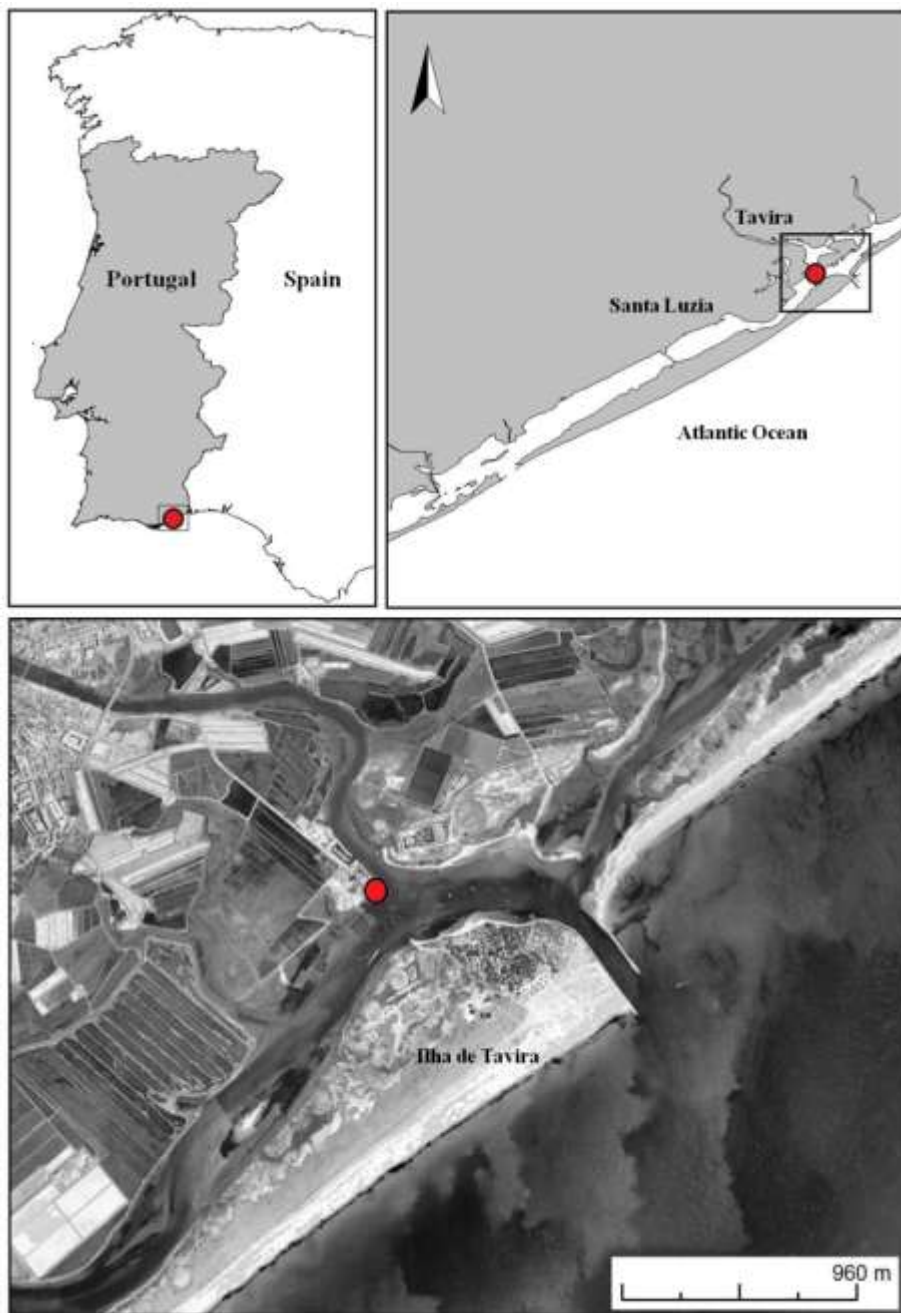
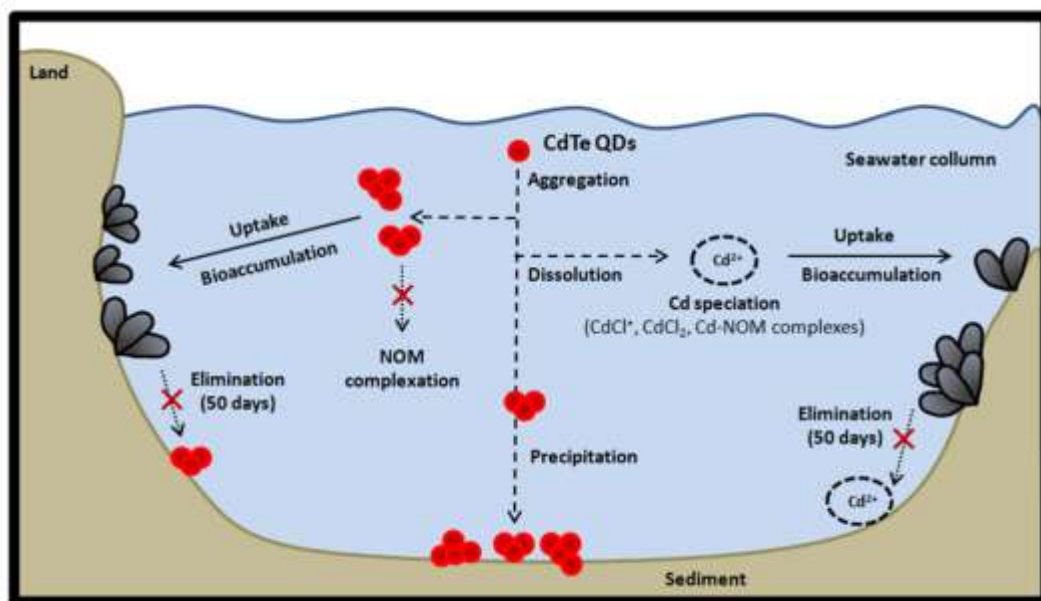


Figure 1.16. Map showing the collection site (red circle), located in the Ria Formosa Lagoon, Southeast of Portugal ($37^{\circ}06'59.4''\text{N}$, $7^{\circ}37'45.0''\text{W}$).

CHAPTER II

Toxicokinetics and tissue distribution of cadmium-based quantum dots in the marine mussel *Mytilus galloprovincialis*



Part of this Chapter was published in:

- Rocha, T.L., Gomes, T., Pinheiro, J.P., Sousa, V.S., Nunes, L.M., Teixeira, M.R., Bebianno, M.J., 2015. Toxicokinetics and tissue distribution of cadmium-based Quantum dots in the marine mussel *Mytilus galloprovincialis*. Environmental Pollution 204, 207-214. doi:10.1016/j.envpol.2015.05.008.

Part of this Chapter was presented at:

- Rocha, T.L., Gomes, T., Pinheiro, J.P., Bebianno, M.J., 2014. Tissue-specific accumulation and metallothionein induction in mussels *Mytilus galloprovincialis* exposed to quantum dots and soluble cadmium. 2nd Marine NanoEcoSafety Workshop, Palermo, Italy.

Abstract

Environmental health hazards of Quantum dots (QDs) are of emergent concern, but limited data is available about their toxicokinetics (TK) and tissue distribution in marine bivalves. This study investigated the QDs behavior in seawater, their TK and tissue distribution in *Mytilus galloprovincialis*, in comparison with dissolved Cd. Mussels were exposed to CdTe QDs and dissolved Cd for 21 days at 10 µg Cd L⁻¹ followed by a 50 days depuration. TK of QDs in mussels is related to the homo-aggregate uptake, surface charge, aggregation and precipitation as key factors. There were tissue- and time-dependent differences in the TK of both Cd forms, and dissolved Cd is the most bioavailable form. Digestive gland is the preferential site for QDs storage and both Cd forms are not easily eliminated by the mussel ($t_{1/2} > 50$ d). Results indicate that the TK model of CdTe QDs in marine mussels is distinct from their dissolved counterparts.

Keywords: Nanoparticles, nanotoxicology, CdTe quantum dots, cadmium, bioaccumulation, bivalve, *Mytilus galloprovincialis*.

2.1. Introduction

The wide development of nanotechnology and the application of ENPs in several commercial products have raised concern about their environmental risk. QDs are fluorescent semiconductor nanocrystals (diameter = 1 - 10 nm) made of several metal complexes, such as Cd-based (CdS, CdTe, CdSe, CdSeS, CdSe/ZnS) or Cd-free QDs (InP, InAs, GaAs and GaN) and these ENPs are applied in many fields due to their physico-chemical properties and biological interactions (Rizvi et al., 2010; Blanco-Canosa et al., 2014).

Increasing production and use of a large scale Cd-based QDs will likely lead to their release into the aquatic environment, as well as to the inevitable increase of Cd concentration. Cd is a highly toxic metal to aquatic biota classified as a priority substance by the European Water Framework Directive. In contrast, the impact of Cd-based QDs in the aquatic organisms remains unclear. Bivalve molluscs are a target group for ENPs ecotoxicology because they uptake, accumulate, transform, store and biodeposit ENPs (Moore, 2006; Canesi et al., 2012; Montes et al., 2012; Corsi et al., 2014). Furthermore, ENPs accumulated by bivalves are potentially transferred in aquatic food webs (Farrell and Nelson, 2013).

Despite the ENPs bioaccumulation, their toxicokinetics (TK) and tissue-specific distribution in bivalves are scarce. Only the TK of Ag and CuO NPs in *C. islandica* (10 - 20 nm and 70 - 80 nm; 151 ng Ag L⁻¹; accumulation 12 h, depuration 8 w) and *M. balthica* (< 100 nm; 200 µg Cu g⁻¹ d. w. sediment; accumulation 35 d, depuration 15 d) were studied (Al-Sid-Cheikh et al., 2013; Dai et al., 2013). Different kinetic models between ENPs and their dissolved counterpart exist and the accumulation rate decreased with increasing ENPs size.

The uptake and *in vitro* toxicity of Cd-based QDs in bivalves is associated with particle-induced oxidative stress and Cd²⁺ release (Gagné et al., 2008; Peyrot et al., 2009; Bruneau et al., 2013; Katsumiti et al., 2014a). Moreover, CdTe QDs induce immunotoxic effects mediated by changes in hemocytes types, lysosomal and DNA damage in *M. galloprovincialis* (6 nm; 10 µg Cd L⁻¹; 14 d) (Rocha et al., 2014). However, to the best of our knowledge, this is the first study of long-time exposure of TK and tissue distribution of Cd-based QDs on marine bivalves.

Accordingly, the objective of this work was to determine Cd accumulation and elimination kinetics in different tissues of the mussel *M. galloprovincialis* exposed to two Cd forms (CdTe QDs and dissolved Cd at 10 µg Cd L⁻¹) for 21 days (accumulation

period) followed by a 50 days depuration period. The accumulation and depuration models and TK parameters were estimated to predict and understand the ENPs TK in different tissues of *M. galloprovincialis*. A *Mytilus* model was chosen since they are a unique target group for aquatic nanotoxicology and a valuable bioindicator for environmental pollution studies (Moore, 2006; Canesi et al., 2012).

2.2. Materials and Methods

2.2.1. QDs characterization

Orange CdTe QDs (diameter = 2 - 7 nm) were obtained from PlasmaChem GmbH (Berlin, CAS#1306-25-8) with an emission wavelength of 590 ± 5 nm and a core coated by carboxyl groups (-COOH) to prevent aggregation. A QDs stock solution was prepared using Milli-Q water (100 mg Cd L^{-1}), sonicated for 30 min (Ultrasonic bath VWR International, 230 V, 200 W, 45 KHz frequency) and kept in constant shaking. Dissolved cadmium stock solution was identically prepared using $\text{Cd}(\text{NO}_3)_2 \cdot 4\text{H}_2\text{O}$ (Merck) without sonication. QDs were characterized relatively to particle size in Milli-Q water using Transmission Electron Microscopy (TEM), hydrodynamic diameter (d_h) and zeta potential (ζ -potential) in seawater by Dynamic Light Scattering (DLS) and Electrophoretic Light Scattering (ELS), respectively, using a ZetaSizer Nano analyser (ZS90, Malvern, Inc.), see Rocha et al. (2014) (Chapter 4).

2.2.2. Aggregation of QDs with NOM

The aggregation of QDs with different natural organic matter (NOM) was measured by DLS. NOM stock solutions (50 mg C L^{-1}) were made in Milli-Q water and natural seawater (salinity = 36.3 ± 0.07) using commercial Aldrich humic acid (HA - high MW and hydrophobic) (Sigma-Aldrich), tannic acid (TA - intermediate MW and hydrophobicity) (VWR) and salicylic acid (SA - low MW and hydrophilic) (Merck), sonicated for 30 min and kept at 4 °C. The dissolved organic carbon (DOC) in stock solutions was analyzed in a Shimadzu TOC5000A analyzer (50 ppb - 4000 ppm) using high-temperature combustion method (Sousa and Teixeira, 2013). After this, QDs (40 mg L^{-1}) were suspended in Milli-Q water and natural seawater with the three types of NOM at 2, 4, 6 and 10 mg C L^{-1} , pH 8.0 and sonicated for 15 min. A similar analysis was performed without NOM. The DLS and ELS techniques were performed as previously described by Sousa and Teixeira (2013).

2.2.3. Cd speciation

The free Cd ion (Cd^{2+}) and total labile Cd concentrations in seawater from control and exposure groups were determined by Absence of Gradients and Nernstian Equilibrium Stripping (AGNES) and Stripping Chronopotentiometry (SCP) techniques using Eco Chemie μ Autolab III potentiostat, Metrohm 663VA stand, GPES 4.9 software (Eco Chemie) and disposable polystyrene cups (VWR 611-1366) in order to avoid losses to the container walls according to Rocha et al. (2007) and Domingos et al. (2011). The following parameters were used for AGNES analysis: initial purge time 600 s, deposition potential -0.705 V, deposition time 240 s, stripping current 4 μA . For SCP experiments the parameters used were: deposition potential -0.80 V, deposition time 90 s, stripping current 4 μA . Calibrations for AGNES and SCP were performed using a Cd concentrations range from 1×10^{-8} to 1×10^{-7} M in sterilized seawater (salinity = 36.3 ± 0.07) at pH 8.0 after ozone treatment at 30 min (Sander Ozonisorator 200; $200 \text{ mg O}_3 \text{ h}^{-1}$). The experiments were performed at 23 °C under an oxygen-free nitrogen atmosphere in triplicate using identical volumes (20 mL). The program Visual MINTEQ (version 2.5.3) (Allison et al., 1999) was used to determine the Cd speciation along the calibration. The calibrations were always linear up to the highest concentration used, i. e. 100 nM. The limit of detection (LOD) and limit of quantification (LOQ) are based in 8 calibration plots and determined by the method of the standard deviation of the residuals. For SCP (free plus labile metal) the LOD and LOQ are respectively 3.2 and 10.7×10^{-9} M and for AGNES (free metal) the LOD and LOQ are respectively 5.3 and 17.6×10^{-9} M.

2.2.4. Experimental design

Mussels *M. galloprovincialis* (60 ± 5 mm shell length) were collected in the Ria Formosa Lagoon (Figs. 1.15 and 1.16) and acclimated during 14 days in natural seawater at 16 °C with constant aeration. Afterwards, ninety mussels were placed in 30 L seawater tanks ($3.6 \text{ mussels L}^{-1}$) in a duplicate design and exposed to either CdTe QDs or dissolved Cd at the same nominal concentration $10 \mu\text{g Cd L}^{-1}$ for 21 days, jointly with a control group. After this, mussels were transferred to clean seawater for 50 days. Ten mussels were collected from each tank at initial time and after 3, 7, 14 and 21 days of exposure and after 15, 20, 30 and 50 days of depuration. Water was changed daily with redosing after each change and experiments were conducted in a static-renewal condition under 12 h:12 h light/dark cycles with salinity, temperature, pH and

oxygen saturation measured daily (36.3 ± 0.07 , 16.6 ± 1.2 °C, 7.9 ± 0.1 , 103 ± 1.3 %, respectively). Mussels were only fed with natural seawater which was changed every other day providing animals with food to avoid starvation and any effects resulting from the interaction of QDs and food. No significant mortality was observed between the three treatments by the end of the accumulation (control: 1.3 ± 0.6 %; QDs: 4.0 ± 1.4 %; dissolved Cd: 2.5 ± 0.7 %; $p > 0.05$) and depuration period (control: 2.9 ± 0.6 %; QDs: 4.5 ± 2.1 %; dissolved Cd: 4.5 ± 2.1 %; $p > 0.05$).

2.2.5. Cd concentrations in seawater and mussel tissues

Cd concentration in seawater was analyzed immediately after QDs and dissolved Cd addition and after the accumulation (14 and 21 days) and depuration (50 days) periods. The QDs dissolution and Cd speciation in experimental seawater over 24 h of exposure were determined by AGNES and SCP as described above for Cd speciation analysis.

For Cd concentrations determination, gills, digestive gland and remaining tissues (mantle, foot and adductor muscles) were dissected, weighed, and hemolymph collected from the posterior adductor muscle using a 1 mL syringe with a 25G needle. Cd concentration was determined in dried mussel tissues (80 °C, 48 h) after wet acid digestion with HNO₃ (80 °C, 4 h) by graphite furnace atomic absorption spectrometry (AAS, AAnalyst 800-PerkinElmer). Accuracy was assured with certified reference material (TORT-II, Lobster Hepatopancreas) from the National Research Council (Canada) and results were similar to the certified values (28.5 ± 4.5 mgCd kg⁻¹ and 26.7 ± 0.6 mgCd kg⁻¹). Cd levels are expressed as µg g⁻¹ of dry weight tissue.

2.2.6. Condition index

The condition index (CI) was calculated as the percentage (%) of the ratio between drained weight of the soft tissues (g) and total weight (g) according to Gomes et al. (2013).

2.2.7. Kinetic models

The accumulation model was estimated by a first-order kinetic model (Serafim et al., 2007), in which the accumulation kinetic is described using the Eq. 2.1.

$$C_B = K_d / K_l C_W (1 - e^{-K_l t}) \quad (\text{Eq. 2.1})$$

where C_B is the Cd concentration in the tissues ($\mu\text{g g}^{-1}$ d. w. tissue), C_w is the Cd concentration in seawater ($\mu\text{g Cd L}^{-1}$), K_a is the accumulation rate ($\text{L g}^{-1}\text{d}^{-1}$), K_l is the loss rate during the accumulation period (d^{-1}), and t is time during the exposure period (d). Both K_a and K_l were estimated by the Ordinary Least Squares method using the nonlinear curve-fitting. During the depuration period, C_w is considered zero and the elimination kinetic was described by Eq. 2.2.

$$C_B = C_{B0} e^{-K_e t} \quad (\text{Eq. 2.2})$$

where C_{B0} is the initial Cd concentration in the depuration period ($\mu\text{g g}^{-1}$ d. w.) and K_e the rate of elimination during the depuration period (d^{-1}). This constant was used to determine the Cd half-life ($t_{1/2}$) in mussel tissues according to the relation $t_{1/2} = \ln 2 / K_e$. The bioconcentration factor (BCF) considers that C_B reaches a steady state and was estimated according to the relationship $\text{BCF} = K_a / K_e$.

2.2.8. Biodeposits

Biodeposits (BDs) were removed from the tanks before the water change, filtered with a $7 \mu\text{m}$ filter (MN 640), washed with seawater and dried at 80°C (48 h). BDs production rate was estimated as the ratio between dried weight of BDs (mg) and total weight of mussel (g) *per day*. Cd concentration was determined in dried BDs (80°C , 48 h) by AAS, as described above.

2.2.9. Statistical analysis

Statistical analyses were carried out using the Statistica 7.0 software (Statsoft Inc., 2005, USA). The results were compared using parametric tests (two-way ANOVA, followed by the Tukey's test) and/or non-parametric test (Kruskal-Wallis), depending on data distribution and variances homogeneity (Shapiro-Wilk and Levene's tests). Results were significant when $p < 0.05$.

2.3. Results

2.3.1. QDs characterization

TEM analysis of CdTe QDs in Milli-Q water show isolated spheroid particles (diameter = 6.1 ± 1.5 nm) and confirm the presence of QDs aggregates in the aqueous

medium (Fig. 2.1A). DLS and ELS indicate that salinity induces the formation of small and large QDs aggregates [$d_h = 563 \pm 435$ nm ($n > 80\%$) and 2973 ± 1332 nm ($10 < n < 80\%$)] (Fig. 2.1B), with negative surface charge (ζ -potential = -9.4 ± 1.2 mV) at pH 8.0.

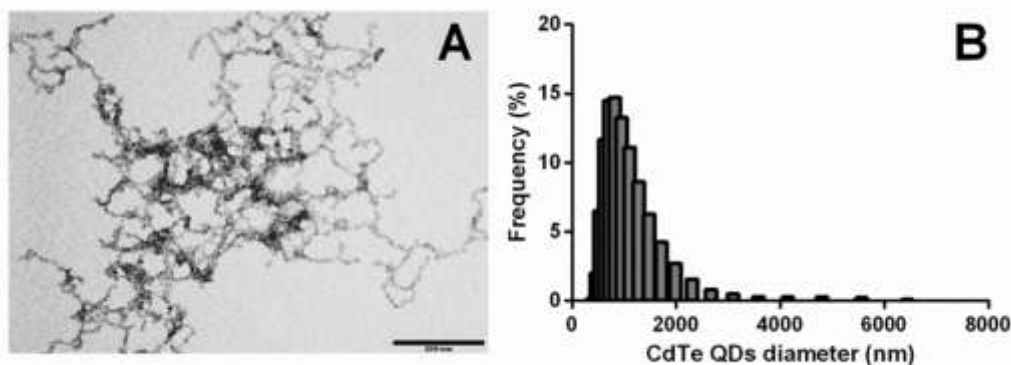


Figure 2.1. Transmission Electron Microscopy (TEM) image of CdTe quantum dots (QDs) (A) and hydrodynamic diameter histogram of QDs suspended in seawater at pH 8.0 (B).

2.3.2. Aggregation of QDs with NOM

DLS and ELS show that d_h and ζ -potential of water-dissolved QDs remains unchanged with the addition of NOM (SA, TA and HA) at different concentrations (0 - 10 mg C L⁻¹) in milli-Q or in seawater (Fig. 2.2). Thus QDs aggregation increase is related with the salinity increase and no hetero-aggregation was observed in both medium.

2.3.3. QDs dissolution and Cd speciation

SCP and AGNES results in seawater collected immediately after the addition of QDs and dissolved Cd show that total Cd concentrations decreased over 24 h exposure ($p < 0.05$; Fig. 2.3A). Results demonstrate that 27.6 % of the initial total Cd concentration (4.2×10^{-8} M) in QDs exposure media were as free ionic form (Fig. 2.3A), indicating that the majority of Cd present in QDs exposure is in the nanoparticulate form. On the other hand, for dissolved Cd exposure media, 24 % of the Cd is free Cd²⁺ and 76 % are Cd-chloro-complexes (CdCl⁺ and CdCl₂) (Fig. 2.3A). In contrast, Cd

concentrations were always below the LOD of the SCP ($\text{LOD} = 3.49 \times 10^{-9} \text{ M}$) during the depuration (Fig. 2.3B).

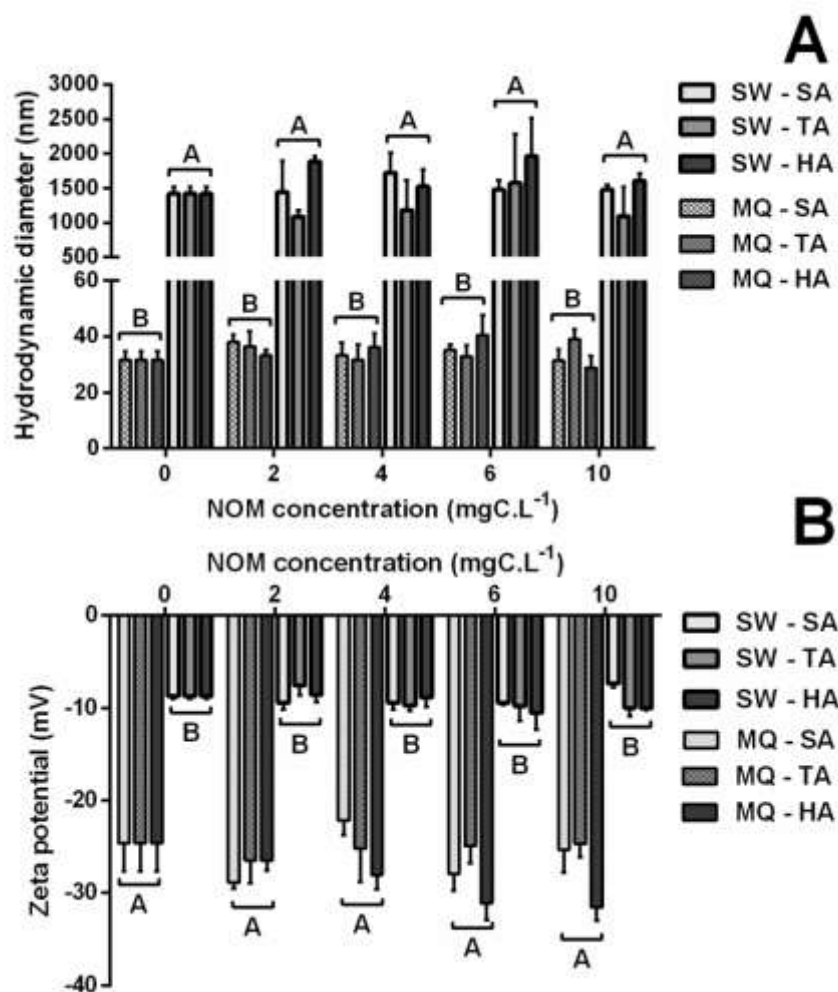


Figure 2.2. Hydrodynamic diameter (mean \pm std nm) (A) and zeta potential (mean \pm std mV) (B) of CdTe quantum dots (QDs) suspended in Milli-Q water (MQ) and seawater (SW) with three types of natural organic matter (NOM): salicylic acid (SA), tannic acid (TA) and humic acid (HA) at pH 8.0. Capital letters indicate significant differences between suspension at each concentration of NOM ($p < 0.05$).

2.3.4. Condition Index (CI)

No significant CI changes were observed between the three treatments by the end of the accumulation (control: 45 ± 5 ; QDs: 43 ± 6 ; dissolved Cd: 44 ± 7 ; $p > 0.05$) and the depuration period (control: 40 ± 4 ; QDs: 42 ± 6 ; dissolved Cd: 38 ± 2 ; $p > 0.05$),

with the exception of unexposed (48 ± 4) and QDs exposed mussels (42 ± 4) after 7 d of exposure ($p < 0.05$).

2.3.5. Cd accumulation

Cd levels in unexposed mussels are tissue dependent and remain unchanged during the whole experiment (Fig. 2.4A-J). Mussels exposed to both Cd forms showed that CdTe QDs and dissolved Cd are bioavailable to the different tissues and that accumulation kinetic is Cd form and tissue dependent (Fig. 2.4A-E; Table 2.1). Cd accumulation followed a first-order kinetic model in whole soft tissues in both exposure conditions, but more slowly accumulated in QDs-exposed mussels (K_a : $0.07 \text{ L g}^{-1} \text{ d}^{-1}$) than in dissolved Cd-exposed ones (K_a : $0.23 \text{ L g}^{-1} \text{ d}^{-1}$; $p < 0.05$). Mussels exposed to QDs accumulate less Cd in whole soft tissues (2.2-fold less) than those exposed to dissolved Cd ($p < 0.05$; Fig. 2.4A).

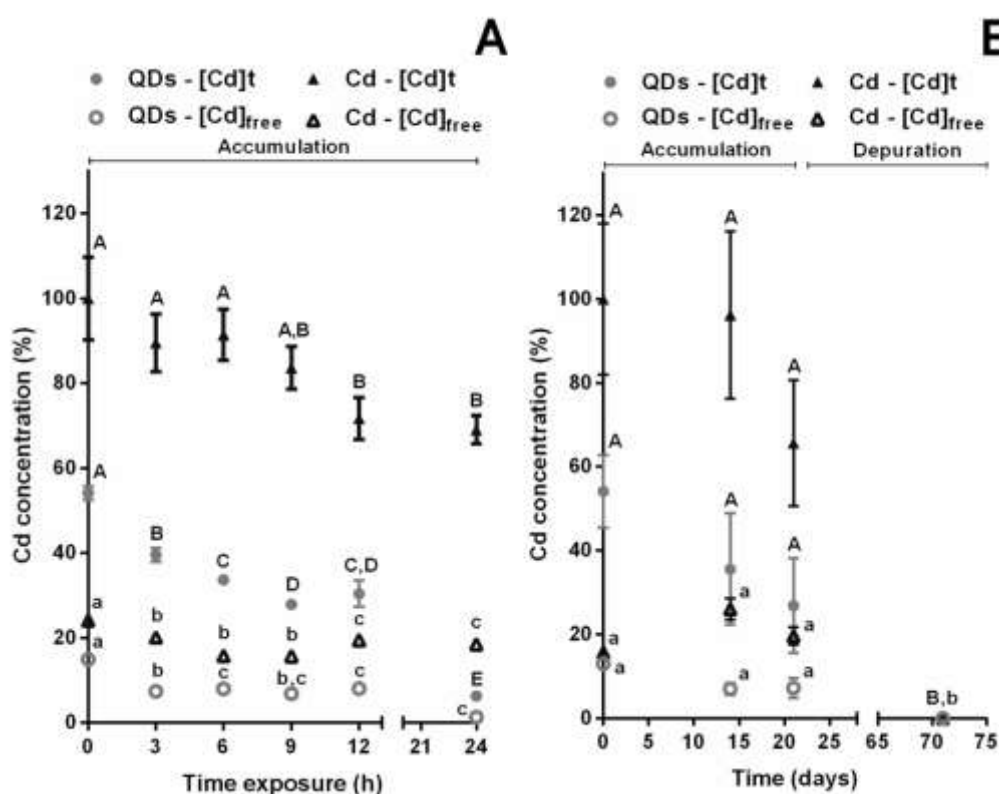


Figure 2.3. Cd concentration (mean \pm std M) in water after exposure to CdTe Quantum dots (QDs) and to dissolved cadmium (Cd) for 24 h (A) during accumulation (21 d) and depuration (50 d) periods (B). Capital and lower letters indicate significant differences between total Cd concentration determined by SCP and free Cd concentration determined by AGNES for each treatment during the experimental time ($p < 0.05$).

A similar Cd tissue distribution was observed in mussel tissues exposed to both Cd forms: digestive gland > gills > remaining tissues > hemolymph ($p < 0.05$; Fig. 2.4B-E). Cd accumulation in the gills and remaining tissues was significantly lower in QDs-exposed mussels (2.6- and 2.7-fold lower, respectively) than in those exposed to dissolved Cd after 21 d ($p < 0.05$; Fig. 2.4B,E). Exposure to both Cd forms induce a linear Cd accumulation, with lower Ka in QDs-exposed mussels (gill: $0.13 \text{ L g}^{-1} \text{ d}^{-1}$; remaining tissues: $0.07 \text{ L g}^{-1} \text{ d}^{-1}$) compared to Cd-exposed ones (gill: $0.27 \text{ L g}^{-1} \text{ d}^{-1}$; remaining tissues: $0.12 \text{ L g}^{-1} \text{ d}^{-1}$) ($p < 0.05$; Table 2.1).

In contrast to the other tissues, Cd accumulation model in the hemolymph differs and is Cd form dependent. Results showed an initial linear Cd increase in the hemolymph of mussel exposed to QDs (14-fold) and Cd (14.8-fold) compared to unexposed ones after 3 days of exposure ($p < 0.05$). After this time, in QDs-exposed mussels, Cd accumulation reached a steady state, while in those exposed to dissolved form, Cd continue to linearly increase until 14 days of exposure reaching then, like in the digestive gland, a steady state (Fig. 2.4C). Ka and BCF in the hemolymph were higher in QDs exposed mussels ($Ka = 0.03 \text{ L g}^{-1} \text{ d}^{-1}$; BCF = 1.9) compared to those exposed to dissolved Cd ($Ka = 0.004 \text{ L g}^{-1} \text{ d}^{-1}$; BCF = 0.16) ($p < 0.05$; Table 2.1). Thus, the high Ka associated with higher Kl in QDs-exposed mussels promotes a steady state, reflecting a dynamic between accumulation and elimination of QDs in the hemolymph.

Cd accumulation in the digestive gland in QDs-exposed mussels corresponds to the linear part of the first-order kinetic model, indicating that much longer periods of exposure are required to reach the steady state, well beyond the 21 days (Fig. 2.4D). On the other hand, in mussels exposed to dissolved Cd there is an initial uptake phase (up to 14 d), reaching a steady state at the end of the accumulation period (Fig. 2.4D). Cd accumulation model in the digestive gland is Cd form dependent, with lower Ka in QDs-exposed mussels ($Ka = 0.34 \text{ L g}^{-1} \text{ d}^{-1}$) compared to those exposed to dissolved Cd ($Ka = 1.39 \text{ L g}^{-1} \text{ d}^{-1}$) ($p < 0.05$; Table 2.1). Cd levels in digestive gland from QDs-exposed mussels were lower (1.5-fold) than in Cd-exposed ones after 21 days ($p < 0.05$). The results show that the digestive gland is the preferential site for Cd storage in mussels exposed to either of the Cd forms.

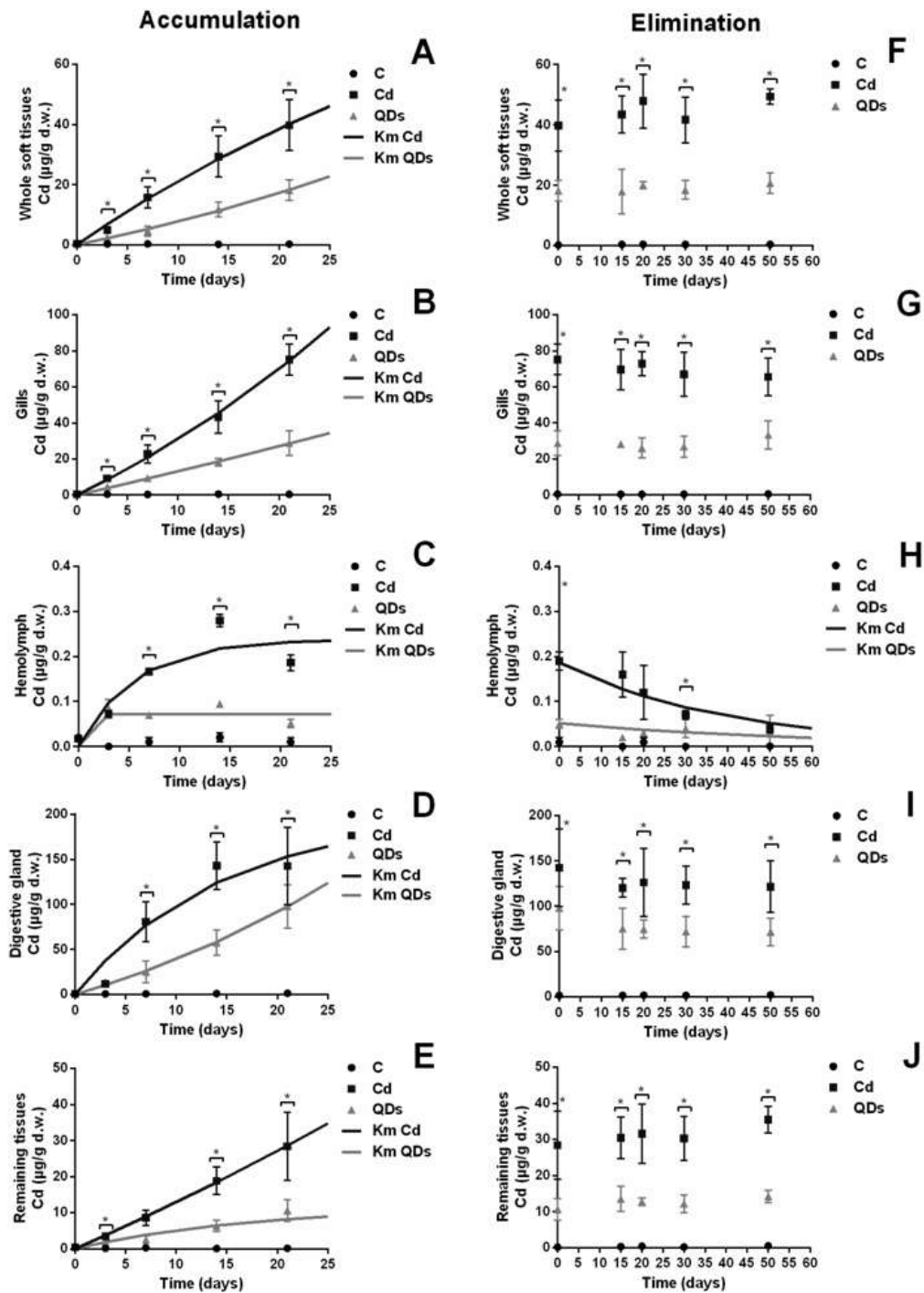


Figure 2.4. Cd concentration (mean \pm std $\mu\text{g g}^{-1}$ d. w. tissue) and first-order kinetic model (Km) of Cd accumulation (A-E) and elimination (F-J) in the whole soft tissues (A,F), gills (B,G), hemolymph (C,H), digestive gland (D,I) and remaining tissues (E,J) of mussels *M. galloprovincialis* from controls (C), exposed to CdTe Quantum dots (QDs) and to dissolved cadmium (Cd) during the accumulation period (21 days) (A-E) and the depuration period (50 days) (F-J). * indicate significant differences between all treatments at each time of exposure ($p < 0.05$).

2.3.6. Cd elimination

At the end of the depuration period (50 days), Cd concentrations in the mussel tissues remains unchanged compared to that at the end of the accumulation period ($p > 0.05$; Fig. 2.4F-J). Due to the high Cd retention rate in the whole soft tissues, gills, digestive gland and remaining tissues, it was impossible to estimate the $t_{1/2}$ in these organs (Table 2.1). In opposite to other tissues, Cd levels in the hemolymph remained high in mussels exposed to QDs (62 % of Cd retention and Ke : 0.016 d^{-1} ; $p > 0.05$) and decrease linearly in mussels exposed to Cd over depuration time (24% of Cd retention and Ke : 0.025 d^{-1} ; $p < 0.05$; Fig. 2.4H). The tendency of QDs to remain longer bound to the hemolymph is supported by the estimated $t_{1/2}$ in this tissue, which was higher for QDs ($t_{1/2} = 42.1$ days) when compared to dissolved Cd ($t_{1/2} = 27.2$ days) (Table 2.1).

Table 2.1. Accumulation rate (Ka), loss rate (Kl), elimination rate (Ke), half-life ($t_{1/2}$) and bioconcentration factor (BCF) in *M. galloprovincialis* tissues from controls (C), exposed to CdTe quantum dots (QDs) and to dissolved cadmium (Cd) during the accumulation (21 days) and depuration (50 days) periods^a.

Exposure	Tissues ^a	Accumulation period			Depuration period			BCF
		$K_a (\text{L g}^{-1} \text{d}^{-1})$	$K_l (\text{d}^{-1})$	r	$K_e (\text{d}^{-1})$	$t_{1/2} (\text{d})^b$	r	
QDs	Total	0.07	-	0.95	-	> 50	0.32	-
	DG	0.34	-	0.93	-	> 50	0.34	-
	G	0.13	-	0.95	-	> 50	0.24	-
	RT	0.07	0.06	0.73	-	> 50	0.29	-
	H	0.03	4.14	0.72	0.016	43	0.37	1.9
Cd	Total	0.23	0.02	0.94	-	> 50	0.20	-
	DG	1.39	0.07	0.90	-	> 50	0.13	-
	G	0.27	-	0.97	-	> 50	0.23	-
	RT	0.12	-	0.94	-	> 50	0.17	-
	H	0.004	0.18	0.90	0.025	28	0.86	0.16

^a Tissues: DG = digestive gland; G = gills; RT = remaining tissues; H = hemolymph.

^b Half-life ($t_{1/2}$) corresponds to $\ln 2/Ke$; BCF corresponds to Ka/Ke ;

2.3.7. Production and Cd concentration of biodeposits

No significant alterations in the BDs production was detected in mussels exposed to both Cd forms during experimental periods ($p > 0.05$, Table 2.2), except for a decrease in QDs-exposed mussels after 14 days and in those exposed to dissolved Cd after 7 days when compared to controls ($p < 0.05$, Table 2.2). Cd concentrations in the BDs were Cd form dependent and confirm the aggregation and precipitation of QDs in

seawater over 24 h. Cd was always higher in QD-exposed mussels compared to those unexposed and exposed to dissolved Cd after 7 days of exposure ($p < 0.05$). In opposition to QDs, no significant Cd levels were observed in BDs from mussels exposed to dissolved Cd after 21 days of accumulation ($p > 0.05$, Table 2.2). Thus, in the depuration period, there are no Cd levels in BDs from mussel exposed to both Cd forms ($p > 0.05$), except for those exposed to dissolved Cd after 15 days depuration ($p < 0.05$, Table 2.2). Cd concentration in BDs during the depuration period confirms that QDs are retained in the mussel tissues, as no elimination through the feces was detected after 50 days.

Table 2.2. Production rate (mean \pm std mg g⁻¹ d. w. tissue *per day*) and Cd concentration in biodeposits (mean \pm std μ g g⁻¹ d. w.) of mussel *M. galloprovincialis* from controls (C), exposed to CdTe quantum dots (QDs) and to dissolved cadmium (Cd) during the accumulation (21 days) and depuration periods (50 days). Capital and lower letters indicate significant differences between treatments at each time of exposure day and within treatment during the exposure period ($p < 0.05$).

Time (days)	Biodeposit production rate (mg g ⁻¹ of d. w. tissue <i>per day</i>)			Cd concentration in the biodeposit (μ g g ⁻¹ d. w.)		
	C	QDs	Cd	C	QDs	Cd
Accumulation						
0	0.48 \pm 0.15 ^{Aa}	0.48 \pm 0.15 ^{Aa}	0.48 \pm 0.15 ^{Aab}	0.14 \pm 0.01 ^{Aa}	0.14 \pm 0.01 ^{Ab}	0.14 \pm 0.01 ^{Ab}
3	0.38 \pm 0.1 ^{Aa}	0.16 \pm 0.16 ^{Aa}	0.39 \pm 0.00 ^{Aa}	0.22 \pm 0.1 ^{Aa}	36.68 \pm 2.4 ^{Aab}	21.76 \pm 29A ^b
7	0.41 \pm 0.21 ^{Aa}	0.07 \pm 0.04 ^{ABa}	0.14 \pm 0.01 ^{Bab}	0.35 \pm 0.1 ^{Ba}	103.4 \pm 41.9 ^{Aab}	34.68 \pm 7.5 ^{ABb}
14	0.23 \pm 0.09 ^{ABa}	0.34 \pm 0.17 ^{Ba}	0.09 \pm 0.02 ^{Aab}	0.16 \pm 0.1 ^{Ba}	199.40 \pm 135.9 ^{Aa}	44.25 \pm 17.7 ^{ABa}
21	0.51 \pm 0.19 ^{Aa}	0.14 \pm 0.06 ^{Aa}	0.12 \pm 0.13 ^{Aab}	0.27 \pm 0.1 ^{Ba}	232.52 \pm 133.7 ^{Aa}	66.12 \pm 68.3 ^{ABa}
Depuration						
15	0.21 \pm 0.07 ^{Aa}	0.20 \pm 0.19 ^{Aa}	0.12 \pm 0.03 ^{Aab}	0.45 \pm 0.2 ^{Ba}	0.75 \pm 0.3 ^{ABab}	10.43 \pm 10.9 ^{Ab}
20	0.25 \pm 0.16 ^{Aa}	0.24 \pm 0.09 ^{Aa}	0.15 \pm 0.06 ^{Aab}	1.62 \pm 1.9 ^{Aa}	6.53 \pm 4.2 ^{Aab}	5.95 \pm 4.5 ^{Ab}
30	0.67 \pm 0.04 ^{Aa}	0.65 \pm 0.17 ^{Aa}	0.52 \pm 0.21 ^{Ab}	0.14 \pm 0.1 ^{Aa}	0.12 \pm 0.1 ^{Ab}	0.84 \pm 0.2 ^{Ab}
50	0.58 \pm 0.22 ^{Aa}	0.59 \pm 0.10 ^{Aa}	0.53 \pm 0.17 ^{Aab}	0.17 \pm 0.2 ^{Aa}	0.29 \pm 0.3 ^{Ab}	0.19 \pm 0.1 ^{Ab}

2.4. Discussion

Estuarine and coastal environments are the potential sinks for ENPs, where behavior, bioavailability, fate, ecological and toxicological impacts depend on their intrinsic physico-chemical properties (size, shape, crystallography, composition surface charge and chemistry), characteristics of the surrounding media (salinity, pH, water hardness) and presence of organic and inorganic components (Lowry et al., 2012; Misra et al., 2012; Sousa and Teixeira, 2013; Corsi et al., 2014). The AGNES and SCPs

results show that several different Cd physico-chemical forms exist during exposure of mussels to CdTe QDs: 72 % are small and larger homo-aggregates of CdTe QDs while 27.6 % is free ionic Cd (Cd^{2+}), inorganic (CdCl^+ and CdCl_2) and organic Cd complexes resulting from Cd release from the QDs core (Cd-NOM-complex). Compared to other QDs (Gagné et al., 2008; Peyrot et al., 2009; Morelli et al., 2012), the CdTe QDs used have similar dissolution in seawater (27.6 %), confirming that the majority of the Cd present in QDs exposure is in the nanoparticulate form and that QDs homo-aggregates are primarily responsible for Cd accumulation. Furthermore, the release of ionic Te from the CdTe QD core and its speciation in seawater cannot be excluded (Domingos et al., 2011), but these parameters were not followed.

The DLS and ELS results show that the aggregation of CdTe QDs in milli-Q and seawater remains unchanged when NOM with different MW and hydrophobicity (SA, TA and HA) are present at different environmentally relevant concentrations ($< 10 \text{ mg C L}^{-1}$). These results indicate that the coating of QDs by ionizable carboxylic groups confers negative surface charge and prevents interaction between QDs and NOM due to repulsion forces. On the other hand, the interaction between NOM and other ENPs with positive surface charge (e. g. 42 nm Ag NPs and 31 nm CuO NPs) increase the stability and residence time of ENPs in the water column, decrease their aggregation state and modify their bioavailability and toxicity for aquatic organisms (Sousa and Teixeira, 2013; Corsi et al., 2014). Furthermore the surface charge and interaction with NOM are different between nanoparticulate and dissolved Cd forms in seawater, since ionic Cd exists as Cd^{2+} and their complexation with NOM was previously described (Koopal et al., 2005; Wu et al., 2012).

As for Cd concentrations in QDs exposure media, a significant decrease was observed over 24 h, in which total labile Cd levels decrease 8.6-fold while dissolved Cd decrease 11-fold (Fig. 2.2A). These decreases are caused by the aggregation and precipitation of QDs and by the large filtration rate ($> 1 \text{ L h}^{-1}$) and accumulation capacity of mussels. Mussels exposed to QDs also uptake free ionic Cd released from QD core (around 27.6 %) which also contribute to Cd accumulation. Conversely, dissolved Cd is the most bioavailable Cd form, so lower Cd levels in QDs-exposed mussels is due to fast homo-aggregation, sedimentation, low dissolution rate and speciation of Cd from QDs core in seawater (Fig. 2.2) (Rocha et al., 2014). The aggregation and surface charge of ENPs are important nano-specific factors to reduce bioavailability and toxicity for bivalve species, since large aggregates prevent passive

transport or carrier-mediated transport and some aggregates would be retained in the gills (Gagné et al., 2008; Hanna et al., 2014).

The ENPs kinetics in bivalves is an emerging issue for understanding the ENPs impact in the aquatic environment and their potential action mode. Results highlighted a complex and dynamic uptake process, storage, transformation, elimination and regulation of CdTe QDs in mussel tissues (Fig. 2.4). Both Cd forms are accumulated and systemically distributed in mussel tissues (Fig. 2.4), as previously reported for other QDs (Hull et al., 2013; Rocha et al., 2014), carbon-based NPs, metal and metal oxide NPs in the *Mytilus* spp. (i. e. Canesi et al., 2010; Gomes et al., 2011, 2012; Hanna et al., 2013; Muller et al., 2014). The TK of Cd in *Mytilus* spp. is well known (Borchardt, 1983; Soto et al., 1996; Hervé-Fernández et al., 2010; Amachree et al., 2013), but to the best of our knowledge, this is the first study about TK and tissue distribution of Cd-based QDs in marine bivalves.

Cd levels in tissues of unexposed mussels remained unchanged over time (Fig. 2.4) and below levels detected in mussels collected in the Ria Formosa Lagoon (Cravo et al., 2009), and the maximum level ($1 \text{ mg Cd kg}^{-1} \text{ d. w. tissue}$) established by the European Commission (Directive 2001/22/EC). As for CdTe QDs, results show that the Cd accumulation model is tissue and Cd form dependent, with QD-exposed mussels showing a general lower accumulation in tissues when compared to its dissolved form (Fig. 2.4A-E). In mussel whole soft tissues exposed to QDs, Cd is assimilated faster at the beginning and accumulates linearly over time (Fig. 2.4A; Table 2.1), indicating that during the accumulation period Cd elimination is very slow or negligible. Similarly, both Cd forms are not easily eliminated during 50 days depuration, since higher Cd retention was observed in exposed mussels (Fig. 2.4F).

QDs and dissolved Cd are accumulated by mussels over exposure and the key role of digestive gland in storage and detoxification of both Cd forms was confirmed by higher Cd levels in this organ when compared to gills (QDs: 3.4-fold; Cd: 1.9-fold) or remaining tissues (QDs: 9.2-fold; Cd: 5-fold) (Fig. 2.4B, D-E). This different tissue distribution is in agreement with previous studies with mussels exposed to uncoated CdTe (Peyrot et al., 2009), PEG-CdSe/ZnS QDs (Hull et al., 2013) and to other ENPs (Ag NPs, CuO NPs, C₆₀ fullerenes) (Dai et al., 2013; Al-Subiai et al., 2012; Gomes et al., 2012, 2014) indicating that the digestive gland is, like for dissolved Cd, target for Cd-based QDs toxicity.

Cd concentration associated to fast Cd accumulation (high K_a ; $0.004 \text{ L g}^{-1} \text{ d}^{-1}$) and elimination (high K_e ; 0.025 d^{-1}) in the hemolymph from mussels exposed to both Cd forms supports the role of hemolymph in the transport, distribution and regulation of QDs and dissolved Cd. The QDs transfer from the digestive system to the hemolymph and circulating hemocytes was also observed in previous studies (Gagné et al., 2008; Hull et al., 2013; Rocha et al., 2014) and CdTe QDs (6.1 nm ; $10 \text{ } \mu\text{g Cd L}^{-1}$; 14 d) transport in the hemolymph is limited by the number of circulating hemocytes and Cd concentration affects the immune function by changing hemocyte types, lysosomes and DNA damage (Rocha et al., 2014). CdS QDs internalization by *Mytilus* hemocytes *via* endocytosis or phagocytosis was previously confirmed (Katsumiti et al., 2014b) and the Cd kinetics in the hemolymph show that this tissue has an important role in nano and dissolved Cd transport between tissues, especially during depuration (Fig. 2.4H; Table 1).

The uptake of ENPs aggregates in the digestive gland is *via* endocytosis (nanoaggregates: $\leq 10^2 \text{ nm}$) and phagocytosis (microaggregates: $10^2 - 10^6 \text{ nm}$) jointly with its storage and/or transfer to the hemolymph (Moore, 2006; Canesi et al., 2012; Baker et al., 2014). Although the mode of interaction and uptake of QDs in invertebrates remains poorly understood, several studies in vertebrate models showed that uncoated QDs adhere to cell surfaces by interactions with glycoproteins and/or glycolipids in plasma membrane and are incorporated *via* endocytic mechanisms by a variety of cell types (Hardman, 2006). The present results suggest that QDs are uptake mainly through the digestive gland cells *via* endocytotic mechanisms, distributed and accumulated in the organism due to low specificity of coverage with carboxylic acid and dissolution of the QDs. Furthermore, the ionic Cd released from QDs core and Cd-chloro-complexes entering in the gills by passive diffusion or *via* active transport pumps for essential metal (Ca^{2+} -channels), rapidly binding to intracellular ligands (e. g. metallothioneins - MTs) being thus transported to lysosomes where it is released into hemolymph by exocytose and incorporated to circulating hemocytes and/or binding to MT to be removed (Marigómez et al., 2002). Furthermore, the permanence of QDs in the mussel digestive system facilitates their digestion and absorption, and lead to the release of free Cd ions in the digestive system (Wu et al., 2012; Al-Sid-Cheikh et al., 2013). The uptake difference between QDs and dissolved Cd in the digestive gland (1.5-fold) and gills (2.6-fold) confirms that QDs contribute more for Cd accumulation in the digestive gland and dissolved Cd is more responsible for Cd levels in the gills (Fig.

2.3B, D). However, future studies and new technologies are needed to differentiate QDs from other forms of accumulated Cd in bivalve tissues.

Cd accumulation and retention by mussels exposed to both Cd forms were also confirmed by $t_{1/2}$ of Cd in the mussel tissues (Fig. 2.4A-E; Table 2.1) associated with no significant Cd elimination during depuration (Fig. 2.4F-J). BDs production by mussels and Cd concentration during depuration indicate that QDs have different metabolic pathways in bivalve species when compared to other ENPs. The ENPs repackaging by mussels in highly concentrated BDs was already reported (Montes et al., 2012; Wegner et al., 2012), but Cd from CdTe QDs is not eliminated in the BDs during 50 days of depuration. Cd concentration in BDs during the accumulation period is related to QDs aggregation and precipitation due to its fast sedimentation rate (0.7 h^{-1}) in seawater (Rocha et al., 2014; Chapter 4).

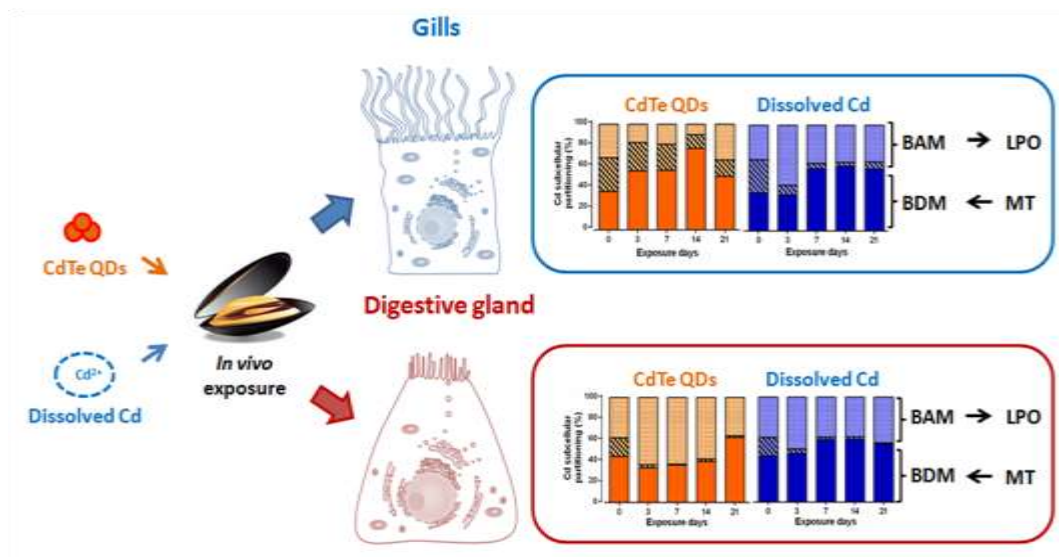
The estimated biologic $t_{1/2}$ of CdTe QDs for *M. galloprovincialis* ($t_{1/2} > 50 \text{ d}$; Table 2.1) is longer than for other ENPs in bivalves, such as Ag NPs ($t_{1/2}$ ranging from 1.4 to 4.3 days and 17 - 50 days for fast and slow compartments) and CuO NPs ($t_{1/2} > 15 \text{ days}$) (Al-Sid-Cheikh et al., 2013; Dai et al., 2013) and confirms that *Mytilus* spp. are high accumulators of both Cd forms when compared to other bivalves (Hervé-Fernández et al., 2010; Rocha et al., 2014). Cd concentration during the depuration period indicates that Cd is not equally distributed between tissues and that digestive gland and gills represent the major storage for QDs and dissolved Cd accumulation. The high Cd sequestration in these tissues from dissolved Cd-exposed mussels is related to the presence of MTs (Serafim and Bebianno, 2007). MTs induction in bivalves exposed to Cd-based QDs was only reported for the freshwater mussel *E. complanata* exposed to CdTe QDs ($1.6 - 8 \text{ mg L}^{-1}$; 24 h), which showed an increase in MTs levels in the digestive gland, and a decrease in the gills related with QDs-mediated oxidative stress (Peyrot et al., 2009). Thus the detoxification mechanism of ENPs in bivalve species remains poorly understood and more studies are needed to determine the elimination process of Cd-based QDs in mussels. The $t_{1/2}$ for dissolved Cd is in agreement with previous studies ($t_{1/2}$ between 96 and 300 days for dissolved Cd in *Mytilus* spp.) (Borchardt, 1983), and the $t_{1/2}$ of QDs ($> 50 \text{ days}$) in *M. galloprovincialis* indicates that Cd accumulation due to the increase production and use of Cd-based QDs is an emerging environmental problem.

2.5. Conclusions

Overall, the TK of CdTe QDs and dissolved Cd in mussels are mediated by different mechanisms of uptake, tissue-specific distribution, storage and elimination, and directly related to QDs aggregation and precipitation in seawater. Dissolved Cd is the most bioavailable form and the exposure to both Cd forms induces Cd accumulation in mussel tissues followed by no efficient elimination during 50 days depuration, although higher in the dissolved form. Results also confirm the digestive gland key role in ENPs storage, while the hemolymph is the route for QDs and metal mobilization between tissues, highlighting *M. galloprovincialis* as an important target for *in vivo* QDs toxicity. However, the regulatory mechanism of ENPs TK in bivalves is unclear and represents one of the most important areas of research in nanoecotoxicology over the coming years. These results support the hypothesis that the mussel *Mytilus* spp. is suitable model for characterizing the potential impact of ENPs in marine environment (Moore, 2006; Canesi et al., 2012). Furthermore, the ENPs accumulation in marine bivalves is an environmental concern considering their potential nanotoxic effects, trophic transfer and potential increase in individual and population susceptibility to diseases, predator or environmental stress conditions, as well as possible impact on human health due to consumption of QDs-contaminated shellfish.

CHAPTER III

Subcellular partitioning kinetics, metallothionein response and oxidative damage in the marine mussel *Mytilus galloprovincialis* exposed to cadmium-based quantum dots



Part of this Chapter was published in:

- Rocha, T.L., Gomes, T., Durigon, E. G., Bebianno, M.J., 2016. Subcellular partitioning kinetics, metallothionein response and oxidative damage in the marine mussel *Mytilus galloprovincialis* exposed to cadmium-based quantum dots. Science of the Total Environment 554-555, 130-141. doi: 10.1016/j.scitotenv.2016.02.168

Part of this Chapter was presented at:

- Rocha, T.L., Gomes, T., Pinheiro, J.P., Bebianno, M.J., 2014. Tissue-specific accumulation and metallothionein induction in mussels *Mytilus galloprovincialis* exposed to quantum dots and soluble cadmium. 2nd Marine NanoEcoSafety Workshop, Palermo, Italy.
- Rocha, T.L., Gomes, T., Durigon, E.G., Bebianno, M.J., 2015. Bioaccumulation, subcellular partitioning and metabolism of CdTe quantum dots in the marine mussel *Mytilus galloprovincialis*. 25th SETAC Europe Annual Meeting, Barcelona, Spain.

Abstract

The environmental health impact of metal-based nanomaterials is of emerging concern, but their metabolism and detoxification pathways in marine bioindicator species remains unclear. This study investigated the role of subcellular partitioning kinetics, metallothioneins (MTs) response and oxidative damage (lipid peroxidation - LPO) in the marine mussel *Mytilus galloprovincialis* exposed to CdTe quantum dots (QDs) in comparison with its dissolved counterpart. Mussels were exposed to QDs and dissolved Cd for 21 days at $10\ \mu\text{g Cd L}^{-1}$ followed by a 50 days depuration. Higher Cd concentrations were detected in fractions containing mitochondria, nucleus and lysosomes, suggesting potential subcellular targets of QDs toxicity in mussel tissues. Tissue specific metabolism patterns were observed in mussels exposed to both Cd forms. Although MT levels were directly associated with Cd in both forms, QDs subcellular partitioning is linked to biologically active metal (BAM), but no increase in LPO occurred, while in the case of dissolved Cd levels are in the biologically detoxified metal (BDM) form, indicating nano-specific effects. Mussel gills showed lower detoxification capability of QDs, while the digestive gland is the major tissue for storage and detoxification of both Cd forms. Both mussel tissues were unable to completely eliminate the Cd accumulated in the QDs form (estimated half-life time > 50 days), highlighting the potential source of Cd and QDs toxicity for human and environmental health. Results indicate tissue specific metabolism patterns and nano-specific effects in marine mussel exposed to QDs.

Keywords: Nanoparticles, CdTe Quantum dots, cadmium, oxidative stress, Metallothionein, lipid peroxidation, *Mytilus galloprovincialis*.

3.1. Introduction

Cd is a metal with no known biological function widespread in estuarine and coastal environments, which at environmentally relevant concentrations ($0.5 - 10 \mu\text{g Cd L}^{-1}$) induces several toxic effects in marine organisms (e. g. Soto et al., 2002; Eisler, 2007; Serafim and Bebianno, 2007; Macías-Mayorga et al., 2015). Ecotoxicity of Cd was extensively studied in marine bivalves, but few studies exist on the ecotoxicological impact of Cd-based ENPs, such as QDs (Katsumiti et al., 2014; Munari et al., 2014; Rocha et al., 2014, 2015a,b,c). Due to the increasing production and use of QDs (e. g. electronic, chemistry, nanomedicine, cell and molecular biology), the impact of Cd concentration from QDs core and their potential environment risk need to be investigated.

Marine bivalves are useful for characterizing the environmental impact of ENPs in the marine environment (Moore, 2006; Canesi et al., 2012; Rocha et al., 2015b). Among bivalve species, *M. galloprovincialis* have the capacity to accumulate high QDs concentrations, which can induce several cellular damage, such as decrease of LMS, genotoxicity on hemocytes, ROS production and changes in antioxidant capacity in the gills and digestive gland after *in vivo* exposure (CdTe QDs 6 nm; $10 \mu\text{g Cd L}^{-1}$; 14 d) (Rocha et al., 2014; 2015c). CdS QDs toxicity was also associated with extra- and intracellular release of Cd^{2+} ions and oxidative damage in *M. galloprovincialis* hemocytes and gills cells after *in vitro* exposure (5 nm; $10^{-4} - 10^2 \text{ mg Cd L}^{-1}$; 24 h) (Katsumiti et al., 2014). In freshwater mussel *E. complanata*, oxidative stress and genotoxicity were observed after exposure to CdTe QDs ($1.6 - 8 \text{ mg L}^{-1}$; 24 h) (Gagné et al., 2008; Peyrot et al., 2009), while larger CdS-CdTe QDs aggregates were more immunotoxic than smaller ones (1 - 10 nm; $0.05 - 2.7 \mu\text{g L}^{-1}$; 21 h) (Bruneau et al., 2013).

The MoA and toxicity of metal-based ENPs in bivalve cells depend on their subcellular localization and interaction to organelles and/or ligands (Rocha et al., 2015b). However, few studies have addressed subcellular localization of metal-based ENPs in bivalves and their metabolism and detoxification pathways remain unclear. On the other hand, the MoA, toxicity and detoxification mechanisms of dissolved metals in marine organisms are related to their subcellular partitioning and threshold concentration in the biologically active metal form (BAM) or in the biologically detoxified metal form (BDM) (Wallace et al., 2003; Ng and Wang, 2005; Campana et al., 2015).

Cd subcellular partitioning is related to metallothioneins (MTs) which are cysteine-rich proteins with the ability to bind up to 7 divalent or up to 20 monovalent metal ions. In invertebrates, MT molecule can bind at least six Cd atoms (Bebianno and Langston, 1989) and play an important role in the regulation of essential metals (Cu, Zn), detoxification of non-essential metals (Ag, Cd and Hg), scavenging of free radicals and protection against oxidative stress (Palmiter, 1998; Gagné et al., 2008). Furthermore, MTs induction is recognized as a biomarker of metal exposure in monitoring environmental quality (Geret et al., 2003; Cravo et al., 2009). Recent studies highlighted the MT role in metal-based ENPs metabolism and protection against oxidative stress in *M. galloprovincialis* exposed to CuO NPs (< 50 nm; 10 µg L⁻¹; 15 d) (Gomes et al., 2011; 2012) and to Ag NPs (< 100 nm; 10 µg L⁻¹; 15 d) (Gomes et al., 2014).

The impact of QDs in aquatic organisms has been associated with QDs dissolution, release of metal ions (e. g. Cd²⁺), ROS production, oxidative stress and genotoxicity (Gagné et al., 2008; Peyrot et al., 2009; Tang et al., 2013; Rocha et al., 2014, 2015c; Buffet et al., 2015) (Chapters 4 - 5). On the other hand, oxidative damage at DNA level (nuclei and mitochondria) was more sensitive to QDs toxicity than to lipid membrane (Gagné et al., 2008). Therefore, no increase in lipid peroxidation (LPO) was reported in the marine clam *S. plana* (Buffet et al., 2015), nor in the freshwater fish *F. heteroclitus* (Blickley et al., 2014) or in *O. mykiss* (Gagné et al., 2008) after exposure to different QDs, indicating that the mechanisms of defense and detoxification is robust enough to prevent QDs-induced oxidative damage according to concentration and exposure time.

In this context, the hypothesis of this study was to assess the subcellular partitioning kinetics, BAM and BDM concentrations of Cd-based QDs, MTs response and oxidative damage to describe the MoA and to predict the ecotoxicological effects of Cd-based ENPs in marine organisms. Accordingly, the aim of this study was to analyze Cd subcellular partitioning in different tissues (gills and digestive gland) of the marine mussel *M. galloprovincialis* exposed to CdTe QDs and to its dissolved counterpart during a 21 days exposure period followed by a 50 days depuration period. Furthermore, the relationships between Cd subcellular partitioning, MTs response and oxidative damage (LPO) in mussels exposed to both Cd forms (nanoparticulate and dissolved form) were examined to identify which subcellular fraction was more important in the accumulation, detoxification and toxicity of Cd-based QDs.

3.2. Materials and Methods

3.2.1. Experimental design

Mussels *M. galloprovincialis* (60 ± 5 mm shell length) were collected in the Ria Formosa Lagoon (Portugal) (Figs. 1.15 and 1.16) and acclimated during 14 days in static tanks containing natural seawater from the sampling site (salinity = 36.3) at 16 °C and constant aeration. CdTe QDs (6 ± 1 nm) and dissolved Cd ($\text{Cd}(\text{NO}_3)_2 \cdot 4\text{H}_2\text{O}$) stock solutions were prepared in ultrapure water and characterized according to the method described by Sousa and Teixeira (2013). Data on characterization and behaviour of CdTe QDs in seawater were previously reported in Rocha et al. (2014, 2015a) (Chapter 4) and are summarized in the Table 3.1.

After the acclimation period, ninety mussels were placed in 30 L tanks filled with 25 L of seawater (3.6 mussels L^{-1}) and exposed to $10 \mu\text{g Cd L}^{-1}$ of CdTe QDs and to the same concentration of their soluble counterpart, jointly with a control group kept in clean seawater in a duplicate design (2 tanks *per* treatment) for 21 days (exposure period). Seawater was changed daily with redosing of the QDs and dissolved Cd concentration, as previously described in Rocha et al. (2015a) (Chapter 4). At the end of exposure period, mussels were transferred to clean seawater for 50 days (depuration period). Mussels were only fed with natural seawater providing animals with food to avoid starvation and any effects resulting from the interaction of QDs and food (Rocha et al., 2015a; Chapter 2).

Ten mussels from each experimental condition were collected at the beginning of the experiment and after 3, 7, 14 and 21 days of exposure and 15, 20, 30 and 50 days of depuration. Experiments were conducted in a static-renewal condition under 12h:12h light/dark cycles and abiotic parameters was analyzed daily by measuring salinity (36.3 ± 0.07), temperature (16.6 ± 1.2 °C), pH (7.9 ± 0.1) and oxygen saturation (103 ± 1.3 %). No mortality was observed between unexposed mussels and those exposed to both Cd forms by the end of accumulation and depuration periods. Collected mussels were dissected into gills and digestive gland that were immediately frozen in liquid nitrogen and stored at -80 °C until further use.

3.2.2. Subcellular partitioning

Mussel tissues (gills and digestive gland) were divided into five pools (each pool containing two tissues), homogenized in 20 mM Tris-HCl buffer pH 8.6 in an ice bath

(the tissue-to-buffer ratio was 1:5 w. w. tissue/volume of buffer) and subject to differential centrifugation using a biofuge stratus 230V centrifuge (Thermo scientific, Germany) following a procedure adapted from Bebianno and Langston (1989) and Campbell et al. (2005) (Fig. 4.1). An aliquot from whole soft tissue homogenate (Ht) was used to determine total Cd concentration and the remaining homogenate (3 mL) was centrifuged at 30000 g (45 min, 4 °C) and two aliquots of the supernatant were used for LPO (500 µL) and total proteins (100 µL) determination. The resulting pellet comprise the insoluble fraction (IF), which consist of the unbroken cells, cell debris, nuclei, cell membranes, granules and mitochondria. The remaining supernatant was heat-treated at 80 °C (10 min) and re-centrifuged at 30000 g (45 min, 4 °C) to separate the high molecular weight proteins (HMW) (containing lysosomes, peroxisomes and microsomes) and low molecular weight proteins (LMW) which corresponds to heat-stable proteins and MT fraction. An aliquot of the LMW fraction (500 µL) was used for the quantification of MTs concentrations. Cd concentration was analyzed in the three fractions (IF, HMW and LMW) and classified in two categories: BAM (IF + HMW fractions) and BDM (LMW fraction) (Fig. 4.1).

3.2.3. Cd concentrations

For the determination of Cd concentrations, Ht samples and all subcellular fractions were dried (80 °C, 48 h), digested in HNO₃ (80 °C, 4 h) and analyzed by graphite furnace atomic absorption spectrometry (AAS AAnalyst 800 - PerkinElmer). Accuracy of the analytical procedure was assured with certified reference material (TORT-II, Lobster Hepatopaneas) from the National Research Council (Canada) and results agreed with the certified values (certified value: 26.7 ± 0.6 mg Cd kg⁻¹; samples: 28.5 ± 4.5 mg Cd kg⁻¹). Total Cd concentration (Cd-total) (sum from all fractions) and in the subcellular fractions are expressed as µg g⁻¹ of dry weight tissue.

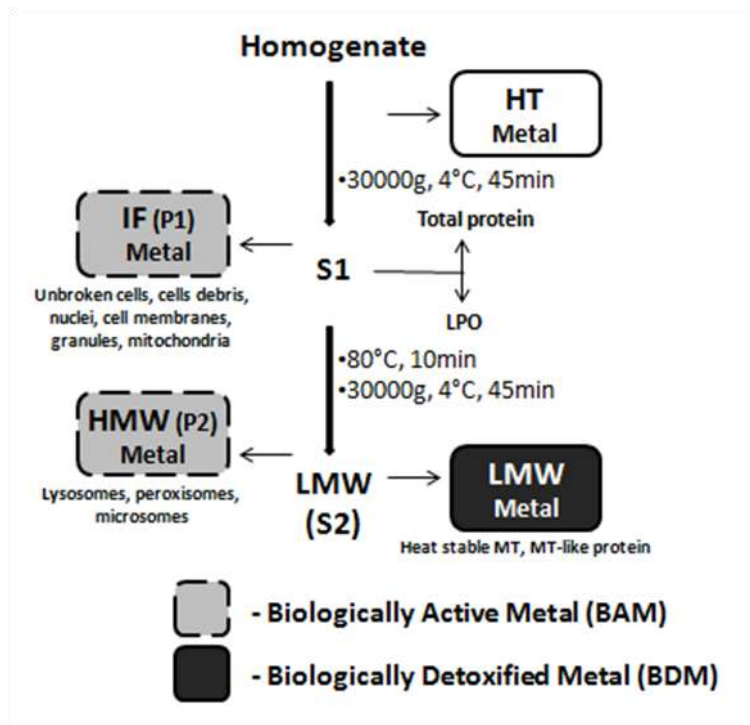


Figure 3.1. Analytical procedure for the subcellular fractionation of mussel tissues by differential centrifugation. After tissue homogenization in Tris-HCl 20 mM pH 8.6 buffer, differential centrifugation and heat treatment steps were used to obtain three subcellular fractions: insoluble fraction (IF: unbroken cells, cells debris, membranes, granules and mitochondria), high-molecular-weight protein fraction (HMW: lysosomes, peroxisomes and microsomes) and low-molecular-weight protein fraction (LMW: heat stable MT and MT-like protein). Cd subcellular partitioning was classified in two categories: biologically active metal (BAM) which included IF and HMW fractions and biologically detoxified metal (BDM) consisted of the LWM fraction. HT = total homogenate; P = pellet; S = supernatant.

3.2.4. Subcellular kinetic models

The accumulation model in the subcellular fractions was estimated by a first-order kinetic model (Serafim et al., 2007), in which the accumulation kinetic is described using the Eq. 3.1.

$$C_B = K_a/K_l C_W (1 - e^{-K_l t}) \quad (\text{Eq. 3.1})$$

where C_B is the Cd concentration in the fractions ($\mu\text{g g}^{-1}$ d. w.), C_W is the Cd concentration in seawater ($\mu\text{g Cd L}^{-1}$), K_a is the accumulation rate ($\text{L g}^{-1} \text{d}^{-1}$), K_l is the loss rate during the accumulation period (d^{-1}), and t is the time during the exposure period (days). Both K_a and K_l were estimated by the Ordinary Least Squares method

using the nonlinear curve-fitting. During the depuration period, C_w is considered zero and the elimination kinetic is described by Eq. 3.2.

$$C_B = C_{B0} e^{-K_e t} \quad (\text{Eq. 3.2})$$

where C_{B0} is the initial Cd concentration in the depuration period ($\mu\text{g g}^{-1}$ d. w.) and K_e the elimination rate during the depuration period (d^{-1}). This constant was used to determine the Cd half-life time ($t_{1/2}$) in mussel tissues subcellular fractions according to the relationship $t_{1/2} = \ln 2 / K_e$. The bioconcentration factor (BCF) considers that C_B reaches a steady state and was estimated according to the relationship $\text{BCF} = K_a / K_e$.

3.2.5. Net accumulation rates

Net accumulation rates for total accumulated Cd ($\text{Cd-total}_{\text{rate}}$), BAM (BAM_{rate}) and BDM (BDM_{rate}) were calculated using Eq. 3.3 following a procedure adapted from Campana et al. (2015):

$$\text{Net accumulation rate}_i = ([\text{Cd}_i]_{\text{exp}} - [\text{Cd}_i]_{\text{control}}) / t \quad (\text{Eq. 3.3})$$

where i is either Cd-total, BAM or BDM; $[\text{Cd}_i]_{\text{exp}}$ is the Cd concentration ($\mu\text{g g}^{-1}$ d. w.) in organisms exposed to QDs or dissolved Cd measured at a time t (day); and $[\text{Cd}_i]_{\text{control}}$ is the mean Cd concentration measured in the unexposed mussels.

3.2.6. Metallothioneins

MTs concentrations were determined by differential pulse polarography, using the standard addition method (Bebianno and Langston, 1989). In the absence of a mussel MTs standard, MTs quantification was based on rabbit liver MT (Sigma-Aldrich; MT-I at 10 mg L^{-1}) and results are expressed as mg g^{-1} of wet weight tissue.

3.2.7. Lipid peroxidation

LPO was evaluated by determining malondialdehyde (MDA) and 4-hydroxyalkenals (4-HNE), both sub-products of polyunsaturated fatty acid peroxidation, using malondialdehyde bis-(dimethyl acetal) (Sigma-Aldrich) as a standard and maximal absorbance at 586 nm (Erdelmeier et al., 1998). LPO levels are expressed as $\text{nmol MDA} + 4\text{-HNE g}^{-1}$ wet weight tissue. Kinetic model parameters (K_a , K_l , K_e and

$t_{1/2}$) of MTs and LPO in the gills and digestive gland of mussels were estimated by a first-order kinetic model (Serafim et al., 2007), as described above.

3.2.8. Total protein concentration

The total protein concentration was measured in the cytosolic fraction according to Bradford method (Bradford, 1976) using Bovin Serum Albumin (Sigma-Aldrich) as a standard. Protein concentrations are expressed as mg g^{-1} wet weight tissue.

3.2.9. Statistical analysis

Statistical analyses were carried out using the Statistica 7.0 software (Statsoft Inc., 2005, Tulsa, OK, USA). The results were compared using parametric tests (two-way ANOVA, followed by the Tukey's test) and/or non-parametric test (Kruskal-Wallis), depending on the distribution of the data and homogeneity of variance (Shapiro-Wilk and Levene's tests). Linear and nonlinear regression analyses were also applied to verify existing relationships between variables.

Principal component analysis (PCA) was used to evaluate the relationship between total Cd concentration in mussel tissues (gills and digestive gland) and in different subcellular fractions (IF, HMW, LMW), levels of MTs and LPO in both tissues of unexposed mussels and Cd-exposed mussels (QDs and dissolved Cd) during the exposure (21 days) and depuration periods (50 days). Results were considered significant when $p < 0.05$.

3.3. Results and discussion

3.3.1. Cd accumulation

QDs tend to aggregate/agglomerate in seawater due to its ionic strength and this behaviour is an important factor for QDs accumulation and subcellular partitioning in *M. galloprovincialis*. The coating of QDs by ionizable carboxylic groups confers negative surface charge in seawater (ζ -potential: -9.4 ± 1.2 mV) and prevents interactions between QDs and different natural organic matter (Rocha et al., 2015a; Chapter 4). Thereby, QDs behaviour in seawater indicates that the QDs homo-aggregates/agglomerates uptake is the major source of Cd for the marine mussels exposed to CdTe QDs. QDs aggregates/agglomerates can be broken in the gills by cilia action and/or taken up by endocytosis in the digestive gland, while gills accumulate principally individual QDs and dissolved Cd (Rocha et al., 2015a,b; Chapter 2).

Therefore, Cd accumulation in both tissues of the marine mussel exposed to CdTe QDs is the result of Cd uptake in different forms: individual QDs (6 ± 1.5 nm), small and large homo-aggregates and free ionic Cd and/or Cd complexes resulting from QDs dissolution (27.6 %) in seawater (Table 3.1; Rocha et al., 2014; 2015a; Chapters 2 and 4).

Table 3.1. Characterization of CdTe quantum dots (QDs) in aqueous medium using different analytical techniques.

Parameters ¹	Techniques ²	Data ³
Individual particle size (nm) ^a	TEM	$2-7^a$; 6 ± 1^b
Shape ^a	TEM	Spheroid ^{a,b}
Hydrodynamic diameter (nm) ^b	DLS	1014 ± 187^b
Polydispersity index ^b	DLS	0.5 ± 0.1^b
ζ -potential (mV) ^b	ELS	-9.4 ± 1.2^b
Isoelectric point (pH) ^b	ELS	10 - 12 ^b
Sedimentation rate - SR (1/h) ^b	THR	Fast SR = $0.88 \pm 5 \times 10^{-4b}$; Slow SR = $0.009 \pm 8.45 \times 10^{-4b}$
Dissolution rate (%) ^b	AGNES, SCP	27.6 ^c
NOM stabilization ^{a,b}	DLS	No stabilization ^c

¹Aqueous medium: Milli-Q water (^a) and seawater (^b).

²TEM: Transmission Electron Microscopy; DLS: Dynamic Light Scattering; ELS: Electrophoretic Light Scattering; THR: Turbidimeter of high resolution; AGNES: Absence of Gradients and Nernstian Equilibrium Stripping; SCP: Stripping Chronopotentiometry.

³Data from the manufacturer PlasmaChem GmbH (^a), Rocha et al., 2014 (Chapter 4) (^b), Rocha et al., 2015a Chapter 2 (^c).

3.3.2. Subcellular partitioning strategy

Most of the research on ecotoxicity of metal-based ENPs in marine organisms is based on total metal concentration in whole soft tissues as a parameter of accumulation and toxicity. However, to the best of our knowledge, this is the first study of metal subcellular partitioning in bivalve species exposed to metal-based ENPs. A first-order kinetic model of tissue specific subcellular partitioning patterns was applied in mussels exposed to Cd-based QDs and dissolved Cd (Figs. 4.1 - 4.3), indicating that ENPs concentrations in the BAM or BDM forms in mussel tissues are important to assess the ENPs accumulation and toxicity patterns in marine bivalves.

Subcellular distribution in *M. galloprovincialis* is Cd form and tissue dependent, with high Cd accumulation in the digestive gland compared to the gills (Figs. 4.1 and

4.2A-B). These results agree with previous ones about tissue specific accumulation of ENPs in bivalve species (Moore et al., 2006; Hull et al., 2011; Gomes et al., 2012; Rocha et al., 2015b; Chapter 2), confirming the importance of digestive gland in the metabolism and detoxification process in bivalve molluscs exposed to ENPs.

3.3.2.1. Gills response

The proportional distribution of each subcellular Cd fraction to the BAM and BDM forms in the gills are in Fig. 4.2A-C. Higher BAM percentage was observed in the gills after exposure to QDs for 21 days (49.2 %) when compared to dissolved Cd (41.6 %). Cd subcellular partitioning for both Cd forms followed a first-order kinetic model and results indicate that the partition of Cd accumulation in QDs-exposed mussels was quicker in the BAM (Ka : $0.48 \text{ L g}^{-1} \text{ d}^{-1}$; Kl : 0.14 d^{-1}) when compared to the BDM form (Ka : $0.15 \text{ L g}^{-1} \text{ d}^{-1}$; Kl : 0.11 d^{-1}) (Fig. 2A; Table 1), indicating that the gills are also a target of Cd-based QDs toxicity. In contrast, in those exposed to dissolved Cd, Cd was more slowly accumulated in the BAM (Ka : $0.17 \text{ L g}^{-1} \text{ d}^{-1}$; Kl : 10^{-7} d^{-1}) than in the BDM form (Ka : $0.41 \text{ L g}^{-1} \text{ d}^{-1}$; Kl : 0.17 d^{-1}). Cd in both forms (BAM and BDM) reached a steady state after 14 days of exposure to QDs, while in those exposed to dissolved Cd, Cd in the BAM form continue linearly to increase until 21 days (BAM $\mu\text{g g}^{-1} \text{ d. w.} = 1.618t + 1.306$, $r = 0.91$, $p < 0.05$) and in the BDM form reached a steady state after 14 days of exposure but with higher levels than in QDs (Fig. 4.3A). These results indicate that mussels may regulate the BDM fraction for both Cd forms, while BAM fraction is partially regulated in mussels exposed to QDs.

The majority of Cd sequestered in the BAM form was distributed in the IF (QDs: 33.7 %; dissolved Cd: 34.5 %) and HMW fraction (QDs: 15.5 %; dissolved Cd: 7.1 %) (Fig. 4.2A-C; Table 4.2). After 3 days of exposure, the Cd accumulation kinetic model in the gills showed an initial linear increase of Cd in the IF of mussels exposed to QDs (1.7-fold) that was even higher in dissolved Cd (20-fold) when compared to unexposed ones ($p < 0.05$). After this time, Cd levels in the IF of QDs-exposed mussels continue to linearly increase until the end of the exposure period (Ka : $0.03 \text{ L g}^{-1} \text{ d}^{-1}$; Kl : $\geq 10^{-7} \text{ d}^{-1}$), while in those exposed to dissolved form, Cd levels in the IF reached a steady state (Ka : $0.51 \text{ L g}^{-1} \text{ d}^{-1}$; Kl : 0.39 d^{-1}) (Table 4.2). This increase of Cd accumulated in the IF that contains mitochondria and nucleus is in agreement with previous studies about QDs toxicity, which showed that QDs induce mitochondrial and

DNA damage in mammals and bivalve cells (Gagné et al., 2008; Li et al., 2011; Aye et al., 2013; Munari et al., 2014; Rocha et al., 2014) (Chapter 4).

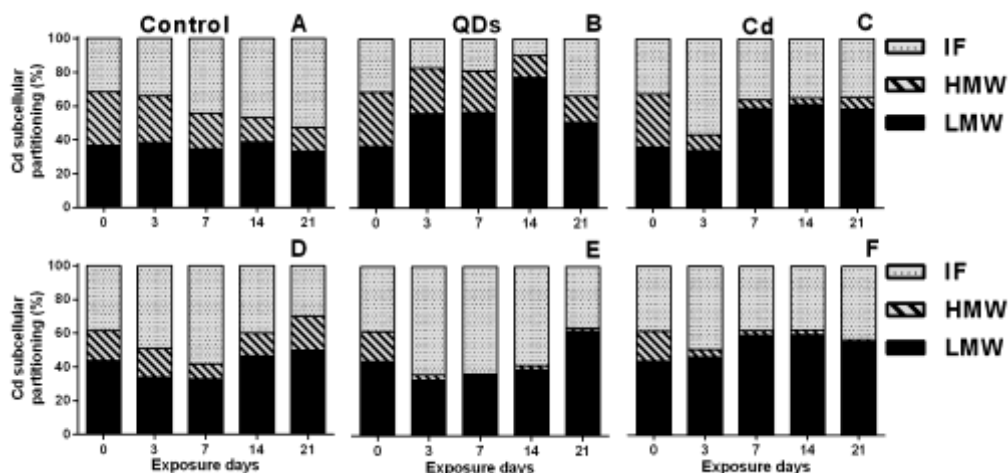


Figure 3.2. Cd distribution (%) in the insoluble (IF), high-molecular-weight proteins (HMW) and low-molecular-weight proteins (LMW) fractions of the gills (A-C) and digestive gland (D-F) of mussels *M. galloprovincialis* from control (A,D), exposed to CdTe quantum dots (QD) (B,E) and to dissolved Cd (C,F) during the exposure period (21 days).

Mitochondria was identified as an early target of QDs toxicity in mammal cells (Li et al., 2011), while mitochondrial damage induced by dissolved Cd in bivalve gills can impair whole-organism metabolism because gills are the major site for respiration, nutrient acquisition and ion osmoregulation (Sokolova et al., 2005). Furthermore, QDs can enter the nucleus *via* the nuclear pore complexes and interact with oligonucleotides in mammal cells (Aye et al., 2013). In marine bivalves, DNA damage induced by Cd-based QDs was described in *M. edulis* and *M. galloprovincialis* hemocytes after *in vitro* exposure to CdS QDs (4 nm; 10 mg L⁻¹; 4 h and 5 nm; 0.001 - 100 mg L⁻¹; 24 h, respectively) (Munari et al., 2014; Katsumiti et al., 2014a). Genotoxic effects of CdTe QDs were also observed in *M. galloprovincialis* hemocytes after *in vivo* exposure (6 nm; 10 µg L⁻¹; 14 d) (Rocha et al., 2014; Chapter4) confirming the genotoxic effects of theses ENPs on marine bivalves.

The Cd accumulation kinetic model in the gills HMW fraction showed a similar linear increase after 3 days of exposure to QDs (2.6-fold) and dissolved Cd (4.2-fold) when compared to unexposed mussels ($p < 0.05$; Fig. 4.2A-C), while lower Cd

concentration was observed in the QDs-exposure mussels (4.5-fold) compared to dissolved Cd-exposed ones after 7 days of exposure ($p < 0.05$). After this time, Cd levels in the HWM fraction of QDs-exposed mussels reached a steady state (Ka : $0.021 \text{ L g}^{-1} \text{ d}^{-1}$; Kl : 0.02 d^{-1}), while in those exposed to dissolved form, Cd concentration increase until 21 days of exposure (Ka : $0.014 \text{ L g}^{-1} \text{ d}^{-1}$; Kl : 0.013 d^{-1}) (Fig. 4.2A-C; Table 4.2). In QDs-exposed mussels, higher Cd accumulation in the HMW fraction was observed in gills compared to digestive gland (3.1-fold) after 21 days of exposure, indicating that the intracellular digestion of food particle inside to gills lysosomes and nutritional status are potential target of the QDs exposure. Results agree with previous studies which indicated the presence of metal-based ENPs inside to endocytic-lysosomal system in the gills of bivalve species, such as reported for the oyster *C. gigas* exposed to ZnO NPs (31.7 nm; $50 \mu\text{g L}^{-1}$ - 50 mg L^{-1} ; 96 h) (Trevisan et al., 2014) and for the clam *S. plana* exposed to Au NPs (5 - 40 nm; $100 \mu\text{L}^{-1}$; 16 d) (Joubert et al., 2013).

3.3.2.2. Digestive gland response

QDs uptake is mainly through the digestive gland cells *via* endocytotic mechanisms, following intracellular digestion, storage or dissolution into lysosomes at pH acid (Katsumiti et al., 2014a; Rocha et al., 2015a,b). After 3 days of exposure, subcellular partitioning results indicate a higher proportion of Cd in the BAM form in the digestive gland of QDs-exposed mussels (49.2 %) when compared to dissolved Cd-exposed ones (41.6 %) (Fig. 4.2D-F). However, at the end of the exposure period, lower Cd distribution in the BAM form was observed for QDs (38.2 %) compared to dissolved Cd (44.9 %). In contrast to the gills, Cd subcellular partitioning in the digestive gland show that in QDs-exposed mussels, Cd accumulated in the BAM form reached a steady state after 14 days of exposure to QDs (Ka : $0.44 \text{ L g}^{-1} \text{ d}^{-1}$; Kl : 0.14 d^{-1}), while BDM increased linearly over exposure time ($\text{BDM } \mu\text{g g}^{-1} \text{ d. w.} = 1.75t - 0.7586$, $r = 0.97$, $p < 0.01$; Ka : $0.17 \text{ L g}^{-1} \text{ d}^{-1}$; Kl : 10^{-7} d^{-1}) (Fig. 4.3B; Table 4.2). On the other hand, in dissolved-Cd exposed mussels, Cd in the BAM and BDM form increased linearly over exposure time ($\text{BAM } \mu\text{g g}^{-1} \text{ d. w.} = 1.588t + 0.9066$, $r = 0.92$, $p < 0.05$; Ka : $0.16 \text{ L g}^{-1} \text{ d}^{-1}$; Kl : 10^{-7} d^{-1} and $\text{BDM } \mu\text{g g}^{-1} \text{ d. w.} = 2.077t + 0.5022$, $r = 0.97$, $p < 0.05$; Ka : $0.18 \text{ L g}^{-1} \text{ d}^{-1}$; Kl : 10^{-7} d^{-1} , respectively) and levels reached in the BDM form were similar to those of the mussels exposed to QDs (Fig. 4.3B; Table 4.2). The linear increase and the similar levels of Cd accumulated in BDM form in the digestive

gland of mussels exposed to both Cd forms confirm the role of digestive gland in the storage and detoxification of QDs and dissolved Cd.

Table 3.2. Accumulation rate (Ka), loss rate (Kl), elimination rate (Ke), half-life ($t_{1/2}$) and bioconcentration factor (BCF) in the gills and digestive gland of mussels *M. galloprovincialis* from controls (C), exposed to CdTe QDs and to dissolved Cd (Cd) during the exposure (21 days) and the depuration (50 days) periods.

Type of exposure	Tissue ^a	Subcellular fraction (Biologically metal form)	Accumulation			Depuration			BCF ^c
			Ka (L g ⁻¹ d ⁻¹)	Kl (d ⁻¹)	R	Ke (d ⁻¹)	$t_{1/2}$ (d) ^b	r	
QDs	G	IF	0.03	$\geq 10^{-7}$	0.79	0.028	25	0.63	1.1
		HMW	0.02	0.02	0.66	-	> 50	-	-
		IF + HMW (BAM)	0.48	0.14	0.83	0.01	68.8	-	48
		LMW (BDM)	0.15	0.11	0.86	-	> 50	-	-
	DG	IF	0.26	$\geq 10^{-7}$	0.91	0.012	57	-	21.7
		HMW	0.01	0.007	0.55	0.009	75	0.42	1.1
		IF + HMW (BAM)	0.44	0.14	0.81	0.011	64.7	-	40
		LMW (BDM)	0.17	$\geq 10^{-7}$	0.91	0.018	38	0.30	8.3
Cd	G	IF	0.51	0.39	0.78	-	-	-	-
		HMW	0.014	0.013	0.24	-	-	-	-
		IF + HMW (BAM)	0.17	$\geq 10^{-7}$	0.95	-	-	-	-
		LMW (BDM)	0.41	0.17	0.92	-	-	-	-
	DG	IF	0.16	$\geq 10^{-7}$	0.95	-	-	-	-
		HMW	0.03	0.21	0.74	-	-	-	-
		IF + HMW (BAM)	0.16	$\geq 10^{-7}$	0.95	-	-	-	-
		LMW (BDM)	0.18	$\geq 10^{-7}$	0.88	-	-	-	-

^a G - gills; DG - digestive gland;

^b Half-life ($t_{1/2}$) = $\ln 2/K_e$;

^c BCF = K_a/K_e

Similarly to the gills, Cd accumulated in the BAM form was higher in the IF after exposed to QDs (36.5 %; Ka : 0.26 L g⁻¹ d⁻¹; Kl : 10^{-7} d⁻¹) and dissolved Cd (43.5 %; Ka : 0.16 L g⁻¹ d⁻¹; Kl : 10^{-7} d⁻¹), indicating that Cd-based QDs can also induce mitochondrial and DNA damage in the digestive gland cells. Cd accumulation in the HMW fraction that contains lysosomes was low in mussels exposed to QDs (1.7 %; Ka : 0.01 L g⁻¹ d⁻¹; Kl : 0.007 d⁻¹) and dissolved Cd (1.4 %; Ka : 0.03 L g⁻¹ d⁻¹; Kl : 0.21 d⁻¹) for 21 days (Fig. 4.2D-F) indicating that free Cd²⁺ released from QDs core into lysosomes may first be directed to LMW fraction for detoxification. However, the

accumulation of QDs in the HMW fraction induce changes in size and structure of lysosomes, resulting in a decrease in the LMS and cellular stress (Katsumiti et al., 2014a; Rocha et al., 2014). LMS damage in bivalve molluscs exposed to different ENPs (e. g. Ag, Au, C₆₀, TiO₂ NPs) was previously reported (Tedesco et al., 2008; Moore et al., 2009; Barmo et al., 2013; Hu et al., 2015), confirming that the endocytic and lysosomal pathways are target of ENPs toxicity in bivalve cells. However, knowledge about digestion time of the ENPs inside lysosomes associated with hydrolytic potential of the ENP-containing lysosomes is not available and is of major interest for future studies of lysosomal biomarkers in mussel digestive cells.

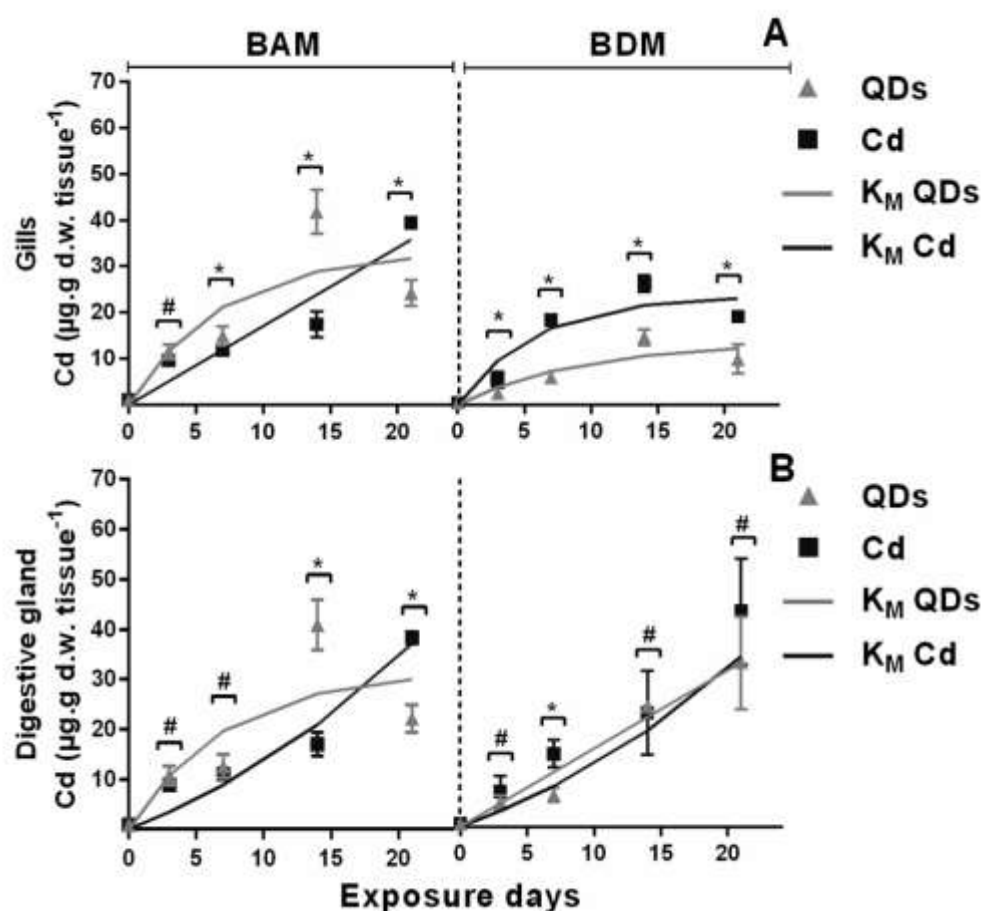


Figure 3.3. Cd concentration (mean \pm std $\mu\text{g g}^{-1}$ d. w. tissue) and first-order kinetic model (K_M) of the Cd accumulated in the biologically active (BAM) and detoxified (BDM) form in the gills (A) and digestive gland (B) from mussels *M. galloprovincialis* exposed to CdTe quantum dots (QDs) and to dissolved Cd during the exposure period (21 days). Symbols # and * indicate significant differences between unexposed and Cd-exposed mussels (QDs or dissolved Cd) and between all treatments at each time of exposure, respectively ($p < 0.05$).

3.3.3. Net accumulation rates

Net Cd-total, BAM and BDM accumulation rates in mussels exposed to both Cd forms are Cd-form and tissue dependent (Fig. 4.4A-F). Interestingly, similar Cd accumulation rates were observed in the BAM form for both mussel tissues during the exposure period for both Cd forms (21 days; $p > 0.05$), while lower BDM rates were observed in the gills compared to digestive gland (3.6-fold, $p < 0.05$). QDs induced higher BAM rate in the gills (7 and 14 days) and digestive gland (14 days) when compared to dissolved Cd ($p < 0.05$), whilst lower BDM rate was identified in the gills from QDs-exposed mussels (1.8 - 3.3 folds, $p < 0.05$) (Fig. 4.4A-F). On the other hand, both Cd forms induced similar BDM rates in the digestive gland at the end of exposure period (QDs: $1.7 \pm 0.5 \mu\text{gCd g}^{-1} \text{ d}^{-1}$; dissolved Cd: $2.2 \pm 0.5 \mu\text{gCd g}^{-1} \text{ d}^{-1}$, $p > 0.05$). These results show that the net accumulation rate of QDs in the BAM and BDM forms are tissue-specific and indicate that the gills have lower detoxification capacity of Cd accumulation in the nanoparticulate form. The increase or decrease in Cd-total and BAM rates of QDs were observed over the exposure time, suggesting that alterations of QDs accumulation rates might occur due to the different QDs behaviour in seawater. Similarly, the ENPs aggregation/agglomeration kinetics affects their distribution in the environment and the route of uptake by estuarine and marine invertebrates (Matranga and Corsi et al., 2012; Minetto et al., 2014; Rocha et al., 2015b).

3.3.4. Cd elimination

During the depuration period, differential tissue elimination responses were observed in QDs-exposed mussels. Although total Cd concentration in QDs-exposed mussels tend to decrease during the depuration period (50 days), both mussel tissues were unable to completely eliminate the Cd accumulated in the QDs form (Fig. 4.5A-B), which is supported by the Cd half-life time ($t_{1/2}$) calculated for BAM and BDM in the gills (BAM $t_{1/2} = 68.8$ days; BDM $t_{1/2} > 50$ days) and digestive gland (BAM $t_{1/2} = 64.7$ days; BDM $t_{1/2} = 38$ days) (Fig. 4.5A-B; Table 4.2; Fig. 4.6). In the mussel gills, while Cd was eliminated from the BAM form ($Ke: 0.01 \text{ d}^{-1}$) it increased in the BDM form showing a Cd redistribution. However, in the digestive gland, Cd decreases in both forms at a similar rate (BAM $Ke: 0.011 \text{ d}^{-1}$; BDM $Ke: 0.018 \text{ d}^{-1}$). On the other hand, BAM and BDM levels in mussels exposed to dissolved Cd significantly increased in the gills (BAM: 2.2-fold; BDM: 1.7-fold) and digestive gland (BAM: 42-fold; BDM: 66.2-fold) at the final depuration phase when compared to the initial of the depuration phase

($p < 0.05$). Due to the reduced number of data in the Cd dissolved-exposed mussels during the depuration phase, the $t_{1/2}$ in subcellular fractions was unable to be determined but was longer than 50 days (Table 4.2). Although no data is available for Ke and $t_{1/2}$ in the subcellular fractions of marine invertebrates exposed to ENPs, similar results of dissolved Cd $t_{1/2}$ was also reported for the subcellular fractions of the marine clam *R. decussatus* exposed to $40 \mu\text{g L}^{-1}$ of dissolved Cd ($Ke = 0.010 - 0.023 \text{ d}^{-1}$; $t_{1/2} = 30 - 71$ days) (Serafim and Bebianno, 2007).

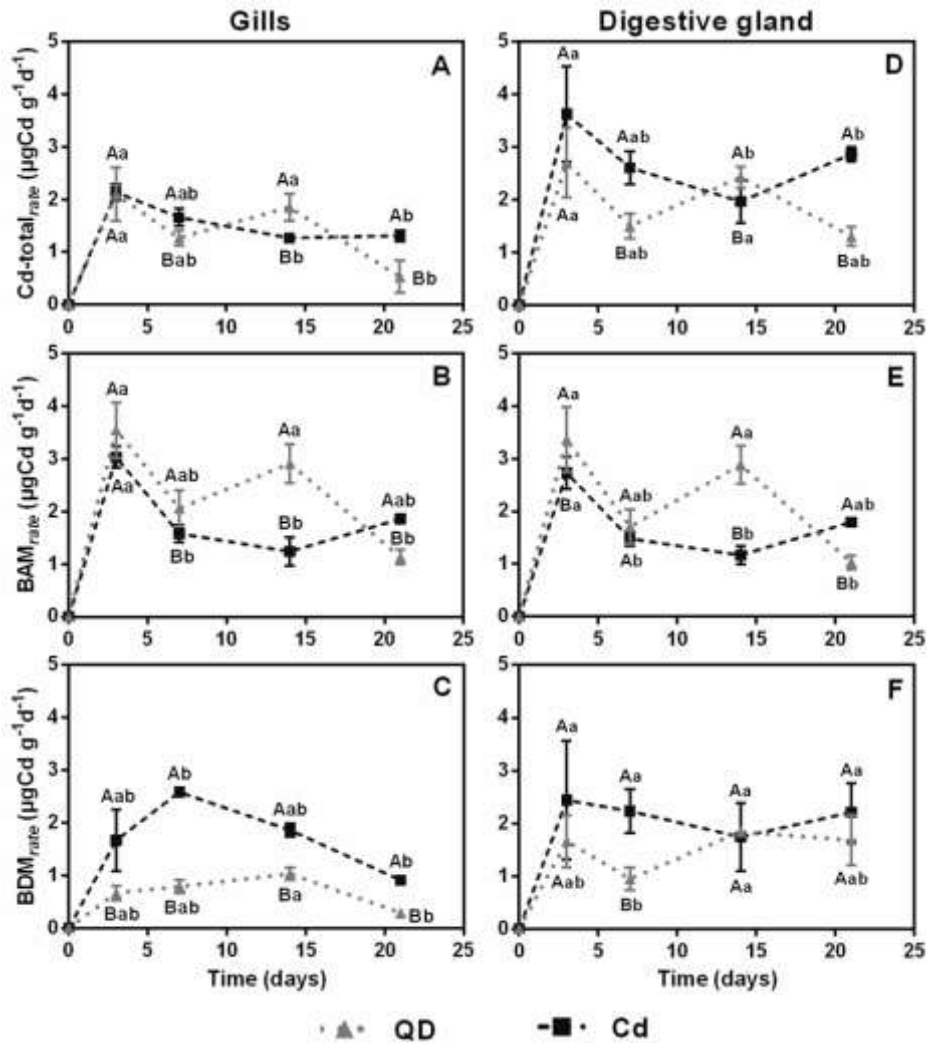


Figure 3.4. Net accumulation rates for total accumulated Cd (Cd-total), biologically active metal (BAM) or biologically detoxified metal (BDM) in the gills (A-C) and digestive gland (D-E) from mussels *M. galloprovincialis* exposed to CdTe quantum dots (QDs) and to dissolved Cd during the exposure period (21 days). Capital and lower letters indicate significant differences between treatments at each time of exposure and within treatment during the exposure period, respectively ($p < 0.05$).

The estimated $t_{1/2}$ of CdTe QDs for *M. galloprovincialis* subcellular fractions is longer than $t_{1/2}$ of Ag NPs (10 - 80 nm; $110 - 151 \text{ ng L}^{-1}$; 12 h) for scallop *Chlamys*

islandica whole soft tissues ($t_{1/2}$: 1.4 - 4.3 days and 17 - 50 days for fast and slow compartments; Al-Sid-Cheikh et al., 2013) and CuO NPs (< 100 nm; 200 $\mu\text{g g}^{-1}$ d. w. sediment) for marine clam *M. balthica* whole soft tissues ($t_{1/2}$ > 15 days; Dai et al., 2013). These results show that the *M. galloprovincialis* accumulate significant concentration of QDs during the exposure period (21 days) followed by a no efficient elimination process from both mussel tissues.

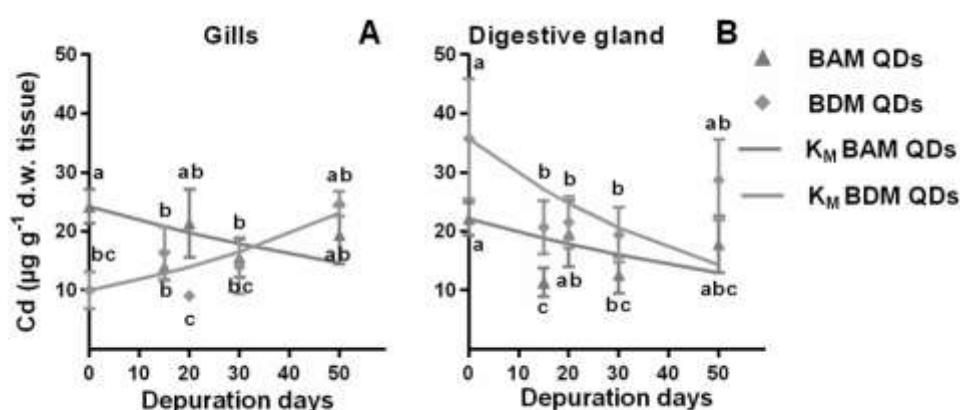


Figure 3.5. Cd concentration (mean \pm std $\mu\text{g g}^{-1}$ d. w. tissue) and first-order kinetic model (K_M) of the Cd in the biologically active (BAM) and detoxified (BDM) forms in the gills (A) and digestive gland (B) from mussels *M. galloprovincialis* exposed to CdTe quantum dots (QDs) and to dissolved Cd during the depuration period (50 days). Different letters indicate significant differences of each treatment during the depuration period ($p < 0.05$).

Even after 50 days of depuration, Cd concentrations in both mussel tissues exposed to Cd-based QDs and dissolved Cd were higher than the Environmental Quality Standard established by European Community (1 $\mu\text{g Cd g}^{-1}$ w. w. tissue) and by Hong Kong, Australia and New Zealand (2 $\mu\text{g Cd g}^{-1}$ w. w. tissue) and United States (3.7 $\mu\text{g Cd g}^{-1}$ w. w. tissue) (Kruzynski, 2003), highlighting the potential source of Cd and QDs toxicity for human health if QDs will be present in this species at these levels. Furthermore, these results are relevant in environmental health assessment since previous studies reported trophic transfer of Cd-based QDs (Bouldin et al., 2008; Lewinski et al., 2011; Werlin et al. 2011; Jackson et al. 2012; Lee and An, 2014). Furthermore, trophic transfer of metals is dependent on the subcellular metal partitioning in prey and on the digestive capacity of the predator (Rainbow and Smith,

2010; Freitas et al., 2012), indicating the importance of subcellular partitioning of ENPs to predict its potential toxicological effects in the trophic web.

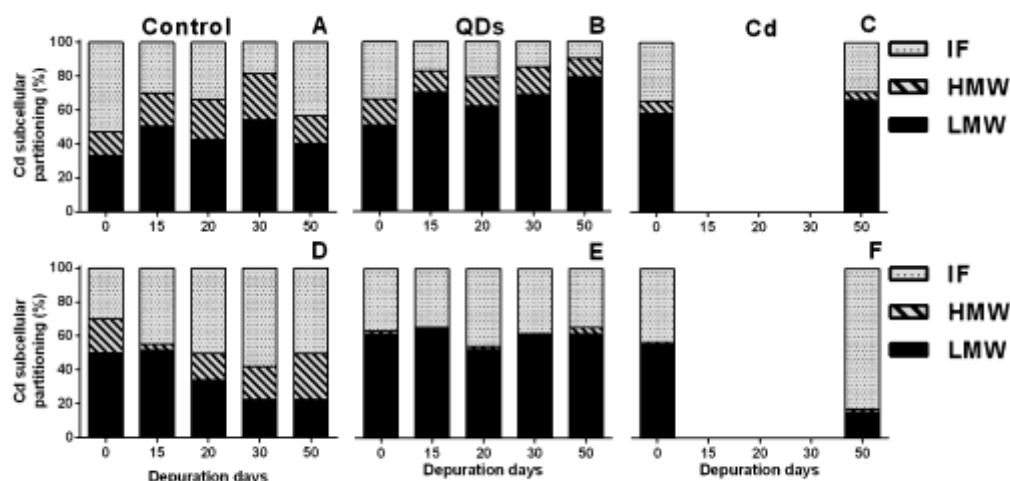


Figure 3.6. Cd distribution (%) in the insoluble (IF), high-molecular-weight protein (HMW) and low-molecular-weight protein fractions (LMW) subcellular fractions of the gills (A-C) and digestive gland (D-F) of mussels *M. galloprovincialis* from control (A,D), exposed to CdTe quantum dots (QDs) (B,E) and to dissolved Cd (C,F) during the depuration period (50 days).

3.3.5. MTs response

Although some toxic effects of Cd-based QDs and other ENPs in bivalves have been described in previous studies (i. e. Gagné et al., 2008; Peyrot et al., 2009; Bruneau et al., 2013; Katsumiti et al., 2014; Rocha et al., 2014; 2015b,c) (Chapters 2,4 and 5), the information regarding the metabolism and detoxification mechanism of metal-based ENPs in marine organisms is scarce. On the other hand, Cd detoxification in bivalve tissues involves Cd binding in the cytosol to metal-binding proteins like MTs to form Cd-MTs complexes followed by biomineralization (transfer and incorporation of Cd-MTs in lysosomes) (Bebianno and Langston, 1993; Viarengo and Nott, 1993; Marigómez et al., 2002; Liu and Wang et al., 2011). MTs response in mussels exposed to Cd-based QDs is, like for dissolved Cd, tissue-specific, with higher MTs levels in the digestive gland compared to the gills (Fig. 4.7A). After 3 days of exposure, MTs induction in the gills of QDs-exposed mussels was higher compared to dissolved Cd-exposed ones (0.22-fold, $p < 0.05$), while the opposite occurred after 7 (0.34-fold) and 14 days of exposure (0.80-fold, $p < 0.05$; Fig. 4.7A). At the end of the exposure period, MTs in the gills of mussels exposed to both Cd forms return to basal levels ($p > 0.05$).

MTs response in the gills seems to be associated with Cd in the BDM fraction (LMW) only for dissolved Cd (MTs $\mu\text{g g}^{-1}$ d. w. tissue = $3.707 [\text{Cd}_{\text{BDM}}] + 130.4$, $r = 0.79$, $p < 0.05$; Fig. 4.7A), indicating different MTs response in the gills of QDs-exposed mussels and an alternative elimination pathways in this organ.

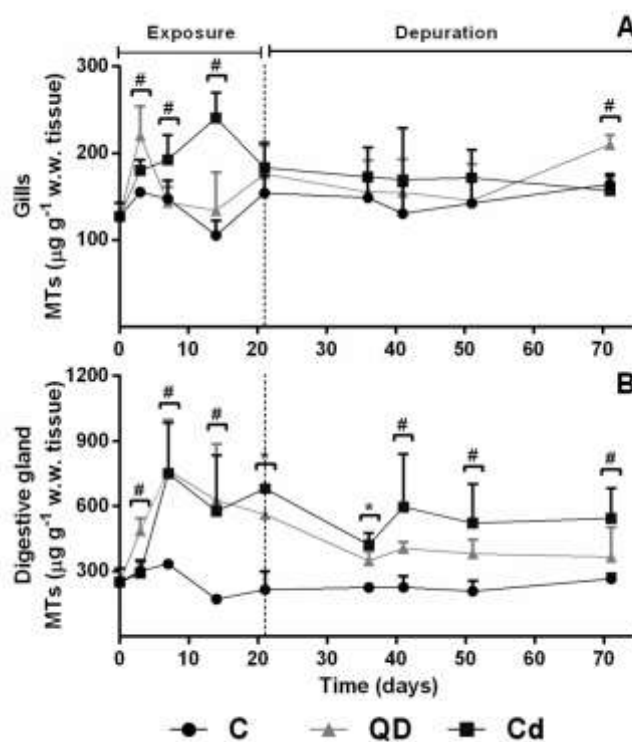


Figure 3.7. MTs concentration (mean \pm std $\mu\text{g g}^{-1}$ w. w. tissue) in the gills (A,B) and digestive gland (C,D) of mussel *M. galloprovincialis* from controls (C), exposed to CdTe quantum dots (QDs) and to dissolved Cd (Cd) during the exposure period (21 days) (A,C) and depuration (50 days) periods (B,D). Symbols # and * indicate significant differences between Cd-exposed mussels (QDs or dissolved Cd) and to unexposed and between all treatments at each time of exposure, respectively ($p < 0.05$).

In seawater, Cd is released from QDs core (27.6 % in this case) and Cd-chloro-complexes are taken up in the gills by passive diffusion and/or via active transport pumps for the essential metals (Ca^{2+} - channels) (Marigómez et al., 2002; Hull et al., 2013; Rocha et al., 2015a) (Chapter 2). Cd released from QDs core is detoxified in the BDM form where Cd is bound to MT forming a Cd-MT complex that can either be transported by the hemolymph to other tissues or precipitate into lysosomes (in the HMW fraction) and be eliminated by exocytosis (Soto et al., 2002; Marigómez et al.,

2002). On the other hand, the presence of QDs aggregates/agglomerates leaves a small role for MTs in the gills, where they are mainly broken down by cilia action and transported to the digestive gland for further detoxification (Joubert et al. 2013; Katsumiti et al., 2014; Rocha et al., 2015b) (Chapter 2). Overall, results confirm that the gills have lower detoxification capability for Cd-based QDs compared to their dissolved counterparts probably due to the presence of aggregates/agglomerates. In an ecotoxicological context, MTs results are similar to those from the freshwater mussel *E. complanata* exposed to CdTe QDs (1.6 - 8 mg L⁻¹; 24 h), where the decrease of MTs levels in the gills was associated with oxidative stress originated by the production of the radical superoxide anion (O₂^{•-}) (Peyrot et al., 2009). The gills of mussels *M. galloprovincialis* exposed to CdTe QDs (CdTe QDs 6 nm; 10 µg Cd L⁻¹; 14 days) was also more susceptible to changes in the antioxidant system compared to the digestive gland, suggesting ROS formation (Rocha et al., 2015c) (Chapter 5), which can also explain the results obtained for MT induction in this tissue.

In the digestive gland, MTs response was similar in mussels exposed to both Cd forms (Fig. 4.7B). After 3 days of exposure, similarly to the gills, a quicker MTs induction occurred in the digestive gland of mussels exposed to QDs compared to dissolved-Cd exposed ones (0.67-fold, $p < 0.05$) but, after 7 days, MTs levels were similar in mussels exposed to both Cd forms (1.3 and 1.2-fold for QDs and dissolved Cd, respectively; $p > 0.05$; Fig. 4.7B). After this period, MTs levels reached a steady state with similar levels between both forms (764 ± 233 and 752 ± 241 µg g⁻¹ w. w. tissue for QDs and dissolved Cd exposure, respectively).

Similarly to what was detected in the accumulation period, MTs levels were higher in the digestive gland compared to the gills during the depuration period (Fig. 4.7A-B). In fact, MTs concentrations in the gills slowly decreased during the depuration period in QDs-exposed mussel (Ke : 0.002 d⁻¹) and dissolved Cd-exposed ones (Ke : 0.003 d⁻¹) but with similar rates (Table 4.3). However, at the end of the depuration period, MTs levels in QDs-exposed mussels increased and were significantly higher compared to unexposed mussels (1.38-fold) and lower compared to dissolved Cd-exposed mussels (2.0-fold, $p < 0.05$; Fig. 5A). In *M. galloprovincialis* exposed to QDs, detoxification mechanism is related to the Cd-MTs turnover (synthesis and degradation), where Cd released from Cd-MT complex is sequestered by newly synthesized MTs, like to dissolved Cd (Bebianno and Langston, 1993; Liu and Wang et al., 2011).

The estimated MT $t_{1/2}$ in the gills (QDs: 433 days; dissolved Cd: 201 days) is longer compared to the digestive gland (QDs: 46 days; dissolved Cd: 80 days) (Table 4.3), indicating that MTs turnover in *M. galloprovincialis* exposed to both Cd forms is Cd form and tissue specific. The difference of MTs and Cd $t_{1/2}$ in mussels exposed to QDs and dissolved Cd could result from Cd translocation between subcellular fractions (Fig. 4.6), intracellular QDs dissolution and release of dissolved Cd, as well as speciation of Cd ions with other ligands, and the oxidant intracellular condition induced by both Cd forms (Gagné et al., 2008b; Rocha et al., 2015c) (Chapter 5). The $t_{1/2}$ of Cd in bivalve species is related to MTs turnover (synthesis and degradation), where Cd released from Cd-MT complex is sequestered by newly synthesized MTs (Bebianno and Langston, 1993; Liu and Wang et al., 2011).

Table 3.3. Accumulation rate (Ka), loss rate (Kl), elimination rate (Ke) and half-life ($t_{1/2}$) of MTs and LPO in the gills and digestive gland of mussels *M. galloprovincialis* from controls (C), exposed to CdTe QDs and to dissolved Cd (Cd) during the exposure (21 days) and the depuration (50 days) periods.

Parameter	Type of exposure	Tissue ^a	Accumulation			Depuration		
			Ka (L g ⁻¹ d ⁻¹)	Kl (d ⁻¹)	r	Ke (d ⁻¹)	$t_{1/2}$ (d) ^b	r
MTs	QDs	G	71.3	4.2	-	0.002	433.2	-
	Cd		13.6	0.66	-	0.003	201	0.148
	QDs	DG	35.5	0.55	0.51	0.015	46	0.65
	Cd		19.7	0.29	0.59	0.009	80	-
LPO	QDs	G	43.6	16.6	-	0.006	117	-
	Cd		14.3	3.9	-	-	-	-
	QDs	DG	40.5	19.8	-	0.010	70	0.65
	Cd		0.77	0.07	0.92	0.023	31	0.72

^a G = gills; DG = digestive gland.

^b Half-life ($t_{1/2}$) = $\ln 2 / Ke$.

^c BCF = Ka / Ke

Based in the conceptual framework between the redox cycling of MTs and metal metabolism proposed by Gagné et al. (2008) and the linear increase of SOD activity in the *M. galloprovincialis* gills over the time of exposure to CdTe QDs described by Rocha et al. (2015c) (Chapter 5), the present study suggest that MTs in mussels exposed to QDs function as a scavenging for free radicals limiting the effects of hydroxyl and

superoxide radical by scavenging them and inducing the activity of SOD in the mussel gills more than a detoxification mechanism. As the oxidized MT in bivalve species is more closely related to metal detoxification, while their reduced form is associated with metal transport and oxidative damage (Gagné et al., 2008b), further studies about the relationships between oxidized and reduced MTs levels in mussels Cd-based ENPs are needed. Similarly, the dual role of MTs in the ENPs metabolism and protection against ENP-induced oxidative stress was recently reported in the gills and digestive gland of *M. galloprovincialis* exposed to CuO NPs (< 50 nm; 10 µg L⁻¹; 3 - 15 d) (Gomes et al., 2011; 2012), Ag NPs (< 100 nm; 10 µg L⁻¹; 3 - 15 d) (Gomes et al., 2014) and in the clam *S. plana* exposed to Au NPs (5 and 40 nm; 100 µg L⁻¹; 16 d) (Pan et al., 2012).

Results also indicate that there are nano-specific effects of QDs in the Cd subcellular partitioning during the exposure and depuration periods and highlight the importance of further studies of metal-MTs complex turnover to better understand ENPs detoxification in mussel tissues as well as the use of MTs as a biomarker of metal-based ENPs exposure. Although this is the first time that the data on the interaction between QDs and marine mussel MTs is reported, the *in vitro* interaction between rabbit liver MTs and Cd-based QDs was recently reported (Tmejova et al., 2014, 2015), indicating that QDs size and electrostatic attraction influence the QDs-MTs complex formation.

3.3.6. Oxidative damage

LPO induced by Cd-based QDs in marine mussels is tissue and exposure time dependent, with higher levels in the digestive gland compared to the gills (Fig. 4.8A-B). After 21 days of exposure, LPO levels in the gills significantly decreased in the mussels exposed to QDs compared to unexposed ones (0.94-fold, $p < 0.05$) (Fig. 4.8A) and was negatively correlated with the increase of Cd levels in the IF (LPO nmol g⁻¹ w. w. = $-0.8478 [\text{Cd}_{\text{QDs}}] + 36.05$, $r = 0.85$, $p < 0.05$) and BDM form (LPO nmol g⁻¹ w. w. = $-0.4352 [\text{Cd}_{\text{QDs}}] + 34.1$, $r = 0.85$, $p < 0.05$), while no significant relationship was observed with the Cd in the HMW fraction ($p > 0.05$). In opposite to the gills, LPO levels in the digestive gland of QDs-exposed mussels is significantly higher when compared to unexposed mussels, especially after 3 and 14 days of exposure ($p < 0.05$) but significantly lower than those exposed to dissolved Cd-exposed after 21 days (4.9-fold, $p < 0.05$) (Fig. 4.8B).

During the depuration period, LPO levels in both tissues of QDs-exposed mussels are similar at the end of the exposure period ($p < 0.05$; Fig. 4.8A-B), with

higher $t_{1/2}$ in the gills (117 days) compared to the digestive gland (70 days) (Table 4.3). On the other hand, the estimated LPO $t_{1/2}$ in the digestive of QDs-exposed mussels (117 days) is longer compared to dissolved Cd ones (31 days). Results indicated that Cd subcellular partitioning associated with the increase of antioxidant enzymes, such as SOD, GPx and GST activities (Rocha et al., 2015c) (Chapter 5) may be enough to prevent LPO damage only in the gills. However, cell defense mechanisms (antioxidant enzymes activities and MTs response) in the digestive gland were not enough to prevent LPO. Results disagree with previous studies that showed no increase in LPO levels in whole soft tissues of the clam *S. plana* exposed to CdS QDs (5 - 6 nm; 10 $\mu\text{g Cd L}^{-1}$; 14 d) (Buffet et al., 2015), or in the *O. mykiss* hepatocytes after *in vitro* exposure to cysteamine-coated CdTe QDs (0.4 - 250 $\mu\text{g mL}^{-1}$; 48 h) (Gagné et al., 2008) and in the fish *F. heteroclitus* after dietary exposed to lecithin-encapsulated CdSe/ZnS QDs (10 $\mu\text{g d}^{-1}$; 85 d) (Blickley et al., 2014), indicating that the mussel digestive gland cells are more sensitive to QDs-induced oxidative damage.

In opposite to QDs, dissolved Cd exposure induces a totally different LPO pattern in both tissues. LPO levels were not significantly different in the gills while in the digestive gland LPO linearly increase until 14 days of exposure (LPO nmol g^{-1} w. w. = $0.5061t + 6.984$, $r = 0.93$, $p < 0.05$) and reached a steady state afterwards (Fig. 3.8B). Furthermore, LPO was positively related with Cd levels in the BDM form (LPO nmol g^{-1} w. w. = $0.1257 [\text{Cd}] + 1.554$, $r = 0.83$, $p < 0.05$), while no correlation was observed with Cd in the BAM form ($p < 0.05$). During the depuration, LPO levels in the gills of mussels exposed to dissolved Cd was higher compared to unexposed (1.9-fold) and QDs-exposed ones (1.7-fold) ($p > 0.05$; Fig. 4.8A) and in the digestive gland reached similar levels to unexposed mussels at the end of depuration period (50 days) ($Ke: 0.023 \text{ d}^{-1}$, $r = 0.72$, $p < 0.05$; Fig. 4.8B; Table 4.3). This decrease of LPO levels in the digestive gland is probably related to the mechanism of elimination of the dissolved Cd in digestive gland cells, which decrease their toxicity by complexation with MTs (Marigómez et al., 2002; Serafim and Bebianno, 2007; Liu and Wang et al., 2011).

After exposure to dissolved Cd, the interaction between oxidative damage and MTs response in the gills was observed, where the increase of LPO levels was negatively related with MTs induction (MTs $\mu\text{g g}^{-1}$ w. w. tissue = $-8.323 [\text{LPO}] + 415.5$, $r = 0.89$, $p < 0.05$). This drop of MTs in the gills could also be the result of oxidative stress induced by ROS generation after exposed to dissolved Cd, which can oxidize

MTs and induce the release of Cd from the MT-Cd complex (Atif et al., 2006; Peyrot et al., 2009). On the other hand, no significant relationship between MTs and LPO levels exist in the digestive gland of dissolved Cd-exposure mussels and in both tissues of QDs-exposed mussels ($p > 0.05$), confirming that levels of MT and LPO were not entirely explained by the QDs dissolution and the release of dissolved Cd into digestive gland cells.

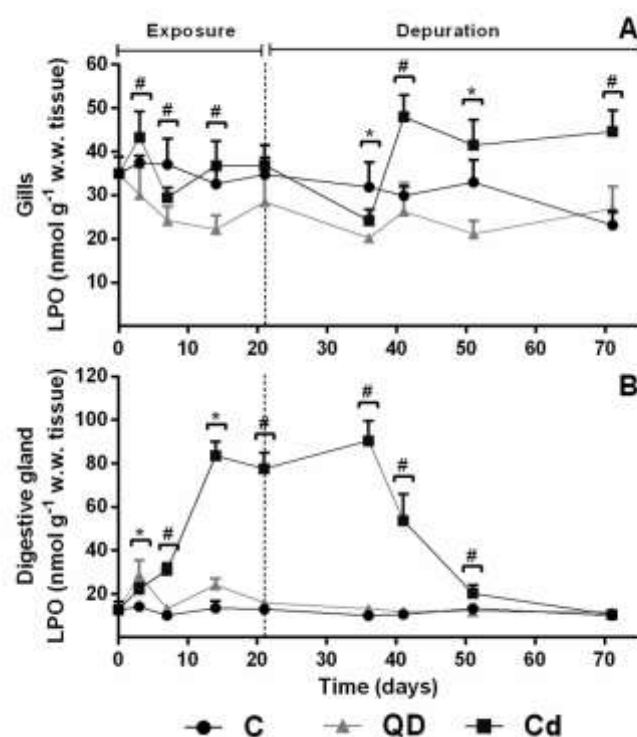


Figure 3.8. LPO levels (mean \pm std MDA + 4-HNE nmol g⁻¹ w. w. tissue) in the gills (A,B) and digestive gland (C,D) of mussel *M. galloprovincialis* from controls (C), exposed to CdTe quantum dots (QDs) and to dissolved Cd (Cd) during the exposure period (21 days) (A,C) and depuration periods (50 days) (B,D). Symbols # and * indicate significant differences between unexposed and Cd-exposed mussels (QDs or dissolved Cd) and between all treatments at each time of exposure ($p < 0.05$).

3.3.7. Tissue specific metabolism pattern

PCA results showed that the two principal components represent 80.2 % and 89.2 % of total variance in the gills (PC1 = 61.9 %, PC2 = 18.2 %) and digestive gland (PC1 = 75.2 %, PC2 = 14.0 %), respectively, and that differential tissue responses are associated with the type of exposure (Fig. 4.9A-D) and depuration periods (Fig. 4.9E-H). In the gills and digestive gland, a clear separation between unexposed mussels and

those exposed to QDs and to dissolved Cd was observed (Fig. 4.9 A-B). After 3 days of exposure, the response in mussel gills exposed to QDs and to dissolved Cd was similar, but with the increase of the time of exposure an opposite behaviour occurred between the two Cd forms confirming that *in vivo* long-time exposure to QDs induced different response in the gills when compared to the dissolved counterpart. The impact of QDs in the mussel gills is closely related to an increase in Cd concentrations in the BAM form, especially in the HMW fraction, and time of exposure (Fig. 4.9A-B). On the other hand, the dissolved Cd exposure was associated to the increase of total Cd concentration, MTs induction, as well as Cd levels in the IF fraction and BDM form (Fig. 4.9A-B). These results are consistent with other studies (Bebianno et al., 1993; Zorita et al., 2007), confirming the role of MTs in the Cd detoxification process through storage in BDM forms and protection against oxidative stress. In the digestive gland of QDs-exposure mussels, QDs effects were related to Cd concentrations in the BAM and in the IF form, and to MTs response while the effects of dissolved Cd were associated to total Cd and to the BDM form, LPO levels and time of exposure (Fig. 4.9C-D). Comparing PCA results for both mussel tissues, QDs exposure was related to BAM, while dissolved Cd exposure was associated to total Cd concentration and BDM, indicating differential metal metabolism patterns according to Cd forms.

In opposite to exposure period, PCA results during the depuration phase indicate that QDs-detoxified mussel gills responses were related to the Cd in the BDM form and in the HMW fraction and to MTs response (Fig. 4.9E-F). Nevertheless, the digestive gland response was related, like for the exposure period, to total Cd and to the BDM form and MT response (Fig. 4.9E-F). On the other hand, dissolved Cd-detoxified mussel gills response was related to total Cd and to changes in BAM, IF and LPO (Fig. 4.9E-F), while the digestive gland response was related to Cd concentration in the BAM (IF and HMW) form (Fig. 4.9G-H). These results confirm the tissue specific detoxification process in mussels exposed to metal-based ENPs.

3.4. Conclusions

In the ecotoxicological context, interactions between ENPs behaviour, nano-specific properties, subcellular partitioning and response of biomarkers of exposure and damage in different mussel tissues are important to assess the environmental health risk of ENPs. Results confirm that the subcellular QDs partitioning kinetics and MTs response are important strategies for accumulation and detoxification of QDs in marine

bivalves. Cd-based QDs are slowly biologically detoxified when compared to dissolved Cd. Consequently, QDs in the BAM form are potentially toxic for mussel tissues due to higher reactivity and capability to induce ROS production and oxidative stress, especially in the fraction containing mitochondrial and nuclei. On the other hand, although Cd accumulated in the BDM form does not correspond to direct toxicity (e. g. no increase in LPO levels), both BAM and BDM forms have higher retention rate in mussel tissues and were not eliminated after 50 days of depuration ($t_{1/2} > 50$ days), indicating potential availability for trophic transfer and risks to human health due to consumption of QDs-contaminated mussels. Differences in subcellular partitioning, MTs response and oxidative damage kinetics between CdTe QDs and dissolved Cd during the exposure and depuration periods indicate that the metal metabolism, detoxification process and toxic effects of metal-based ENPs in marine invertebrates are distinct from that of their dissolved counterpart.

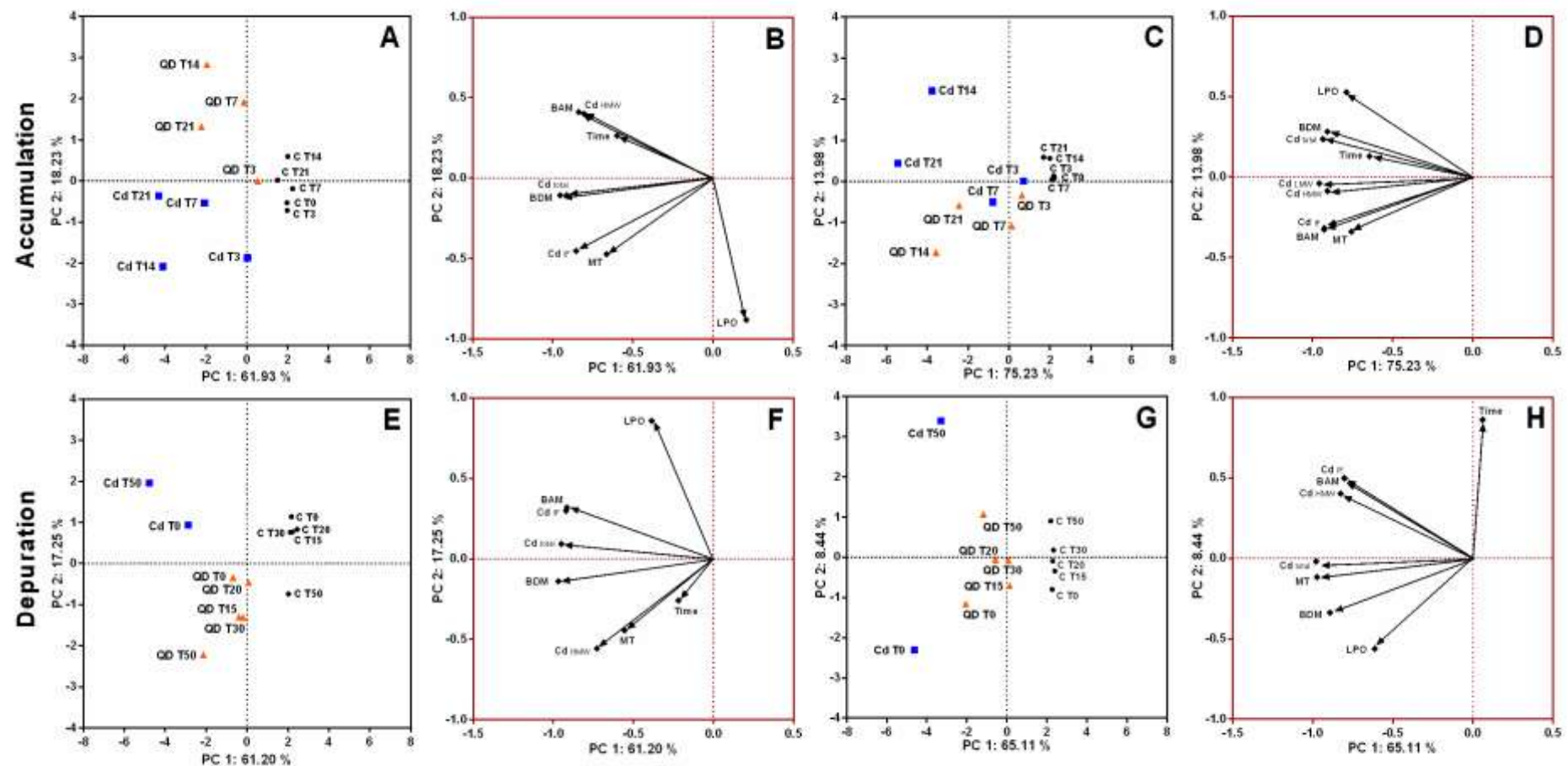
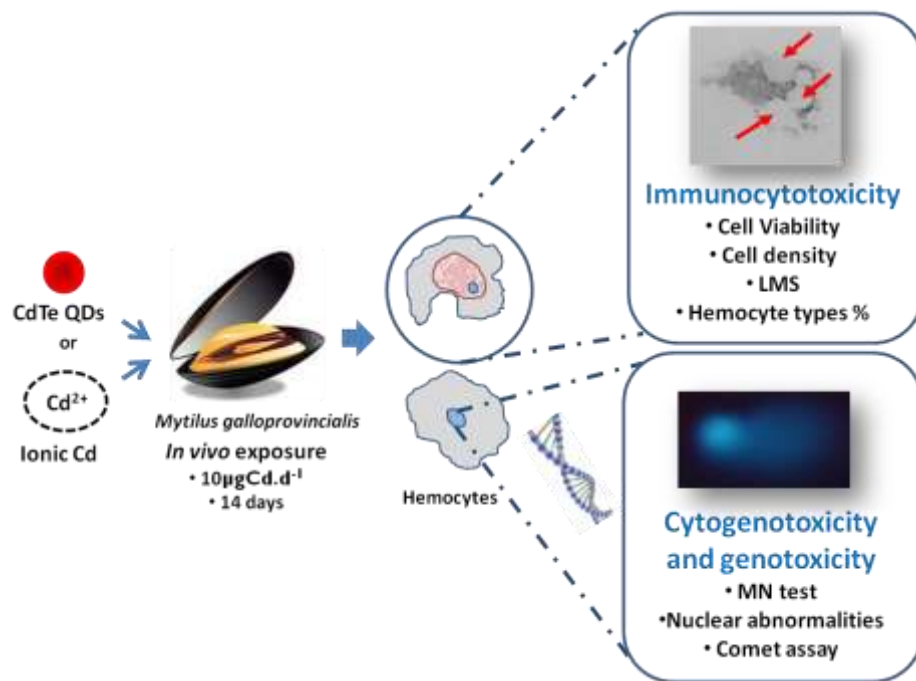


Figure 3.9. PCA analysis between total Cd concentration and in different subcellular fractions (IF, HMW, LMW), MTs and LPO levels in the gills (A-B) and digestive gland (C-D) of mussels *M. galloprovincialis* from controls (C), exposed to CdTe quantum dots (QDs) and to dissolved cadmium (Cd) during 21 days of exposure (A-D) and after 50 days of depuration (E-H). Total Cd concentration and Cd subcellular partitioning in mussel tissues was classified in two categories: the biologically active metal (BAM) which included IF and HMW fractions and the biologically detoxified metal (BDM) consisted of the LWM fraction.

CHAPTER IV

Immunocytotoxicity, cytogenotoxicity and genotoxicity of cadmium-based quantum dots in the marine mussel *Mytilus galloprovincialis*



Part of this Chapter was published in:

- Rocha, T.L., Gomes, T., Cardoso, C., Letendre, J., Pinheiro, J.P., Sousa, V.S., Teixeira, M.R., Bebianno, M.J., 2014. Immunocytotoxicity, cytogenotoxicity and genotoxicity of cadmium-based quantum dots in the marine mussel *Mytilus galloprovincialis*. *Marine Environmental Research* 101C, 29-37. doi:10.1016/j.marenvres.2014.07.009

Part of this Chapter was presented at:

- Rocha, T.L., Gomes, T., Cardoso, C., Letendre, J., Bebianno, M.J., 2014. Citotoxicity and immune response of mussel *Mytilus galloprovincialis* after exposure to Quantum dots and cadmium. 24th SETAC Europe Annual Meeting, Basel, Switzerland.
- Rocha, T.L., Gomes, T., Sousa, V.S., Teixeira, M.R., Pinheiro, J.P., Bebianno, M.J., 2014. Characterization and behavior of CdTe Quantum dots in the aquatic environment: effects of salinity, pH and natural organic matter. 24th SETAC Europe Annual Meeting, Basel, Switzerland.
- Rocha, T.L., Gomes, T., Cardoso, C., Mestre, N., Bebianno, M.J., 2015. Comparative effects of cadmium-based quantum dots and dissolved cadmium exposure in the marine mussel *Mytilus galloprovincialis*. 18th International symposium on Pollutant Responses in Marine Organisms (PRIMO18), Trondheim, Norway.
- Rocha, T.L., Gomes, T.C., Cardoso, C., Mestre, N., Sousa, V. S., Bebianno, M.J., 2015. Multibiomarker assessment of cadmium-based quantum dots effects in the marine mussel *Mytilus galloprovincialis*. 10^o Congreso Ibérico y 7^a Iberoamericano de Contaminación y Toxicología Ambiental - CICTA, Vila Real, Portugal.

This Chapter was awarded

- “Prêmio Jovem Cientista do Ano - Fluviação 2014”. Fluviação de Mora, Portugal.

Abstract

There is an increased use of quantum dot (QDs) in biological and biomedical applications, but little is known about their marine ecotoxicology. So, the aim of this study was to investigate the possible immunocytotoxic, cytogenotoxic and genotoxic effects of cadmium telluride QDs (CdTe QDs) on the marine mussel *Mytilus galloprovincialis*. Mussels were exposed to 10 $\mu\text{g Cd L}^{-1}$ of CdTe QDs or to dissolved Cd for 14 days and Cd accumulation, immunocytotoxicity [hemocyte density, cell viability, lysosomal membrane stability (LMS), differential cell counts (DCC)], cytogenotoxicity (micronucleus test and nuclear abnormalities assay) and genotoxicity (comet assay) were analyzed. Results show that after *in vivo* exposure to QDs, Cd is accumulated in mussel soft tissues and hemolymph and induce immunotoxic effects mediated by a decrease in LMS, changes in DCC, as well as genotoxicity (DNA damage). However, QDs do not induce significant changes in hemocytes density, cell viability and cytogenetic parameters in opposition to Cd^{2+} . Dissolved Cd is the most cytotoxic and cytogenotoxic form on *Mytilus* hemocytes due to a higher accumulation of Cd in tissues. Results indicate that immunotoxicity and genotoxicity of CdTe QDs and Cd^{2+} are mediated by different modes of action and show that *Mytilus* hemocytes are important targets for *in vivo* QDs toxicity.

Keywords: Nanoparticles, CdTe quantum dots, immunotoxicity, DNA damage, genotoxicity, hemocyte, *Mytilus galloprovincialis*.

4.1. Introduction

The widespread production and use of ENPs will likely increase their release into the aquatic environment, as well as their interaction, bioaccumulation or transfer in aquatic food webs (Jackson et al., 2012; Farrell and Nelson, 2013, Ma and Lin, 2013). An example of ENPs are QDs, which are semiconductor metalloid-crystal structures with a nanometer diameter (2 - 10 nm) and contain a metalloid crystalline core (usually Cd-based) coated with a shell or ligands. A great capacity to recognize specific cellular targets, strong fluorescence at narrow and size-tunable wavelengths, resistance to photobleaching, electronic and catalytic properties, makes QDs one of the most exploited ENPs not only in nanomedicine but also in pharmacy, biology and electronics (Michalet et al., 2005; Rizvi et al., 2010; Zhang et al., 2012). So far, few studies exist on the ecotoxicological effects of these ENPs in marine organisms, focusing mainly in algae (Morelli et al., 2012), mussels (Gagné et al., 2008; Peyrot et al., 2009; Bruneau et al., 2013; Katsumiti et al., 2014; Munari et al., 2014), crustaceans (Jackson et al., 2012; Feswick et al., 2013) and fish (Tang et al., 2013; Zhang et al., 2013).

The ecotoxicology of QDs has been mainly related to two main mechanisms, the release of Cd^{2+} ions from the ENPs core and/or the generation of free radicals or reactive oxygen species (ROS) (Gagné et al., 2008; Peyrot et al., 2009; Morelli et al., 2012; Tang et al., 2013). Cd is a non-essential metal classified as a priority substance in the field of water policy by European Water Framework Directive (Directive 2008/105/EC), as human carcinogen by the International Agency for Research on Cancer (IARC, 1993) and the US Environmental Protection Agency (EPA, 1999) and its carcinogenic and genotoxic effects towards aquatic organisms well studied (Emmanouil et al., 2007; Vincent-Hubert et al., 2011; Chandurvelan et al., 2013). Given the capacity of Cd-based QDs to induce oxidative stress and Cd^{2+} release, the immunocytotoxic, cytogenotoxic and genotoxic effects of QDs in aquatic species need to be thoroughly investigated.

Bivalve molluscs, mainly the mussel *Mytilus spp.*, are good bioindicators to assess the toxicity and environmental risk of ENPs in aquatic ecosystems (Canesi et al., 2012; Ciacci et al., 2012; Montes, 2012). The immune system of bivalves is also a sensitive target of NPs toxicity (Canesi and Procházková, 2014). *Mytilus spp.* lack adaptive immunity, but the blood cells (hemocytes) are responsible for cell-mediated immunity *via* phagocytosis, production of ROS and RNS, cytotoxic reactions, secretion of antimicrobial peptides and probably wound healing (Canesi et al., 2010; 2012).

Mytilus hemocytes classified as granular hemocytes (eosinophilic) and agranular hemocytes (hyalinocytes and basophils) possess high, low and no phagocytic capability, respectively (Le Foll et al., 2010). Particle composition, size, shape, aggregation state and concentration are key elements for determining the cytotoxicity, immunoactivity and immunoefficiency of QDs to bivalve species, in combination with exposure routes (saltwater, freshwater, sediments), differences within and among species and time of exposure (Gagné et al., 2008; Peyrot et al., 2009; Bruneau et al., 2013; Katsumiti et al., 2014). Furthermore, it was recently demonstrated that different QDs induce significant effects on hemocytes immune parameters of the marine mussels *M. edulis* and *M. galloprovincialis* and the freshwater mussel *E. complanata* (Gagné et al., 2008; Peyrot et al., 2009; Bruneau et al., 2013; Katsumiti et al., 2014). However, the mechanism of *in vivo* toxicity of ENPs on different types of hemocytes is still unclear.

In terms of biomarkers of cytogenotoxicity, the MN and nuclear abnormalities assay has been applied to measure chromosomal damage in mussels (Burgeot et al., 1996; Vincent-Hubert et al., 2011; Bolognesi and Fenech, 2012; Canesi et al., 2014). The comet assay is a sensitive technique for the detection of DNA strand breaks induced by NPs in bivalve hemocytes and provides a marker for genotoxic effects (Al-Subiai et al., 2012; Gomes et al., 2013). Therefore, the combination of different genotoxicity and cytogenotoxicity tests (comet assay, MN test and nuclear abnormalities assay) allows a more realistic analysis of the immunogenotoxic effects of pollutants in bivalve molluscs.

Accordingly, the aim of this work was to characterize the CdTe QDs behaviour in aquatic systems and analyze their possible immunocytotoxic, cytogenotoxic and genotoxic effects on *M. galloprovincialis* hemocytes after long-term exposure (14 days). Immunocytotoxicity of QDs was evaluated by measuring several functional parameters, as hemocyte density, cell viability, LMS and DCC of circulating hemocytes, and cytogenotoxic effects analyzed by the MN test, nuclear abnormalities and comet assay. Furthermore, the immunotoxic effects of QDs were compared with those of their dissolved counterpart Cd²⁺ after *in vivo* exposure to an environmentally realistic Cd concentration.

4.2. Materials and Methods

4.2.1. QD characterization

4.2.1.1. Stock solution

Orange CdTe QDs (2 - 7 nm diameter, emission wavelength at 590 ± 5 nm) was purchased from PlasmaChem GmbH (Berlin, CAS# 1306-25-8), and according to the supplier they consist of a CdTe core coated by carboxyl groups (-COOH) to prevent aggregation. A QD stock solution was made using Milli-Q water (100 mg Cd L^{-1}), sonicated for 30 min (Ultrasonic bath VWR International, 230 V, 200 W, 45 KHz frequency) and kept in constant shaking. Dissolved cadmium stock solution (Cd^{2+}) was prepared identically but not sonicated using cadmium nitrate ($\text{Cd}(\text{NO}_3)_2 \cdot 4\text{H}_2\text{O}$) (Merck).

4.2.1.2. Morphology, size, surface charge and aggregation kinetics

Particle shape and size was characterized using TEM and DLS, while the zeta potential determined by ELS. For TEM analysis, a drop of the stock solution was deposited onto a 300 mesh copper grid coated with a carbon layer and the excess solution was removed with tissue paper and allowed to dry at room temperature. The images were obtained in a JEOL (JEM-1011) microscope, using image analysis software (Soft Imaging System). The hydrodynamic diameter (d_h) of QDs was determined by DLS using a ZetaSizer Nano (ZS 90, Malvern, Inc.) analyzer. A He-Ne laser (633 nm wavelength) was used as a light source and the intensity of scattered light was measured at 90° . In these measurements, 12 mm square disposable polystyrene cells (DTS0012, Malvern, Inc.) were used. Zeta potential (ζ -potential) was determined using the same equipment in a disposable polycarbonate capillary cell (DTS1061, Malvern Inc.) at 25°C . The aggregation kinetics of QDs under environmentally relevant conditions of salinity and pH was determined by time-resolved DLS measurements. Each measurement was performed over a time period of 12 h. The polydispersity index (PDI) was also determined during a cycle of 12 h by DLS. For these analysis, CdTe QDs (40 mg Cd L^{-1}) were suspended in two aqueous media, Milli-Q water ($18 \text{ M}\Omega/\text{cm}$) and natural seawater ($S = 36.3$), over a wide range of pH (1.7 - 12), sonicated for 15 min and the pH changed using HNO_3 or NaOH .

4.2.1.3. Sedimentation rate (SR)

The sedimentation rate (SR) of CdTe QDs (40 mg Cd L^{-1}) was measured by the change in turbidity with time (0 - 24 h), as described in Sousa and Teixeira (2013). The

SR is related to the normalized nanoparticle turbidity C/C_0 , where C is the turbidity at time t and C_0 the initial turbidity at time 0. The SR is $\delta(C/C_0)/\delta t$, estimated from the initial 5 % decrease in normalized particle turbidity which occur within the first hour for the fast sedimentation (fast SR) conditions and within 12 - 24 h for slow sedimentation (slow SR) conditions (Keller et al, 2010).

4.2.1.4. Spectral properties

QDs optical properties were investigated in Milli-Q water at pH 8.0 by means of UV-Vis absorption spectra using a spectrophotometer (Jasco V-650) controlled with Jasco's Spectra Manage™ software and fluorescence spectra by Infinite 200 PRO multimode reader (TECAN) equipped with Tecan i-Control™ software, using the excitation and emission spectra of 530 and 545 nm, respectively.

4.2.2. Exposure experiments

Mussels *M. galloprovincialis* (60.1 ± 5.1 mm shell length) were collected from Ria Formosa Lagoon (South of Portugal) (Figs. 1.15 - 1.16) and acclimated for 14 d in static tanks containing natural seawater ($S = 36.3$) at 16 °C and constant aeration. After acclimation, fifty mussels were placed in 30 L tanks filled with 25 L of seawater (2.0 mussels L^{-1}) and exposed to $10 \mu g Cd L^{-1}$ of CdTe QDs and to their dissolved counterpart (Cd^{2+}) jointly with a control group kept in clean seawater in a triplicate design (3 tanks *per* treatment). Exposure experiments were conducted in static conditions under 12h:12h light/dark cycles and abiotic parameters in seawater were analysed daily by measuring salinity, temperature, pH and oxygen saturation (36.3 ± 0.07 , 16.6 ± 1.2 °C, 7.9 ± 0.1 , 103.0 ± 1.3 %, respectively). The animals were collected at the beginning of the experiment and after 3, 7 and 14 days of exposure. Due to the tendency of QDs to agglomerate in seawater, water was changed daily with redosing of QDs and Cd^{2+} concentrations. Mussels were not fed and no mortality was observed. At the end of the exposure period, hemolymph was collected from the posterior adductor muscle using a 1 mL syringe with a 25G needle and kept on ice for subsequent assays.

4.2.3. Cd concentration

Cd concentration was determined in dried tissues and hemolymph (80 °C, 48 h) after acid digestion with HNO_3 (80 °C, 4 h) followed by graphite furnace AAS (Analyst 800 - PerkinElmer). Accuracy of the analytical procedure was assured with certified

reference material (TORT-II, Lobster Hepatopancreas) from the National Research Council (Canada) and results agreed with the certified values (samples: 28.5 ± 4.5 mg Cd kg⁻¹; certified value: 26.7 ± 0.6 mg Cd kg⁻¹). Cd levels are expressed as µg g⁻¹ of dry weight tissue.

4.2.4. Immunocytotoxicity assessments

4.2.4.1. Cell viability and hemocyte density

After collection, hemolymph was centrifuged at 3000 *rpm* (3 min, 4 °C) and cell viability assessed by measuring the percentage of live cells with a Neubauer chamber (400 cells *per* condition) using Trypan blue (0.4 % in physiological solution; v/v). Hemocyte density was determined based on the cell using the Eq. 3.1.

$$\text{Concentration (Cell mL}^{-1}\text{)} = \frac{\text{Number of cells} \times 10\,000}{\text{Number of squares}} \times \text{Dilution factor} \quad (\text{Eq. 3.1})$$

4.2.4.2. Lysosomal Membrane Stability

Lysosomal Membrane Stability (LMS) was evaluated using the Neutral Red Retention Time (NRRT) assay, as previously described by Canesi et al. (2008) and Moore et al. (2009). Hemolymph from 10 animals *per* treatment was quickly extracted, mixed with saline solution (1:1 v/v) and aliquots of 40 µL were transferred onto glass slides and incubated with 40 µL of neutral red (final concentration 57.6 µg mL⁻¹ from a stock solution of NR 28.8 mg mL⁻¹ DMSO). Analysis was made using light microscopy (40x lens) 15 min after application of NR, then after 30, 60, 90, 120, 150 and 180 min. For each time, 9 - 10 fields were randomly analyzed, each containing around 8 - 10 cells (score at least 100 cells *per* animal). The endpoint of the assay was defined as the time at which 50 % or more hemocytes presented increased lysosomal volume, or when the lysosomal membrane was damaged and the NR solution leaked into the cytosol.

4.2.2.3. Differential Cell Count, Micronucleus test and Nuclear Abnormalities assay

DCC, MN test and nuclear abnormalities assay were measured according to the protocol described by Bolognesi and Fenech (2012). Hemolymph was mixed with PBS buffer 0.01 M pH 7.4 (1:1; v/v) and aliquots of 100 µL were placed onto glass slides (three slides *per* animal; 10 mussels *per* treatment), allowed to adhere for 15 min and fixed with 100 % methanol. Cell staining for microscopy was performed by immersion

in 10 % Giemsa solution (v/v). Nuclear abnormalities and DCCs of hemocytes were scored in at least 1000 cells *per* slide using light microscopy and expressed as percentage (%). Cytogenotoxicity (nuclear abnormalities) was measured by determining the frequency of hemocytes with MN or Buds and binucleated hemocytes (BN). The DCC was determined by frequency of hemocyte types: eosinophils, basophils, hyalinocytes and hemocyte aggregates. The cytogenotoxicity and DCC were analyzed at the end of the exposure period and *Mytilus* hemocyte subpopulations and nuclear abnormalities were classified according to Le Foll et al. (2010) and Bolognesi and Fenech (2012).

4.2.2.4. Comet assay

Genotoxicity was estimated using the comet assay (DNA damage) in a slightly modified version of that by Singh et al. (1988) and described in Gomes et al. (2013). Briefly, microscopic slides were coated with 0.65 % normal melting point agarose (NMA) in Tris-acetate EDTA. After collection, hemolymph cells for each mussel were centrifuged at 3000 *rpm* (3 min, 4 °C) and the pellets with isolated cells suspended in 0.65 % low melting point agarose (LMA, in Kenny's salt solution) and casted on the microscope slides. Afterwards, the slides with the embedded cells were immersed in a lysis buffer (2.5 M NaCl, 100 mM EDTA, 10 mM Tris, 1 % Triton X-100, 10 % Dimethylsulfoxide, 1 % Sarcosil, pH 10, 4 °C) for 1 h, for the diffusion of cellular components and DNA immobilization in agarose. Following the lysis step, slides were gently placed in an electrophoresis chamber containing electrophoresis buffer (300 mM NaOH, 1 mM EDTA, adjusted at pH 13, 4 °C) and left for 15 min to permit DNA unwinding. The electrophoresis was carried out for 5 min at 25 V and 300 mA. Once the electrophoresis was concluded, the slides were removed and immersed in neutralizing solution (0.4 mM Tris, pH 7.5), rinsed with bi-distilled water and left to dry overnight. Afterwards, slides were stained with 4,6-diamidino-2-phenylindole (DAPI, 1 µg mL⁻¹) and the presence of comets was analysed using an optical fluorescence microscope (Axiovert S100) coupled with a camera (Sony). The Komet 5.5 image analysis system (Kinetic Imaging Ltd) was used to score 50 randomly chosen cells for each slide (25 in each gel from each individual mussel) at a total magnification of 400x. Amount of DNA in the comet tail (tail DNA %) was used as parameter of the comet and results are expressed as mean ± SEM. Cells were also categorized for grade of damage (using tail DNA %) based on the criteria referred in Almeida et al. (2011): zero or

minimal (10 %), low damage (10 - 25 %), mid damage (25 - 50 %), high damage (50 - 75 %) and extreme damage (> 75 %). During the entire procedure, great care was taken to avoid exposing cells and slides to light and heat.

4.2.5. Statistical analysis

The statistical analyses were carried out using the Statistica 7.0 software (Statsoft Inc., 2005, Tulsa, OK, USA). The results were compared with parametric tests (two-way ANOVA, followed by the Tukey's test) and non-parametric test (Kruskal-Wallis), depending on the distribution of the data and homogeneity of variances, according to the Shapiro-Wilk test and Levene's test. Linear regression analysis was also applied to verify existing relationships between variables and determine the rates of metal accumulation and comet parameter versus time. Results were considered significant when $p < 0.05$.

4.3. Results

4.3.1. QDs characterization

TEM analysis of CdTe QDs demonstrates isolated spheroid particles with an mean size of 6.1 ± 1.5 nm, along with the presence of QDs aggregates in the aqueous medium (Fig. 4.1A-B). CdTe QDs have maximum absorption and luminescent wavelength at 530 nm and 530 - 545 nm, respectively. ζ -potential measurements show that QDs have lowest negative surface charge in seawater (-9.37 ± 1.16 mV) than in Milli-Q water (-42.64 ± 0.55 mV) at pH 8.0 ($p < 0.05$; Fig. 4.2A). DLS measurements show that the d_h of QDs is higher in seawater (1014.5 ± 187.2 nm) compared to Milli-Q water (14.79 ± 1.7 nm) at pH 8.0 ($p < 0.05$; Fig. 4.2B).

ζ -potential and d_h of water-dissolved QDs are highly affected by salinity and pH (Fig. 4.2). The DLS results indicate that salinity changes the isoelectric point of QDs because ζ -potential is near zero at pH 1.7 for Milli-Q water and at pH 10 - 12 for seawater (Fig. 4.2A). At the isoelectric point, QDs have little or no charge, leading to NPs adherence and formation of large aggregates. QDs have highest d_h in seawater at pH 10 (1574.7 ± 63.7 nm) and in Milli-Q water at pH 1.7 - 2.0 (759.9 ± 64.3 nm to 866.5 ± 118.7 nm) (Fig. 4.2B). In addition, results demonstrate that ζ -potential varied with pH for Milli-Q water, while for seawater no significant differences exist. ($p < 0.05$; Fig. 4.2A).

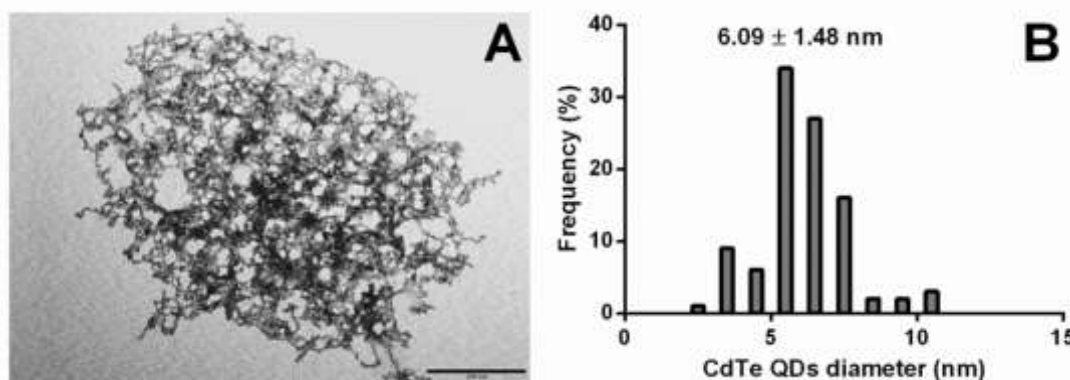


Figure 4.1. Transmission Electron Microscopy (TEM) image of CdTe quantum dots (QDs) in Milli-Q water (A) and particle size histogram of QDs obtained from TEM images (B).

The effect of salinity on aggregation kinetics is identified over time (Fig. 4.3). During 12 h, salinity induces the formation of two large aggregate groups at pH 8.0 [562.9 ± 435.3 nm ($n > 80$ %) and 2973 ± 1331 nm ($10 < n < 80$ %)] compared with small aggregates (42.1 ± 11.3 nm) in Milli-Q water at pH 8.0 (Fig. 4.3A). Additionally, high PDIs are observed in seawater (0.52 ± 0.1) and Milli-Q water (0.69 ± 0.12) over time, reflecting the presence of a polydisperse system comprised of both large and small aggregates (Fig. 4.3B). The higher PDI in seawater also indicates the presence of smaller aggregates that are likely masked in the DLS signal by the presence of larger ones.

Turbidity (C/C_0) of CdTe QDs suspensions is measured to assess the changes in SR (Fig. 4.3C). Higher decrease in turbidity over time (24 h) is observed in seawater (91.8 %) compared to Milli-Q water (67.7 %) ($p < 0.05$). As a consequence of formation of large aggregates, a decrease in turbidity and an increase in SR are observed in seawater (Fig. 4.3D), showing that QDs tend to sediment rapidly in this medium (fast SR = $0.88 \pm 5 \times 10^{-4}$ 1/h; slow SR = $0.009 \pm 8.45 \times 10^{-5}$ 1/h) compared to Milli-Q water (fast SR = 0.70 ± 0.002 1/h; slow SR = $0.03 \pm 3.03 \times 10^{-5}$ 1/h; $p < 0.05$).

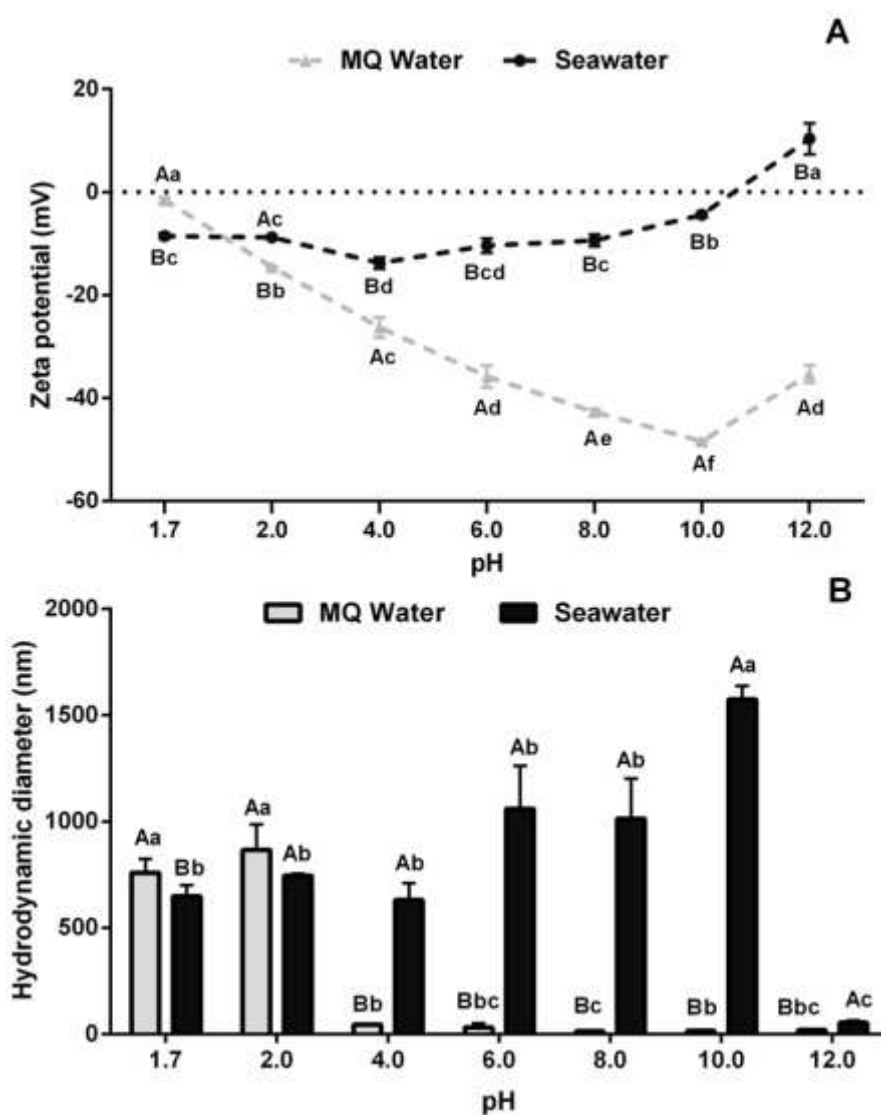


Figure 4.2. ζ -potential (A) and hydrodynamic diameter (B) of CdTe QDs suspended in Milli-Q water and natural seawater at pH between 1.7 and 12. Capital and lower letters represent statistical differences between suspensions at each pH and differences for each suspension at different pH, respectively ($p < 0.05$).

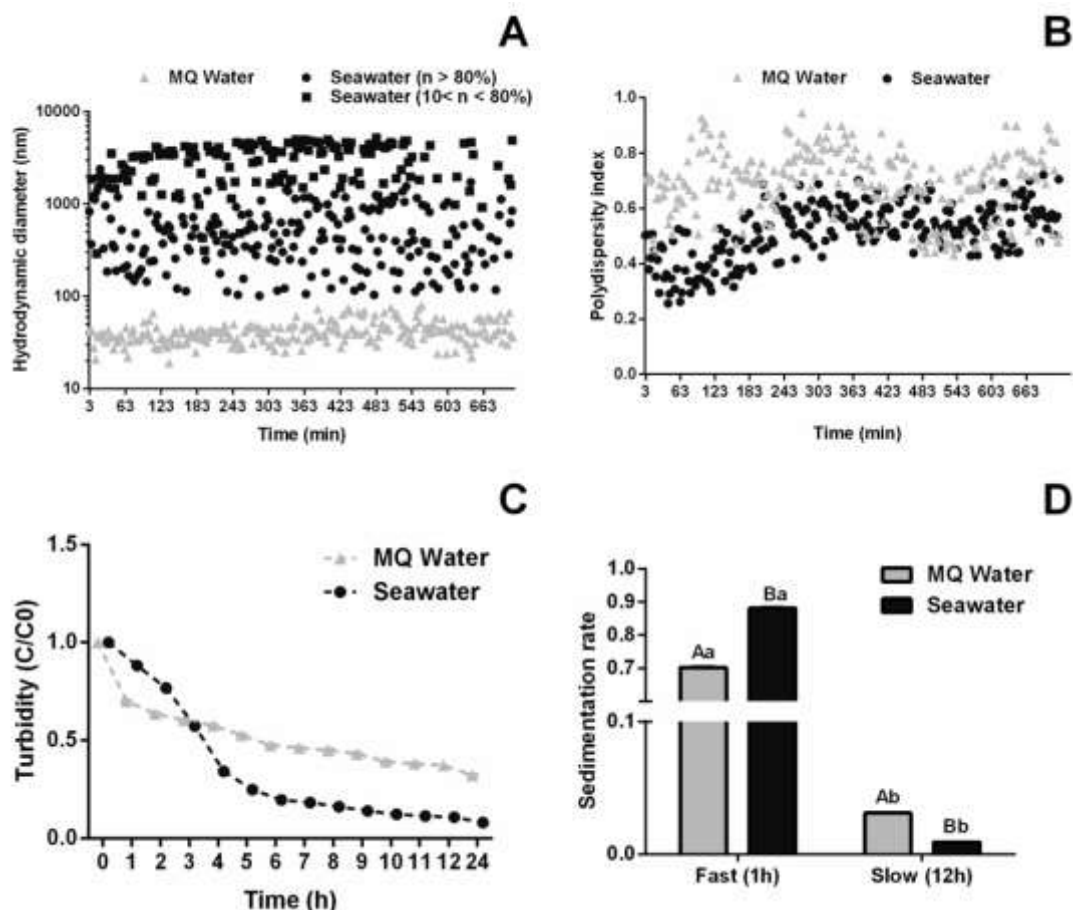


Figure 4.3. Hydrodynamic diameter (A), polydispersity index (B), turbidity (C) and sedimentation rate (D) of CdTe quantum dots (QDs) suspended in Milli-Q water and natural seawater at pH 8.0 over time. Capital and lower letters represent statistical differences between suspensions at each time and differences for each suspension at different time, respectively ($p < 0.05$).

4.3.2. Cd concentration

The exposure of mussels to QDs and to dissolved Cd results in a significant Cd accumulation in mussel whole soft tissues when compared to unexposed mussels (Fig. 4.4A) during 14 days of exposure that is Cd form dependent. Cd concentrations in mussel tissues increase linearly with time for QDs ($0.83 \mu\text{g g}^{-1} \text{d}^{-1}$; $r^2 = 0.87$, $p < 0.001$) and Cd^{2+} ($2.13 \mu\text{g g}^{-1} \text{d}^{-1}$; $r^2 = 0.89$, $p < 0.001$) exposed mussels, with a higher accumulation in the latter (2.1-, 3.5- and 2.5-fold at 3, 7 and 14 days, respectively).

Higher Cd accumulation is also observed in the hemolymph of exposed mussels, compared to unexposed ones (Fig. 4.4B), with concentrations also increasing linearly with time for dissolved Cd. Nevertheless, a lower accumulation rate is found for QDs exposed mussels ($0.004 \mu\text{g g}^{-1} \text{d}^{-1}$; $r^2 = 0.48$; $p < 0.05$) compared to those exposed to dissolved Cd ($0.019 \mu\text{g g}^{-1} \text{d}^{-1}$; $r^2 = 0.99$; $p < 0.001$), even though with a similar

accumulation in the first 3 days of exposure (QDs: $0.08 \pm 0.02 \mu\text{g g}^{-1} \text{ d. w.}$; dissolved Cd: $0.07 \pm 0.003 \mu\text{g g}^{-1} \text{ d. w.}$; $p > 0.05$).

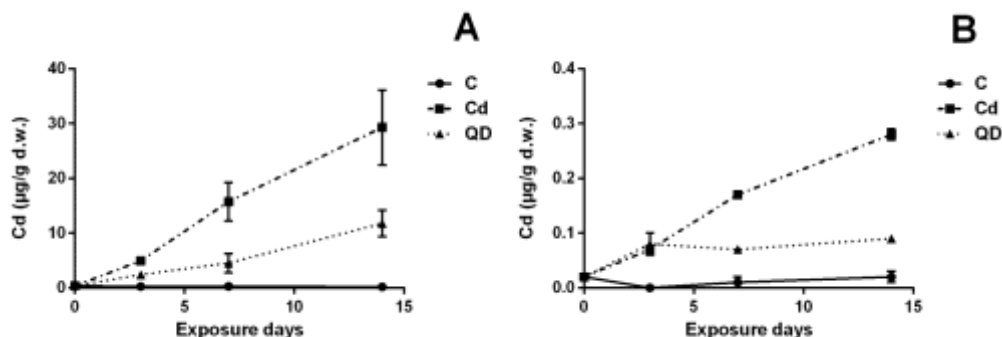


Figure 4.4. Cd accumulation in whole soft tissue (A) and hemolymph (B) of mussels *M. galloprovincialis* ($\mu\text{g g}^{-1} \text{ d. w. tissue}$) from controls (C), exposed to CdTe quantum dots (QDs) and dissolved Cd (Cd^{2+}) for 14 days (mean \pm std).

4.3.3. Immunocytotoxicity

4.3.3.1. Hemocyte viability and density

The different immunocytotoxic effects of CdTe QDs and their dissolved counterpart were analyzed by cell viability and density of hemocytes (Table 4.1). Dissolved Cd is the most immunocytotoxic form, causing a significant decrease in cell viability after 7 and 14 days of exposure and cell density of circulating hemocytes after 14 days ($p < 0.05$). On the other hand, no immunocytotoxic effects is observed on cell viability and density in hemocytes exposed to QDs ($p > 0.05$).

4.3.3.2. LMS

Cellular stress at the lysosomal level (LMS) induced by both Cd forms was analyzed by NRRT (Fig. 4.5). After 3 days of exposure, a significant decrease in LMS is observed in mussels exposed to QDs ($39 \pm 12.6 \text{ min}$) and dissolved Cd ($58.5 \pm 17.9 \text{ min}$) compared to controls ($93 \pm 9.5 \text{ min}$) ($p < 0.05$). These cytotoxic effects remain until the end of the exposure period (14 days), with no significant differences between the two Cd forms ($p > 0.05$). The reduction rate of NRRT is lowest in QDs exposed mussels (-3.3 min d^{-1} ; $r^2 = 0.29$; $p < 0.001$) compared to dissolved Cd exposed ones (-4.8 min d^{-1} ; $r^2 = 0.58$; $p < 0.001$).

Table 4.1. Cell viability and hemocyte density in mussels *M. galloprovincialis* from controls (C), exposed to dissolved cadmium (Cd) and CdTe quantum dots (QDs) for 14 days (mean \pm std). Capital and lower letters represent statistical differences between treatments at each time of exposure day and treatment during the exposure period ($p < 0.05$).

Time	Cell viability (%)			Cell density ($\times 10^6$)		
	C	QDs	Cd	C	QDs	Cd
0	80.71 \pm 0.79 ^a	-	-	1.87 \pm 0.24 ^a	-	-
3	85.79 \pm 2.54 ^{Aa}	84.73 \pm 2.96 ^{Aa}	87.17 \pm 3.79 ^{Aa}	1.17 \pm 0.06 ^{Aa}	1.07 \pm 0.14 ^{Aa}	1.20 \pm 0.18 ^{Aa}
7	83.38 \pm 2.77 ^{Aa}	80.88 \pm 1.97 ^{ABa}	76.95 \pm 3.33 ^{Ba}	1.20 \pm 0.10 ^{Aa}	1.30 \pm 0.36 ^{Aa}	1.32 \pm 0.12 ^{Aa}
14	84.82 \pm 2.52 ^{Aa}	79.66 \pm 1.78 ^{Aa}	80.06 \pm 4.41 ^{Ba}	1.63 \pm 0.08 ^{Aa}	1.71 \pm 0.11 ^{ABa}	1.22 \pm 0.21 ^{Ba}

4.3.3.3. DCC

The impact of both Cd forms in the cell-mediated immunity after 14 days of exposure was analyzed by DCC (Fig. 4.7). Frequency of hemocytes (eosinophils, basophils, hyalinocytes and aggregates) is modulated in accordance with Cd forms. QDs exposed mussels show a significant decrease in the frequency of eosinophils (-2.1-fold; $p < 0.05$; Fig. 4.7A), while in those exposed to dissolved Cd the frequency of basophils (-1.6-fold) decreases compared to controls ($p < 0.05$; Fig. 4.7B). Both Cd forms induce a significant increase in the frequency of hyalinocytes (3.1- and 4.5-fold for QDs and dissolved Cd, respectively; $p < 0.05$; Fig 4.7C). The effects are not observed in the frequency of hemocytes aggregates between conditions ($p > 0.05$; Fig 4.7D).

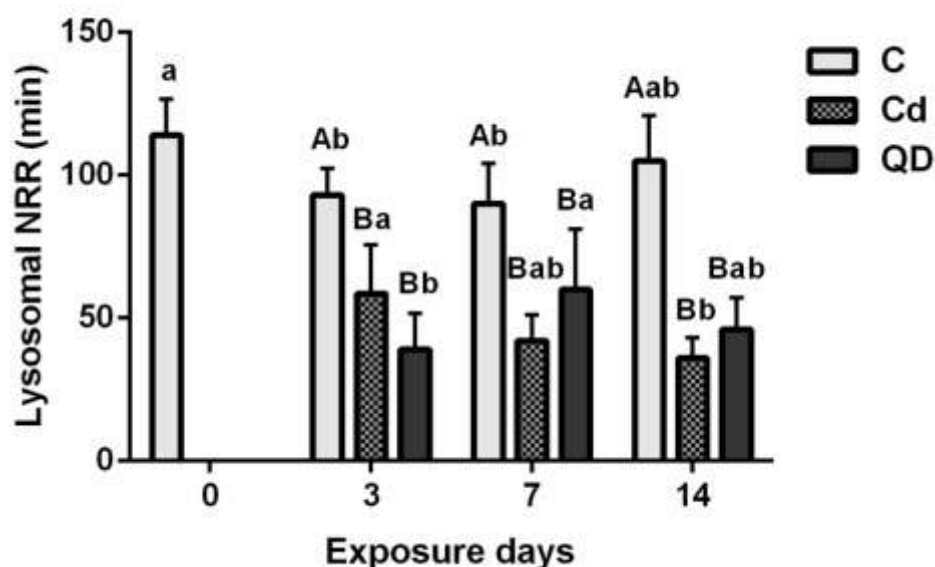


Figure 4.5. Lysosomal membrane stability (LMS) (mean \pm std) in mussels *M. galloprovincialis* from controls (C), exposed to CdTe Quantum dots (QDs) and dissolved cadmium (Cd) for 14 days. Capital and lower letters represent statistical differences between treatments at each time of exposure and for each treatment during the exposure period ($p < 0.05$).

4.3.4. Cytogenotoxicity

4.3.4.1. Micronucleus Assay and Nuclear Abnormalities

Chromosomal damage induced by both Cd forms after 14 days of exposure was analyzed by MN and nuclear abnormalities assay (Fig. 4.7A). Cytogenotoxicity is Cd form dependent, where dissolved Cd is the most cytogenotoxic in mussel hemocytes. A higher frequency of BN hemocytes is observed in dissolved Cd exposed mussels (13.1-fold; $p < 0.05$), with no significant alterations in those exposed to QDs (3.7-fold; $p > 0.05$) compared to the control condition.

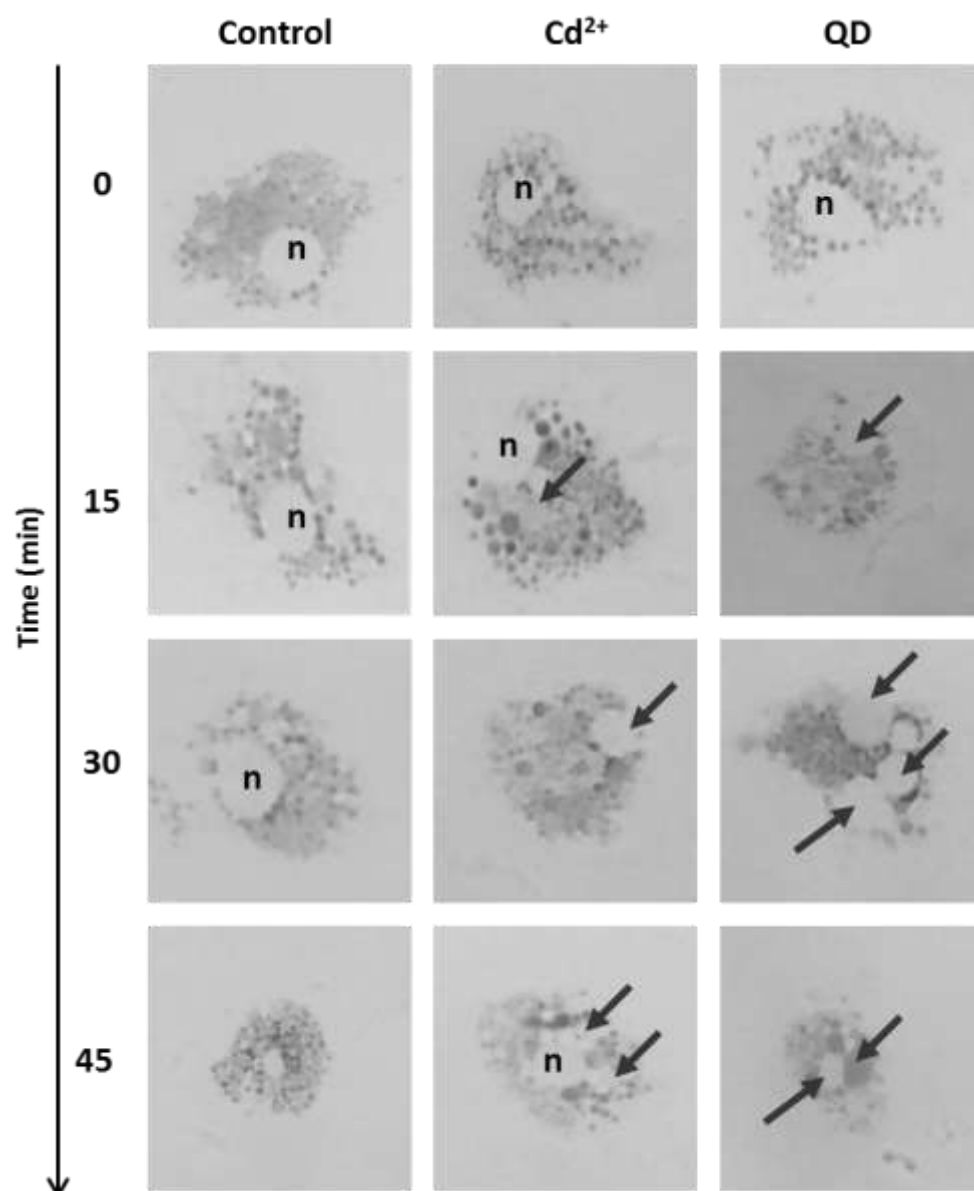


Figure 4.6. Light microscopic image of hemocytes in mussels *M. galloprovincialis* from controls (C), exposed to CdTe quantum dots (QDs) and dissolved Cd (Cd²⁺) for 14 days. Analysis was made using light microscopy (total magnification 400x) and time after application of neutral red (NR) was expressed in min. The arrows indicate increased lysosomal volume, damaged lysosomal membrane and NR solution leaked into the cytosol or near the nucleus (n).

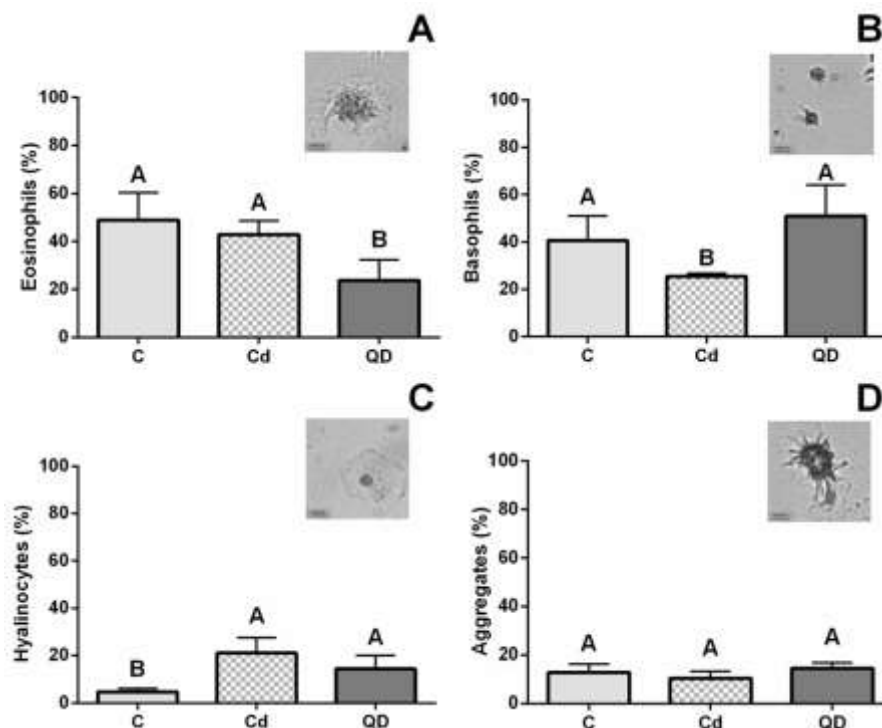


Figure 4.7. Frequency of hemocytes types (mean \pm std) of mussels *M. galloprovincialis* from controls (C), exposed to CdTe quantum dots (QDs) and dissolved C (Cd) at 14 days expressed as Eosinophils % (A), Basophils % (B), Hyalinocytes % (C) and hemocytes aggregates % (D). Capital letters represent statistical differences between treatments ($p < 0.05$).

4.3.5. Genotoxicity

4.3.5.2. Comet assay

Genotoxic effects of both Cd forms analyzed by comet assay and expressed as % of tail DNA are in Figs. 4.8B and 4.9. DNA damage is always higher in exposed mussels than in controls, throughout the exposure period ($p < 0.05$) and dependent on the Cd form. QDs are more genotoxic than dissolved Cd in the first 7 days of exposure (1.9- to 1.7-fold for QDs and 1.3- to 1.4-fold for Cd²⁺; $p < 0.05$), while the opposite occurred at the end of the experiment (2.1-fold for QDs compared to 2.6-fold for dissolved Cd; $p < 0.05$). This result in a higher induction rate for dissolved Cd (1.03 % d⁻¹; $r^2 = 0.26$; $p < 0.01$) compared to QDs (0.67 % d⁻¹; $r^2 = 0.12$; $p < 0.01$) (Figs. 4.8B, 4.9).

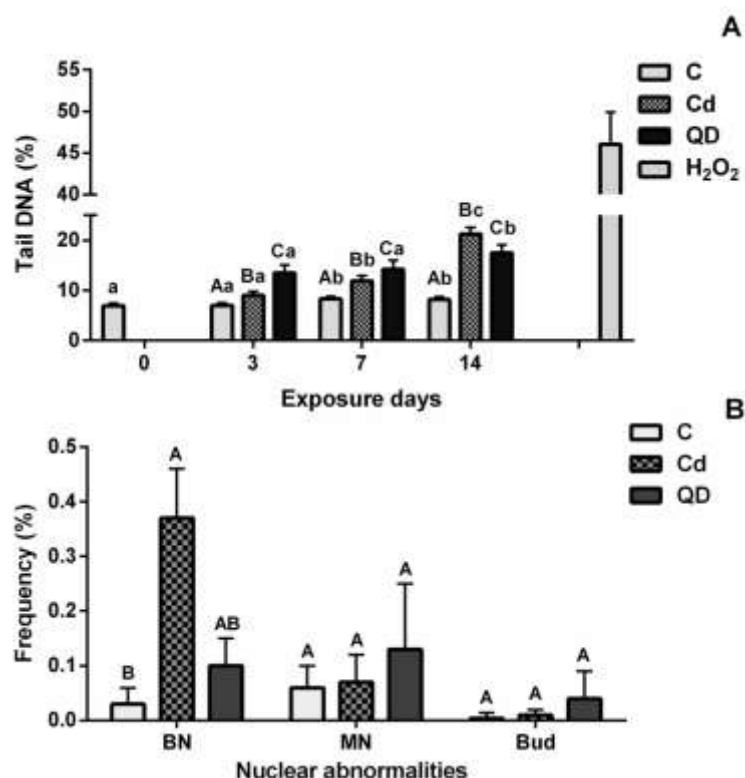


Figure 4.8. Genotoxic effects of CdTe quantum dots (QDs) and dissolved cadmium (Cd^{2+}) in mussels *M. galloprovincialis* exposed for 14 days. (A). Frequency of nuclear abnormalities (mean \pm std) expressed as frequency of binucleated cells (BN), micronucleus (MN) and Bud. Capital letters represent statistical differences between treatments ($p < 0.05$). (B). DNA damage (mean \pm SEM) expressed as tail DNA %. Capital and lower letters represent statistical differences between treatments at each time of exposure and for each treatment during the exposure period ($p < 0.05$).

The % of tail DNA was also used to grade DNA damage in exposed and unexposed mussels (Table 4.2). Hemocytes from unexposed mussel show minimal or low damage along the exposure period (from 98 to 97.8 %). This grading system confirm that QDs are more genotoxic at 3 and 7 days of exposure, since the percentage of hemocytes with mid and high damage (13 to 15.4 %) is higher compared to dissolved Cd (6.2 to 10 %). However, after 14 days, dissolved Cd exposed mussels show higher percentage of hemocytes with mid and high damage (31.5 %) compared to those exposed to QDs (17.6 %). There is no extreme DNA damage in the mussels exposed to both Cd forms after 14 days of exposure.

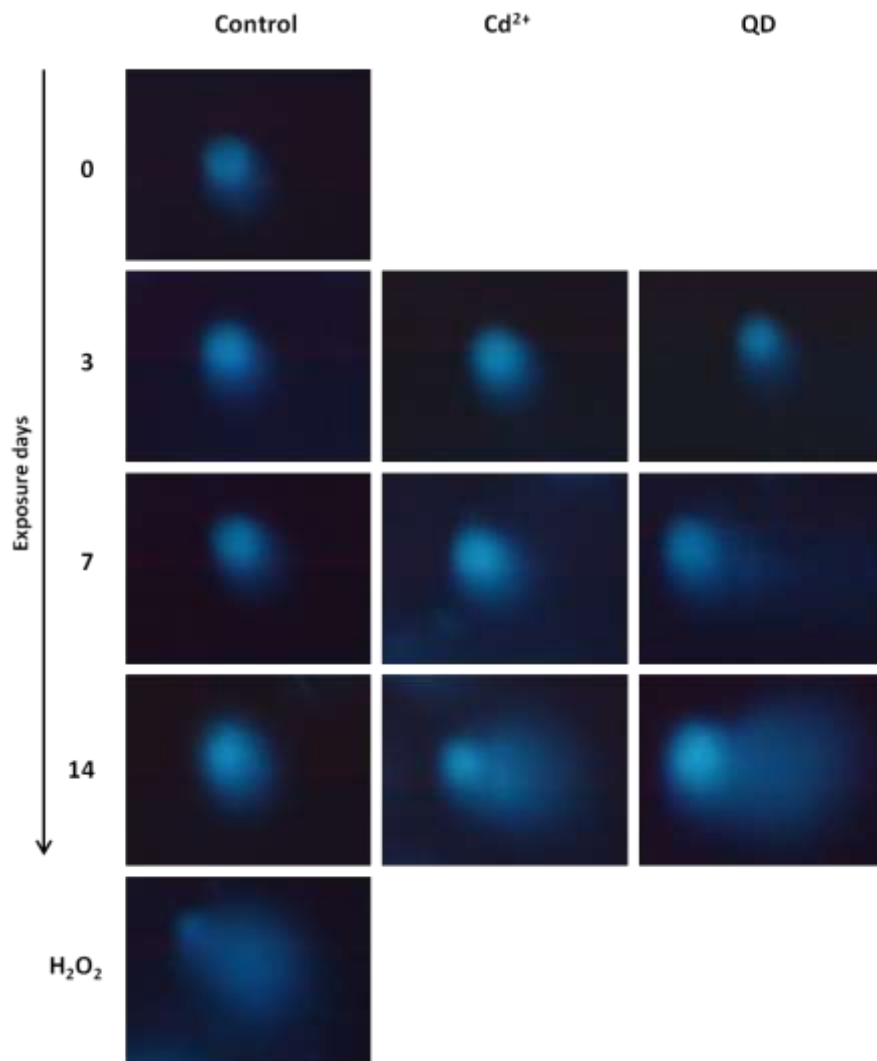


Figure 4.9. Comet assay images of hemocytes in mussels *M. galloprovincialis* from controls (C), exposed to CdTe quantum dots (QDs) and dissolved Cd (Cd^{2+}) for 14 days (total magnification 400x). H_2O_2 was the positive control.

Table 4.2. Frequency of hemocytes (%) distributed by grade of DNA damage in *M. galloprovincialis* from controls (C), exposed to dissolved cadmium (Cd) and CdTe quantum dots (QDs) for 14 days.

DNA damage criteria	C				QDs			Cd			H_2O_2
	0	3	7	14	3	7	14	3	7	14	
Minimal	76.6	76.2	67.0	70.2	38.0	39.52	23.4	56.8	49.4	18.53	2.0
Low	21.4	21.6	30.0	27.6	49.0	45.11	59.0	37.0	41.6	50.0	18.5
Mid	2.0	2.2	3.0	2.2	12.4	14.77	17.0	6.0	8.8	28.69	35.0
High	0	0	0	0	0.6	0.6	0.6	0.2	0.2	2.79	35.5
Extreme	0	0	0	0	0	0	0	0	0	0	9

4.4. Discussion

The growing development and use of QDs leads to their release into the aquatic environment but knowledge about its impact on the marine environment and human health is still in its infancy. Since different types of NPs may induce immunomodulation or immunotoxicity in bivalves (Gagné et al., 2008; Ciacci et al., 2012; Barmo et al., 2013), the cell-mediated immunity is considered a primary target and important model for understanding the MoA of NPs in invertebrates. To the best of our knowledge, this is the first *in vivo* study of immunotoxicity and cytogenotoxicity in marine mussels exposed to QDs.

The impact of NPs on marine molluscs is dependent of their physicochemical properties and behaviour in the aquatic environment. Results of NPs characterization show that CdTe QDs (6.1 ± 1.5 nm) tend to significantly aggregate in seawater over time (Fig. 4.2). This is in accordance with the QDs salinity-dependent propensity to aggregate verified for CdSe/ZnS QDs, CdSe QDs, CdS/CdTe and CdS QDs in previous studies, with the presence of aggregates with different sizes (Jackson et al., 2012; Morelli et al., 2012; Bruneau et al., 2013; Katsumiti et al., 2014). ζ -potential measurements show that the ionized carboxylic groups confer low negative surface charge of CdTe QDs in seawater (-9.37 ± 1.16 mV, at pH 8), confirming the tendency of these NPs to aggregate due to low repulsion forces (Fig. 4.2). These large aggregates tend to sediment and induce changes in the seawater turbidity and higher sedimentation rate for QDs in seawater compared with Milli-Q (Fig. 4.3). Consequently, during the exposure period, mussels *M. galloprovincialis* can interact with different aggregation states of QDs: (1) individual QDs (6.09 ± 1.48 nm); (2) small aggregates (562.9 ± 435.3 nm; $n > 80$ %); (3) large aggregates (2973.2 ± 1331.6 nm; $10 < n < 80$ %).

Cd accumulation in mussel tissues and hemolymph is Cd form dependent (particulated or dissolved Cd). Mussels accumulate less Cd in their whole tissues after exposure to CdTe QDs than from dissolved Cd (Fig. 4.4A), indicating a higher bioavailability of its dissolved form. This result is consistent with previous studies showing that NPs aggregation reduces surface area to volume ratio, increase sedimentation and decrease their bioavailability and consequently alter their toxicity (Lowry et al., 2012). However, in freshwater mussels *E. complanata* exposed to uncoated CdTe ($0 - 8$ mg L⁻¹, 24 h), the bioaccumulation factor of Cd from CdTe was similar to dissolved Cd (Peyrot et al. 2009). This result is not in agreement with the results obtained from CdTe QDs coated with carboxylic acid (Fig. 4.4A) and indicates

that coverage of QDs alters their dissolution and bioavailability and consequently their toxicity in mussels *M. galloprovincialis*. Furthermore, results indicate that the carboxyl polymer may modulate the toxicity of QDs in mussels *M. galloprovincialis*, as reported for others invertebrates, *Daphnia spp.* (8 nM, 24 h) (Feswick et al., 2013) and *L. plumulosus* (3.6 mg L⁻¹, 96 h) (Jackson et al., 2012), where in QDs with negative charge (COOH-CdSe/ZnS QD) induce more Cd accumulation than QDs with positive charge (NH₂-PEG- CdSe/ZnS QD) or uncharged QD (PEG- CdSe/ZnS QD).

As for the hemolymph, exposed mussels to dissolved Cd accumulate Cd linearly with time (0.019 µg g⁻¹ d⁻¹), while in QDs, Cd concentrations remain unchanged until the end of exposure period after an increase in the first 3 days (0.004 µg g⁻¹ d⁻¹) (Fig. 4.4B). The presence of QDs in mussel hemolymph is related to the transport of the NPs from the digestive system into the hemolymph, reflecting the phagocytic capacity of the hemocytes (Barmo et al., 2008; Browne et al., 2008) and suggesting the transfer of both forms of Cd to tissues during detoxification processes. Thereby, results indicate that the transport of QDs in the hemolymph is limited by the number of circulating hemocytes, since the frequency of eosinophils (granulocytes hemocytes with high phagocytic capability) decreased in mussels exposed to QDs after 14 days (Fig. 4.7). Additionally, the hypothesis that Cd-based QDs speciation in the hemolymph cannot be excluded, since Cd binds to inorganic ions in the plasma and produces chloro-complexes (CdCl⁺, CdCl₂ and CdCl₃⁻) or is associated to bind a plasma protein, the histidine-rich glycoprotein (HRG), as seen in mussels *M. edulis* exposed to dissolved Cd (Nair and Robinson, 2001).

Even though no significant changes were found in hemocytes viability and density, both QDs and dissolved Cd induce immunocytotoxicity mediated by lysosome damage, changes in frequency of hemocytes types (eosinophils and hyalinocytes) and DNA damage. The lysosomal cytotoxicity of CdTe QDs and dissolved Cd measured by NRRT show significant decrease of LMS in the hemocytes, which is related to impaired cellular immunity, cell injury or cell death (Moore et al., 2009). Both Cd forms induce similar effects at lysosomal level, probably due to dissolution of QDs and release of Cd²⁺ ions inside the lysosomes at acidic pH around 5.0, as suggested by Katsumiti et al. (2014). Cytotoxicity and cellular mechanisms of *in vitro* CdS QDs exposure in *Mytilus* hemocytes was also associated with internalization of QDs by endocytosis or phagocytosis, intracellular release of Cd²⁺, increase the lysosomal acid phosphatase (ACP), ROS production and ROS-mediated DNA damage (Katsumiti et al., 2014).

However, immunotoxicity of QDs cannot be completely related to Cd release, and NP-specific effects have been suggested by Bruneau et al. (2013), according to QDs composition, shape, size, surface area, coverage, agglomeration state and charge.

In studies of NPs immunotoxicity, hemocytes are generally considered as a single cellular type, but important three subpopulations of hemocytes exist in *Mytilus sp.* (Le Foll et al., 2010): eosinophils (granulocytes hemocytes with high phagocytic capability), basophils and hyalinocytes (agranular hemocytes with no and low phagocytic function, respectively). *In vivo* exposure to CdTe QDs or dissolved Cd changes the immune response of mussels, but the immunomodulation of hemocyte types is dependent of Cd form (Fig. 4.7). In general, literature reports that different mechanisms may promote changes in the frequency of types of hemocytes in bivalves: 1. The decrease of frequency by selective cell death; 2. Changes in the frequency by hematopoiesis and specific cellular differentiation; 3. Decrease of frequency by differential diapedesis and migration to tissues according to the cell type (Pipes and Coles, 1995; Chandurvelan et al., 2013). The immunomodulation analyzed by DCC show a decrease in frequency of eosinophils only in mussels exposed to QDs, which may be related to the phagocytosis of QDs by eosinophils (probably in the form of aggregates), induction of pro-apoptotic processes and stimulation of migration of these cells to tissues due to their high phagocytic capacity, ROS and NO production, and release of hydrolytic enzymes in the eosinophils hemocytes compared to agranular hemocytes (Le Foll et al., 2010; Canesi and Procházková, 2014). As for dissolved Cd, only the frequency of basophils decreases (Fig. 3.7), that confirms a specific role of basophils in metal detoxification, since this decrease might be expected as they transport Cd to tissues for storage and/or elimination, which is in accordance with the higher accumulation of dissolved Cd in tissues (Chandurvelan et al., 2013). On the other hand, both Cd forms induce an increase in the frequency of hyalinocytes, probably due to the stimulation of hematopoiesis as a compensatory response to the decrease in the frequency of circulating eosinophils and basophils (Fig. 4.7). The hematopoiesis process in bivalves is unknown, but it probably occurs in hemolymph or connective tissues with granulocytes that have agranular precursors (Hine, 1999). Nevertheless, the role of each hemocyte type in QDs and dissolved Cd toxicity should be further characterized, mainly because the origin, life cycle and life span of hemocytes remain unknown. The frequency of aggregates show that both Cd forms do not change the adhesion between hemocytes types (Fig. 4.7), since the aggregates are formed by adhesion between

basophilic hemocytes (aggregate core) and eosinophilic hemocytes (aggregate corona) (Le Foll et al., 2010).

The cytogenotoxic and genotoxic properties of CdTe QDs and dissolved Cd were analyzed by chromosomal damage (MN test and nuclear abnormalities assay) and DNA damage (Comet assay) (Figs. 4.8 and 4.9). The MN assay is considered a sensitive tool to determine chromosomal damage induced by clastogenic (DNA breakage) or aneugenic (abnormal segregation), while the alkaline comet assay enables the identification of DNA strand breaks (single and double) (Almeida et al., 2011; Bolognesi and Fenech, 2012). These methodologies were also used to evaluate genotoxic effects in bivalves exposed to other NPs, as C₆₀ fullerenes, CuO NPs, Ag NPs and CdS QDs (Al-Subiai et al., 2012; Gomes et al., 2013; Katsumiti et al., 2014). The cytogenotoxic effects of Cd are dependent on the metal form and Cd accumulation in tissues. CdTe QDs do not have significant cytogenetic effects in *Mytilus* hemocytes, as no significant chromosomal damage was detected in exposed mussels (BN, MN and Bud). On the other hand, dissolved Cd induces a significant cytogenetic effect in hemocytes associated with increases in the BN cells frequency after 14 days of exposure (Fig. 4.8A). A high cytotoxicity of dissolved Cd was also observed in the gills of freshwater mussel *D. polymorpha* (10 µg L⁻¹; 11 d) (Vincent-Hubert et al., 2011) and in the marine mussel *Perna canaliculus* (200 - 2000 µg L⁻¹; 28 d) (Chandurvelan et al., 2013). This suggests the potential cellular internalization and interaction of Cd²⁺ with cell cycle components during hematogenesis, because the emergence of BN cells is the result of the impairment of cytokinesis (Bolognesi and Fenech, 2012). Furthermore, results denote a cytogenotoxic potential of QDs in *Mytilus* hemocytes after subchronic and chronic exposure, as no significant increase of different nuclear changes (BN, MN and Bud) was identified after 14 days of exposure (Fig. 4.8A).

Early genotoxic effects of CdTe QDs and dissolved Cd were confirmed by the comet assay, indicating that both Cd forms induce DNA strand-breaks in exposed hemocytes via different MoA. QDs at a non-cytotoxic concentration (10 µg Cd L⁻¹, Table 4.1) induce higher DNA strand-breaks in hemocytes than dissolved Cd after 3 and 7 days of exposure, even though a lower Cd accumulation from QDs was detected in tissues (Fig. 4.3). This result shows that Cd accumulation patterns do not reflect the genotoxic potential of these particles and confirms the specific nano-effects. After 14 days, the opposite happens, with higher DNA damage in dissolved Cd exposed mussels, reflected by an increase in the % of DNA tail and in the frequency of hemocytes with

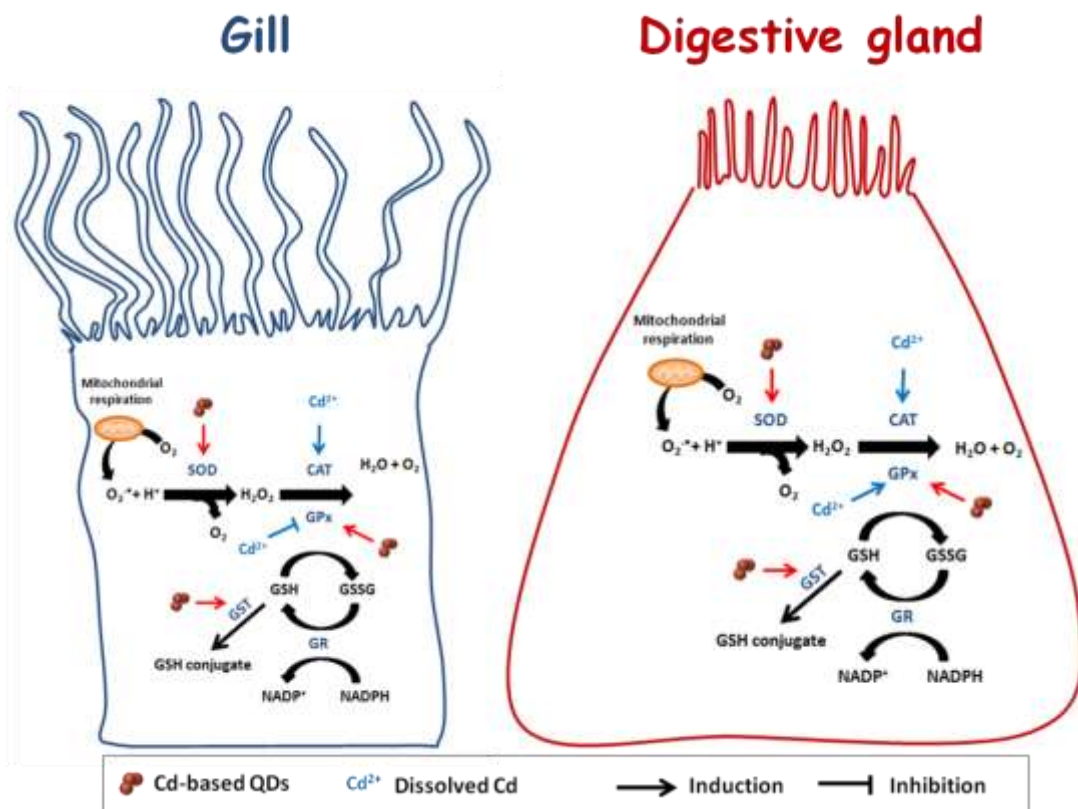
mid and high damage (Figs. 4.8B, 4.8; Table 4.2). These results are related to a higher DNA damage and Cd accumulation rates (whole soft tissues and hemolymph) in mussels exposed to dissolved Cd after 14 days compared to QDs. This increase in DNA damage is also related to the cytotoxic effect of dissolved Cd after 14 days in terms of decrease of viability and cell density. As for QDs, due to the small size (2 - 10 nm), they penetrate in the nucleus *via* nuclear pore complexes, promote DNA strand-breaks through direct interaction with DNA or nuclear proteins, intracellular release of Cd²⁺ ions from the core and produce ROS which lead to DNA damage (Gagné et al., 2008; Aye et al., 2013). Furthermore, the intracellular release of Te²⁻ anion from the QD core and the production of its derivatives cannot be excluded, but the determination of Te concentration in tissues was not measured. On the other hand, dissolved Cd induces DNA damage by three mechanisms: direct DNA interaction, oxidative stress and inhibition of DNA repair system (Vincent-Hubert et al., 2011; Tang et al., 2013).

3.4. Conclusions

Overall, *in vivo* exposure to CdTe QDs affects the immune response and induces DNA damage in mussels *M. galloprovincialis*, which could lead to a possible increase in individual and population susceptibility to diseases or adaptation to environmental stress conditions. The immunocytotoxicity, cytogenotoxicity and genotoxicity of CdTe QDs and its dissolved counterpart are mediated by different mechanisms and not directly related to Cd accumulation in tissues, especially in the case of QDs. Dissolved Cd is the most cytotoxic and cytogenotoxic form on *Mytilus* hemocytes and the genotoxic capacity of QDs is time-dependent. In addition, the results obtained in this study confirm that cell-mediated immunity is one of the most relevant targets of CdTe QDs toxicity and that hemocytes are important models for monitoring the impact of NPs in the marine environment.

CHAPTER V

Tissue specific responses to cadmium-based quantum dots in the marine mussel *Mytilus galloprovincialis*



Part of this Chapter was published in:

- Rocha, T.L., Gomes, T., Mestre, N.C., Cardoso, C., João, M., 2015. Tissue specific responses to cadmium-based quantum dots in the marine mussel *Mytilus galloprovincialis*. *Aquatic Toxicology* 169, 10-18. doi:10.1016/j.aquatox.2015.10.001

Part of this Chapter was presented at:

- Rocha, T.L., Gomes, T., Cardoso, C., Bebianno, M.J., 2014. Cellular and biochemical responses in *Mytilus galloprovincialis* exposed to Quantum dots. 29th ESCPB Congress, Glasgow, Scotland.
- Rocha, T.L., Gomes, T.C., Cardoso, C., Mestre, N., Sousa, V. S.; Bebianno, M.J., 2015. Multibiomarker assessment of cadmium-based quantum dots effects in the marine mussel *Mytilus galloprovincialis*. 10^o Congreso Ibérico y 7^a Iberoamericano de Contaminación y Toxicología Ambiental - CICTA, Vila Real, Portugal.

Abstract

In recent years, Cd-based quantum dots (QDs) have generated interest from the life sciences community due to potential applications in nanomedicine, biology and electronics. However, these engineered nanomaterials can be released into the marine environment, where their environmental health hazards remain unclear. This study investigated the tissue specific responses related to alterations in the antioxidant defence system induced by CdTe QDs, in comparison with its dissolved counterpart, using the marine mussel *Mytilus galloprovincialis*. Mussels were exposed to CdTeQDs and dissolved Cd for 14 days at $10\ \mu\text{g Cd L}^{-1}$ and biomarkers of oxidative stress [superoxide dismutase (SOD), catalase (CAT), glutathione peroxidases (total, Se-independent and Se-dependent GPx) and glutathione-S-transferase (GST)] were analyzed along with Cd accumulation in the gills and digestive gland of mussels. Results show that both Cd forms changed mussel's antioxidant responses with distinct modes of action (MoA). There were tissue- and time-dependent differences in the biochemical responses to each Cd forms, wherein QDs are more pro-oxidant when compared to dissolved Cd. The gills are the main tissue affected by QDs with effects related to the increase of SOD, GST and GPxs activities, while those of dissolved Cd was associated to the increase of CAT activity, Cd accumulation and exposure time. Digestive gland is a main tissue for accumulation of both Cd forms, but changes in antioxidant enzymes are lower when compared to the gills. A multivariate analysis revealed that the antioxidant patterns are tissue dependent, indicating nano-specific effects possibly associated to oxidative stress and changes in redox homeostasis.

Keywords: Nanomaterials, metal-based nanoparticle, CdTe Quantum dots, ecotoxicology, oxidative stress, antioxidant enzymes, *Mytilus galloprovincialis*.

5.1. Introduction

QDs are engineered semiconductor nanocrystals with a nanometer diameter (2 - 10 nm) comprising a metalloid core usually coated with a shell or ligands, which enhances its optical and electronic properties while reducing metal leaching. Cd-based QDs have been used in different nanotechnologies including biomedical imaging, cancer detection, targeted drug delivery, electronic, pharmacy and as chemosensors in analytical chemistry (Michalet et al., 2005; Rizvi et al., 2010). The increasing production and use of these ENPs will likely increase their release into the aquatic environment. Although QDs concentrations in the environment are unavailable, there are increasing concerns about its possible ecological risks and toxicity to human health (Hardman, 2006; Rocha et al., 2014, 2015a).

Ecotoxicological impact of Cd-based QDs in aquatic organisms has been reported in several studies using *in vitro* and *in vivo* exposure (Gagné et al., 2008a; Peyrot et al., 2009; Katsumiti et al., 2014; Rocha et al., 2014; 2015a; Buffet et al., 2015) (Chapters 2 and 4). However, the mechanisms of QDs-mediated toxicity are not well established and depend on size, chemical composition, surface coating and exposure conditions. Many studies suggested that the QDs toxicity is mainly related to QDs dissolution and extra- and intracellular release of Cd^{2+} ions (Peyrot et al., 2009, Domingos et al., 2011; Katsumiti et al., 2014). On the other hand, other studies indicated that the generation of free radicals or ROS associated to oxidative damage are the major MoA of Cd-based QDs (Gagné et al., 2008a; Buffet et al., 2015).

QDs are efficient energy donors and have the ability to generate ROS in aqueous solutions under exposure to ultraviolet or visible electromagnetic radiation (Ipe et al., 2005). In this condition, QDs can promote the delocalization of an electron (e^-) from the valence band (v_b) to conduction band (c_b) creating an electron-hole pair ($e_{cb}^- + h_{vc}^+$), which can undergo redox reactions with surface adsorbed molecules (Ribeiro et al., 2012). Band-gap energy of CdTe QDs is between 1.8 and 2.4 eV for v_b and c_b , respectively, that is potentially sufficient to reduce O_2 and to oxidize H_2O molecules to produce ROS, such as superoxide radical ($\text{O}_2^{\cdot-}$) and hydroxyl radical (OH^{\cdot}) (Santana et al., 2015). Furthermore, the type and quantity of ROS generated depends on the QDs composition and on the fact that QDs photo-activation is size dependent (Ipe et al., 2005; Ribeiro et al., 2012; Santana et al., 2015).

From the context of aquatic nanotoxicology, bivalve species have the higher capacity to concentrate Cd-based QDs from water, which can induce several tissue and

cellular damage (Gagné et al., 2008a; Peyrot et al., 2009; Rocha et al., 2014; 2015a; Buffet et al., 2015) (Chapters 1 - 4). *In vitro* toxicity of CdS QDs (5 nm; 10^{-4} - 10^2 mg Cd L⁻¹; 24 h) in *M. galloprovincialis* hemocytes and gill cells was associated with extra- and intracellular release of Cd²⁺ ions and consequent oxidative damage (Katsumiti et al., 2014). QDs-induced oxidative stress and DNA damage were also reported in the freshwater mussel *E. complanata* exposed to CdTe QDs (1.6 - 8 mg L⁻¹; 24 h), whereby the ROS generation induced by QDs lead to an immunosuppressive effect and inflammatory condition (Gagné et al., 2008a; Peyrot et al., 2009). These studies also observed inhibition and induction of MTs in the gills and digestive gland, respectively, while LPO increased in gills and decreased in the digestive gland (Gagné et al., 2008a; Peyrot et al., 2009). *In vivo* exposure to CdTe QDs (6 nm; 10 µg Cd L⁻¹; 14 d) also induced immunotoxic and genotoxic effects in the marine mussel *M. galloprovincialis* (Rocha et al., 2014) (Chapter 4) and CdS QDs (5 - 6 nm; 10 µg Cd L⁻¹; 14 d) induced behaviour and biochemical impairment in whole soft tissues of the marine clam *S. plana* (Buffet et al., 2014a). The estimated $t_{1/2}$ of CdTe QDs for *M. galloprovincialis* ($t_{1/2} > 50$ d) is longer than for other ENPs in bivalves and results indicated the digestive gland role in QDs storage, while the haemolymph is the route for QDs and dissolved Cd distribution between tissues (Rocha et al., 2015a) (Chapters 2 and 4). However, to the best of our knowledge, this is the first *in vivo* study of tissue specific response related to oxidative stress in marine mussels exposed to Cd-based QDs.

Differential tissue responses are involved in the uptake, accumulation and detoxification processes in bivalve species exposed to ENPs. Recent studies suggested that the gills were more susceptible to dissolved metal toxicity, while digestive gland was more sensitive to ENPs (McCarthy et al., 2013; Gomes et al., 2012). Higher ENPs concentrations were found in the digestive gland compared to gills from bivalves exposed to different ENPs, such as fullerenes, Au NPs, Ag NPs, CuO NPs and CdTe QDs (Tedesco et al., 2010; Al-Subiai et al., 2012; Gomes et al., 2012; McCarthy et al., 2013; Rocha et al., 2015a) (Chapters 1 and 2). This differential tissue accumulation was related to highly developed processes for the cellular internalization of nano- and microscale particles (endocytosis and phagocytosis) in the digestive gland cells (Moore et al., 2006; Canesi et al., 2012), nevertheless it has been demonstrated that gills can also be a main target for ENPs (Koehler et al., 2008; Trevisan et al., 2014). Thereby, more studies are required to investigate the tissue specific differences in ENPs toxicity,

which are essential elements to understand their MoA and nano-specific effects in aquatic organisms.

The tissue specific toxicity of metals, including Cd, is well known in aquatic molluscs (Bebianno et al., 1993; Soto et al., 1996; Marigómez et al., 2002). However, there is a lack of knowledge on the tissue specific responses to ENPs exposure in marine organisms. Accordingly, the aim of this study was to analyse the antioxidant capacity and tissue specific responses in the marine mussel *M. galloprovincialis* after *in vivo* exposure (14 days) to Cd-based QDs and dissolved Cd. Activities of antioxidant enzymes, such as SOD, CAT, GST, total GPx, Se-I GPx and Se-D GPx were measured in mussel gills and digestive gland along with Cd accumulation in both tissues. PCA was applied to all the data obtained for the gills and digestive gland to explain the effects of both Cd forms (CdTe QDs and dissolved Cd) and the tissue specific responses.

5.2. Materials and Methods

5.2.1. QDs characterization

Orange CdTe QDs were obtained from PlasmaChem GmbH (Berlin, CAS# 1306-25-8) with declared purity of 99.9 %, particle size of 2 - 7 nm, an emission wavelength at 590 ± 5 nm and a core coated by carboxyl groups (-COOH). A QDs stock solution was made using Milli-Q water (100 mgCd L^{-1}), sonicated for 30 min (Ultrasonic bath VWR International, 230 V, 200 W, 45 KHz frequency) and kept in constant shaking. Suspensions of QDs in Milli-Q water and natural seawater ($S = 36.3$) were characterized by a combination of analytical techniques (TEM, DLS, ELS) as described in Rocha et al. (2014, 2015a) (Chapters 2 and 4). Dissolved cadmium stock solution was prepared identically but not sonicated using cadmium nitrate ($\text{Cd}(\text{NO}_3)_2 \cdot 4\text{H}_2\text{O}$) (Merck).

5.2.2. Experimental design

Mussels *M. galloprovincialis* (60 ± 5 mm shell length) were collected in the Ria Formosa Lagoon (Portugal) (Figs. 1.15 -1.16) and acclimated during 14 days in tanks containing natural seawater ($S: 36.3$) at 16°C and constant aeration. After acclimation, fifty mussels were placed in 30 L tanks filled with 25 L of seawater ($2.0 \text{ mussels L}^{-1}$) and exposed to $10 \mu\text{g Cd L}^{-1}$ of CdTe QDs and their dissolved counterpart jointly with a control group kept in clean seawater in a triplicate design (3 tanks per treatment) for

14 days of exposure, as described in Rocha et al. (2014) (Chapter 4). Seawater was changed daily with redosing of the Cd concentrations and exposure experiments were conducted in a static-renewal condition under 12h: 12h light/dark cycles. Seawater quality was analysed daily by measuring salinity (36.3 ± 0.07), temperature (16.6 ± 1.2 °C), pH (7.9 ± 0.1) and oxygen saturation (103 ± 1.3 %). Mussels were only fed with the plankton existent in the natural seawater and no significant mortality was observed between unexposed mussels and those exposed to both Cd forms by the end of the exposure period. Mussels from each experimental condition were collected at the beginning of the experiment and after 3, 7 and 14 days of exposure. After sampling, gills and digestive gland were dissected and immediately frozen in liquid nitrogen and stored at -80 °C until further use.

5.2.3. Cd concentration

Cd concentration was determined in dried mussel tissues (80 °C, 48 h) after wet acid digestion with HNO₃ (80 °C, 4 h) by graphite furnace AAS (Analyst 800-PerkinElmer). Accuracy was assured with certified reference material (TORT-II, Lobster Hepatopancreas) from the National Research Council (Canada) and results were similar to the certified values (28.5 ± 4.5 mg Cd kg⁻¹ and 26.7 ± 0.6 mg Cd kg⁻¹, respectively). Cd levels are expressed as µg g⁻¹ of dry weight.

5.2.4. Antioxidant enzymes

Antioxidant enzymes (SOD, CAT, GST, total GPx, Se-I GPx and Se-D GPx) activities were measured in the gills and digestive gland cytosolic fraction of five mussels from unexposed mussels and exposed to each Cd form. Mussel tissues were homogenized in 0.02 M Tris-HCl buffer (pH 7.6), containing 1 mM of EDTA, 0.5 M of sucrose, 0.15 M of KCl and 1 mM of DTT, in an ice bath for 2 min (the tissue-to-buffer ratio was 1:5 wet weight tissue/volume of buffer). The homogenates were centrifuged at 500 g (15 min, 4 °C) and the supernatant was re-centrifuged at 12000 g (45 min, 4 °C) to produce the cytosolic fraction (Gomes et al., 2012).

SOD activity was determined by reduction of cytochrome c by the xanthine oxidase/hypoxanthine system at 550 nm, using a molar extinction coefficient (ϵ) of 50 M⁻¹ cm⁻¹ (McCord and Fridovich, 1969) and results expressed in U mg⁻¹ total protein. CAT activity was analysed by the decrease in absorbance due to H₂O₂ consumption at 240 nm (ϵ = of 40 M⁻¹ cm⁻¹) (Greenwald, 1985) and results expressed as

$\mu\text{molmin}^{-1} \text{ mg}^{-1}$ of total proteins. GST activities were measured following the conjugation of reduced glutathione (GSH) with 1-chloro 2,4 dinitrobenzene (CDNB) at 340 nm ($\epsilon = 9.6 \text{ mM}^{-1} \text{ cm}^{-1}$) (Habig et al., 1974) and results expressed as $\mu\text{molmin}^{-1} \text{ mg}^{-1}$ of total proteins. The SE-I GPx and Se-D GPx activities were measured by using cumene hydroperoxide and H_2O_2 as substrates, respectively. GPx activities were measured following NADPH oxidation in the presence of excess glutathione reductase, reduced glutathione and cumene hydroperoxide or H_2O_2 as substrate at 340 nm ($\epsilon = 6.22 \text{ mM}^{-1} \text{ cm}^{-1}$) according to the method described by Flohe and Gunzler (1984) and adapted to a microplate reader (McFarland et al., 1999). Total GPx activity was calculated as the sum of Se-I GPx and Se-D GPx activities. GPx results are expressed as $\text{nmolmin}^{-1} \text{ mg}^{-1}$ of total proteins.

5.2.5. Total protein concentration

The determination of total protein concentration was measured in the cytosolic fraction according to the Bradford method (Bradford, 1976) and adapted to a microplate reader (Infinite[®] 200 PRO-Tecan), using Bovin Serum Albumin (Sigma-Aldrich) as a standard. Protein concentrations are expressed as mg g^{-1} wet weight tissue.

5.2.6. Statistical analysis

Statistical analyses were carried out using the Statistica 7.0 software (Statsoft Inc., 2005, Tulsa, OK, USA). Significant differences between the different treatments for the analyzed variables were identified using parametric tests (two-way ANOVA, followed by the Tukey's test) and/or non-parametric tests (Kruskal-Wallis), depending on the distribution of data and homogeneity of variances (Shapiro-Wilk and Levene's tests). Linear and nonlinear regression analyses were also applied to verify significant relationships between variables.

PCA was also used to evaluate the relationship between the different treatments [unexposed mussels and Cd-exposed mussels (QDs and dissolved Cd)] and the analysed variables [antioxidant enzymes (SOD, CAT, GST, total GPx, Se-I GPx and Se-D GPx) activities] in the gills and digestive gland and along the exposure period (14 days). The PCA was performed to differentiate tissue specific responses and MoA of both Cd forms. Results were considered significant when $p < 0.05$.

5.3. Results and discussion

5.3.1. Characterization and behaviour of QDs in seawater

Data on characterization of CdTe QDs in the aqueous medium used in this work are summarized in Table 3.1. QDs have spheroid shape and particle size reported by the manufacturer is 2 - 7 nm, which is in agreement with the size obtained by TEM (6 ± 1 nm) (Table 3.1). DLS results indicate that the hydrodynamic diameter (dh) and polydispersity index of QDs aggregates/agglomerates in natural seawater at pH 8.0 is 1014 ± 187 nm and 0.5 ± 0.1 , respectively. ELS analysis show isoelectric point in seawater at pH 10 - 12 and confirm negative surface charge of QDs aggregates/agglomerates at pH 8.0 (ζ -potential = -9.4 ± 1.2 mV). This finding is supported by other studies with QDs (Morelli et al., 2012; Hull et al., 2013) and confirms the tendency of these ENPs to aggregate/agglomerate in seawater and quickly settle on the bottom of the exposure tanks. Dissolution rate of QDs in seawater at pH 8.0 (27.6 %) was previously described (Rocha et al., 2015a) (Chapter 2) and confirm that dissolved Cd is more bioavailable than QDs for mussel *M. galloprovincialis*, where QDs have fast homo-aggregation, sedimentation, low dissolution rate and speciation of Cd from QDs core in seawater (Rocha et al., 2014, 2015a).

5.3.2. Cd accumulation

Cd concentration in mussel tissues significantly increased after 14 days of exposure to QDs (gills: 35-fold; digestive gland: 55-fold) and dissolved Cd (gills: 84-fold; digestive gland: 135-fold) when compared to unexposed mussels ($p < 0.05$) (Table 5.1). Cd accumulation in the gills was lower when compared to the digestive gland (3.18- and 3.3-fold lower for QDs and dissolved Cd, respectively) (Table 5.1). QDs aggregation/agglomeration in seawater associated their uptake mainly through the digestive gland cells via endocytotic mechanisms, and these results confirm the digestive gland role in storage and detoxification of both Cd forms. Therefore, Cd levels in mussel tissues are Cd form and tissue dependent and the dissolved Cd is the most bioavailable form (Hull et al., 2013; Rocha et al., 2015a) (Chapter 2). On the other hand, these results disagree with previous studies that showed similar Cd accumulation in whole soft tissues of the marine clam *S. plana* exposed to CdS QDs (5 - 6 nm; $10 \mu\text{gCd L}^{-1}$; 14 d) (Buffet et al., 2015) and in the gills and digestive gland of the freshwater mussel *E. complanata* exposed to CdTe QDs ($1.6 - 8 \text{ mg L}^{-1}$; 24 h) (Peyrot et

al., 2009). In this study, tissue specific Cd accumulation in *M. galloprovincialis* exposed to CdTe QDs may be related besides the route and time of exposure to different cell type composition, as well as tissue-specific expression of protein related to metal metabolism (e. g. MTs) (Zorita et al., 2007).

5.3.3. Antioxidant responses

Antioxidant enzymes activities of unexposed mussels did not changed over time ($p > 0.05$; Fig. 5.1 A-J). However, tissue specific biochemical responses were observed after exposure to CdTe QDs and dissolved Cd (Fig. 5.1 A-J). SOD, CAT, GPxs and GST activities changed after exposure to QDs, suggesting that these ENPs have potential redox properties with the capacity to generate ROS and oxidative stress in marine mussels. An overview of the results shows that alterations in enzymatic activities were more pronounced in the gills after exposure to Cd-based QDs.

Table 5.1. Cd concentration (mean \pm std $\mu\text{g g}^{-1}$ d. w. tissue) in the gills and digestive gland of mussels *M. galloprovincialis* from controls (C), exposed to CdTe quantum dots (QDs) and to dissolved cadmium (Cd) for 14 days. Different capital and lower letters indicate significant differences between treatments at each time of exposure and within treatment during the exposure period, respectively ($p < 0.05$).

Time (days)	Gill ¹			Digestive gland ¹		
	C	QDs	Cd ²⁺	C	QDs	Cd ²⁺
0	0.43 \pm 0.15 ^{Aa}	0.43 \pm 0.15 ^{Ac}	0.43 \pm 0.15 ^{Ac}	0.99 \pm 0.19 ^{Aa}	0.99 \pm 0.19 ^{Ac}	0.99 \pm 0.19 ^{Ac}
3	0.46 \pm 0.12 ^{Ca}	4.57 \pm 1.31 ^{Bc}	9.25 \pm 1.39 ^{Ab,c}	0.97 \pm 0.23 ^{Ba}	14.01 \pm 3.82 ^{Ab,c}	11.74 \pm 2.38 ^{Ac}
7	0.42 \pm 0.05 ^{Ca}	9.40 \pm 1.95 ^{Bb}	22.82 \pm 5.08 ^{Ab}	0.93 \pm 0.22 ^{Ca}	25.34 \pm 12.13 ^{Bb}	80.9 \pm 22.1 ^{Ab}
14	0.52 \pm 0.12 ^{Ca}	18.21 \pm 2.2 ^{Ba}	43.33 \pm 8.98 ^{Aa}	1.05 \pm 0.12 ^{Ca}	57.85 \pm 14.01 ^{Ba}	143.4 \pm 42.7 ^{Aa}

¹ Data from Rocha et al. (2015a) (Chapter 2).

In mussels exposed to QDs, SOD activity in the gills increased linearly over time of exposure ($\text{SOD U mg}^{-1} \text{ prot} = 0.599x + 2.564$, $r = 0.98$, $p < 0.05$), suggesting $\text{O}_2^{\cdot-}$ generation. On the other hand, in mussels exposed to dissolved Cd, SOD activity only increased between 3 and 7 days of exposure (1.7-fold and 1.8-fold, respectively, $p < 0.05$) and remained unchanged after 14 days when compared to unexposed mussels ($p > 0.05$) (Fig. 5.1 A). For the digestive gland, SOD activity only increased in QDs-exposed mussels after 14 days of exposure (4-fold, $p < 0.05$) and no significantly

changes were observed in dissolved Cd-exposed ones ($p > 0.05$; Fig. 5.1 B). Overall, after 14 days of exposure, QDs induced higher SOD activity in the gills when compared to dissolved Cd (gills: 3-fold, digestive gland: 1.5-fold, $p < 0.05$), indicating nano-specific tissue effects.

The increase in SOD activity in both mussel tissues during QDs exposure was not followed by the increase in CAT activity (Fig. 5.1 B-E). In both tissues, CAT activity only increase after 3 days of exposure to QDs (gill: 1.7-fold, digestive gland: 2.3-fold, $p < 0.05$) (Fig. 5.1 C-D), decreasing afterwards to levels similar to controls. However, in mussels exposed to dissolved Cd, CAT activity increased after 3 and 7 days of exposure in the digestive gland (1.7-fold) and gills (2-fold), respectively ($p < 0.05$). These higher CAT activities remained until the end of the exposure period to dissolved Cd (14 days), showing significant differences between the two Cd forms. CAT induction in dissolved Cd versus QDs was 1.4- and 2.8-folds for gills and digestive gland, respectively ($p < 0.05$), indicating that the dissolved Cd possibly induced higher H_2O_2 than Cd-based QDs. Similarly, gills cells of the *M. galloprovincialis* showed higher CAT activity after *in vitro* exposure to dissolved Cd when compared to CdS QDs (5 nm; 10^{-4} - 10^2 mg Cd L⁻¹; 24 h) (Katsumiti et al., 2014), confirming lower release of Cd²⁺ from QDs core and lower H_2O_2 production mediated by QDs in mussel tissues.

In QDs-exposed mussels, the increase in total GPx activity was concomitant with an increase in SOD activity (Figs. 5.1 E-F and 5.2), suggesting a compensatory mechanism between antioxidant enzymes under QDs-mediated ROS formation. On the other hand, in mussels exposed to dissolved Cd for 14 days, total GPx activity decreased in the gills (2.3-fold) and increased in the digestive gland (1.8-fold) (Figs. 5.1 E-F and 5.2), suggesting either a depletion of substrate necessary for the activation of this enzyme or an alteration of its conformation rendering it inactive.

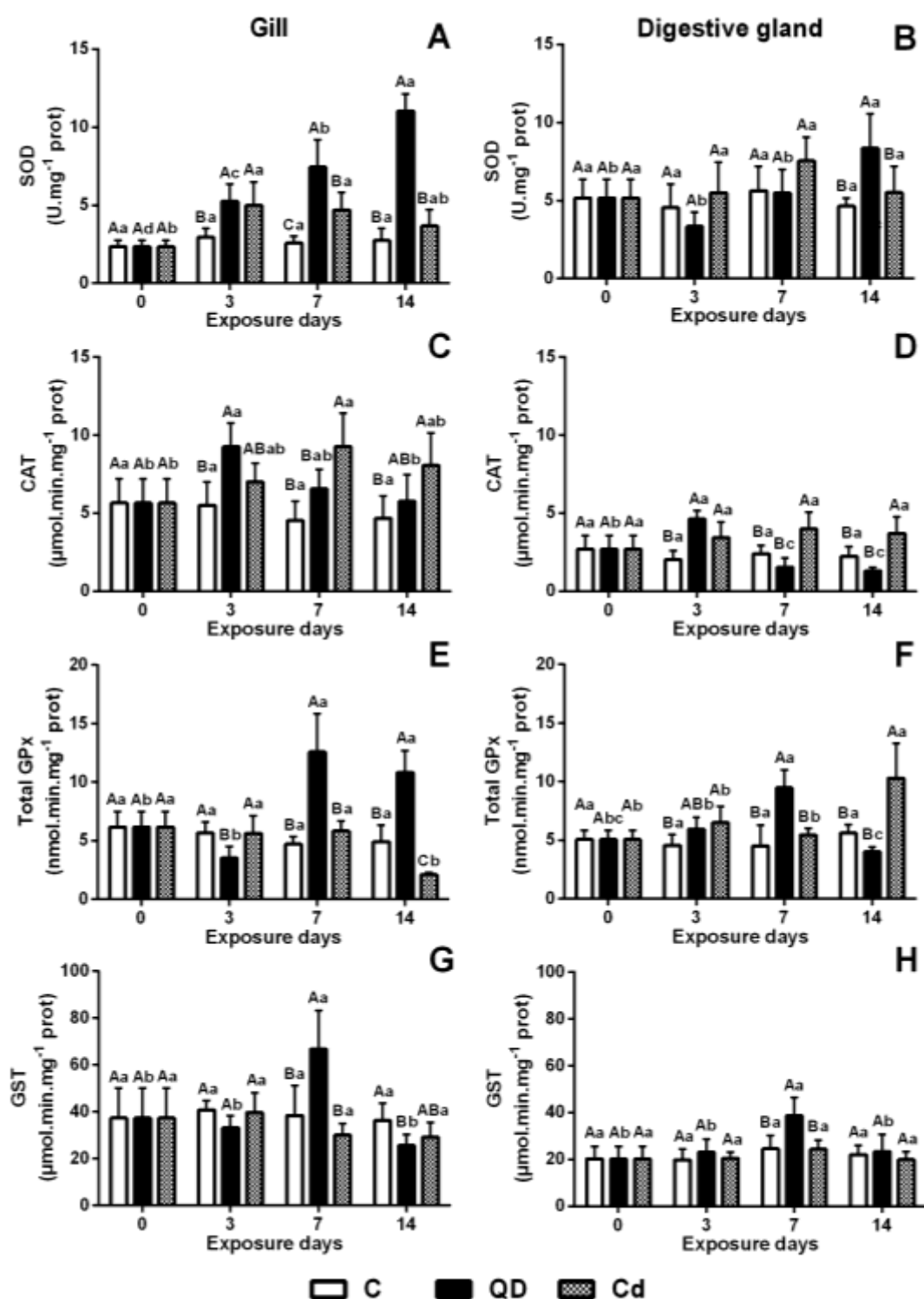


Figure 5.1. Superoxide dismutase (SOD) (A-B), catalase (CAT) (C-D), total glutathione peroxidase (Total GPx) (E-F) and glutathione-S-transferase (GST) (G-H) activities in the gills and digestive gland of mussels *M. galloprovincialis* from controls (C), exposed to CdTe quantum dots (QDs) and to dissolved cadmium (Cd) for 14 days (mean \pm std).

In QD-exposed mussels, Se-D GPx and SOD activities in the gills generally followed the same pattern, showing that the Se-D GPx is a more sensitive enzyme of defence responding to Cd-based QDs than Se-I GPx (Fig. 5.2). In both tissues of QDs-exposed mussels, Se-I GPx and Se-D GPx activities increased after 7 days of exposure ($p < 0.05$) (Fig. 5.2). After this time, both GPxs activities remained high in the gills (Se-I GPx: 1.6-fold; Se-D GPx: 3.1-fold; $p < 0.05$), but returned to similar control levels in the digestive gland of QDs-exposed mussels ($p > 0.05$). On the other hand, exposure to dissolved Cd increased Se-I GPx in the digestive gland only after 14 days (1.7-fold; $p < 0.05$) and induced Se-D GPx after 3 and 14 days of exposure (2.2- and 2.4-fold, respectively; $p < 0.05$) (Fig. 5.2). Furthermore, lower Se-D GPx activity (5.3-fold) was observed in the digestive gland of mussels exposed to QDs compared to dissolved Cd ($p < 0.05$), indicating nano-specific effects. The observed results agree with previous studies about the oxidative stress in bivalve species induced by Cd-based QDs (i. e. CdS and CdTe QDs) (Gagné et al., 2008a; Buffet et al., 2015), showing that the impairment or overcome of the antioxidant defences in *M. galloprovincialis* exposed to CdTe QDs promotes oxidative stress, which may be related to genotoxic, immunotoxic and cytogenotoxic effects (Rocha et al., 2014; 2015c) (Chapters 3 and 4).

GSTs are multifunctional isoenzymes involved in the cellular detoxification of reactive electrophilic compounds, regulation of redox homeostasis and innate immune responses in mussels (Wang et al., 2013). After 7 days of exposure to Cd-based QDs, GST activity increased in the mussel gills (1.7-fold) and digestive gland (1.6-fold) ($p < 0.05$; Fig. 5.1 I-J). Afterwards, GST activity decreased in the gills (1.4-fold; $p < 0.05$) and similar levels to controls were observed in the digestive gland ($p > 0.05$). On the other hand, in dissolved Cd-exposed mussels no significant changes were detected in GST activity for both tissues during the 14 days of exposure ($p > 0.05$; Fig. 5.1 I-J). Results agree with a previous study that showed higher GST activity in the whole soft tissues of *S. plana* exposed to CdS QDs (5 - 6 nm; 10 $\mu\text{g Cd L}^{-1}$; 14 d) when compared to dissolved Cd (Buffet et al., 2015), confirming the role of this enzyme in redox homeostasis in bivalves exposed to Cd-based QDs.

GST has the capacity to metabolize reactive products from the LPO process and oxidative metabolism, such as organic hydroperoxides, alkenals and epoxides (Canesi et al., 1999; Pickett and Lu, 1989). An increase of this enzyme was also observed in bivalves exposed to others metals and metal-based ENPs (e. g. Ag NPs, CuO NPs, CdS QDs) (Canesi et al., 1999; Buffet et al., 2013, 2015; Gomes et al., 2012), confirming

that the GST represent an important defense response against metals and metal-based ENPs toxicity. Thereby when the bivalve antioxidant response is not sufficient to prevent the ENPs-induced oxidative degradation of lipids (LPO), GST can act as a compensatory mechanism and reduce the toxicity of the compounds derived from LPO.

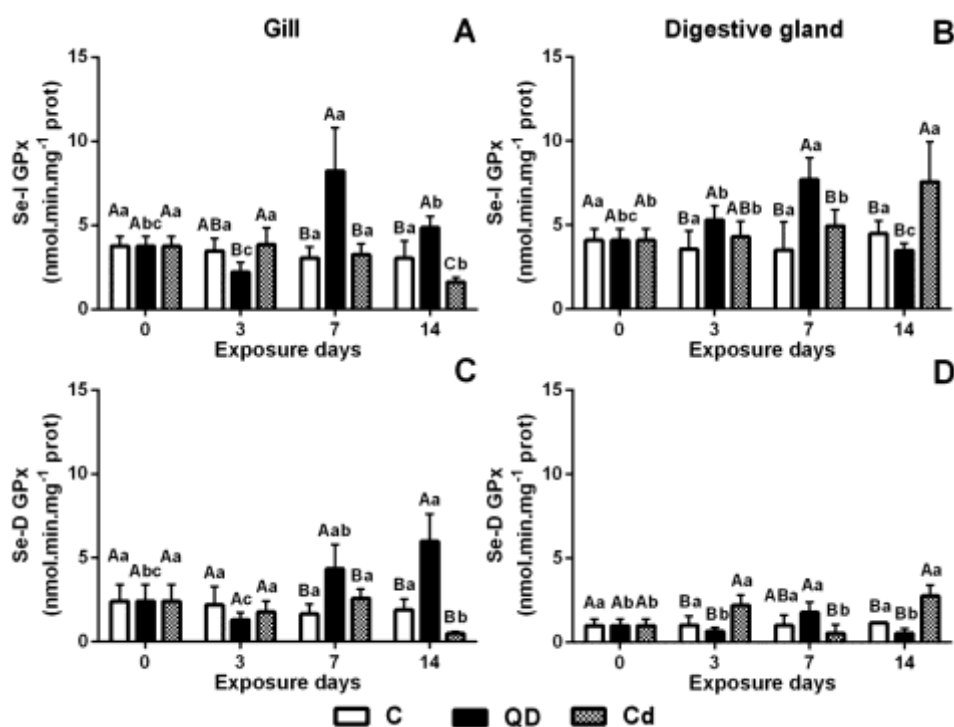


Figure 5.2. Se-independent glutathione peroxidase (Se-I GPx) (A-B) and Se-dependent glutathione peroxidase (Se-D GPx) (C-D) activities in the gills (A, C) and digestive gland (B, D) of mussels *M. galloprovincialis* from controls (C), exposed to CdTe quantum dots (QDs) and to dissolved cadmium (Cd) for 14 days (mean \pm std). Different capital and lower letters indicate significant differences between treatments at each time of exposure and within treatment during the exposure period, respectively ($p < 0.05$).

Results of antioxidant enzymes activities show a higher response in the gills compared to digestive gland, suggesting that the gills may be more susceptible to ROS generation and oxidative stress, principally in QDs-exposed mussels. Gills are principally responsible for uptake of ionic Cd released from QDs core and from Cd-chloro-complexes by passive diffusion and/or via active transport pumps for essential metals (Ca²⁺- channels) (Marigómez et al., 2002; Hull et al., 2013; Rocha et al., 2015a) (Chapter 2). This differential response in the gills may relate to its direct contact with water and/or pollutants and physiological roles in respiration, ionic osmoregulation and

higher oxygen content (Regoli et al., 1995). Furthermore, QDs aggregates/agglomerates can be broken by cilia action in the gills (Joubert et al. 2013; Katsumiti et al., 2014; Rocha et al., 2015b) (Chapter 2). Branchial epithelium is the first contact between the body surface and different Cd forms (QDs and or Cd^{2+} ions released from QDs core). Probably this epithelium is also in contact with ROS generated by QDs photo-activation (i. e. $\text{O}_2^{\cdot-}$ and OH^{\cdot}) in aqueous solution (Ipe et al., 2005; Ribeiro et al., 2012; Santana et al., 2015), which may contribute to a higher response in the antioxidant system in the gills when compared to digestive gland. Furthermore, in the nano-bio interaction scenario (Ma and Lin, 2013), the physical contact can be another mechanism contributing to the Cd-based QDs toxicity in aquatic organisms, but these parameters were not followed.

Digestive gland cells are highly adapted for endocytosis of large particles (< 100 nm) and represent main organ for ENPs-aggregates/agglomerates uptake and storage in the bivalves (Moore et al., 2006; Canesi et al., 2012; Gomes et al., 2012). In this tissue, QDs aggregates/agglomerates can be broken in microvillus border and under an intracellular digestion process inside digestive gland lysosomes where the Cd-based QDs can change size, shape, charge, shell and release Cd^{2+} ions in the digestive system of the *M. galloprovincialis* (Joubert et al. 2013; Katsumiti et al., 2014; Rocha et al., 2015b). In bivalve molluscs, digestive gland is the main site for metabolic regulation, detoxification and elimination of xenobiotics, besides participating in the regulation of homeostasis, immune defense and reproductive process (Gomes et al., 2012; Marigómez et al., 2012). These tissue specific responses were previously reported in bivalves exposed to other ENPs, such as Ag NPs in mussels *M. galloprovincialis* (42 ± 9.6 nm; $10 \mu\text{g L}^{-1}$; 15 d) (Gomes et al., 2014) and in oysters *C. virginica* (20 - 30 nm; $0.02 - 20 \text{ mg L}^{-1}$; 48 h) (McCarthy et al., 2013), indicating differential biophysicochemical interactions at the interfaces between metal-based ENPs and marine organisms when compared to its dissolved counterparts.

5.3.4. Tissue specific antioxidant patterns

The PCA on the data for the gills and digestive gland confirm differential tissue response and MoA of both Cd forms in the marine mussels (Fig. 5.3 A-D). In both tissues, the overall PCA indicates a clear separation between unexposed mussels and those exposed to both Cd-forms. Similar responses were observed between unexposed mussels (Fig. 5.3 A-D), showing lower biomarkers variance in both tissues with time in

the control group. The two principal components represent 80.0 % and 74.4 % of total variance in the gills (PC1 = 49.3 %, PC2 = 30.7 %) and digestive gland (PC1 = 51.3 %, PC2 = 23.1 %), respectively. After 3 days of exposure, QDs-exposed mussels showed higher response when compared to the dissolved Cd-exposed ones, indicating early response of the antioxidant system in short-time of exposure to QDs. However, a clear separation between times of exposure was observed in both Cd forms, confirming that the tissue specific response and changes in antioxidant capacity induced by Cd-based QDs in *M. galloprovincialis* is time and Cd form dependent. Similar biomarkers variation with time of exposure was also observed in *M. galloprovincialis* exposed CuO NPs (31 nm; 10 $\mu\text{g L}^{-1}$; 15 d) (Gomes et al., 2012), confirming that the oxidative stress mediated by ENPs are more pronounced after *in vivo* long-time exposure (> 7 days).

Gills were more susceptible to changes in the antioxidant system after exposure to QDs compared to digestive gland. PCA results showed that there are different MoA between both Cd forms in the gills, especially after 7 and 14 days of exposure (Fig. 5.3A-B). QDs toxicity in the mussel gills is closely related to changes in antioxidant enzymes, especially SOD, GST, total GPx, Se-I GPx and Se-D GPx activities (PC1). On the other hand, dissolved Cd exposure was associated to the increase of total Cd concentration, CAT induction and increase of exposure time (PC2) (Fig. 5.3A-B). The changes in antioxidant enzymes in the QDs-exposed mussels did not follow Cd accumulation in both mussel tissues, indicating that the QDs effects are not only attributed to QDs dissolution and release of Cd^{2+} ions, as observed in *E. complanata* exposed to CdTe QDs (1.6 - 8 mg L^{-1} ; 24 h) (Gagné et al., 2008a), *M. edulis* exposed to CdS-CdTe QDs (1 - 10 nm; 0 - 2.7 $\mu\text{g L}^{-1}$; 21 h) (Bruneau et al., 2013) and in *S. plana* exposed to CdS QDs (5 - 6 nm; 10 $\mu\text{g Cd L}^{-1}$; 14 d) (Buffet et al., 2015). Results indicate that the CdTe QDs remained in the nanoparticulate form in the mussel tissues, but the detoxification mechanism of QDs in bivalve remains poorly understood (Rocha et al., 2015a, b).

The PCA results showed that the biochemical response in the digestive gland is more significant after 14 days of exposure to both Cd forms (Fig. 5.3 C-D), indicating different antioxidant patterns between QDs and dissolved Cd. After long-time exposure to QDs (14 days), biochemical response in digestive gland was related to the increase in SOD activity and exposure time (PC2), while the response to dissolved Cd was associated to total Cd accumulation and changes in GST, total GPx, Se-I GPx and Se-D activities (PC1). Cd accumulation is higher in the digestive gland compared to the gills

(3.2-fold), confirming the role of digestive gland in QDs storage (Rocha et al., 2015a,c) (Chapters 2 and 3), while the gills have a key role in the protection against pro-oxidant effects of Cd-based QDs.

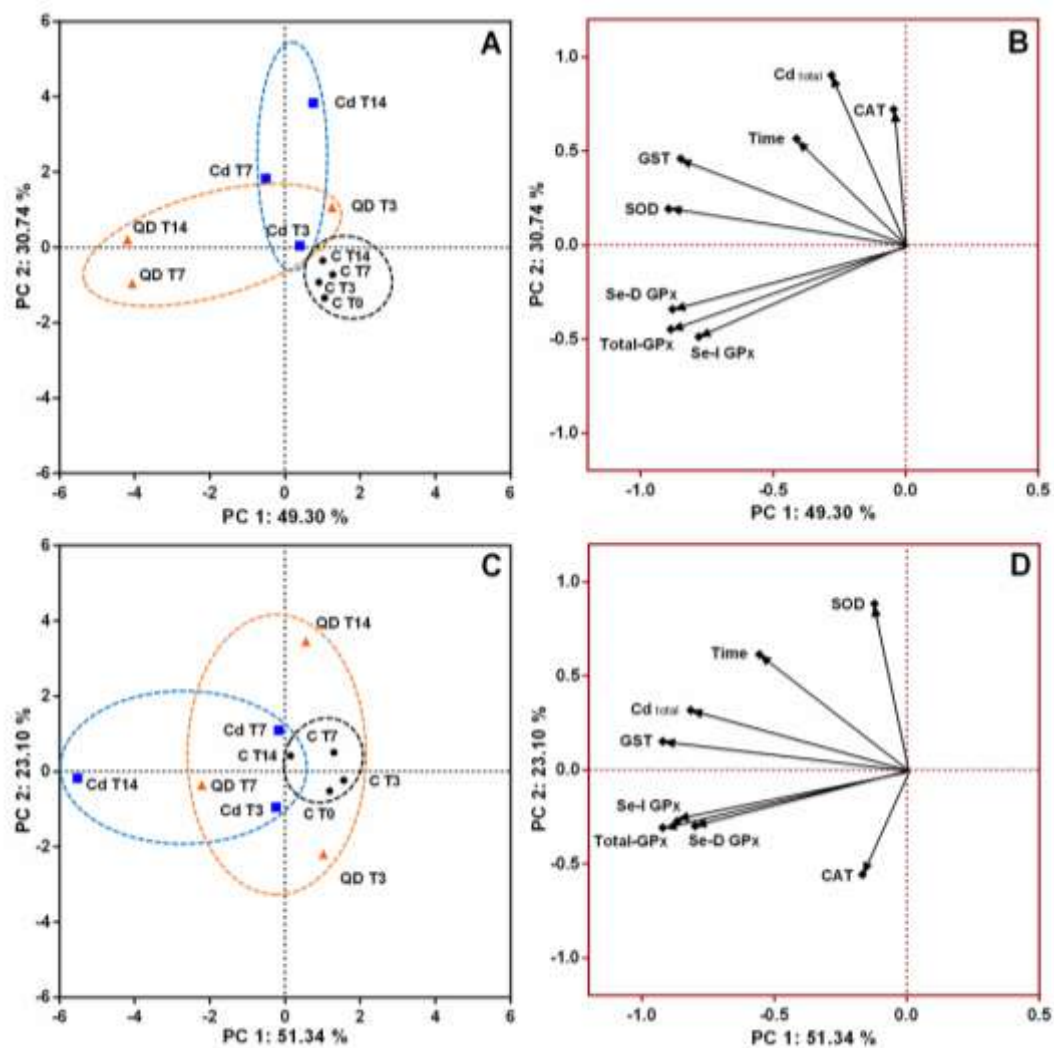


Figure 5.3. Principal component analysis (PCA) of Cd accumulation and of a battery of biomarkers (SOD, CAT, total GPx, Se-I GPx, Se-D GPx and GST activities) in the gills (A-B) and digestive gland (C-D) of mussels *M. galloprovincialis* from controls (C), exposed to CdTe Quantum Dots (QDs) and to dissolved cadmium (Cd) for 14 days.

The alterations of the antioxidant capacity in QDs-exposed mussels observed in this study may be associated with genotoxic and immunotoxic effects in mussels *M. galloprovincialis* exposed to CdTe QDs (6 nm; 10 $\mu\text{g Cd L}^{-1}$; 14 d) (Rocha et al., 2014) (Chapter 4) and with inflammatory condition and oxidative damage described in *E. complanata* exposed to CdTe QDs (1.6 - 8 mg L^{-1} ; 24 h) (Gagné et al., 2008a). ROS generation and oxidative damages induced by Cd-based QDs were already reported at various trophic levels in the aquatic environment, such as algae *C. reinhardtii* and *T. pseudonana* (Domingos et al., 2011; Zhang et al., 2013), cnidarians *Hydra vulgaris* (Ambrosone et al., 2012), ragworms *H. diversicolor* (Buffet et al., 2014b), bivalve molluscs *E. complanata*, *M. galloprovincialis* and *S. plana* (Gagné et al., 2008a; Rocha et al., 2014; 2015c; Buffet et al., 2015) (Chapters 3 and 4) and fishes *O. mykiss* and *G. aculeatus* (Gagné et al., 2008b; Sanders et al., 2008), indicating that the MoA of Cd-based QDs is mainly mediated by ROS production and oxidative stress.

5.4. Conclusions

In conclusion, the present study investigated the effects of CdTe QDs and dissolved Cd in the antioxidant defence system of the marine mussel *M. galloprovincialis* and showed Cd-form specific antioxidant patterns that may be related to changes in redox homeostasis, ROS production and oxidative stress. Overall, the toxicity of Cd-based QDs and dissolved Cd are mediated by different pathways. The long-time exposure to Cd-based QDs resulted in more severe changes in the antioxidant defense system than dissolved Cd, suggesting that the MoA of Cd-based QDs are mediated not only by release of Cd^{2+} ions but also from the nano-specific properties and ROS generated from them (Fig. 5.4 A-B).

Results showed that both Cd forms induced tissue-specific responses in mussel's antioxidant capacity (Fig. 5.4 A-B), which provided an additional knowledge of the toxic effects mediated by ENPs in marine invertebrates, and might give a better understanding of the ecotoxicological impact of these nanoparticles in marine and estuarine organisms. SOD, GPx and GST activities were the most sensitive biomarkers of oxidative stress induced by CdTe QDs in marine mussels (Fig. 5.4 A-B). Such tissue specific biochemical responses, GPxs activities in the gills increased and decreased in QDs and dissolved Cd exposure, respectively, while this enzyme in both Cd forms increased in the digestive gland. Considering the results of this study, further studies about tissue specific expression profile of antioxidants enzymes isoforms are needed to

understand the tissue specific susceptibility to oxidative stress and toxic effects induced by ENPs in aquatic organisms. Furthermore, further studies about response of different cell types of the gills and digestive gland in mussels exposed to ENPs are needed to understand the cellular target involved in uptake, metabolism and toxicity of ENPs in aquatic organisms.

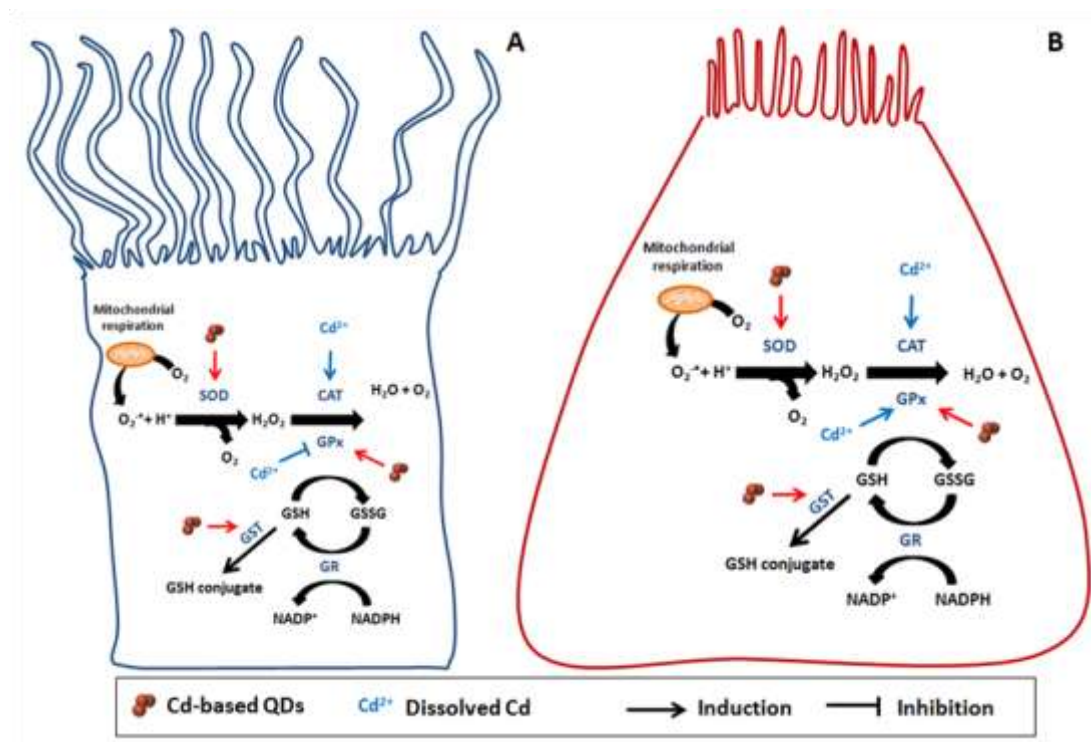
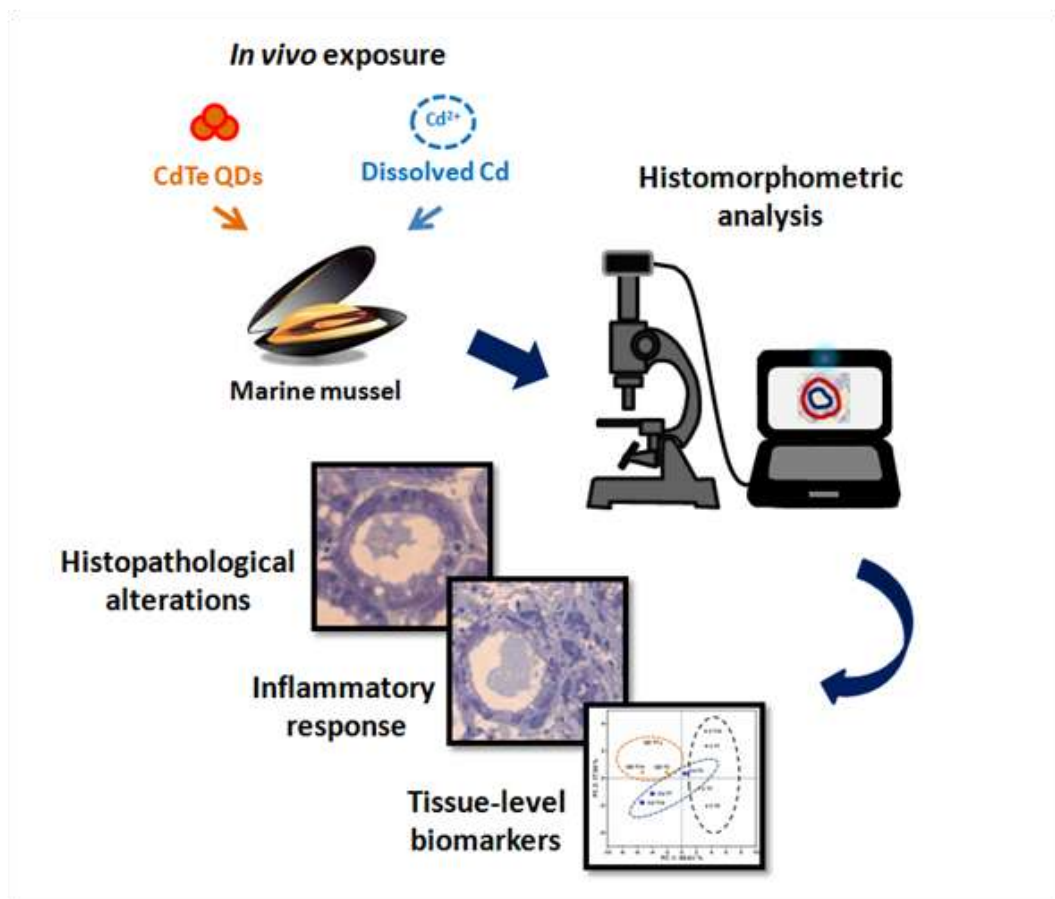


Figure 5.4. General scheme illustrating the tissue specific response in the gills (A) and digestive gland (B) of mussel *M. galloprovincialis* exposed to CdTe quantum dots (QDs) and to dissolved cadmium (Cd) for 14 days.

CHAPTER VI

Histopathological assessment and inflammatory response in the digestive gland of marine mussel *Mytilus galloprovincialis* exposed to cadmium-based quantum dots



Part of this Chapter was submitted to:

- Rocha, T.L., Sabóia-Morais, S.M.T., Bebianno, M.J. Histopathological assessment and inflammatory response in the digestive gland of marine mussel *Mytilus galloprovincialis* exposed to cadmium-based quantum dots. Aquatic Toxicology.

Part of this Chapter was presented at:

- Rocha, T.L., Gomes, T., Tomazett, M.V., Sabóia-Morais, S.M.T., Bebianno, M.J., 2016. Quantum dot localization and quantitative histopathological assessment in the digestive gland of marine mussel *Mytilus galloprovincialis*. In: SETAC Europe 26th Annual Meeting, Nantes, France.

Abstract

Although the tissue-level biomarkers have been widely applied in environmental toxicology studies, the knowledge about this approach in marine invertebrates exposed to engineered nanomaterials (ENMs) remains limited. This study investigated histopathological alterations and inflammatory response induced by Cd-based quantum dots (QDs), in comparison with its dissolved counterpart, in the marine mussel *Mytilus galloprovincialis*. Mussels were exposed to CdTe QDs and dissolved Cd at the same concentration ($10 \mu\text{g Cd L}^{-1}$) for 14 days and a total of 15 histopathological alterations and 17 histomorphometric parameters were analyzed in the digestive gland along with the determination of histopathological condition indices (I_h). A multivariate analysis showed that the mussel response to QDs was more related to exposure time, inflammatory condition (frequency of haemocytic infiltration and granulocytomas) and changes of cell-type composition (especially the rate between basophilic and digestive cells), while the response to dissolved Cd was associated to histomorphometric parameters of the epithelium and lumen of digestive tubules and increase of the atrophic tubule frequency. Both Cd forms induce higher I_h compared to unexposed mussels indicating a significant decrease in the health status of digestive gland in a Cd form and time dependent pattern. Results indicate that the multiparametric tissue-level biomarkers in the digestive gland provide a suitable approach to assess the ecotoxicity and mode of action of metal-based ENMs in marine bivalves.

Keywords: Nanoecotoxicology, nanoparticle, CdTe Quantum dots, cadmium, tissue-level biomarkers, histopathology, *Mytilus galloprovincialis*.

6.1. Introduction

The ecotoxicological impact of metal-based ENMs is an emerging concern worldwide due to its nano-specific properties, transformation in the environment, release of toxic metals and biophysicochemical interactions (Misra et al., 2012; Lowry et al., 2012; Corsi et al., 2014; Rocha et al., 2015a) (Chapter 1). Among these ENMs, QDs are semiconductor nanocrystals (2 - 10 nm in diameter) used as a new class of imaging probes for biology and medicine and with application in pharmacy and electronics due to their unique optical and electronic properties (Rizvi et al., 2010). Although QDs concentrations in the aquatic environment are unknown, their increasing production and use will likely increase their release into the marine environment, which are known to induce toxic effects at different trophic levels, such as algae (Morelli et al., 2013), polychaete (Buffet et al., 2014a), nematode (Zhou et al., 2015), molluscs (Buffet et al., 2015; Katsumiti et al., 2014; Rocha et al., 2014, 2015b,c) (Chapters 2 - 5) and fish (Blickley et al., 2014).

Bivalve molluscs are a target group of the ENMs toxicity and have been indicated as sentinel species for characterizing the environmental impact of ENMs (Canesi et al., 2012; Rocha et al., 2015a) (Chapter 1). The marine mussel *M. galloprovincialis* exposed to CdTe QDs (6 ± 1 nm; $10 \mu\text{g Cd L}^{-1}$; 14 days) has the capacity to take up and accumulate QDs from seawater, which induce several toxic effects, such as immunotoxicity and genotoxicity by LMS decrease and DNA damage in circulating haemocytes, as well as changes in antioxidant enzyme activities in the gills and digestive gland in a tissue specific pattern (Rocha et al., 2014, 2015b,c) (Chapters 2 - 5). Behaviour and biochemical impairment were reported in the marine clam *S. plana* exposed to CdS QDs (5 - 6 nm; $10 \mu\text{g Cd L}^{-1}$; 14 days) (Buffet et al., 2014b), while QDs-related oxidative stress, genotoxic and immunosuppressive effects associated with inflammatory condition were reported in the freshwater mussel *E. complanata* exposed to CdTe QDs ($1.6 - 8 \text{ mg L}^{-1}$; 24 h) (Gagné et al., 2008a; Peyrot et al., 2009).

Despite the emerging literature about the toxicity and MoA of ENMs in bivalve molluscs (Rocha et al., 2015a) (Chapter 1), information about histopathological effects and tissue-level biomarkers in marine bivalves exposed to metal-based ENMs remain unclear and scarce (Vale et al., 2014). On the other hand, changes in the morpho-functional state of bivalve species have been widely investigated and used in biomonitoring programmes worldwide (Costa et al., 2013; Cuevas et al., 2015). Tissue-

level biomarkers and histopathological alterations in the bivalve digestive gland are some of the most important approaches to assess the health status of individuals and of populations (Garmendia et al., 2011; Costa et al., 2013; Cuevas et al., 2015) and allows to differentiate the aetiology of pathological conditions associated to functional damage of cells, tissues and organs (Carella et al., 2015).

Although the histopathological alteration induced by Cd-based QDs in marine invertebrates remains poorly understood, recent studies indicated different tissue injuries in bivalve species exposed to other metal-based ENMs. Qualitative histopathological alterations were observed in the digestive gland of the freshwater clam *C. fluminea* exposed to nTiO₂ (0.1 - 1 mg L⁻¹; 10 d), showing an enlargement or widening of the tubule lumen and a reduction in thickness of the digestive tubule epithelium, indicating inflammatory response in the digestive gland (Vale et al., 2014). The increasing presence of pigmented brown cells was observed in different organs of the blue mussel *M. edulis* exposed to CuO NPs (400 - 10³ µg Cu L⁻¹; 1 h) (Hu et al., 2014), while similar patterns of diffuse and focal haemocytic infiltration were observed in *M. galloprovincialis* after exposure to CuO NPs (10 µg Cu L⁻¹; 21 days) compared to bulk CuO and ionic copper (Ruiz et al., 2015). However few studies conducted to date have evaluated semi-quantitative and quantitative morphological changes in bivalve species exposed to ENMs.

The bivalve immune system have been considered as a sensitive target of ENMs toxicity (Canesi and Procházková, 2014; Rocha et al., 2014, 2015a) (Chapters 1 and 4). Bivalve molluscs have only innate immunity, including humoral and cellular effectors, which hemocytes (also called immunocytes) are responsible for cell-mediated immunity mainly *via* phagocytosis, ROS and NO production, hydrolytic enzymes and antimicrobial peptides (Canesi et al., 2012; De Vico and Carella, 2012). Immunotoxicity induced by Cd-based QDs in bivalve molluscs are dependent of nano-specific properties (e. g. size, composition, shape, surface coating and aggregation state), type of exposure (*in vivo* or *in vitro*), exposure conditions, as well as bivalve species analyzed (Gagné et al., 2008; Peyrot et al., 2009; Bruneau et al., 2013; Katsumiti et al., 2014; Rocha et al., 2014) (Chapters 1 and 4). These studies reported that the immune-mediated and inflammatory response in bivalves exposed to Cd-based QDs is mainly related to QDs dissolution, extra- and intracellular release of Cd²⁺ ions and ROS production that lead to changes in immune parameters (e. g. cell viability/density, phagocytosis activity and LMS), as well as modifications in the frequency of hemocyte types and DNA damage.

However, the morphology of the inflammatory response and the role of hemocytes in the metabolism, transport and detoxification of metal-based ENMs are not well established.

Accordingly, the aims of this study were (i) to identify and quantify the histopathological alterations induced by Cd-based QDs through histomorphometric analysis of epithelium and lumen of digestive tubules and semi-quantitative approach based on histopathological indices for the digestive gland; (ii) to describe the inflammatory response in the digestive gland after exposure to Cd-based QDs; (iii) to compare results between QDs-exposed mussels and dissolved Cd-exposed ones in order to differentiate the nano-specific effects at cellular and tissue levels.

6.2. Materials and Methods

6.2.1. Experimental design

Mussels *M. galloprovincialis* (60 ± 5 mm shell length) were collected in the Ria Formosa Lagoon (Portugal) (Figs. 1.15 -1.16) and acclimated during 14 days in static tanks containing natural seawater (salinity = 36) at 16 °C and constant aeration. CdTe QDs (6 ± 1 nm) and dissolved Cd ($\text{Cd}(\text{NO}_3)_2 \cdot 4\text{H}_2\text{O}$) stock solutions were prepared in ultrapure water and characterized according to the method described by Sousa and Teixeira (2013). Data on characterization and behaviour of CdTe QDs in the seawater were previously reported in Rocha et al. (2014, 2015b) (Chapters 2 and 4) and are summarized in Table 3.1.

After the acclimation, ninety mussels were placed in 30 L tanks filled with 25 L of seawater (3.6 mussels L^{-1}) and exposed to $10 \mu\text{g Cd L}^{-1}$ of CdTe QDs and to the same concentration of dissolved counterpart, jointly with a control group kept in clean seawater in a triplicate design (3 tanks *per* treatment) for 14 days. Seawater was changed daily with redosing of QDs and dissolved Cd concentration. Mussels were only fed with natural seawater providing animals with food to avoid starvation and any effects resulting from the interaction of QDs and food (Rocha et al., 2015b).

Ten mussels from each experimental condition were collected at the beginning of the experiment and after 3, 7 and 14 days of exposure. Experiments were conducted in a static-renewal condition under 12h:12h light/dark cycles and abiotic parameters were analyzed daily by measuring salinity (36.3 ± 0.07), temperature (16.6 ± 1.2 °C), pH (7.9 ± 0.1) and oxygen saturation (103 ± 1.3 %). No mortality was observed

between unexposed mussels and those exposed to both Cd forms by the end of the exposure period.

6.2.2. Cd concentrations

For the determination of Cd concentrations, digestive gland was dried (80 °C, 48 h), digested in HNO₃ (80 °C, 4 h) and analyzed by graphite furnace atomic absorption spectrometry (AAS AAnalyst 800 - PerkinElmer). Accuracy of the analytical procedure was assured with certified reference material (TORT-II, Lobster Hepatopancreas) from the National Research Council (Canada) and results agreed with the certified values (certified value: 26.7 ± 0.6 mg Cd kg⁻¹; samples: 28.5 ± 4.5 mg Cd kg⁻¹) as previously described in Rocha et al. (2015b) (Chapter 2). Data on Cd concentrations in mussel tissues are expressed as µg g⁻¹ of dry weight tissue and were previously reported in Rocha et al. (2015b) (Chapter 2) and summarized in Table 4.1.

6.2.3. Histopathological assessment

Digestive gland (n = 10 *per* treatment) from unexposed and exposed mussels were carefully excised and immediately fixed by immersion in 4 % paraformaldehyde in 0.1 M phosphate buffer (PBS) at pH 7.0. Afterwards, portions of the digestive gland were embedded in glycol-methacrilate resin (Historesin, Leica, Germany), sectioned into 2.5 µm thick slices (10 sections *per* slide; 3 slides *per* animal; n = 300 sections *per* treatment) and stained with 1 % toluidine blue (TB) pH 8.5. Histological analysis and digital image capture were performed in the light microscope (Olympus CH30) associated with the Moticam 230 digital camera and the Motic Images Plus 2.0 software.

6.2.3.1. Histomorphometry

Histomorphometric analyses were conducted by evaluating epithelium and tubular lumen modification of digestive tubules. Images of TB-stained sections were randomly captured at 400x magnification (30 images *per* animal; 300 images *per* treatment) and analyzed using the imaging program (Motic Images Plus 2.0 software). Proportion of each digestive tubule type *per* animal (P_k) was analyzed by a visual count of 300 random tubules *per* experimental group, indicating three main phases (type I: holding phase; type II: absorptive phase; type III: disintegrating or atrophic phase) (Marigómez et al., 1990; Owen, 1996; Carella et al., 2015).

Digestive tubule status was analyzed in terms of the epithelial layer area (S_0), digestive tubule lumen area (S_i), tubule perimeter (P_0), lumen perimeter (P_i), mean epithelial thickness (h) [$h = 2(S_0 - S_i) / P_0 + P_i$] (Marigómez et al. 1990) and circularity (c) [$c = 4\pi (S_0 / P_0^2)$] (Carella et al., 2015). Cell type composition of the digestive tubule epithelium was analyzed in terms of the basophilic and digestive cell frequency (%), rate between number of both digestive tubule cell types ($R_{Bas/Dig}$) (Calvo-Ugarteburu et al., 1995), hemocyte frequency (%) and total cell number *per* digestive tubule and *per* epithelial layer area (S_0). Scheme of the procedure used to measure the histomorphometric parameters is in Fig. 6.1).

6.2.4. Inflammatory response

Inflammatory response in the mussel digestive gland was analyzed through microscopy examination from each individual using the method from Villalba et al. (1993) and modified by Carella et al. (2015). Defensive changes were morphologically classified as infiltrates and haemocytic aggregates and categorized for grade of inflammatory response, ranging from 0 to 4 (0: zero or minimal 10% inflammation; 1: 25 % inflammation; 2: 50 % inflammation; 3: 75 % inflammation; 4: > 90 % inflammation).

6.2.5. Histopathological condition indices

Semi-quantitative histopathological condition indices (I_h) for the digestive gland were estimated for each mussel, according to weighted indices approach originally described by Bernet et al. (1999) and Costa et al. (2009) for fish and then modified for clam (Costa et al., 2013) and mussel species (Cuevas et al., 2015). Briefly, histopathological alterations in the digestive gland were classified in four reaction patterns (tubular, intertubular alterations, parasitosis and neoplasia) (Table 6.1). An importance factor (w) ranging from 1 (minimally severe) to 3 (severe) was attributed to each type of tissue damage (Table 6.1). The I_h was calculated according to Costa et al. (2013) using the following formula:

$$I_h = \frac{\sum_1^j w_j a_j h}{\sum_1^j M_j} \quad (1)$$

Where: I_h = histopathological index for each individual h ; W_j = relative weight of the j th histopathological alteration; a_{jh} the score value selected for the j th alteration and M_j is the attributable maximum (weight x maximum score) for j th alteration. The denominator of the equation standardises the indices to a value between 0 and 1, to allow comparisons between different conditions (Costa et al., 2013).

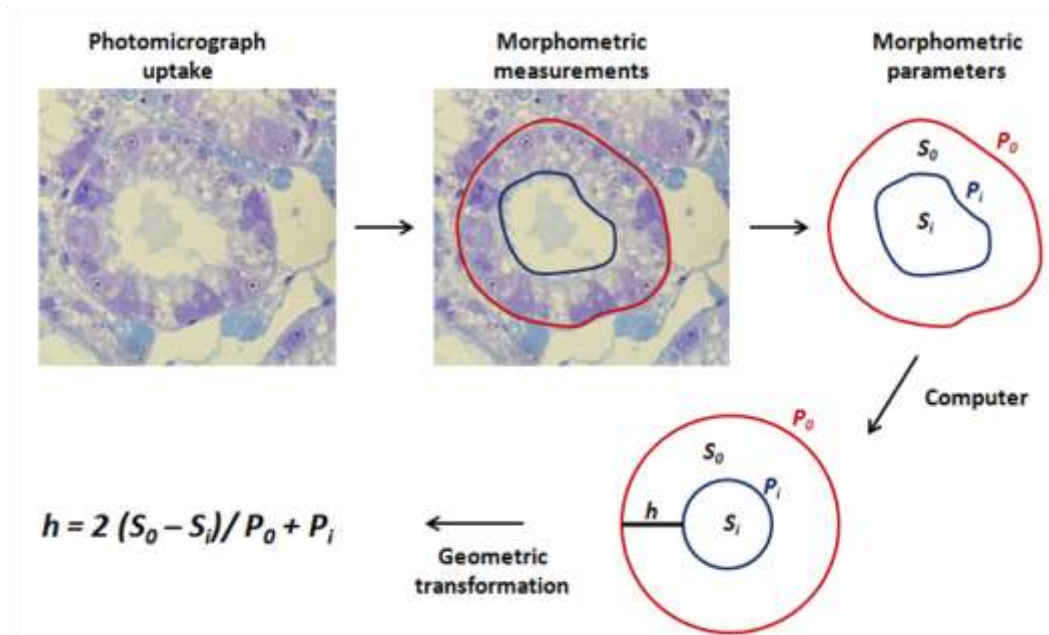


Figure 6.1. Scheme of the procedure used to measure the histomorphometric parameters of digestive tubules in mussels *M. galloprovincialis* (adapted from Marigómez et al. 1990). S_0 : area of epidermal layer; S_i : area of lumen; P_0 : perimeter of the tubule; P_i : perimeter of the lumen; h : mean epithelial thickness.

6.2.6. Statistical analysis

Statistical analyses were carried out using the Statistica 7.0 software (Statsoft Inc., 2005, Tulsa, OK, USA). The results were compared using parametric tests (two-way ANOVA, followed by the Tukey's test) and/or non-parametric test (Kruskall-Wallis), depending on the distribution of the data and homogeneity of variances (Shapiro-Wilk and Levene's tests). Linear and nonlinear regression analyses were also applied to verify existing relationships between variables. PCA was used to evaluate the relationship between Cd concentration in the digestive gland, histomorphometric parameters, histopathological indices and inflammatory response of unexposed mussels and Cd-exposed mussels (QDs and dissolved Cd) during the exposure period (14 days). Results were considered significant when $p < 0.05$.

Table 6.1. Histopathologies in the digestive gland of mussel *M. galloprovincialis* and their importance weight (*w*).

Reaction pattern ¹	Histopathological alteration	<i>w</i> ²
Tubular alteration	Haemocytes infiltration	1 ^a
	Lipofuscin aggregates	1 ^a
	Vacuolization	1 ^b
	Atrophy	2 ^b
	Epithelium hyperplasia	2 ^a
	Epithelium hypertrophy	2 ^a
	Tubule regression	2 ^a
	Nuclear alteration	2 ^b
	Necrosis	3 ^a
Intertubular alteration	Haemocytes infiltration	1 ^a
	Lipofuscin aggregates	1 ^a
	Fibrosis	2 ^a
	Granulocytoma	2 ^a
	Necrosis	3 ^a
Parasitosis	Bacteria	2 ^a
	Protozoa	3 ^a
Neoplasia	Fibroma	2 ^a
	Haemic neoplasia	3 ^a

¹ Reaction patterns according to Costa et al. (2013).

² Importance factor (*w*) according to Costa et al. (2013) (^a) and described in the present study (^b).

6.3. Results and discussion

6.3.1. Characterization of QDs in seawater and bioaccumulation

Data on CdTe QDs characterization in the aqueous medium used in this study are summarized in Table 3.1 and previously described by Rocha et al. (2014, 2015b) (Chapters 2 and 4). TEM results showed QDs with spheroid shape and primary size of 6 ± 1 nm, such as reported by the manufacturer (2 - 7 nm). In natural seawater at pH 8.0, QDs formed aggregates/agglomerates with a hydrodynamic diameter of 1014 ± 187 nm, negative surface charge of -9.4 ± 1.2 mV and PDI of 0.5 ± 0.1 (Table 3.1), confirming the QDs aggregation/agglomeration following by sedimentation in natural seawater, such as described by previous studies with other QDs (Morelli et al., 2012; Hull et al., 2013). Furthermore no QDs stabilization with different natural organic matter (NOM) and low QDs dissolution rate (27.6 %) followed by speciation of Cd²⁺ released from QDs core have been reported (Rocha et al., 2015b) (Chapter 2), indicating

that the majority of QDs remain as homo-aggregates in seawater, which are responsible for Cd accumulation in mussel tissues.

Both Cd forms are accumulated in the digestive gland over exposure period (14 days) in a Cd form dependent pattern, wherein Cd accumulation from QDs was lower when compared to its dissolved counterpart (Table 5.1). Kinetic model for Cd accumulation in the digestive gland of *M. galloprovincialis* during 21 days of exposure to both Cd forms was estimated by Rocha et al., (2015b) (Chapter 2), indicating lower Cd accumulation rate (Ka) in QDs-exposed mussels compared to those exposed to dissolved Cd ($Ka = 0.34$ and $1.39 \text{ L g}^{-1} \text{ d}^{-1}$, respectively). Similarly recent studies indicated that different types of QDs aggregates/agglomerates are mainly uptaken by marine mussels *via* endocytotic pathways in the digestive system, while individual NP and dissolved form are uptaken in the gills (Hull et al. 2013; Rocha et al., 2015b) (Chapter 2), confirming that the digestive gland is a important target for storage and toxicity of Cd-based QDs. However, to the best of our knowledge, this is the first study of the histopathological assessment and morphology of the inflammatory response in bivalve species exposed to Cd-based QDs.

6.3.2. Histomorphometry

6.3.2.1. Morphological phases of digestive tubules

Qualitative analyses showed that the digestive gland of *M. galloprovincialis* surrounds stomach and is structurally formed by clusters of blind-ending alveolo-tubular units, which connect to stomach by way of non-ciliated secondary ducts and ciliated main ducts (Owen, 1996). The normal phasic activity of the digestive gland was observed in unexposed mussels, which showed more than 95 % of digestive tubules in the holding and absorbing phase (90 ± 3 % and 7 ± 2 %, respectively) (Figs. 6.2 and 6.3A-B), such as previously reported (Cajaraville et al., 1992; Carella et al., 2015). However, frequency of digestive tubules in atrophic phase (tubules showing large lumen and thin epithelium) increase significantly after 3 days of exposure to QDs (16.3-fold) and dissolved Cd (5.7-fold) when compared to unexposed mussels, indicating higher effects of QDs compared to its dissolved counterparts (2.8-fold; $p < 0.05$; Figs. 6.2 and 6.3C-F). Moreover, mussels exposed to both Cd forms showed similar profile of the atrophic status, with significant differences with unexposed ones ($p < 0.05$; Figs. 6.2 and 6.3C-F), indicating that the frequency of digestive tubule atrophy in bivalve species is a biomarker of general stress induced by pollutants, such as metals (e. g. Cd) (Da Ros

et al., 1995), water accommodated fraction (WAF) of oils (Cajaraville et al., 1992) and biotoxins (Carella et al., 2015), including metal-based ENMs, and are one the most prevalent lesions identified in mussels in environmental pollution biomonitoring programmes (Costa et al., 2013; Cuevas et al., 2015). Overall, results show that the increase in the frequency of atrophic tubules after exposure to both Cd forms is associated to epithelial thinning and consequently lead to failure of digestive gland functions, such as digestion, metabolic and homeostatic regulation (e. g. calcium, hemolymphatic pH, cell volume) and immune defence (Owen, 1996; Marigómez et al., 1999). Digestive tubule atrophy is considered an initial process of necrosis in mussels exposed to Cd (Da Ros et al., 1995) and can occur in association with degenerative processes, indicating systemic pathological conditions in bivalves (Carella et al., 2015).

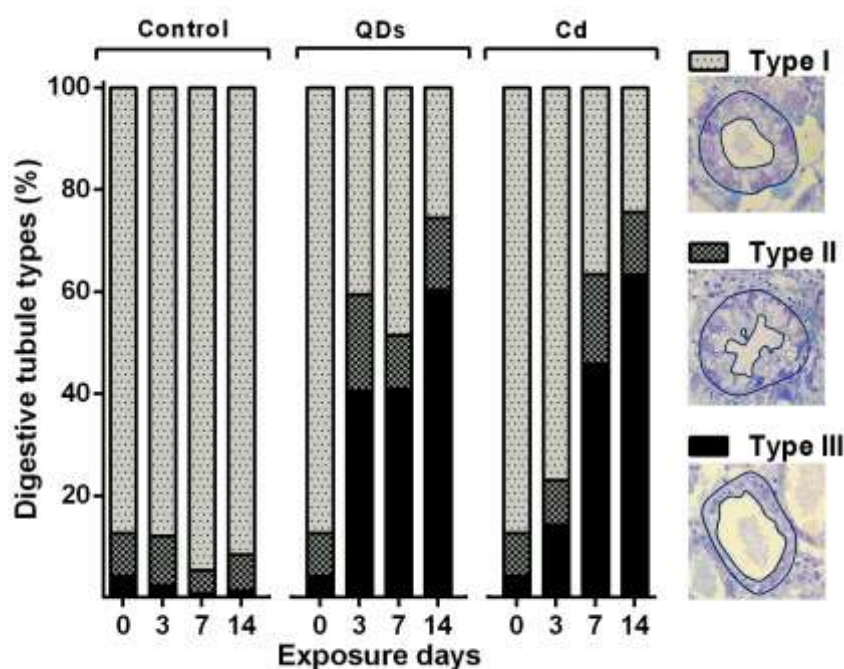


Figure 6.2. Digestive tubule types (%) in mussels *M. galloprovincialis* from control (C), exposed to CdTe quantum dots (QDs) and to dissolved Cd (Cd) for 14 days. Digestive tubules were classified in type I (holding), type II (adsorbing) and type III (disintegrating or atrophic).

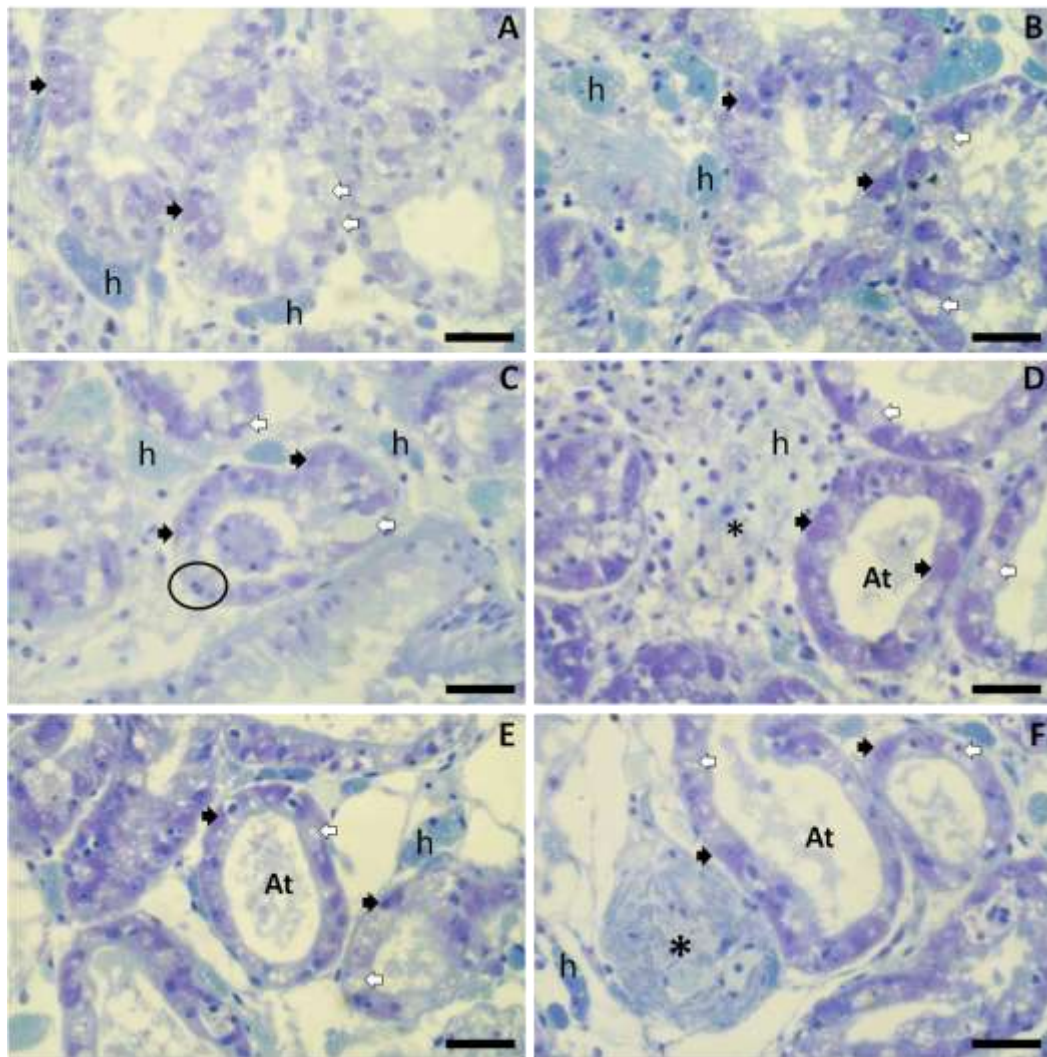


Figure 6.3. Photomicrographs of the digestive gland of mussels *M. galloprovincialis* from control (A-B), exposed to CdTe quantum dots (QDs) (C-D) and to dissolved Cd (E-F) for 14 days. A-F: Digestive and basophilic cells in the digestive tubule epithelium (black and white arrows, respectively) and haemocytes (h). C-F: Nuclear alteration (karyorrhexis) (circle) in the digestive tubule epithelium, atrophic tubules (At) haemocytic infiltrations (asterisks) in the digestive gland of mussels exposed to QDs (C-D) and to dissolved Cd for 14 days. Technique (A-F): sections of the digestive gland embedded in glycol-methacrilate resin and stained with 1 % toluidine blue pH 8.5. Scale bars: 100 μ m.

6.3.2.2. Digestive tubule status

Histomorphometric parameters measured in the digestive gland of unexposed mussels and those exposed to both Cd forms are in Fig. 6.4A-F. Unexposed mussels showed similar planimetric parameters over the experimental period, except for a decrease in Pi (14 days) and Si (7 - 14 days) ($p < 0.05$; Fig. 6.4B,D). After 14 days of

exposure, QDs exposure decreased the circularity (1.1-fold; $p < 0.05$) but did not produce other significant histomorphometric changes when compared to unexposed mussels (Fig. 6.4F), while lower changes of epithelium and lumen parameters of digestive tubules were observed compared to dissolved Cd-exposed ones (Fig. 6.4A-F). In opposite to QDs exposure, mussels exposed to dissolved Cd showed an increase in the Pi (1.2-fold) and Si (1.6-fold), which is followed by a decrease in the mean epithelial thickness (h) and in circularity (1.6-fold and 1.2-fold decrease, respectively; $p < 0.05$; Fig. 6.4A-F). Results agree with previous studies that showed that the height of digestive tubule epithelium decrease in response to Cd exposure (Marigómez et al., 1990), while in QDs exposure no changes in the digestive tubule status in terms of epithelial and lumen area, perimeter of the tubule and lumen, as well as circularity and epithelial thickness were observed.

6.3.2.3. Cell-type replacement

Digestive tubules of *M. galloprovincialis* are constituted by single epithelium formed by two main cell types, namely digestive and basophilic cells (Cajarville et al., 1990; Marigómez et al., 1999) (Fig. 6.3A-F). In unexposed mussels, digestive cells have columnar shape and are the most abundant cell type (60 ± 4.3 %), while basophilic cells are pyramidal cells and represent 40 ± 4.3 % of the digestive tubule epithelium and this composition did not change after 14 days ($p > 0.05$; Fig. 6.5A-B). However the exposure to QDs and dissolved Cd decrease the digestive cell frequency, followed by an increase in the basophilic cell frequency and higher rate between both cell types ($R_{\text{Bas/Dig}}$) ($p < 0.05$; Fig. 6.5A-C). Results obtained represent the first data on the cell composition changes in the digestive tubule of marine bivalves exposed to metal-based ENMs and showed that both Cd forms induces a cell-type replacement over time, acting as epithelial modulation factor.

After 3 days of exposure, QDs-exposed mussels showed a significant decrease in the digestive cell frequency when compared to unexposed (1.2-fold) and dissolved Cd-exposed ones (1.1-fold) ($p < 0.05$; Fig. 6.5A-B), while a significant increase in the basophilic cell frequency was observed compared to unexposed mussels (1.2-fold; $p < 0.05$). On the other hand, this cell-type replacement was delayed in the dissolved Cd-exposed mussels and was only observed after 7 and 14 days of exposure ($p < 0.05$), while no significant differences between both Cd forms exist after 7 and 14 days ($p > 0.05$) (Fig. 6.5A-B).

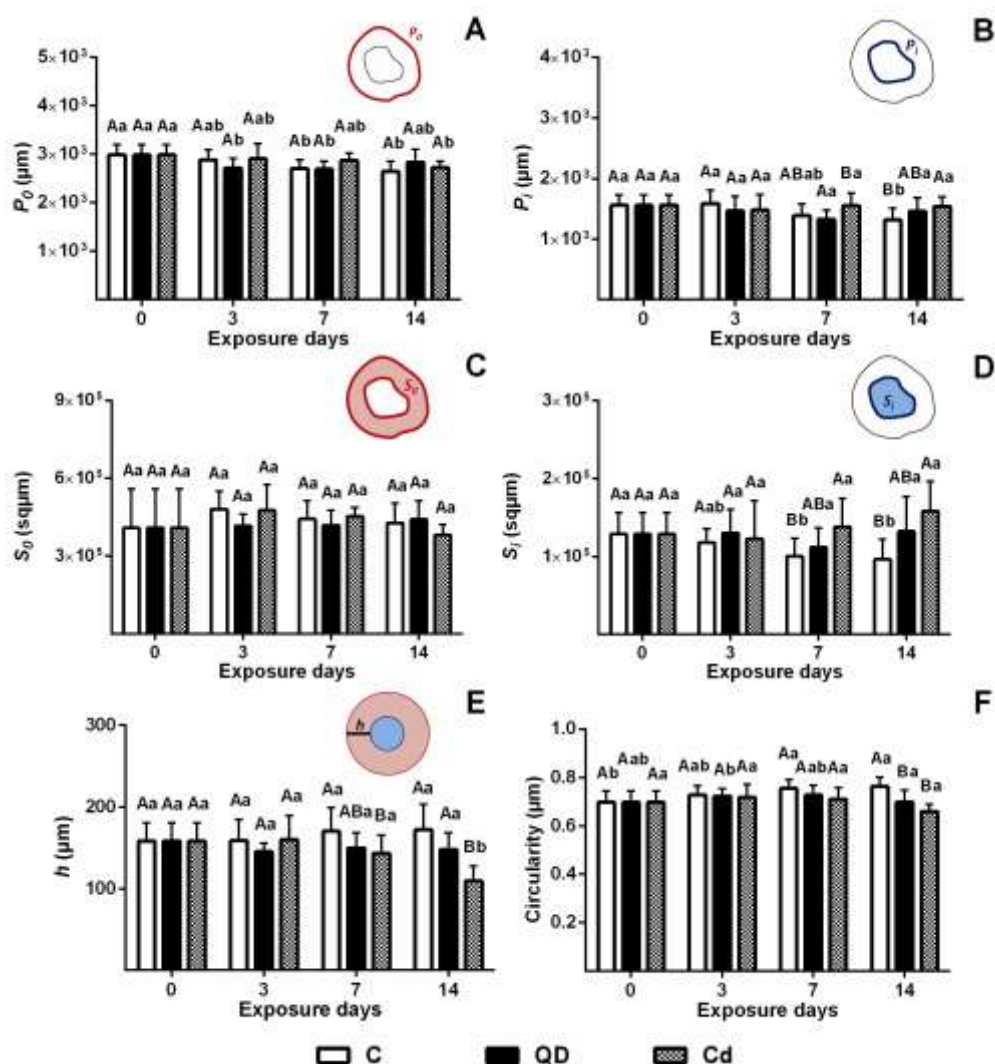


Figure 6.4. Histomorphometric parameters (mean \pm std) of digestive tubules in mussels *M. galloprovincialis* from control (C), exposed to CdTe quantum dots (QDs) and to dissolved Cd (Cd) for 14 days: tubule perimeter (P_0) (A), lumen perimeter (P_i) (B), epithelial layer area (S_0) (C), lumen area (S_i) (D), mean epithelial thickness (h) (E) and circularity (F). Different capital and lower case letters indicate significant differences between treatments at each time of exposure and within treatment during the exposure period, respectively ($p < 0.05$).

The impact of both Cd forms in the cell composition of the digestive tubules was confirmed by the measurement of $R_{\text{Bas/Dig}}$, which increased linearly over time in mussels exposed to QDs ($R_{\text{Bas/Dig}} = 0.09192t + 0.515$; $r = 0.96$; $p < 0.05$) and dissolved Cd ($R_{\text{Bas/Dig}} = 0.06139t + 0.8266$; $r = 0.92$; $p < 0.05$), indicating higher effects of QDs as epithelial modulation factor in the digestive tubule compared to dissolved Cd (Fig. 6.5C). A significant increase in $R_{\text{Bas/Dig}}$ was observed after 3 days of exposure to QDs (1.4-fold) and dissolved Cd (1.2-fold) when compared to unexposed ones ($p < 0.05$; Fig.

6.5C). At the end of exposure period, $R_{\text{Bas/Dig}}$ remained higher in both Cd-exposed mussels compared to control (QDs: 2.6-fold; dissolved Cd: 2.0-fold; $p < 0.05$), with higher response in QDs-exposed mussels (2.1 ± 0.59) when compared to dissolved Cd-exposed ones (1.61 ± 0.36) ($p < 0.05$; Fig. 6.5C). However, no significant tendency was observed in the frequency of haemocytes in the digestive tubule epithelium, as well as in the total number cell *per* tubule or *per* epithelial area (S_0) (Fig. 6.5D-F), confirming that the $R_{\text{Bas/Dig}}$ is a more sensitive biomarker of cell-type replacement than frequency of each cell type in the digestive gland of the marine mussel exposed to both Cd forms. Results agree with previous studies that showed higher basophilic cell volume density (V_{VBAS}) in *M. galloprovincialis* exposed to Cd ($80 \mu\text{g L}^{-1}$; 21 days) (Soto et al., 2003) or after exposure to Cd ($200 \mu\text{g L}^{-1}$) and Cu ($40 \mu\text{g L}^{-1}$) for 9 days (Zorita et al., 2007), highlighting the role of basophilic cells in the metabolism of metal-based ENMs and its dissolved counterpart.

Although the MoA of metal-based ENMs in the digestive tubule epithelium of bivalves remains unavailable, several studies showed that the epithelial turnover in the digestive tubule of mussels *M. galloprovincialis* is mediated by mature cell division, where both digestive and basophilic cells are able to proliferate (Marigómez et al., 1999; Zaldibar et al., 2008). After 14 days of exposure, basophilic cells with mitotic nucleus (metaphase) was identified in QDs-exposed mussels, confirming the epithelial cell renewal by this cell type, while the presence of nuclear alterations in basophilic and digestive cells (e. g. pyknotic nuclei, karyorrhexis and karyolysis) indicate cell death (apoptosis and/or necrosis) in the digestive tubules induced by Cd-based QDs (Fig. 6.3C). These cellular alterations were related to the increase in the basophilic cell frequency and $R_{\text{Bas/Dig}}$ (Fig. 6.5C), indicating the need of the epithelial cell renewal due to loss of digestive cells, leading to a replacement of the cell loss and regeneration of damaged digestive tubules. Results suggest that more studies are needed on the role of cell-type replacement and cell death, especially related to the role of basophilic cells, in the physiological response of bivalve molluscs exposed to metal-based ENMs.

Previous studies showed that digestive cells have microvilli on the apical surface and a cytoplasm with a well-developed endo-lysosomal system, and are responsible for the intracellular digestion of food particle and detoxification of xenobiotics. On the other hand, basophilic cells do not have microvilli and display a highly developed rough endoplasmic reticulum and numerous secretory granules, which confers them their characteristic basophilic, and are responsible for the synthesizes and secretes hydrolytic

enzymes for extracellular digestion (Owen, 1972; Cajaraville et al., 1990; Dimitriadis et al., 2004). Due to these specific functions performed by both cell types, the cell-type replacement induced by both Cd forms (Fig. 6.5A-C) possibly provokes failure in food digestion, storage and xenobiotic metabolism, as well as metabolic and homeostatic impairments. Furthermore, toxic effects of QDs observed in the digestive gland of *M. galloprovincialis* may also compromise nutritional status, growth and reproduction, such as indicated for oyster *C. virginica* exposed to Ag NPs (20 - 30 nm; 0.02 - 20 $\mu\text{g L}^{-1}$; 48 h) (Ringwood et al., 2009; McCarthy et al., 2013).

6.3.3. Inflammatory response

Unexposed mussels showed minimal or low defensive responses (score 1 to 2) along the experimental period, but mussels exposed to both Cd forms showed an increase in the inflammatory response characterized by a focal or diffuse haemocytic infiltration and formation of haemocytic aggregates (also called granulocytomas) in the interstitial tissue of the digestive gland (Fig. 6.6A-B; Fig. 6.6). After 3 days of exposure, a similar significant increase in the haemocytic infiltration was identified in mussels exposed to QDs and dissolved Cd (3.7-fold, respectively) when compared to unexposed ones ($p < 0.05$), and this inflammatory response remain higher until the end of the exposure period (QDs: 6.4-fold; dissolved Cd: 5.1-fold; $p < 0.05$; Fig. 6.6A). Similar intensity of the haemocytic infiltration (mean of grades of inflammation) was observed in mussels exposed both Cd forms for 14 days (QDs: 3.2 ± 0.8 ; dissolved Cd: 2.5 ± 0.9 ; $p > 0.05$; Fig. 6.6A), while the frequency of mussels showing haemic infiltrates of grades 2 - 4 is Cd form and time exposure dependent (Fig. 6.6A-F). After 14 days, the inflammatory condition in the QDs exposure was more severe compared to dissolved Cd exposure, since the percentage of QDs-exposed mussels with inflammation of grades 3 and 4 (80 %) was higher compared to dissolved Cd-exposed ones (30 %) (Fig. 6.7). Hemocytes infiltrates were observed in association with digestive tubules showing regressive changes, such as cell swelling, vacuolization and atrophy, confirming that the inflammatory response induced by QDs exposure is mediated by recruitment of hemocytes in damaged tissue (Rocha et al., 2014) (Chapter 4), where they could phagocytose QDs and/or cell debris.

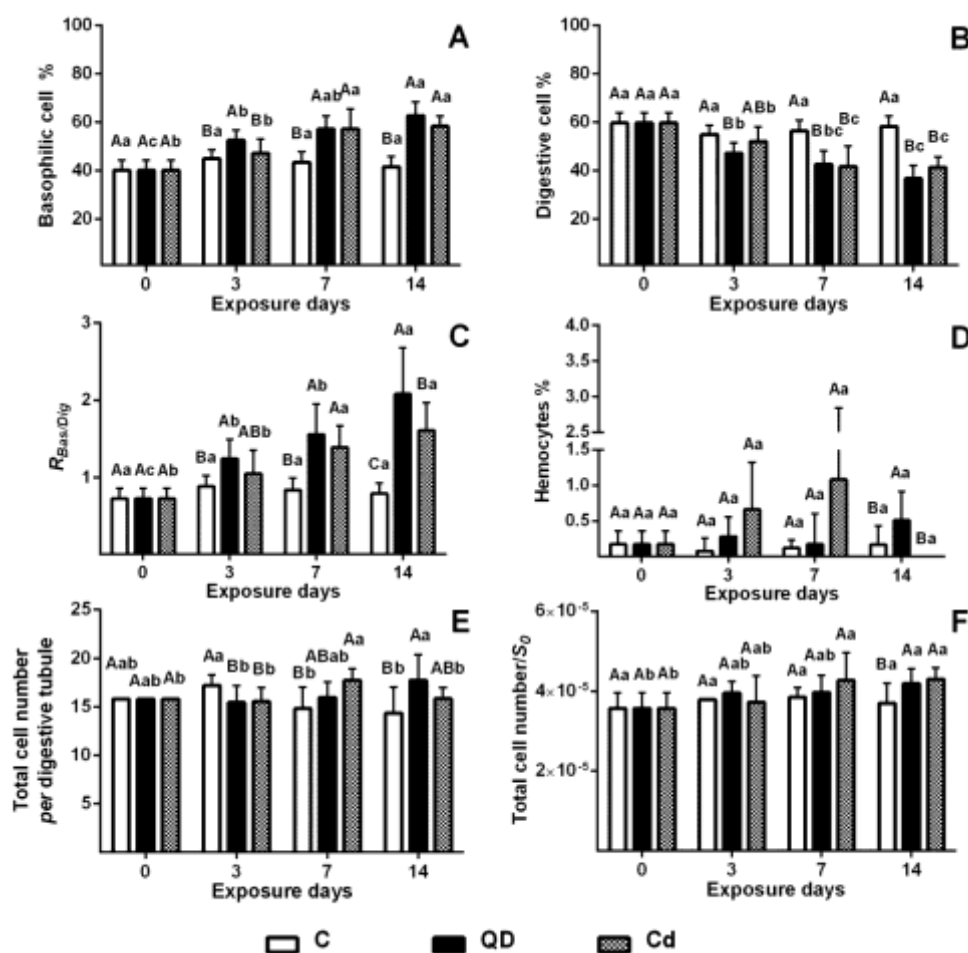


Figure 6.5. Cell type composition (mean \pm std) of the digestive tubule epithelium in mussels *M. galloprovincialis* from control (C), exposed to CdTe quantum dots (QDs) and to dissolved Cd (Cd) for 14 days: basophilic cell frequency (%) (A), digestive cell frequency (%) (B), rate between both digestive tubule cell types ($R_{Bas/Dig}$) (C), hemocyte frequency (%) (D), total cell number *per* digestive tubule (E) and *per* epithelial layer area (S_0) (F). Different capital and lower case letters indicate significant differences between treatments at each time of exposure and within treatment during the exposure period, respectively ($p < 0.05$).

In opposite to haemocytic infiltration, significant increase of the intensity of granulocytomas was observed in mussels exposed to QDs for 7 and 14 days when compared to unexposed ones (16- and 14-fold, respectively; $p < 0.05$), while no significant effects were observed in those exposed to dissolved Cd ($p > 0.05$; Fig. 6.6D-F), indicating that the mussel defence response related to haemocytic aggregates is Cd form and time dependent. Results agree with previous studies that showed that this type of inflammatory response in molluscs is usually observed when small particles

should be phagocytised (Vico and Carella, 2012). Nevertheless, granulocytomas frequencies observed in QDs-exposed mussels are higher when compared with mussels exposed to CuO NPs (40 - 500 nm, 10 $\mu\text{g Cu L}^{-1}$, 21 days) (Ruiz et al., 2015), showing that the Cd-based QDs induces higher inflammatory condition in marine mussels compared to others metal based-ENMs.

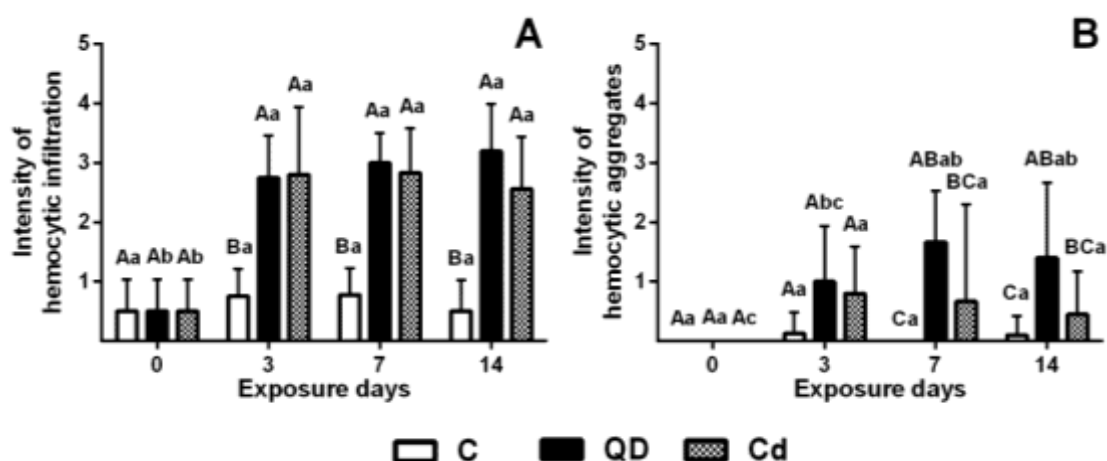


Figure 6.6. Inflammatory response (mean \pm std) in the digestive gland of mussels *M. galloprovincialis* from control (C), exposed to CdTe quantum dots (QDs) and to dissolved Cd (Cd) for 14 days: intensity of the haemocytic infiltration (A) and haemocytic aggregates (B). Different capital and lower case letters indicate significant differences between treatments at each time of exposure and within treatment during the exposure period, respectively ($p < 0.05$).

6.3.4. Histopathological condition indices

Fifteen histopathological alterations in the digestive gland were considered for the weighted indices approach (Table 6.1) and results of histopathological indices (I_h) estimated *per* reaction pattern are in Fig. 6.7A-C. No significant differences were observed for all reaction patterns in unexposed mussels during the experimental period ($p > 0.05$; Fig. 6.8A-C), while mussels exposed to both Cd forms showed higher I_h for tubular (I_{h1}) and intertubular (I_{h2}) alterations when compared to unexposed ($p < 0.05$; Fig. 6.8A-B). After 3 days of exposure, QDs-exposed mussels showed a significant increase in I_{h1} and I_{h2} when compared to unexposed (2.5- and 6.2-fold, respectively; $p < 0.05$), while no significant differences were observed between dissolved Cd-exposed and unexposed mussels ($p > 0.05$; Fig. 6.8A-B), confirming early histopathological

lesions after exposure to QDs. Afterwards both Cd forms induce similar I_h levels with higher intensity compared to unexposed mussels until the end of exposure ($p < 0.05$; Fig. 6.8A-B). Although results of total histopathological condition indices (I_{htotal}) indicated similar intensity of histopathological alterations in the digestive gland of mussels exposed to both Cd forms for 14 days (Fig. 6.8C), the analysis of I_h per reaction pattern indicated early histopathological response in a shorter time of exposure to QDs. On the other hand, neoplasias (fibroma or haemic neoplasia) were not observed in the digestive gland of mussels after exposure to both Cd forms for 14 days, indicating that the DNA damage and oxidative stress previously observed in mussels exposed to the same CdTe QDs (6 nm; $10 \mu\text{g L}^{-1}$; 14 days) (Rocha et al., 2014; 2015b) (Chapters 4 and 5) is not directly related to development of neoplasias in the digestive gland of marine mussels in the experimental condition analyzed. Similar results were observed in *M. galloprovincialis* exposed to CuO NPs (40 - 500 nm, $10 \mu\text{g Cu L}^{-1}$, 21 days) (Ruiz et al., 2015), suggesting that further studies are needed to understand the potential effect of metal-based NMs on cancer development in bivalve species.

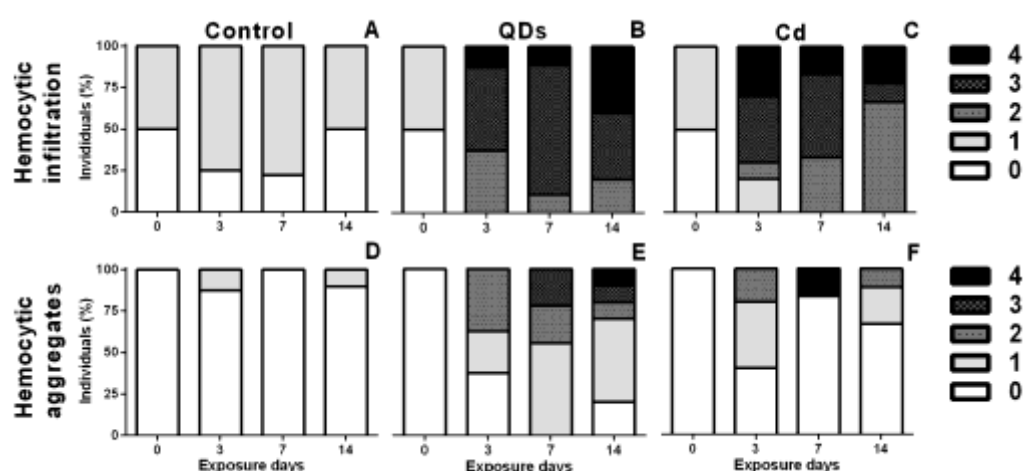


Figure 6.7. Frequency of the haemocytic infiltration (%) (A - C) and haemocytic aggregates (%) (D - F) distributed by grade of the inflammatory response in the digestive gland of mussels *M. galloprovincialis* from control (C) (A and D), exposed to CdTe quantum dots (QDs) (B and E) and to dissolved Cd (Cd) (C and F) for 14 days.

6.3.5. Principal component analysis

Multivariate analysis results indicate differential tissue-level biomarkers and inflammatory responses in marine mussels exposed to QDs when compared to its dissolved counterparts (Fig. 6.9A-B). The two principal components represent 77.1 %

of total variance (PC1 = 59.6 %, PC2 = 17.5 %) and showed a clear separation between unexposed mussels and those exposed to both Cd forms, especially after 14 days of exposure (Fig. 6.9A-B). After 3 days, QDs-exposed mussels showed higher response when compared to those exposed to dissolved Cd, indicating early tissue alterations and inflammatory response in a short-time of exposure to QDs (Fig. 6.9A-B). Similarly, early changes of the antioxidant capacity (in the gills and digestive gland) and immunotoxic effects in circulating hemocytes were observed in *M. galloprovincialis* exposed to CdTe QDs (6 nm, 10 µg Cd L⁻¹, 14 days) (Rocha et al., 2014; 2015c) (Chapters 4 and 5), indicating an association between ROS production, antioxidant capacity and inflammatory conditions in mussels exposed to Cd-based QDs. After long-time exposure to QDs (14 days), mussel response was more related to exposure time, inflammatory response (haemocytic infiltration and aggregation) and changes of the $R_{Bas/Dig}$, while the response to dissolved Cd was related to Cd concentration in the digestive gland and histomorphometric parameters of digestive tubules (e. g. Si and digestive tubule type II or III). QDs are well known to produce oxidative stress, immunotoxicity and inflammatory conditions at different trophic levels in the aquatic environment, such as bivalves (Gagné et al. 2008; Peyrot et al., 2009; Bruneau et al., 2013; Rocha et al., 2014, 2015c) (Chapters 3 and 4), polychaetes (Saez et al., 2015) and fishes (Gagné et al., 2010; Bruneau et al., 2013), confirming the hypothesis that the immune system of invertebrates and vertebrates represent a major target for Cd-based QDs.

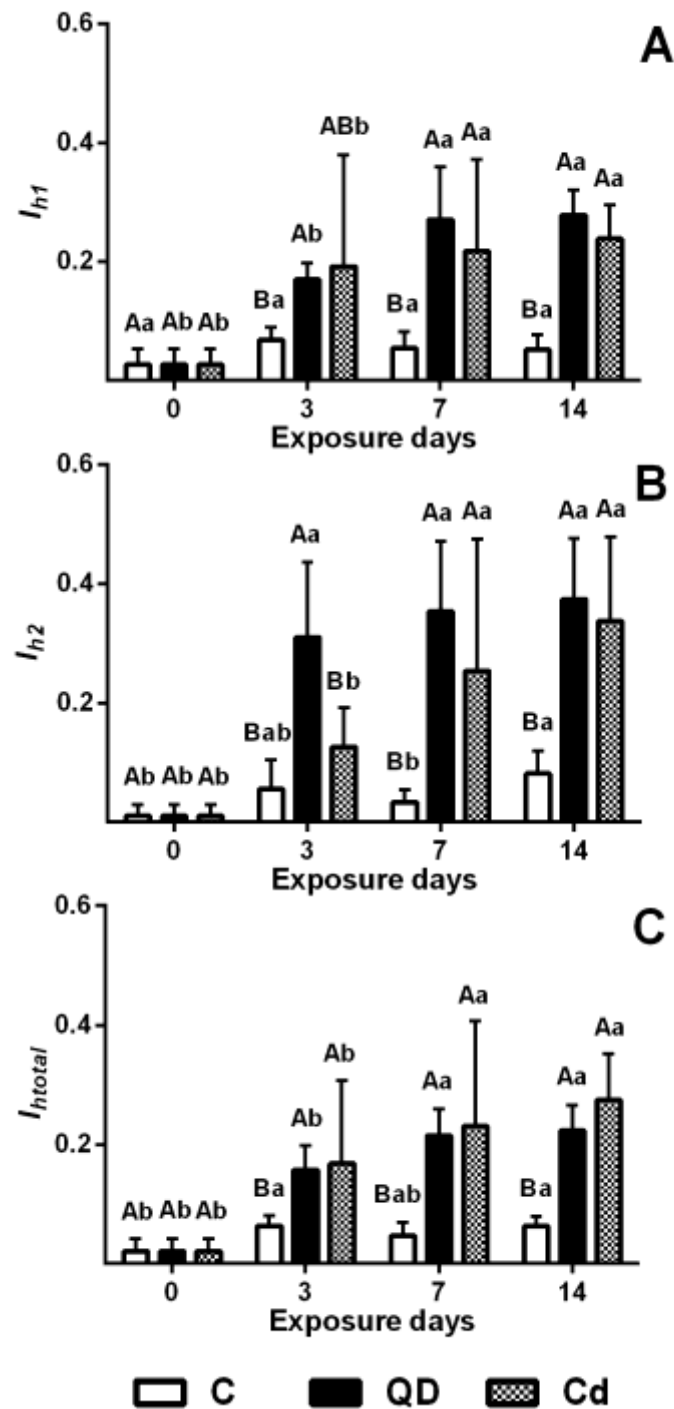


Figure 6.8. Histopathological condition indices (I_h) (mean \pm std) of the digestive gland in mussels *M. galloprovincialis* from control (C), exposed to CdTe quantum dots (QDs) and to dissolved Cd (Cd) for 14 days: tubular alteration index (I_{h1}) (A), intertubular alteration index (I_{h2}) (B) and total histopathological index (I_{htotal}) (C). Different capital and lower case letters indicate significant differences between treatments at each time of exposure and within treatment during the exposure period, respectively ($p < 0.05$).

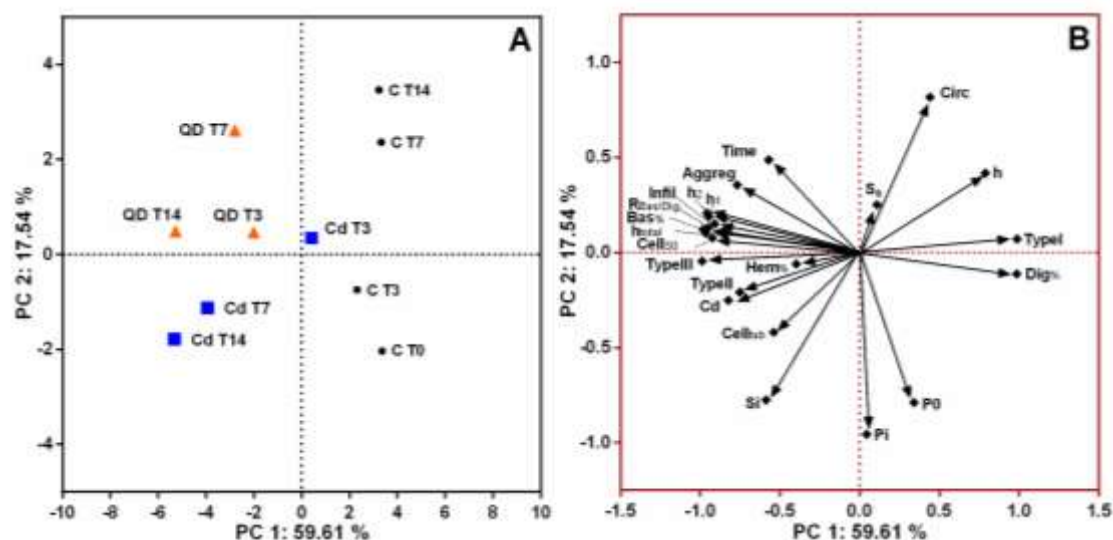


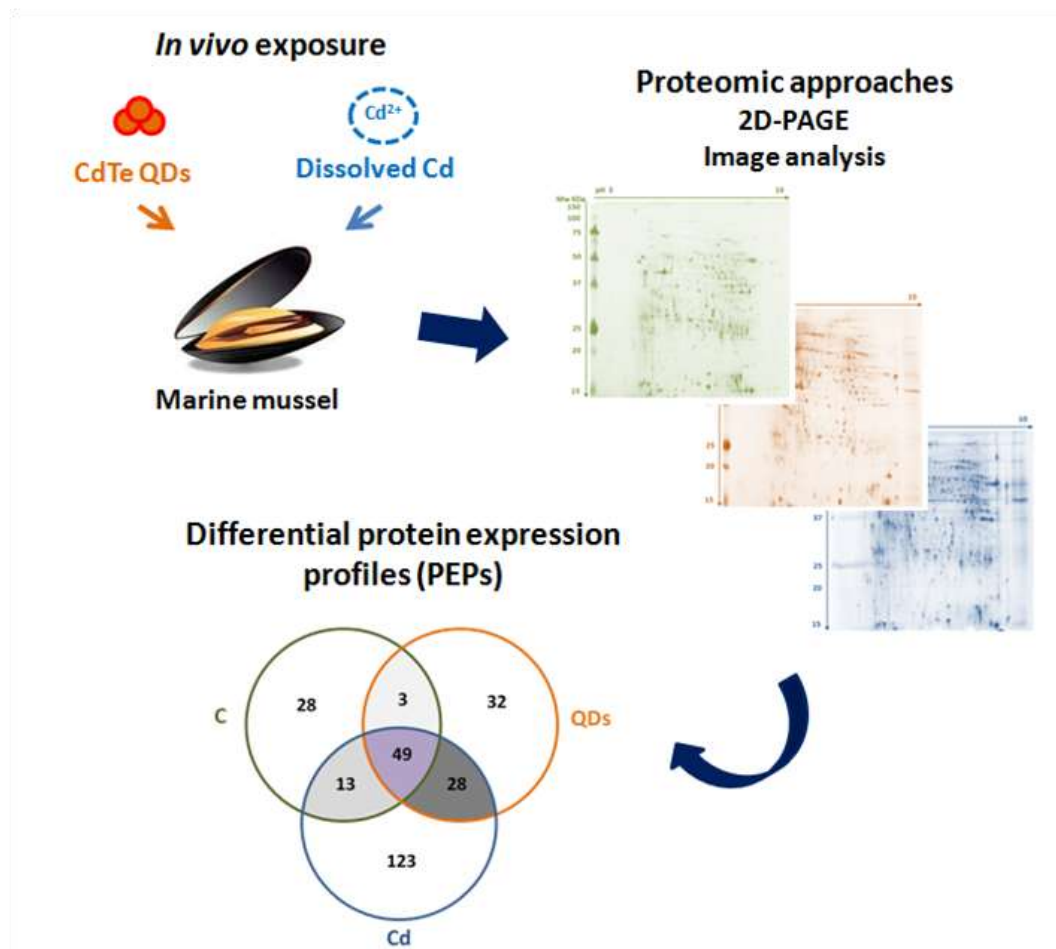
Figure 6.9. Principal component analysis (PCA) of Cd concentration and of a battery of tissue-level biomarkers (histomorphometric parameters of the digestive tubule epithelium and lumen, digestive tubule cell type composition and histopathological indices) and inflammatory response (haemocytic infiltration and aggregation intensities) in the digestive gland of mussels *M. galloprovincialis* from controls (C), exposed to CdTe QDs and to dissolved cadmium (Cd) during 14 days of exposure (A-B).

6.4. Conclusions

In conclusion, the present study analyzed histopathological alterations and inflammatory responses in marine mussels exposed to CdTe QDs and dissolved Cd and showed different mussel responses according to the Cd form and exposure time. Among histomorphometric parameters analyzed, the $R_{Bas/Dig}$ is a more sensitive tissue-level biomarker in mussels exposed to Cd-based QDs and results indicated that the cell-type replacement is an important strategy for maintenance of homeostasis in marine mussels exposed metal-based ENMs. The inflammatory response in mussels is Cd form dependent, wherein higher increase in the frequency of haemocytic infiltrations and granulocytomas is due to QDs exposure, indicating distinct mode of action related to nano-specific properties. This study indicates the utility of health status screening in marine mussel exposed to metal-based ENMs using a multiparametric histopathological assessment associated to immune defence response.

CHAPTER VII

Differential proteomic response to cadmium-based quantum dots in the marine mussel *Mytilus galloprovincialis*



Part of this Chapter is being prepared for submission to:

- Rocha, T.L., Cardoso, C., Bebianno, M.J. Differential proteomic response to cadmium-based quantum dots in the marine mussel *Mytilus galloprovincialis*. Journal of Hazardous Materials.

Part of this Chapter was presented at:

- Rocha, T.L., Cardoso, C., Bebianno, M.J., 2016. Differential protein expression profile in mussels *Mytilus galloprovincialis* exposed to CdTe quantum dots and dissolved cadmium. 30th ESCPB Congress, Barcelona, Spain.

Abstract

Cd is a well-known toxic metal to marine organisms, but its effects at nanoscale (Cd-based quantum dots - QDs) are less known. In the nanoecotoxicological context, proteomics applied on marine invertebrates is a suitable tool to describe their mode of action (MoA), identification of novel or unbiased biomarkers and safety assessment of nanomaterials in aquatic environment. In this work, a proteomic approach was used to assess differential protein expression signatures (PESs) in the digestive gland of the marine mussel *Mytilus galloprovincialis* exposed to CdTe QDs and their dissolved counterpart. Mussels were exposed to CdTe QDs (size: 6 ± 1 nm; $10 \mu\text{g Cd L}^{-1}$) and dissolved Cd (Cd nitrate; $10 \mu\text{g Cd L}^{-1}$) for 14 days and the PESs were analyzed by two-dimensional electrophoresis (2D-PAGE) associated to image analysis, along with the determination of Cd concentration in the tissue. Results showed that both Cd forms induce changes in protein expression in a Cd form dependent pattern, indicating nano-specific effects. PESs show significant differences (≥ 2 folds) in 304 protein spots between mussels exposed to both Cd forms and unexposed ones, wherein 32 and 123 proteins were specific to QDs and dissolved Cd, respectively, and 28 proteins were detected only after the exposure to both Cd forms. Results indicate that the MoA and toxicity of QDs is not only due to QDs dissolution and release of ionic Cd (Cd^{2+}), but also related to its nano-specific properties. To our knowledge, this is the first proteomics study in bivalves exposed to Cd-based QDs.

Keywords: Nanoecotoxicology, nanomaterials, metal-based nanoparticle, CdTe Quantum dots, cadmium, proteomics, *Mytilus galloprovincialis*.

7.1. Introduction

ENMs are a new class of emerging contaminants with potential hazardous effects to human and environmental health, but its mechanistic and toxicological peculiarities related to nano-specific properties remain unclear (Rocha et al., 2015a; Costa and Fadeel, 2016) (Chapter 1). Among the ENMs, QDs are semiconductor nanocrystals with unique optical and biofunctional properties used mainly in biomedical imaging, target drug delivery and electronics (Rizvi et al., 2010). Despite its widespread applications, concerns about the potential hazardous of Cd-based QDs have been reported in the estuarine and marine environment at various trophic levels, such as phytoplankton (Morelli et al., 2013), amphipod (Jackson et al., 2012), polychaete (Buffet et al., 2014), bivalve molluscs (Hull et al., 2013; Katsumiti et al., 2014; Munari et al., 2014; Buffet et al., 2015; Rocha et al., 2014, 2015b,c) (Chapters 2 - 5) and fish (Blickley et al., 2014).

Bivalve molluscs are the most studied marine invertebrate group and have been used as sentinel species for characterizing the potential impact of ENMs in the marine environment (Canesi et al., 2012, 2016; Rocha et al., 2015a) (Chapter 1). The bioaccumulation and ecotoxicity of Cd-based QDs was investigated in the marine mussel *M. galloprovincialis* after *in vitro* exposure to CdS QDs (5 nm; 10^{-4} - 10^2 mg L⁻¹; 24 h) (Katsumiti et al., 2014) and after *in vivo* exposure to CdTe QDs (6 nm; 10 µg L⁻¹; 14 days) (Rocha et al., 2014, 2015b,c) (Chapters 2 - 5), in *M. edulis* exposed to CdS QDs (13.4 nm; 0.01 to 10 mg L⁻¹; 4 h) (Munari et al., 2014) and in the marine clam *S. plana* exposed to CdS QDs (5 - 6 nm; 10 µg L⁻¹; 14 days) (Buffet et al., 2014). Overall, marine bivalves exposed to QDs showed Cd accumulation, behaviour impairment, oxidative stress, LMS decrease, immunotoxic and genotoxic effects in a size, time, concentration, tissue and species dependent manner. Tissue specific responses were observed in *M. galloprovincialis* exposed to CdTe QDs (6 nm; 10 µg L⁻¹; 14 days), wherein QDs aggregates uptake was mainly through the digestive gland cells via endocytotic mechanisms, characterizing the digestive gland as main target organ for accumulation and metabolism of Cd-based QDs, with estimated $t_{1/2}$ of more than 50 days (Rocha et al., 2015b,c) (Chapters 2 - 5).

Cd is a metal with no known biological function in marine organisms (e. g. Serafim and Bebianno, 2007; Macías-Mayorga et al., 2015), but when reduced to the nanoscale (e. g. Cd-based QDs) has different MoA and toxicity. Although the QDs dissolution and release of Cd²⁺ ions from QDs core was confirmed as source of toxicity

in mammals and invertebrate cells, especially for uncoated QDs, nano-specific effects are related to oxidative stress due to ROS production, namely superoxide radical ($O_2^{\cdot-}$) and hydroxyl radical (OH^{\cdot}) (Hardman, 2006; Pelley et al., 2009; Rocha et al., 2015a,c); (Chapters 1 -5). However, the relative contribution of QDs dissolution, ROS production and/or nano-specific properties for QDs toxicity is not well established.

In the ecotoxicological context, proteomic responses to Cd-based QDs are scarce and were only assessed for the marine diatom *P. tricornutum* (Scebba et al., 2016) and for the fish *D. rerio* embryos (Petushkova et al., 2015). Different protein expression profiles were identified in the *P. tricornutum* exposed to CdSe/ZnS QDs (17 nm; 2.5 nM; 4 - 8 days), indicating different molecular mechanisms involved in the algae response to acute versus chronic exposure to QDs (Scebba et al., 2016), while changes in the vitellogenin profile were observed in *D. rerio* embryos exposed to CdSe/ZnS QDs (9.5 nm; 2 μ M; 48 h) (Petushkova et al., 2015). Thus, to the best of our knowledge, this is the first study of differential protein expression pattern in marine mussels exposed to Cd-based QDs.

Proteomic approaches have been applied in the blue mussel *Mytilus spp.* to describe the molecular and cellular mechanisms induced by ENPs, as well as to identify putative new biomarkers to Au NPs, Ag NPs and CuO NPs exposure (Tedesco et al., 2008, 2010a,b; Gomes et al., 2013, 2014; Hu et al., 2014). Differential protein expression analyzed by two-dimensional polyacrylamide gel electrophoresis (2D-PAGE) followed by mass spectrometry (MS) was identified in *M. galloprovincialis* exposed to CuO NPs (31 nm) and Ag NPs (42 nm) at 10 μ g L⁻¹ for 15 days (Gomes et al., 2013, 2014), indicating different MoA between metal-based ENPs and its dissolved counterpart. Furthermore, redox proteomic analysis showed higher protein carbonylation (gills) and ubiquitination (gills and digestive gland) associated to oxidative stress in marine mussels *M. edulis* exposed to Au NPs-citrate (13 nm; 750 μ g L⁻¹; 24 h), while changes in protein thiol oxidation occurred in the digestive gland of *M. edulis* exposed to the same NPs, with higher effects of small (5.3 nm) compared to larger ones (15.6 nm) (Tedesco et al., 2008, 2010a,b). Results point out that nano-specific effects of ENPs in marine invertebrates are size dependent and that proteomics may reveal more specific effects and NPs MoA compared to traditional biomarkers analysis.

Accordingly, the aim of this study was to compare differential protein expression profiles (PEPs) in the digestive gland of mussels *M. galloprovincialis*

exposed to CdTe QDs and to its dissolved counterpart at environmentally relevant concentration of Cd ($10 \mu\text{g Cd L}^{-1}$) for 14 days. 2D-PAGE associated to image analyses were employed to compare PESs in response to CdTe QDs and dissolved Cd in order to identify putative/new biomarkers of Cd-based QDs exposure.

7.2. Materials and Methods

7.2.1. QDs characterization

CdTe QDs (2 - 7 nm) coated by carboxyl groups (-COOH) were obtained from PlasmaChem GmbH (Berlin, CAS# 1306-25-8) with declared purity of 99.9 % and an emission wavelength at $590 \pm 5 \text{ nm}$. A QDs stock solution was made in Milli-Q water (100 mg L^{-1}), sonicated for 30 min (Ultrasonic bath VWR International, 230 V, 200 W, 45 KHz frequency) and characterized according to the method described by Sousa and Teixeira (2013). Suspensions of QDs in natural seawater ($S = 36.3$) were characterized by a combination of multiple analytical techniques (TEM, DLS, ELS, THR, AGNES, SCP) and results were previously reported in Rocha et al. (2014, 2015b) (Chapters 2 and 4) and are summarized in Table 3.1.

7.2.2. Experimental design

Mussels *M. galloprovincialis* ($60 \pm 5 \text{ mm}$ shell length) were collected in the Ria Formosa Lagoon (Portugal) (Figs. 1.16 and 1.17) and acclimated for 14 days in tanks containing natural seawater ($S: 36.3$) at 16°C and constant aeration. After acclimation, fifty mussels were placed in 30L tanks filled with 25 L of seawater ($2.0 \text{ mussels L}^{-1}$) and exposed to $10 \mu\text{g Cd L}^{-1}$ of CdTe QDs and to the same concentration of their dissolved counterpart jointly with a control group kept in clean seawater in a triplicate design (3 tanks *per* treatment) for 14 days, as described in Rocha et al. (2014, 2015b) (Chapters 2 and 4). Exposure experiments were conducted in a static-renewal condition under 12h: 12h light/dark cycles and seawater was changed daily with redosing of the Cd concentrations. Abiotic parameters were analysed daily by measuring salinity (36.3 ± 0.07), temperature ($16.6 \pm 1.2^\circ\text{C}$), pH (7.9 ± 0.1) and oxygen saturation ($103 \pm 1.3 \%$). Mussels were only fed with natural seawater providing animals with food to avoid starvation and any effects resulting from the interaction of QDs and food. No significant mortality was observed between unexposed mussels and those exposed to both Cd forms. Five mussels were collected from each experimental condition after 14 days of

exposure and the digestive gland dissected and immediately frozen in liquid nitrogen and stored at -80 °C until further use.

7.2.3. Cd accumulation

Cd concentration was determined in dried digestive gland (80 °C at 48 h) after wet acid digestion with HNO₃ (80 °C at 4 h) by graphite furnace atomic absorption spectrometry (AAS, AAnalyst 800-PerkinElmer). Accuracy was assured with certified reference material (TORT-II, Lobster Hepatopancreas) from the National Research Council (Canada) and results were similar to the certified values (28.5 ± 4.5 mg Cd kg⁻¹ and 26.7 ± 0.6 mg Cd kg⁻¹, respectively) as previously described in Rocha et al. (2015b) (Chapter 2). Data on Cd concentrations are expressed as µg g⁻¹ of dry weight tissue and were previously reported in Rocha et al. (2015b) (Chapter 2).

7.2.4. Protein extraction and two-dimensional electrophoresis (2-DE)

Pools of five digestive glands for each condition (control, QDs and dissolved Cd) were weighed, homogenized in HEPES-sucrose buffer [10 mM HEPES, 250 mM sucrose, 1 mM DTT, 1 mM EDTA, 1 mM PMSF and 10 % protease inhibitor cocktail (Sigma Aldrich), centrifuged (15000 g, 2 h) at 4 °C and total protein concentration was measured according to the Bradford method (Bradford, 1976) adapted to a microplate reader (Infinite® 200 PRO-Tecan), using Bovin Serum Albumin (Sigma-Aldrich) as a standard.

Proteins were first separated by isoelectric focusing (IEF) followed by SDS-PAGE according to Chora et al. (2009). 100 µg of proteins were precipitated in 10 % trichloroacetic acid (TCA) in cold acetone containing 20 mM DTT (-20 °C; 2 h), centrifuged (10000 g, 30 min, 4 °C), washed with cold acetone, solubilised in 300 µL of rehydration buffer (7 M urea, 2 M thiourea, 4 % CHAPS, 0.8 % pharmalyte, 65 mM DTT and bromophenol blue traces) for 30 min, centrifuged (14000 g, 10 min, 4 °C) and applied onto 18 cm Immobiline™ DryStrip pH 3 - 10 NL (GE Healthcare). IEF was performed on Ettan™ IPGphor II™ at 20 °C using the following programme: 6 h of passive rehydration (0 V), 6 h of active rehydration (50 V) and IEF was carried out (50 µA/strip): 1000 V, 1 h; 4000 V, 1 h; 8000 V, 1 h; 8000 V until 50000 V were reached (~5 h). For the second dimension (SDS-PAGE), strips were reduced with 2 % DTT and alkylated in 2.5 % iodoacetamide in SDS equilibration buffer (6 M urea, 75 mM Tris-HCl, 4% SDS, 29.3 % glycerol and bromophenol blue traces) at pH 8.8.

SDS-PAGE was carried out on 12 % polyacrylamide gels (six gels per condition) using the Ettan™ Dalt six system controlled with Multitemp IV (GE Healthcare) in two steps at 9 °C: 120 V, 90 mA, 30W for 30 min; 500 V, 360 mA, 100 W until separation was finished (~5.5 h). Afterwards gels were silver stained using a protocol compatible with MS analysis (Blum et al., 1987, modified). To ensure the reproducibility of the gels, four replicates of each experimental condition (control, CdTe QDs and dissolved Cd) were prepared.

7.2.5. Image analysis

Silver stained gels were scanned using a GS-800 densitometer (BIORAD, Hercules, CA) and analysed using the PDQuest software (V8.0, BIORAD, Hercules, CA). The protein intensity of each spot was normalized to the total intensity of each gel image and the normalized volumes of the different spots of the digestive gland from mussels exposed QDs and to dissolved Cd were matched against the corresponding ones from control gels. The number of valid protein spots was determined for each gel, as well as the number of proteins matched to every gel, and qualitative and quantitative differences in protein expression between the digestive gland of unexposed and Cd-exposed (QDs and dissolved) mussels were determined. Only spots expressed in 4 replicate gels for each condition were included in the statistical analysis and differences between protein expression were identified using non-parametric Mann-Whitney U-rank. Only spots with 2-fold or higher change in protein expression were considered for protein identification and results were considered significant when $p < 0.05$. Proteins were also categorized according its molecular weight (MW) (higher: $MW > 50$ KDa; medium: $50 > MW > 25$ KDa; low $MW < 25$ KDa) and isoelectric point (pI) (acidic: $pI < 7$; neutral: $7 > pI < 8$; basic: $pI > 8$).

7.3. Results and discussion

7.3.1. QDs behaviour in seawater and bioaccumulation

Data on CdTe QDs characterization and their behaviour in seawater are summarized in Table 3.1 and previously described by Rocha et al. (2014, 2015b) (Chapters 2 and 4). The aggregation behaviour and dissolution of CdTe QDs in seawater as well as differences in their uptake and accumulation in mussel tissues compared to dissolved Cd play pivotal roles in QDs mediated toxicity. In seawater, CdTe QDs have low dissolution rate (27.6 %) and the majority of QDs remain as homo-

aggregates with hydrodynamic diameter of 1014 ± 187 nm and negative surface charge (ζ -potential = -9.4 ± 1.2 mV), which are responsible for Cd accumulation in mussel tissues.

QDs homo-aggregates are uptake by mussels mainly via endocytosis in the digestive system, while individual particle or dissolved Cd is uptake mainly by gills (Rocha et al., 2015b) (Chapter 2). Both Cd forms are accumulated in the digestive gland over exposure period (14 days) in a Cd form dependent pattern, wherein lower Cd accumulation were observed in QDs-exposed mussels when compared to its dissolved counterpart (Table 5.1). Results confirm that the digestive gland of mussels *M. galloprovincialis* is an important target for accumulation and toxicity of Cd-based QDs, especially due to their high capacity to change the protein expression.

7.3.2. Protein expression profiles (PEPs)

Differential PEPs were obtained by 2D-PAGE in the cytosolic fraction of the digestive gland from unexposed mussels and those exposed to CdTe QDs and to dissolved Cd for 14 days (Fig. 7.1A-C). Image analysis allowed discriminating 434, 454 and 575 protein spots in the digestive gland of unexposed mussels and those exposed to QDs and dissolved Cd, respectively (Fig. 7.1A-C).

Both Cd forms induced differential protein expression in the digestive gland of *M. galloprovincialis* in a Cd form dependent pattern (Fig. 7.1A-C). QDs exposure induced significant changes in 181 protein spots (2-fold or higher; $p < 0.05$) compared to unexposed mussels, while dissolved Cd exposure induced alterations in 272 protein spots, indicating that QDs induced lower changes in the total number of differently expressed proteins when compared to their dissolved counterpart. These results may be related to higher Cd accumulation in mussels exposed to dissolved Cd compared to QDs (Table 5.2; Rocha et al., 2015b) (Chapter 2). However, several differently expressed proteins were specific to QDs and to dissolved Cd, while other proteins were common to mussels exposed to both Cd forms, indicating that the MoA and toxicity of QDs are not only due to their dissolution and release of ionic Cd (Cd^{2+}). A Venn diagram was generated to compare the common and differently expressed proteins between unexposed mussels and those exposed to QDs and dissolved Cd (Fig. 7.2). A total of 28, 32 and 123 protein spots were specific to control, QDs and dissolved Cd, respectively. In addition, 3, 13 and 28 differentially expressed proteins were commonly observed between control/QDs, control/dissolved Cd and QDs/dissolved Cd, respectively, while

49 protein spots were differently expressed in all conditions (control, QDs and dissolved Cd) (Fig. 7.2).

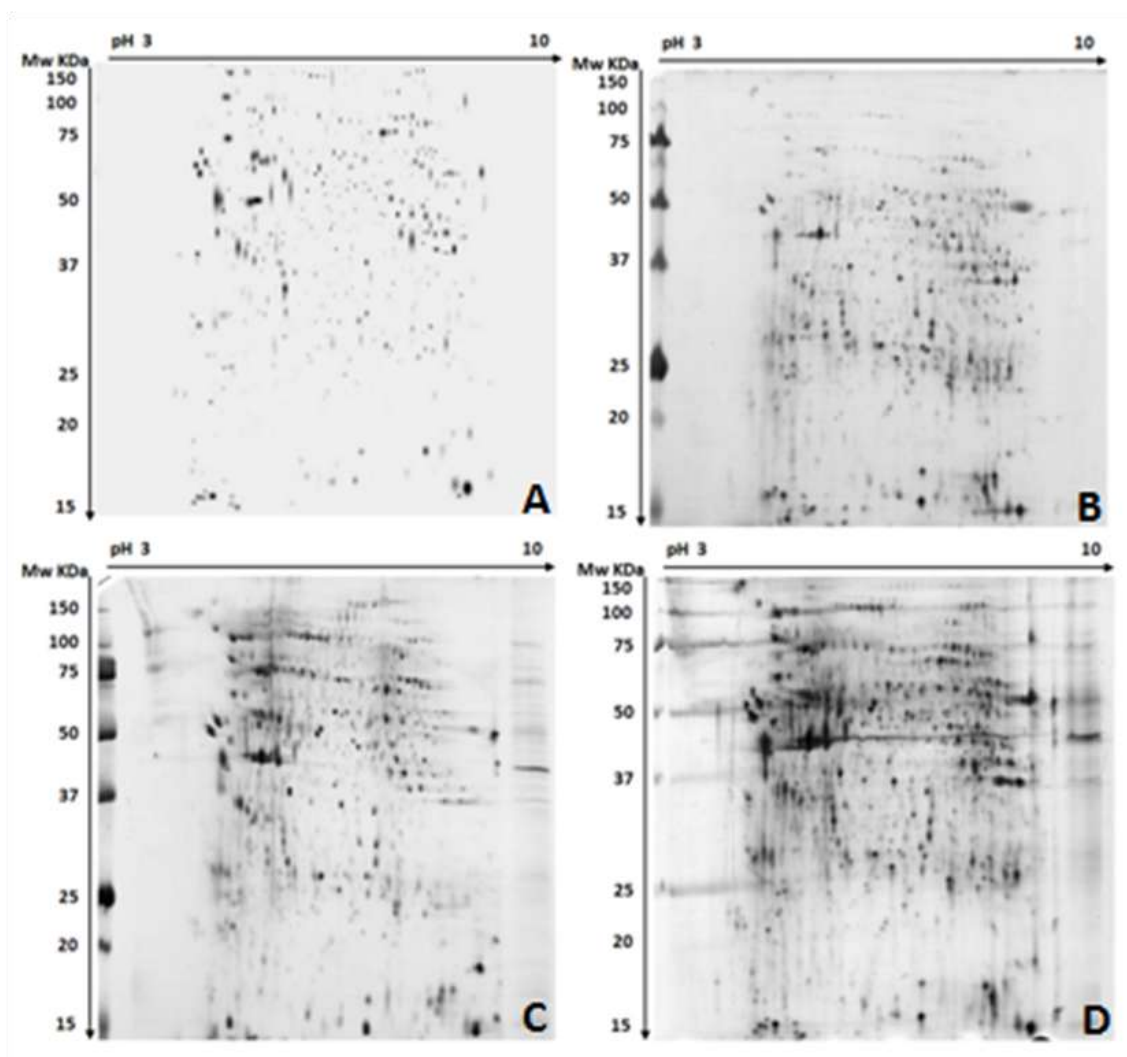


Figure 7.1. Master gel (A) constructed combining the information from the 2-DE gels of the digestive gland of *M. galloprovincialis* from control (B), exposed to CdTe quantum dots (QDs) (C) and to dissolved cadmium (Cd) (D) for 14 days. 100 μ g of protein content was separated on 18 cm IPG strips, in 3 - 10 pH gradients. The second dimension was performed in 12% SDS-PAGE gels, following by silver stain.

Image analysis showed 32 specific proteins spots (Tables 7.1 and 7.2) and 3 differently expressed proteins (Tables 7.1 and 7.3) in the digestive gland of QDs-exposed mussels. These 3 proteins (spot numbers: 5648, 4584 and 46125) were up-regulated compared to unexposed mussels (3.57-, 3.96 and 4.27-fold, respectively), indicating specific effects of QDs in proteins with high and medium MW (67.06, 47.67

and 67.87 KDa, respectively) and acidic pI (6.77, 5.80 and 5.68, respectively) (Fig. 7.3; Tables 7.1). On the other hand, 123 specific protein spots (Tables 7.1 and 7.4) and 13 differently expressed proteins were detected after exposure to dissolved Cd. Among these 13 proteins, 12 were up-regulated (spot number: 6495, 6563, 8255, 7488, 6498, 9618, 8436, 7383, 4480, 7546, 6876, 7555) (3.1-, 3.2-, 3.9-, 4.0-, 5.8-, 6.1-, 7.0-, 7.4-, 8.8-, 10-, 18.4- and 21.1-fold, respectively) and 1 down-regulated (spot number: 5133) (3.4-fold) compared to control (Tables 7.1 and 7.5). In opposite to QDs, dissolved Cd induced specific changes in proteins with higher (34 proteins), medium (66 proteins) and low MW (23 proteins), while pI ranged from acidic (73 proteins), neutral (30 proteins) to basic (20 proteins) (Table 7.5).

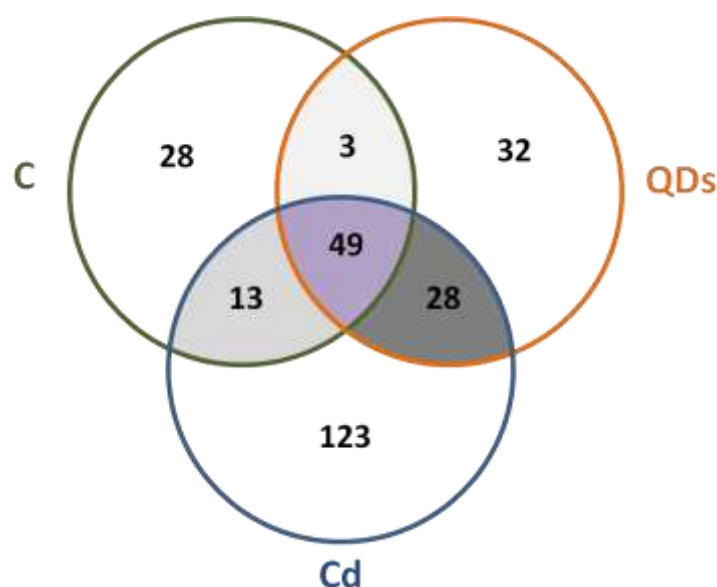


Figure 7.2. Venn diagrams comparing the number of differential expressed proteins in the digestive gland of unexposed mussels and exposed to quantum dot (QDs) and dissolved Cd

In addition, 28 protein spots were only observed in the digestive gland of mussels exposed to both Cd forms (Tables 7.1 and 7.6), which showed lower intensity in QDs-exposure mussels compared to Cd-exposed ones (Fig. 7.4; Table 7.1). Among these 28 proteins, 4 were up-regulated (spot numbers: 64102, 5635, 3223, 7277) (2.42-, 2.64-, 3.3- and 12.2-fold, respectively) and 24 down-regulated (spot numbers: 4779, 6878, 6708, 3665, 3835, 4273, 4337, 7578, 3142, 5121, 2212, 3555, 3834, 63101, 3765, 7380, 7725, 6697, 3442, 4410, 3836, 4412, 3416, 3833) (2.19 to 11.7-fold, respectively) in QDs-exposed mussels compared to dissolved Cd exposed ones (Tables 7.1 and 7.6).

Interestingly, a similar higher number of up-regulated proteins was observed in the marine diatom *P. tricornutum* exposed to CdSe/ZnS QDs (17 nm; 2.5 nM; 4 - 8 days) compared to control cells (Scebba et al., 2016), suggesting that the increase in protein synthesis is an important molecular mechanism in marine organisms exposed to Cd-based QDs. Furthermore, similar tendency to up-regulation was observed in the digestive gland of *M. galloprovincialis* exposed to Ag NPs (42 nm; 10 µg L⁻¹; 15 d) (Gomes et al. 2013), while the opposite was identified after the exposure to CuO NPs (31 nm; 10 µg L⁻¹; 15 d) at the similar metal concentration and exposure time (Gomes et al. 2014).

49 protein spots in unexposed mussels were modulated by both Cd forms (QDs and dissolved Cd) (Table 7.7). Among these proteins, 40 were up-regulated (Table 7.7) and 9 down-regulated (spot numbers: 8406, 7571, 6463, 8402, 7475, 7552, 6496, 7579 and 7550) (21.2-, 19.6-, 8.0-, 6.3-, 5.3-, 5.2-, 4.2-, 3.8- and 2.5-fold, respectively) in QDs-exposed mussels, while in the digestive gland of dissolved Cd-exposed ones 44 were up-regulated (Table 7.7) and 5 down-regulated (spot numbers: 8406, 7571, 6463, 8402 and 6496) (2.8-, 3.7-, 1.9-, 1.1- and 1.4-fold, respectively) (Fig. 7.5; Table 7.7). Interestingly, 4 spots (7475, 7552, 7579 and 7550) were down-regulated and up-regulated after exposure to QDs and dissolved Cd, respectively (Table 7.7), confirming differential protein expression after exposure to both Cd forms. On the other hand, 28 proteins (spot numbers: 2326, 3353, 3571, 4579, 4581, 4582, 4585, 4785, 5554, 5556, 5558, 5655, 61124, 6369, 6468, 6567, 6568, 6569, 7371, 7393, 7394, 7490, 7587, 7591, 7684, 7685, 7735 and 8610) (Table 7.8) were only detected in the control group, indicating that these protein spots were suppressed after exposure to both Cd forms (Table 7.1).

Table 7.1. Number of differentially expressed proteins (≥ 2 fold) in the digestive gland of mussels *Mytilus galloprovincialis* exposed to quantum dots (QDs) and dissolved Cd (Cd) compared with unexposed mussels (C).

Cd form	New proteins		Suppressed proteins		Differentially expressed proteins			
					Common		Specific	
	Common	Specific	Common	Specific	Up regulated	Down regulated	Up regulated	Down regulated
QDs	28	32	28	4	40	0	3	0
Cd		123		0			12	1

Owing to their high surface area and unique surface properties, ENPs may interact with extracellular medium and/or plasma proteins of marine invertebrates, leading to the formation of NP-protein corona (Canesi et al., 2016). Although the QDs-protein corona formation in bivalve species remains unknown, the interaction of QDs with different mammal proteins has been reported, especially for human and bovine serum albumin (HSA and BSA, respectively) (Liang et al., 2008; Lai et al., 2012). These studies showed that the binding of QDs to HSA/BSA form the QDs-HSA/BSA complex by electrostatic interactions, while different interaction mechanism was observed between positively charged QDs and negatively charged QDs. In this context, the differential protein expression profiles observed in the digestive gland of mussels exposed to QDs indicate potential interaction between QDs and mussel cytosolic proteins.

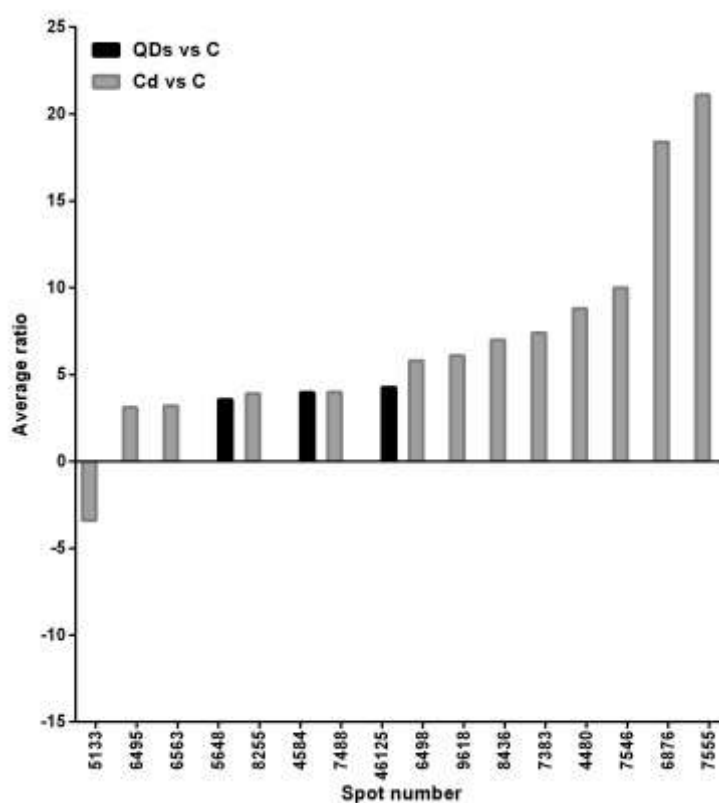


Figure 7.3. Sets of protein spots differently expressed in the digestive gland of mussels exposed to quantum dot (QDs) and dissolved Cd compared to unexposed ones.

Proteomic-based approaches using bivalve species have been used to assess hazard effects of metal-based ENPs and/or identification of putative new biomarkers. In the marine mussel *M. galloprovincialis*, a sets of protein spots differentially expressed

in mussels' gills and digestive gland (caspase 3/7-1, cathepsin L, Zn-finger protein and procollagen-D) were proposed as new putative biomarkers for the CuO NPs exposure (Gomes et al., 2014), while other sets of proteins (major vault protein, paramyosin and ras partial) were associated to Ag NPs toxicity (Gomes et al. 2013). Similarly, differentially expressed proteins observed in this study (Table 7.1 - 7.8) are potential new biomarkers to assess the ecotoxicological impact of Cd-based QDs in the aquatic environment.

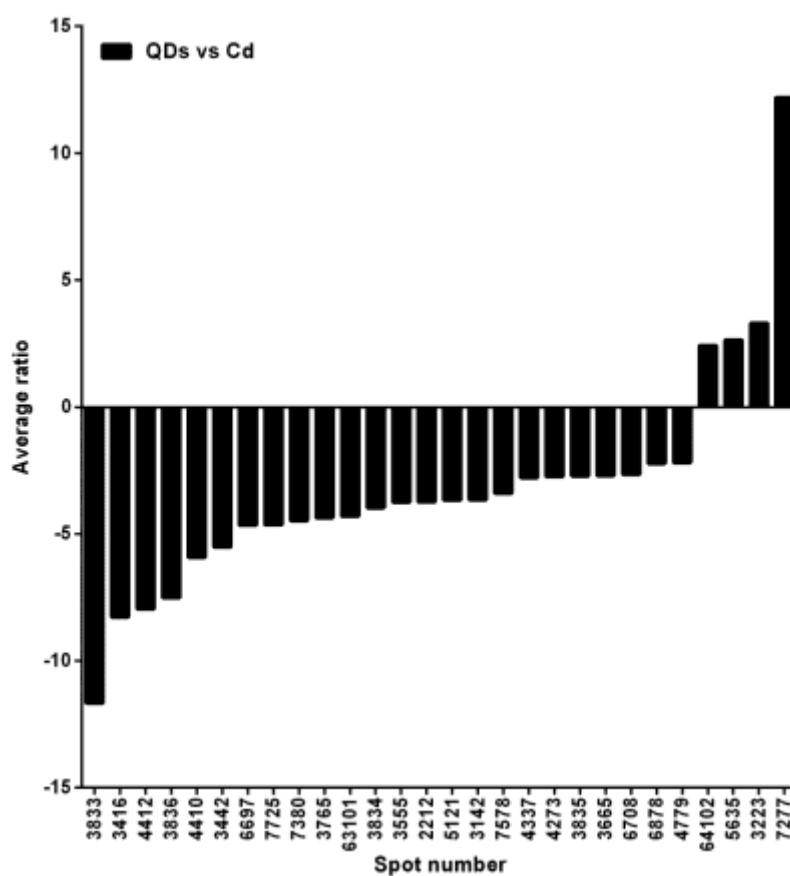


Figure 7.4. Sets of protein spots only observed in the digestive gland of mussels exposed to both Cd forms (QDs vs dissolved Cd) compared to unexposed ones.

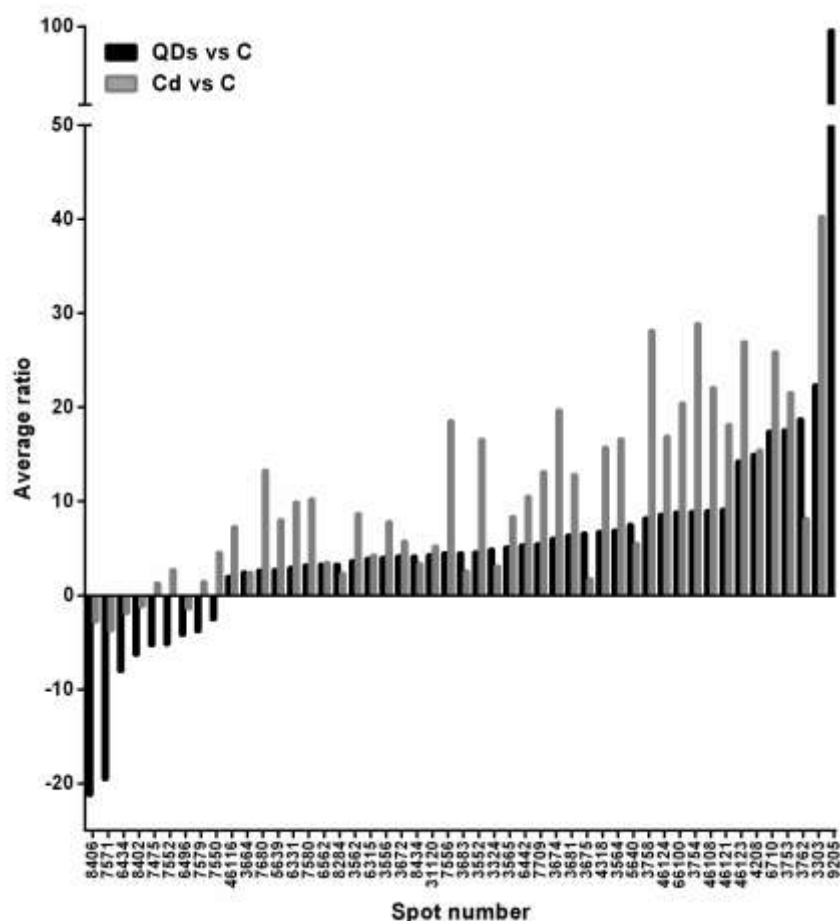


Figure 7.5. Sets of protein spots only differently expressed in the digestive gland of mussels exposed to both Cd form (QDs and dissolved Cd) compared to unexposed ones.

7.4. Conclusions

To the best of our knowledge, this is the first proteomic analysis in bivalve species exposed to Cd-based QDs. This exploratory study provide a first insight of PEPs in *M. galloprovincialis* after exposure to CdTe QDs for 14 days, in comparison to their dissolved counterpart, indicating specific molecular mechanism related to nano properties and several protein spots as potential biomarkers to assess the MoA and toxicity of Cd-based QDs. Both Cd forms showed a higher tendency to up-regulate proteins in the digestive gland in a Cd form dependent pattern. The identification of differentially expressed proteins by MS and bioinformatics was no followed in this study due to technical problems in the equipment, indicating that additional studies are needed to identify proteins modulated by both Cd forms. Overall, results showed nano-specific effects at protein level and confirm that the MoA and toxicity of QDs and their dissolved counterpart are mediated by different pathways.

Table 7.2. List of protein spots in the digestive gland of mussels only exposed to quantum dots (QDs).

Spot Number	Obs. Mw (KDa)	Obs. pI	Normalized volume (QDs)
2426	38.18	4.74	515.3
3350	33.58	5.29	346.0
3360	29.09	5.28	46.30
3362	27.85	5.48	56.90
3566	49.79	5.11	157.4
3567	49.77	5.22	193.0
3570	53.06	5.40	337.6
3687	64.73	5.48	66.70
3688	64.44	5.44	107.2
41115	17.61	5.80	33.30
4375	28.27	6.08	549.9
46128	69.65	6.45	119.2
5651	71.84	6.89	59.40
5652	73.5	6.94	40.30
5653	72.17	6.99	31.30
5761	95.65	7.25	27.60
5868	171.17	7.09	45.90
5869	160.9	7.18	117.1
64103	40.01	7.88	162.3
6570	54.19	8.03	177.9
66104	60.89	7.66	1465.8
6741	84.99	7.85	159.5
6745	96.19	7.93	23.80
6746	95.14	8.02	51.90
6867	153.32	7.65	79.40
6869	167.08	7.70	29.90
6870	164.15	7.76	30.20
6875	160.45	7.47	170.5
7396	35.6	8.47	15.50
7677	74.85	8.73	34.50
8181	17.95	9.12	56.90
8275	19.02	9.61	101.3

Table 7.3. List of protein spots differently expressed in the digestive gland of mussels exposed to quantum dot (QDs) compared to controls and dissolved Cd-exposed mussels.

Spot Number	Obs. Mw (KDa)	Obs. pI	Normalized volume (C)	Normalized volume (QDs)	Mean ratio (QDs vs C)
5648	67.06	6.77	27.9	99.7	3.57↑
4584	47.67	5.8	29.4	116.3	3.96↑
46125	67.87	5.68	23.7	101.3	4.27↑

Table 7.4. List of protein spots in the digestive gland of mussels exposed only to dissolved Cd.

Spot Number	Obs. Mw (KDa)	Obs. pI	Normalized volume (Cd)
11127	18.28	3.69	363.5
21139	17.15	4.42	143.4
2214	28.08	4.65	812.8
2228	18.73	4.25	236.5
2231	19.06	4.66	82.00
2310	22.06	3.93	391.9
2311	21.87	4.09	292.4
2316	35.09	3.99	203.3
2328	27.27	4.24	294.6
2425	41.93	4.80	808.7
2525	55.96	4.39	1806.8
2526	51.76	4.30	1995.3
3206	35.35	4.84	277.9
3216	18.17	5.25	199.3
3217	23.73	4.98	354.5
3222	19.06	5.13	81.00
3306	35.19	4.32	1130.6
3307	34.32	4.32	361.8
3308	28.00	4.35	1443.2
3507	49.51	4.58	256.6
3508	49.32	4.63	142.5
3558	55.18	5.16	217.7
4147	21.18	6.00	26.10
4215	26.34	5.38	49.80
4238	35.37	5.81	138.1
4274	22.94	5.92	26.40
4275	23.14	6.08	33.70
4305	31.59	5.75	275.5

4326	35.79	5.74	194.0
4328	24.46	5.69	230.1
4329	34.12	5.85	490.3
4345	30.09	6.20	69.10
4346	30.98	6.32	43.70
4355	36.41	5.88	452.7
4394	33.21	6.39	51.90
4395	33.93	6.46	37.70
4396	33.76	6.55	20.90
4397	35.61	6.13	78.80
4439	40.30	6.23	134.0
4450	37.29	6.50	86.40
4476	36.37	5.55	176.3
4478	36.23	5.75	319.3
4479	37.43	6.16	93.80
4776	93.60	5.65	116.3
4777	97.65	5.88	99.50
4783	104.77	6.46	27.30
4844	122.5	5.93	40.00
4845	121.81	6.01	23.40
4846	121.81	6.11	32.70
5118	18.36	6.17	37.20
5171	20.81	6.92	29.80
51124	16.70	6.74	341.5
5238	18.66	6.50	24.90
5241	21.98	7.06	21.70
5306	27.00	6.68	139.70
5307	31.9	6.71	103.3
5311	26.37	6.79	1220.3
5314	30.83	6.83	153.8
5319	31.00	7.04	238.6
5351	31.92	6.63	32.10
5365	30.29	7.22	64.40
5366	33.85	7.13	100.8
5367	32.91	6.63	17.40
5368	34.37	6.92	59.70
5369	33.04	6.97	106.1
5371	32.02	6.86	34.50
5408	42.66	6.70	256.8
5414	39.46	6.70	149.0
5448	38.79	7.10	95.10
5451	36.89	6.69	50.30
5452	38.62	6.97	37.70
5458	46.09	7.06	334.5
5451	36.89	6.69	50.30
5452	38.62	6.97	37.70

5553	50.96	7.28	38.60
5642	69.89	6.78	154.0
5643	63.50	6.67	198.8
5644	62.03	6.87	65.70
5645	61.50	7.28	63.40
5646	60.09	7.34	214.4
5754	91.62	6.73	405.1
5755	85.18	7.21	24.00
5756	86.37	7.03	51.60
5759	98.40	6.92	215.6
5760	98.78	7.04	334.3
5863	120.1	7.34	61.30
6146	20.76	7.36	67.50
6279	23.86	8.11	51.00
6286	21.07	7.75	46.30
6302	27.82	7.36	1159.3
6312	34.7	7.10	192.6
6321	32.75	7.48	785.7
6340	39.16	7.19	54.70
6342	38.36	7.26	62.50
6397	27.59	7.56	57.20
63103	35.05	7.90	177.6
6422	39.8	7.58	101.8
6557	55.61	7.54	84.50
6566	51.23	8.13	47.70
6645	59.12	7.67	179.0
6690	70.54	7.61	30.30
6693	59.26	7.47	119.0
6709	119.88	7.93	46.50
6724	92.01	7.29	30.00
6726	87.52	7.65	38.90
7174	16.58	8.31	356.1
7267	26.36	8.86	2076.2
7317	30.02	8.32	127.1
7387	28.72	8.89	465.8
7389	31.94	8.33	110.5
7390	32.32	8.42	147.4
7473	44.19	8.53	178.6
7477	39.25	8.37	242.7
7487	38.15	8.55	535.3
7569	46.92	8.83	373.6
7682	65.02	8.73	156.7
7683	73.79	8.33	49.40
7717	85.99	8.48	202.8
7734	79.85	8.64	175.7
7811	105.08	8.46	45.10

8166	17.36	9.60	922.9
8338	27.96	9.38	105.8
8339	27.98	9.28	93.10

Table 7.5. List of protein spots differently expressed in the digestive gland of mussels exposed to dissolved Cd compared to controls.

Spot Number	Obs. Mw (KDa)	Obs. pI	Normalized volume (C)	Normalized volume (Cd)	Mean ratio (Cd vs C)
5133	17.73	6.22	379.8	111.7	3.4↓
6495	45.05	7.69	43.10	135.5	3.1↑
6563	47.65	7.82	156.9	507.2	3.2↑
8255	32.06	9.01	34.40	135.8	3.9↑
7488	37.78	8.67	406.2	1608	4.0↑
6498	43.76	8.04	113.7	663.2	5.8↑
9618	74.23	9.17	455.2	2771	6.1↑
8436	39.33	9.13	47.80	333.5	7.0↑
7383	27.42	8.91	36.60	270.6	7.4↑
4480	45.90	6.03	372.2	3290	8.8↑
7546	49.34	8.58	153.8	1538	10.0↑
6876	140.91	7.70	15.60	286.3	18.4↑
7555	47.10	8.71	45.60	961.2	21.1↑

Table 7.6. List of protein spots only observed in the digestive gland of mussels exposed to both Cd forms (QDs and dissolved Cd).

Spot Number	Obs. Mw (KDa)	Obs. pI	Normalized volume (QDs)	Normalized volume (Cd)	Mean ratio (QDs vs Cd)
3833	126.04	5.46	23.30	271.7	11.7↓
3416	37.72	4.97	52.40	434.0	8.28↓
4412	38.67	5.35	67.10	533.3	7.95↓
3836	110.54	5.46	36.30	272.9	7.52↓
4410	38.79	5.20	48.20	285.6	5.93↓
3442	47.92	4.76	268.5	1480.3	5.51↓
6697	67.32	7.93	220.1	1026.1	4.66↓
7725	88.21	8.31	31.90	148.0	4.64↓
7380	31.94	8.25	18.70	83.70	4.48↓
3765	77.07	5.40	22.10	96.30	4.36↓
63101	33.45	8.06	28.10	120.8	4.30↓
3834	124.54	5.52	47.90	190.4	3.97↓
3555	50.97	5.22	95.00	356.5	3.75↓
2212	17.73	4.27	58.30	217.7	3.73↓
5121	17.12	6.08	52.70	193.2	3.67↓
3142	20.46	4.77	26.30	96.30	3.66↓
7578	56.53	8.58	287.3	978.0	3.40↓
4337	26.97	5.92	109.2	304.5	2.79↓
4273	22.85	5.74	25.10	68.70	2.74↓
3835	109.88	5.51	31.90	86.90	2.72↓
3665	65.00	5.39	60.50	163.2	2.70↓
6708	119.34	7.88	38.20	101.5	2.66↓
6878	118.66	8.01	39.30	87.70	2.23↓
4779	95.42	6.09	64.50	141.5	2.19↓
64102	38.43	7.83	160.3	66.20	2.42↑
5635	76.15	7.01	45.60	17.30	2.64↑
3223	19.57	5.39	285.3	86.50	3.30↑
7277	18.51	8.90	854.2	70.10	12.2↑

Table 7.7. List of protein spots differently expressed in the digestive gland of mussels exposed to both Cd form (QDs and dissolved Cd).

Spot number	Obs. Mw (KDa)	Obs. pI	Normalized volume (C)	Normalized volume (QDs)	Normalized volume (Cd)	Mean ratio (QDs vs C)	Mean ratio (Cd vs C)
8406	35.70	9.00	17259	812.8	6246	21.23↓	2.76↓
7571	49.68	8.90	5685	290.7	1531	19.56↓	3.71↓
6434	37.43	7.88	271.3	33.70	145.0	8.05↓	1.87↓
8402	35.70	8.69	5482	871.3	4760.5	6.29↓	1.15↓
7475	36.81	8.23	4116	781.5	5389.8	5.27↓	1.31↑
7552	51.58	8.42	436.2	84.10	1192.6	5.19↓	2.73↑
6496	44.27	7.83	2863	682.4	2045.8	4.20↓	1.40↓
7579	54.91	8.51	149.3	39.30	216.9	3.80↓	1.45↑
7550	51.41	8.36	166.0	65.00	757.8	2.55↓	4.57↑
46116	70.50	5.70	169.3	340.1	1232.2	2.01↑	7.28↑
3664	62.21	5.45	84.10	208.5	205.2	2.48↑	2.44↑
7680	65.40	8.50	94.40	254.9	1253.2	2.70↑	13.28↑
5639	66.53	6.93	79.70	218.7	640.1	2.74↑	8.03↑
6331	32.01	7.86	25.10	74.00	248.7	2.95↑	9.91↑
7580	56.80	8.45	36.00	116.1	368.2	3.23↑	10.23↑
6562	47.37	7.74	144.4	481.0	504.9	3.33↑	3.50↑
8284	22.87	9.59	125.4	417.8	294.4	3.33↑	2.35↑
3562	54.79	5.39	295.2	1086.9	2562.9	3.68↑	8.68↑
6315	22.86	7.23	37.30	146.6	160.0	3.93↑	4.29↑
3556	60.01	5.08	81.30	326.1	634.8	4.01↑	7.81↑
3672	70.78	5.24	66.10	275.4	381.5	4.17↑	5.77↑
8434	44.11	9.49	157.2	656.2	528.1	4.17↑	3.36↑
31120	15.73	4.94	103.3	444.8	540.2	4.31↑	5.23↑
7556	51.01	8.55	93.50	421.0	1735.4	4.50↑	18.56↑
3683	69.35	4.84	57.20	257.9	147.1	4.51↑	2.57↑
3552	52.57	5.08	45.10	208.8	747.9	4.63↑	16.58↑
3324	22.40	4.80	105.0	515.8	328.6	4.91↑	3.13↑
3565	50.70	5.34	118.6	608.8	991.1	5.13↑	8.36↑
6442	37.91	8.02	190.9	1023	2010	5.36↑	10.53↑
7709	93.94	8.19	31.60	173.0	415.8	5.47↑	13.16↑
3674	76.33	5.54	19.50	117.7	383.9	6.04↑	19.69↑
3681	67.56	5.54	52.80	337.3	677.8	6.39↑	12.84↑
3675	69.18	4.91	22.10	146.1	38.70	6.61↑	1.75↑
4318	35.61	5.41	24.60	165.7	386.9	6.74↑	15.73↑
3564	54.21	5.32	125.3	866.1	2084.1	6.91↑	16.63↑
5640	66.34	7.10	44.60	335.2	245.9	7.52↑	5.51↑
3758	80.25	5.05	13.10	107.6	368.9	8.21↑	28.16↑
46124	71.37	5.56	50.20	432.9	848.3	8.62↑	16.90↑
66100	62.46	7.92	49.80	439.9	1019	8.83↑	20.45↑
3754	95.78	5.19	30.10	267.5	869.7	8.89↑	28.89↑
46108	78.37	5.24	38.70	347.4	854.4	8.98↑	22.08↑

46121	75.46	5.93	8.10	73.90	147.1	9.12↑	18.16↑
46123	76.04	5.65	15.4	219.1	415.5	14.23↑	26.98↑
4208	16.99	6.32	42.9	642.9	662.6	14.99↑	15.45↑
6710	79.92	7.97	20.6	358.8	533.0	17.42↑	25.87↑
3753	95.05	5.25	25.3	445.2	545.6	17.60↑	21.57↑
3762	94.00	5.14	19.8	371.3	161.3	18.75↑	8.15↑
3303	35.55	4.95	24.9	557.5	1003	22.39↑	40.3↑
9205	19.14	9.24	70.2	6986	1388	99.52↑	19.77↑

Table 7.8. List of spots only observed in the digestive gland of unexposed mussels (C).

Spot Number	Obs. Mw (KDa)	Obs. pI	Normalized volume (C)
2326	28.88	4.58	340.8
3353	31.28	5.01	394.1
3571	59.55	5.53	37.90
4579	55.89	5.70	75.80
4581	54.43	5.79	30.30
4582	51.16	5.70	267.4
4585	49.3	6.15	51.70
4785	92.34	6.02	40.30
5554	53.02	6.83	113.6
5556	52.69	7.12	205.0
5558	52.26	7.33	81.30
5655	70.06	6.62	12.50
61124	17.02	7.51	419.2
6369	35.11	7.41	150.7
6468	42.81	7.66	524.2
6567	50.96	7.36	122.2
6568	49.12	7.45	30.90
6569	54.09	7.78	34.80
7371	31.32	8.74	84.80
7393	33.87	8.98	96.80
7394	27.35	8.72	92.20
7490	36.91	8.67	92.10
7587	55.45	8.84	121.1
7591	55.92	8.53	275.9
7684	71.33	8.67	64.20
7685	70.84	8.76	50.40
7735	80.81	8.32	26.80
8610	71.09	9.07	42.20

CHAPTER VIII

General discussion, conclusions
and future perspectives

8.1. General discussion

8.1.1. Nanomaterials

Recently the European Commission defined nanomaterials (NMs) as “*A natural, incidental or manufactured material containing particles, in an unbound state or as an aggregate or as an agglomerate and where, for 50 % or more of the particles in the number size distribution, one or more external dimensions is in the size range 1 - 100 nm*” (2011/696/EU). Furthermore, the International Organization for Standardization (ISO) defines the term nanoscale as “*length interval approximately from 1 nm to 100 nm*”, while engineered nanomaterials (ENMs) were defined as “*materials with any external dimension in the nanoscale or having an internal surface structure at those dimensions (between 1 and 100 nm) that are designed for a specific purpose or function*” (ISO/TS 27687:2008; ISO/TS 80004-4:2011; ISO/TS 80004-2:2015). ENMs have unique properties and are applied in a wide range of society fields, from industrial applications to medical and environmental sciences.

Among the metal-based ENMs, quantum dots (QDs) were defined by EPA as “*a closely packed semiconductor crystal comprised of hundreds or thousands of atoms, and whose size is on the order of a few nanometers to a few hundred nanometers*” (EPA100/B-07/001:2007). Due to their unique optical and biofunctional properties with widely applications in several fields, such as nanomedicine, biology and electronic (revised in the Chapter 1), QDs were chosen in this study as a model of metal-based ENMs for ecotoxicological assessment of ENMs in the marine environment.

8.1.2. Nanoecotoxicology

Nanotoxicology studies the interaction of NMs with biological systems, especially in humans and mammals (Fischer and Chan, 2007), while the nanoecotoxicology studies the ecotoxicity and environmental risk of NMs. Nanoecotoxicology is an emergent area in the toxicological science, but limited information is available when compared to the nanotoxicology (Kahru and Ivask, 2013) and large knowledge gap still exists, especially for the marine environment (Matranga and Corsi, 2012; Libralato et al., 2013; Baker et al., 2014).

The increasing development of different types of QDs will inevitably lead to their release into the wastewater and marine environment, wherein QDs are considered

as emerging contaminants (Corsi et al., 2014; Rocha et al., 2015a) (Chapter 1). ENMs are not intrinsically hazardous *per se* and have the potential to improve the environmental quality by direct and indirect application, such as in environmental remediation (namely nanoremediation) to reduce the impact of contaminants/pollutants, and in agriculture and food production, and application as sensors and devices for monitoring ecosystem health and preservation of biodiversity (Karn et al., 2009; Peralta-Videa et al., 2011; Corsi et al., 2014; Peijnenburg et al., 2015). Thus, for the development of sustainable nanotechnologies, the knowledge of the environmental impact of ENMs is needed, especially for the aquatic environment.

Aquatic environment represents the ultimate sink for deposition of ENMs and its sub-products by point sources (sewage, effluents, river influx, wastewater treatment) and/or indirectly input (aerial deposition, dumping and run-off) (revised in Chapter 1). Although the concentration of QDs in the aquatic environment is difficult to predict due to the methodology remained not available, potential hazardous effects of Cd-based QDs were reported in estuarine and marine environment at various trophic levels (revised in Chapter 1). Accordingly, the main focus of this thesis was to assess the toxicokinetics, MoA and toxicity of Cd-based QDs in the biomonitor species *M. galloprovincialis* using a multibiomarker approach associated with differential protein expression and comparing their effects to dissolved Cd at an environmentally relevant Cd concentration. In this Chapter, the general discussion is summarised along with the overall conclusions and some suggestions for future research.

8.1.3. Behaviour and fate of QDs in the aquatic environment

Behaviour and fate of QDs in the aquatic environment are highly dependent on their nano-specific properties, such as size, shape, surface charge, functionalization and coating, as well as environmental conditions (Chapter 1). Different processes may influence the behaviour of QDs in the marine environment (namely physicochemical transformation, macromolecular interaction and biologically mediated reactions) (Fig. 1.9), which determines their fate, bioavailability, interaction, accumulation and toxicity in marine organisms (Tables 1.2 - 1.5; Chapter 1).

In this study, QDs characterization was performed by a combination of multiple analytical techniques (TEM, DLS, ELS, THR, UV-Vis spectrophotometry, AGNES and

SCP) using both natural seawater from the Ria Formosa Lagoon (Portugal) and ultrapure water (Milli-Q) (Chapters 2 - 3; Rocha et al., 2014, 2015b). Similar approaches (e. g. TEM, DLS, ELS) were used in previous studies about the ecotoxicity of several ENPs on bivalve species, such as Ag NPs (40 - 50 nm) (Buffet et al., 2013; Gomes et al., 2014), Au NPs (5 - 40 nm) (Pan et al., 2012), CuO NPs (Gomes et al., 2011, 2012) and TiO₂ NPs (10 - 100 nm) (Libralato et al., 2013; Katsumiti et al., 2014b). On the other hand, AGNES and SCP are electrochemical stripping techniques that enable to detect chemical speciation and the dissolution rate of NPs in aqueous medium (Galceran et al., 2004; Rocha et al., 2007). The NPs dissolution associated to metal speciation plays an important role in the aquatic toxicity of metal-based NPs and were also used in previous studies about the bioaccumulation and toxic effects of CdTe/CdS QDs (4.2 - 5.7 nm) on green algae *C. reinhardtii* (Domingos et al., 2011), on the ecotoxicity of ZnO NPs (30 nm) on the crustaceans *D. magna* (Adam et al., 2014) and on the interactive effects between n-TiO₂ (5 - 20 nm) and dissolved Cd in freshwater clam *C. fluminea* (Vale et al., 2014), indicating that the combination of multiple analytical techniques for ENMs characterization provides a more comprehensive analysis for the hazard and risk characterization of ENMs.

The characterization and behaviour of QDs in seawater (primary particle size, shape, hydrodynamic diameter, surface charge, polydispersity index, isoelectric point, aggregation/agglomeration kinetics, stabilization with different NOM, sedimentation and dissolution rates) (Table 3.1) indicated that CdTe QDs used in this study were spheroid ENPs with primary size of 6 ± 1 nm coated by carboxyl groups (-COOH). In natural seawater, these QDs form aggregates/agglomerates with a hydrodynamic diameter of 1014 ± 187 nm and negative surface charge (ζ -potential = -9.4 ± 1.2 mV), which reduced its total surface area in contact with the surrounding environment and bioavailability to marine mussels when compared to their dissolved counterpart (Chapters 2 - 3). QDs dissolution rate in seawater was 27.6 % and its fast and slow sedimentation rates were $0.88 \pm 5 \times 10^{-4}$ and $0.009 \pm 8.45 \times 10^{-4}$, respectively, confirming the tendency of QDs to aggregate/agglomerate and quickly settle, while no stabilization with different NOM (HA, TA and SA) was observed (Chapter 2). Several physico-chemical forms of Cd were identified during the exposure of mussels to CdTe QDs: 72 % were small and larger homo-aggregates of CdTe QDs, while 27.6% were free ionic Cd (Cd²⁺), inorganic (CdCl and CdCl₂) and organic Cd complexes that result from Cd release from the QDs core (Cd-NOM-complex). On the other hand, the release

of ionic Te from the QDs core and its speciation in seawater were not followed in this study, but these parameters require future studies for holistic understanding of the toxicity of CdTe QDs in the marine environment. To our knowledge, there are no studies reporting the Te concentration nor its toxicity in mussel species, while concentrations of 2 and 3 $\mu\text{g Te kg}^{-1}$ were reported in fishes and oysters (Guérin et al., 2011), indicating that further studies about the impact of CdTe QDs in the Te accumulation in marine organisms are need.

8.1.4. Uptake, accumulation and tissue distribution

The uptake, accumulation and tissue distribution of QDs in mussels compared to its dissolved counterpart are summarised in the Figure 8.1. Several physico-chemical forms of QDs in seawater are available for the marine mussel *M. galloprovincialis* and induce Cd accumulation in tissue and time dependent patterns (Chapter 2). As filter-feeders, mussels can uptake QDs from seawater, where aggregation/agglomeration behaviour of QDs changes its uptake route, decreases its bioavailability and induces lower Cd accumulation in mussel tissues compared to dissolved Cd (Chapters 2-3). Similar results were observed for other metal-based ENPs (Chapter 1; Table 1.1). QDs aggregates/agglomerates are uptaken by mussels mainly by endocytosis or phagocytosis in the digestive system, while individual particle or dissolved Cd is mainly uptaken by the gills. QDs are transferred from the digestive system to the hemolymph, following their systemically distribution in mussel tissues (Chapter 2; Fig. 8.1).

A similar Cd tissue distribution was observed in *M. galloprovincialis* exposed to QDs and dissolved Cd (digestive gland > gills > remaining tissues > hemolymph) (Fig. 2.4), while the accumulation kinetics is Cd form dependent (Chapter 2; Fig 2.4; Table 2.1). Digestive gland has an important role in storage, metabolism and detoxification of both Cd forms, while gills have similar functions for dissolved Cd. On the other hand, hemolymph plays several functions in the transport, distribution and regulation of both Cd forms, wherein transport of QDs may be limited by circulating hemocytes number (Chapters 2 - 3; Fig. 8.1). Furthermore, the permanence of QDs in the mussel digestive system facilitates their digestion and dissolution and lead to the release of free Cd ions in the digestive system. Similarly, the uptake of ENPs aggregates by the digestive system following its storage and/or tissue distribution by transport *via* hemolymph were reported for different bivalve species exposed to ENPs (Chapter 1; Table 1.1).

Furthermore, no significant QDs elimination by mussels via biodeposits occurred during the accumulation period, while the Cd concentration in feces and pseudofeces from the bottom of the exposure tanks was associated to QDs aggregation in seawater (Chapter 2).

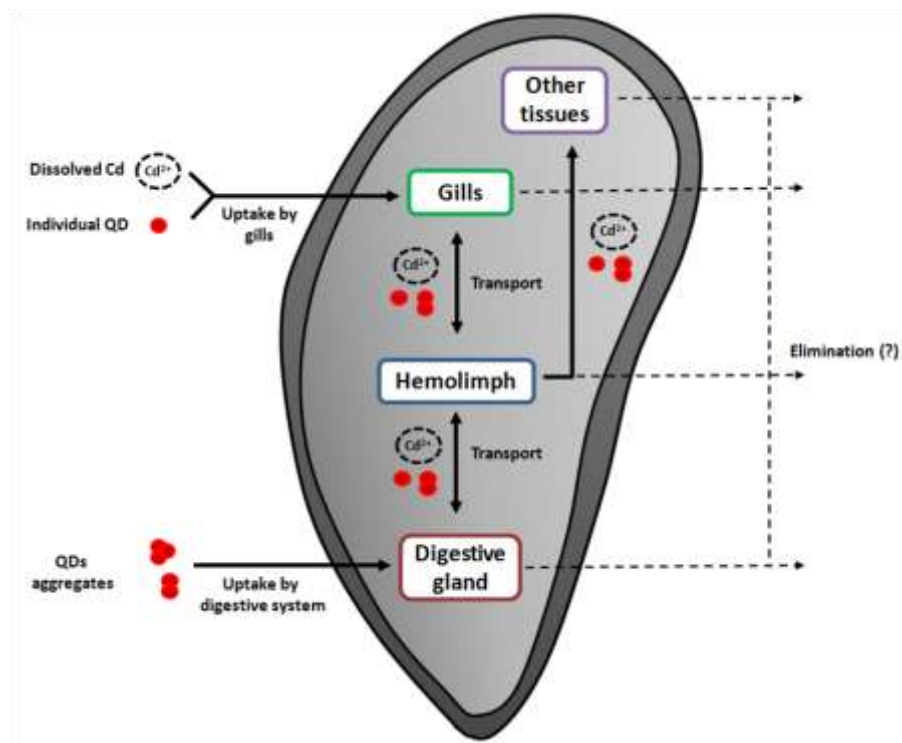


Figure 8.1. General scheme illustrating routes for uptake, tissue distribution and elimination of quantum dots (QDs) and its dissolved counterpart in the marine mussel *M. galloprovincialis*.

8.1.5. Subcellular partitioning and metabolism

The subcellular distribution in *M. galloprovincialis* are important strategies for accumulation and detoxification of QDs and are Cd form and tissue dependent, with high Cd accumulation in the digestive gland compared to the gills (Figs. 4.1, 4.2A-B) (Chapter 4). In both mussel tissues, the metabolism and toxicity of QDs was related to an increase in Cd concentration in the biologically active metal form (BAM), while dissolved Cd was mainly associated to the biologically detoxified metal form (BDM), indicating that QDs are slowly detoxified when compared to dissolved Cd. Thus, QDs in the BAM form is potentially toxic for mussel tissues due to the high reactivity and capability to induce ROS production and oxidative stress. The subcellular partitioning

kinetics showed that the mitochondria, nucleus and lysosomes are potential subcellular targets of CdTe QDs toxicity in mussel tissues (Chapter 4), such as previously indentified in mammal cells (Li et al., 2011). Although the metal subcellular partitioning have been investigated in the goldfish *C. auratus* exposed to ZnO NPs (30 nm; 2 mg L⁻¹; 30 days) (Fan et al., 2013) and in the ragworm *N. diversicolor* exposed to Cu NPs (< 100 nm; 150 µg Cu g⁻¹ d. w. sediment; 10 days) (Thit et al., 2015), to the best of our knowledge, this is the first study of subcellular metal partitioning in bivalve species exposed to metal-based ENPs.

QDs have higher retention rate in mussel tissues and were not eliminated after 50 days of depuration, wherein no Cd levels were detected in biodeposits, confirming that QDs accumulated in mussel tissues are not eliminated through the feces during depuration period. The estimated $t_{1/2}$ of CdTe QDs for the subcellular fractions of mussel gills and digestive gland ($t_{1/2} > 50$ d; Table 4.2) is longer than for other ENPs in bivalves, such as Ag NPs (10 - 80 nm; 110 - 151 ng L⁻¹; accumulation 12 h, depuration 8 weeks) in scallop *C. islandica* whole soft tissues ($t_{1/2}$: 1.4 - 4.3 days and 17 - 50 days for fast and slow compartments) (Al-Sid-Cheikh et al., 2013) and CuO NPs (< 100 nm; 200 µg g⁻¹ d. w. sediment; accumulation 35 days, depuration 15 days) for marine clam *M. balthica* whole soft tissues ($t_{1/2} > 15$ d) (Dai et al., 2013), indicating higher availability of QDs for trophic transfer and risks to human health due to consumption of QDs-contaminated mussels.

8.1.6. Mode of action and toxicity

The MoA and toxicity of CdTe QDs in the marine mussel *M. galloprovincialis* are tissue and exposure time dependent and involve intra- and extra-cellular ROS production, changes in antioxidant enzymes activity, immune response and DNA damage, as well as cell-type replacement in digestive tubules and differential protein expression (Fig. 8.2; Chapters 2 - 7). Similarly, toxic effects of several metal-based ENPs in bivalve species have been directly or indirectly related to ROS production and oxidative stress, which induced immunotoxic and genotoxic effects (Chapter 1; Table 1.1). Tissue specific responses were observed in the marine mussel *M. galloprovincialis* exposed to both Cd forms (Chapter 5), indicating differential biophysicochemical interaction of QDs and antioxidant capacity in the gills and digestive gland. These

differential tissue responses agree with previous studies with *M. galloprovincialis* exposed to CuO NPs (31 nm; 10 $\mu\text{g L}^{-1}$; 15 days) (Gomes et al., 2012), *C. virginica* exposed to Ag NPs (20 - 30 nm; 0.002 - 20 $\mu\text{g L}^{-1}$; 48 h) (McCarthy et al., 2013) and *C. gigas* exposed to ZnO NPs (31.7 nm; 50 $\mu\text{g L}^{-1}$ - 50 mg L^{-1} ; 96 h) (Trevisan et al., 2014), confirming that this approaches provides additional knowledge on MoA and toxicity of ENMs in bivalves species.

CdTe QDs exposure induced ROS production, antioxidant enzymes alterations and oxidative stress in *M. galloprovincialis* in Cd form and tissue dependent pattern, wherein gills showed more pronounced enzymatic activities changes compared to the digestive gland (Chapter 5; Fig. 5.4). Alterations in the antioxidant defense system were higher in QDs-exposed mussels compared to their dissolved counterpart, indicating that QDs-related oxidative stress is not only due to the release of Cd ions, but also associated to nano-specific properties and ROS generated from them (Chapter 5; Figs. 5.4, 8.2). SOD, GPx and GST activities were the most sensitive biomarkers of oxidative stress induced by CdTe QDs in marine mussels (Fig. 8.2). As tissue-specific biochemical responses, total GPx activity in the gills increased and decreased in QDs and dissolved Cd exposure, respectively, while in the digestive gland their activity increased during the exposure period (Fig. 5.4A-B). Furthermore, Se-D GPx showed a similar pattern of the SOD activity, which was considered as the more sensitive enzyme of defence responding to Cd-based QDs compared to Se-I GPx (Fig. 5.2).

The lower LPO levels observed in mussel tissues after exposure to QDs (Chapter 4; Fig. 4.8) may be related to GST activity response (Chapter 5; Fig. 5.1G-H) and its roles in the metabolism of compounds derived from LPO, which reduced toxic effects of QDs at membrane levels. Moreover, MTs response in mussels exposed to Cd-based QDs is, like for dissolved Cd, tissue-specific, with higher MTs levels in the digestive gland compared to the gills (Chapter 2). In opposite to dissolved Cd, MT response in mussels exposed to QDs indicated its function as a scavenging for free radicals limiting the effects of hydroxyl and superoxide radical by scavenging them and inducing the SOD activity in the mussel gills more than a detoxification mechanism. The MoA of Cd-based QDs in *M. galloprovincialis* is mainly mediated by ROS production and oxidative stress, as reported for others micro-organisms, invertebrates and fish species (revised in the Chapter 1; Tables 1.2 - 1.5).

The immune system of mussels *M. galloprovincialis* is a significant target for the QDs toxicity (Chapters 3 and 6). Immunotoxic effects of QDs in mussels are mediated by a decrease in LMS, changes of circulating hemocytes types and DNA damage, while no effects on hemocytes density, cell viability and cytogenetic parameters (frequency of hemocytes with MN or buds and binucleated hemocytes) were observed (Chapter 3), indicating that they are immunocytotoxic and genotoxic, but not cytogenotoxic (Fig. 8.2). On the other hand, the dissolved Cd form is the most cytotoxic and cytogenotoxic on *Mytilus* hemocytes. Furthermore, a decrease in frequency of circulating eosinophils was detected only in mussels exposed to QDs (Chapter 3), which may be related to phagocytosis of QDs by this cell type and to the significant increase in the haemocytic infiltration observed in the digestive gland of QDs-exposure mussels (Chapter 6), confirming the role of hemocytes in the transport, tissue distribution, metabolism and homeostase regulation in marine mussels exposed to Cd-based QDs. These effects on the immune system of mussels exposed to both Cd forms could lead to a possible increase in individual and population susceptibility to diseases or adaptation to environmental stress conditions.

CdTe QDs induced higher DNA damage in *M. galloprovincialis* hemocytes when compared to other metal-based ENPs (e. g. 42 nm Ag NPs and 31 nm CuO NPs) at the same concentration and exposure time ($10 \mu\text{g L}^{-1}$; 14 - 15 days) (Gomes et al. 2011, 2012, 2013a,b, 2014). Similar genotoxic effects of Cd-based QDs were also observed in *Mytilus* spp. hemocytes after *in vitro* exposure to CdS QDs (4 nm; 10 mg L^{-1} ; 4 h) (Munari et al., 2014) and CdS QDs (5 nm; $0.001 - 100 \text{ mg L}^{-1}$; 24 h) (Katsumiti et al., 2014a), in the freshwater mussel *E. complanata* exposed to CdTe QDs ($1.6 - 8 \text{ mg L}^{-1}$; 24 h) (Gagné et al., 2008), in annelids *E. fetida* and *H. diversicolor* exposed to CdSe/ZnS QDs (5.9 nm; $0.001 - 1 \text{ ng g}^{-1} \text{ w.}$; 24 h) (Saez et al., 2014), in *O. mykiss* hepatocytes after *in vitro* exposed to cysteamine-CdTe QDs ($0.4 - 250 \mu\text{g mL}^{-1}$; 48 h) (Gagné et al., 2008) and in *D. rerio* exposed to MPA-CdTe QDs (3.4 nm; $50 - 500 \mu\text{g L}^{-1}$; 24 h) (Tang et al., 2013a), confirming the potential genotoxicity of Cd-based QDs at different trophic levels. On the other hand, the mechanism of genotoxicity of QDs remains less known and can be related to their direct interaction with DNA or nuclear proteins, intracellular release of Cd^{2+} ions from the QDs core and/or DNA strand-breaks through indirect mechanism by ROS production and oxidative stress (Fig. 8.2) (Gagné et al., 2008; Vincent- Hubert et al., 2011; Aye et al., 2013; Tang et al.,

2013; Rocha et al., 2014) (Chapter 4). The present results indicated that genotoxic effects of QDs in *M. galloprovincialis* were mainly related to ROS generation and oxidative stress, but the interaction of QDs with nuclear compounds and the QDs dissolution followed by the release of Cd^{2+} should be considered because Cd accumulation in the mussel subcellular fraction (IF) containing nucleus was observed after QDs exposure (Fig. 4.2A-C; Table 4.2; Chapter 4).

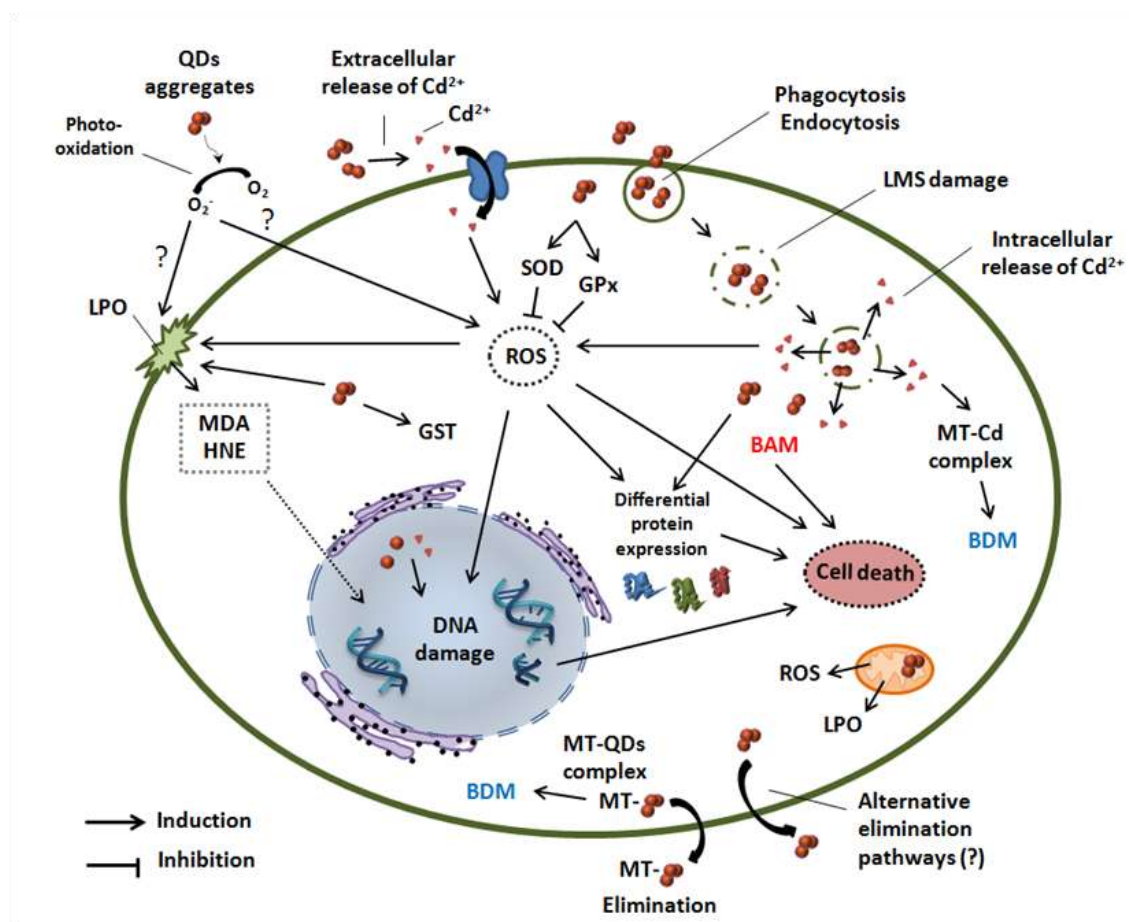


Figure 8.2. General scheme illustrating the mode of action (MoA) and toxicity of CdTe QDs in marine mussels *M. galloprovincialis*. QDs dissolution induces extracellular release of Cd^{2+} , which penetrate the cell by protein-mediated transport and induce oxidative stress by ROS production. Photo-oxidation of QDs can also induce ROS production. Uptake of QDs aggregates by endocytosis decrease lysosomal membrane stability (LMS), release Cd^{2+} , induce intracellular ROS production, increase SOD, CAT and GST activities and promote differential protein expression. Both Cd forms induce lipid peroxidation (LPO) resulting in malondialdehyde (MDA) and 4-hydroxyalkenals (HNE) production. Subcellular partitioning is linked to biologically active metal (BAM) and to biologically detoxified metal (BDM) forms. QDs-related oxidative stress increase DNA damage and may lead to cellular death. QDs elimination may occur via metallothionein (MT) induction and/or via alternative elimination pathways.

8.2. Conclusions

An overview of the final conclusions is summarized as follows:

- The marine mussel *M. galloprovincialis* is an important target for the ecotoxicity of Cd-based QDs and represents a suitable model for characterizing the impact of metal-based ENPs in marine environment.
- The environmental risk assessment (ERA) of QDs in marine environment is dependent on their behaviour and fate in seawater, which strongly influence their bioavailability, uptake, accumulation and toxicity in marine mussels.
- QDs are less bioavailable in seawater than in freshwater and Cd accumulation is lower in mussels *M. galloprovincialis* when compared to their dissolved counterpart.
- The uptake, accumulation, metabolism, toxicity and detoxification of QDs and dissolved Cd in *M. galloprovincialis* are mediated by different pathways.
- QDs aggregates are uptaken by mussels mainly by endocytosis in the digestive system and induce higher proportion of Cd in the BAM form, while dissolved Cd is mainly uptaken by the gills and remains mainly in the BDM form in mussel tissues.
- Main mechanisms of toxicity of CdTe QDs in marine mussels involve intra- and extra-cellular ROS production, changes in antioxidant enzymes activities, immune response induction and DNA damage.
- Tissue-specific sensibility is involved in mussel responses to both Cd forms, wherein CdTe QDs is the more pro-oxidant Cd form and the gills is the more susceptible tissue to QDs-related oxidative stress.
- In gills, QDs toxicity is related to changes in SOD, GST, total GPx, Se-I GPx and Se-D GPx activities, while dissolved Cd is associated with total Cd concentration, CAT activity and exposure time. In opposition, the digestive gland response to QDs was related to SOD activity and exposure time, while the response to dissolved Cd was associated to changes in GST, total GPx, Se-I GPx and Se-D activities.
- The immunocytotoxicity and genotoxicity of CdTe QDs are time dependent and not directly related to Cd accumulation in mussel tissues, indicating different mechanisms compared to their dissolved counterpart.

- QDs exposure induces higher frequency of haemocytic infiltrations and granulocytomas in the digestive gland compared to dissolved Cd, confirming their nano-specific effects in the immune response of mussels.
- The $R_{Bas/Dig}$ is the most sensitive tissue-level biomarker to QDs effects, indicating that the cell-type replacement in digestive tubules of mussels is an important strategy for the maintenance of homeostasis in response to QDs.
- QDs induce different protein expression profiles in the digestive gland of mussels when compared to dissolved Cd and unexposed mussels, indicating potential molecular biomarkers to QDs exposure.
- Accumulation and detoxification processes of Cd-based QDs in mussel tissues are mediated by subcellular partitioning and MT induction, where lower detoxification occurs compared to their dissolved counterpart ($t_{1/2} > 50$ days), indicating their potential trophic transfer and risks to human health due to consumption of QDs-contaminated mussels.
- The multibiomarker assessment represents a sensitive tool to assess the ecotoxicity of QDs in marine mussels, wherein subcellular partitioning (BAM form) and biomarkers of the immunotoxicity (DCC and DNA damage), oxidative stress (SOD, GPx and GST) and tissue-level response ($R_{Bas/Dig}$ and frequency of haemocytic infiltrations and granulocytomas) are related to nano-specific properties of QDs.
- This multibiomarker approach in the marine mussel *M. galloprovincialis* could be incorporated as complementary tools in biomonitoring programmes to assess the risk associated with the presence of metal-based ENPs in the marine environment.

8.3. Future perspectives

Taking in account all the results of this thesis, some key points are suggested for future research to better understand the ecotoxicity and environmental risk of metal-based ENPs in the marine environment:

- Assessment of toxicity of Cd-based QDs to developing embryos and to juveniles of marine mussels.
- Assessment of ontogenesis and cell differentiation of different hemocytes types in marine mussels and their roles in the immunotoxicity induced by ENP exposure.
- Molecular characterization and functional analysis of antioxidant enzymes isoforms from marine mussels exposed to ENPs to understand the tissue-specific susceptibility to oxidative stress related to nano-specific properties.
- Assessment of cell death (apoptosis and necrosis) in mussel tissues after exposure to QDs to confirm the MoA, toxicity and cell-type replacement mechanism.
- Applications of transcriptomics and metabolomics technologies to describe gene expression changes and metabolic profiles in mussels exposed to metal-based ENPs.
- Assessment of ecotoxicity of Cd-based QDs in other relevant environmentally conditions, such as multispecies exposures and mesocosms.

REFERENCES

REFERENCES

- Ali, D., Alarifi, S., Kumar, S., Ahamed, M., Siddiqui, M.A., 2012. Oxidative stress and genotoxic effect of zinc oxide nanoparticles in freshwater snail *Lymnaea luteola* L. *Aquatic Toxicology* 124-125, 83-90.
- Allison, J.D., Brown, D.S., 1999. Novo-Grada MINTEQA2/PRODEFA2, A geochemical assessment model for environmental systems, version 3.0. 3rd edn. In Office of Research and Development U.S. Environmental Protection Agency, Athens.
- Almeida, C., Pereira, C., Gomes, T., Bebianno, M.J., Cravo, A., 2011. DNA damage as a biomarker of genotoxic contamination in *Mytilus galloprovincialis* from the south coast of Portugal. *Journal of Environmental Monitoring* 13, 2559-2567.
- Al-Sid-Cheikh, M., Rouleau, C., Pelletier, E., 2013. Tissue distribution and kinetics of dissolved and nanoparticulate silver in Iceland scallop (*Chlamys islandica*). *Marine Environmental Research* 86, 21-28.
- Al-Subiai, S.N., Arlt, V.M., Frickers, P.E., Readman, J.W., Stolpe, B., Lead, J.R., Moody, A.J., Jha, A.N., 2012. Merging nano-genotoxicology with ecogenotoxicology: an integrated approach to determine interactive genotoxic and sub-lethal toxic effects of C₆₀ fullerenes and fluoranthene in marine mussels, *Mytilus* sp. *Mutation Research* 745, 92-103.
- Amachree, D., Moody, A.J., Handy, R.D., 2013. Comparison of intermittent and continuous exposures to cadmium in the blue mussel, *Mytilus edulis*: accumulation and sub-lethal physiological effects. *Ecotoxicology and Environmental Safety* 95, 19-26.
- Ambrosone, A., Mattera, L., Marchesano, V., Quarta, A., Susa, A.S., Tino, A., Rogach, A.L., Tortiglione, C., 2012. Biomaterials Mechanisms underlying toxicity induced by CdTe quantum dots determined in an invertebrate model organism. *Biomaterials* 33, 1991-2000.
- Atif, F., Kaur, M., Yousuf, S., Raisuddin, S., 2006. *In vitro* free radical scavenging activity of hepatic metallothionein induced in an Indian freshwater fish, *Channa punctata* Bloch. *Chemico-Biological Interactions* 162, 172-180.
- Aye, M., Di Giorgio, C., Berque-Bestel, I., Aime, A., Pichon, B.P., Jammes, Y., Barthélémy, P., De Méo, M., 2013. Genotoxic and mutagenic effects of lipid-coated CdSe/ZnS quantum dots. *Mutation Research* 750, 129-138.
- Baalousha, M., Lead, J.R., 2013. Characterization of natural and manufactured nanoparticles by atomic force microscopy: Effect of analysis mode, environment and sample preparation. *Colloids and Surfaces A: Physicochemical and Engineering Aspects* 419, 238-247.
- Baalousha, M., Manciuola, A., Cumberland, S., Kendall, K., Lead, J.R., 2008. Aggregation and surface properties of iron oxide nanoparticles: influence of pH and natural organic matter. *Environmental Toxicology and Chemistry* 27, 1875-1882.
- Baker, T.J., Tyler, C.R., Galloway, T.S., 2014. Impacts of metal and metal oxide nanoparticles on marine organisms. *Environmental Pollution* 186, 257-271.
- Balbi, T., Smerilli, A., Fabbri, R., Ciacci, C., Montagna, M., Grasselli, E., Brunelli, A., Pojana, G., Marcomini, A., Gallo, G., Canesi, L., 2014. Co-exposure to n-TiO₂ and Cd²⁺ results in interactive effects on biomarker responses but not in increased toxicity in the marine bivalve *M. galloprovincialis*. *Science of the Total Environment* 493C, 355-364.
- Barmo, C., Ciacci, C., Canonico, B., Fabbri, R., Cortese, K., Balbi, T., Marcomini, A., Pojana, G., Gallo, G., Canesi, L., 2013. *In vivo* effects of n-TiO₂ on digestive gland

- and immune function of the marine bivalve *Mytilus galloprovincialis*. *Aquatic Toxicology* 132-133C, 9-18.
- Baun, A., Hartmann, N.B., Grieger, K., Kusk, K.O., 2008. Ecotoxicity of engineered nanoparticles to aquatic invertebrates: a brief review and recommendations for future toxicity testing. *Ecotoxicology* 17, 387-395.
- Bebianno, M.J., Langston, W.J., 1989. Quantification of metallothioneins in marine invertebrates using differential pulse polarography. *Portugaliae Electrochimica Acta* 7, 59- 64.
- Bebianno, M.J., Langston, W.J., 1993. Turnover rate of metallothionein and cadmium in *Mytilus edulis*. *Biometals* 6, 239-44.
- Bebianno, M.J., Nott, J.A., Langston, W.S., 1993. Cadmium metabolism in the clam (*Ruditapes decussatus*): the role of metallothioneins. *Aquatic Toxicology* 27, 315-334.
- Bernet, D., Schmidt, H., Meier, W., Wahli, T., 1999. Histopathology in fish: proposal for a protocol to assess aquatic pollution 25-34.
- Blanco-Canosa, J.B., Wu, M., Susumu, K., Petryayeva, E., Jennings, T.L., Dawson, P.E., Algar, W.R., Medintz, I.L., 2014. Recent progress in the bioconjugation of quantum dots. *Coordination Chemistry Reviews* 263-264, 101-137.
- Blickley, T.M., Matson, C.W., Vreeland, W.N., Rittschof, D., Di Giulio, R.T., McClellan-Green, P.D., 2014. Dietary CdSe/ZnS quantum dot exposure in estuarine fish: bioavailability, oxidative stress responses, reproduction, and maternal transfer. *Aquatic Toxicology* 148, 27-39.
- Blinova, I., Ivask, A., Heinlaan, M., Mortimer, M., Kahru, A., 2010. Ecotoxicity of nanoparticles of CuO and ZnO in natural water. *Environmental Pollution* 158, 41-47.
- Blum, H., Biere, H., Gross, H.J., 1987. Improved silver staining of plant proteins, RNA and DNA in polyacrylamide gels. *Electrophoresis* 8 93-99.
- Bolognesi, C., Fenech, M., 2012. Mussel micronucleus cytome assay. *Nature Protocols* 7, 1125-1137.
- Bolognesi, C., Frenzilli, G., Lasagna, C., Perrone, E., Roggieri, P., 2004. Genotoxicity biomarkers in *Mytilus galloprovincialis*: wild versus caged mussels. *Mutation Research* 552, 153-62.
- Borchardt, T., 1983. Influence of food quantity on the kinetics of cadmium uptake and loss via food and seawater in *Mytilus edulis*. *Marine Biology* 76, 67-76.
- Bouldin, J.L., Ingle, T.M., Sengupta, A., Alexander, R., Hannigan, R.E., Buchanan, R.A., 2008. Aqueous toxicity and food chain transfer of Quantum dots in freshwater algae and *Ceriodaphnia dubia*. *Environmental Toxicology and Chemistry* 27, 1958-63.
- Bradford, M.M., 1976. A rapid and sensitive method for the quantitation of microgram quantities of protein utilizing the principle of protein-dye binding. *Analytical Biochemistry* 72, 248-254.
- Brar, S.K., Verma, M., Tyagi, R.D., Surampalli, R.Y., 2010. Engineered nanoparticles in wastewater and wastewater sludge - evidence and impacts. *Waste Management* 30, 504-520.
- Browne, M.A., Dissanayake, A., Galloway, T.S., Lowe, D.M., Thompson, R.C., 2008. Ingested microscopic plastic translocates to the circulatory system of the mussel, *Mytilus edulis* (L.). *Environmental Science & Technology* 42, 5026-5031.
- Bruneau, A., Fortier, M., Gagne, F., Gagnon, C., Turcotte, P., Tayabali, A., Davis, T.L., Auffret, M., Fournier, M., 2013. Size distribution effects of cadmium tellurium

- quantum dots (CdS/CdTe) immunotoxicity on aquatic organisms. *Environmental Science: Processes & Impacts* 15, 596-607.
- Buffet, P.-E., Amiard-Triquet, C., Dybowska, A., Risso-de Faverney, C., Guibbolini, M., Valsami-Jones, E., Mouneyrac, C., 2012. Fate of isotopically labeled zinc oxide nanoparticles in sediment and effects on two endobenthic species, the clam *Scrobicularia plana* and the ragworm *Hediste diversicolor*. *Ecotoxicology and Environmental Safety* 84, 191-198.
- Buffet, P.-E., Pan, J.F., Poirier, L., Amiard-Triquet, C., Amiard, J.-C., Gaudin, P., Faverney, C.R. De, Guibbolini, M., Gilliland, D., Valsami-Jones, E., Mouneyrac, C., 2013. Biochemical and behavioural responses of the endobenthic bivalve *Scrobicularia plana* to silver nanoparticles in seawater and microalgal food. *Ecotoxicology and Environmental Safety* 89, 117-124.
- Buffet, P.-E., Poirier, L., Zalouk-Vergnoux, A., Lopes, C., Amiard, J.-C., Gaudin, P., Risso-de Faverney, C., Guibbolini, M., Gilliland, D., Perrein-Ettajani, H., Valsami-Jones, E., Mouneyrac, C., 2014b. Biochemical and behavioural responses of the marine polychaete *Hediste diversicolor* to cadmium sulfide quantum dots (CdS QDs): waterborne and dietary exposure. *Chemosphere* 100, 63-70.
- Buffet, P.-E., Richard, M., Caupos, F., Vergnoux, A., Perrein-Ettajani, H., Luna-Acosta, A., Akcha, F., Amiard, J.-C., Amiard-Triquet, C., Guibbolini, M., Risso-De Faverney, C., Thomas-Guyon, H., Reip, P., Dybowska, A., Berhanu, D., Valsami-Jones, E., Mouneyrac, C., 2013a. A mesocosm study of fate and effects of CuO nanoparticles on endobenthic species (*Scrobicularia plana*, *Hediste diversicolor*). *Environmental Science & Technology* 47, 1620-1628.
- Buffet, P.-E., Tankoua, O.F., Pan, J.-F., Berhanu, D., Herrenknecht, C., Poirier, L., Amiard-Triquet, C., Amiard, J.-C., Bérard, J.-B., Risso, C., Guibbolini, M., Roméo, M., Reip, P., Valsami-Jones, E., Mouneyrac, C., 2011. Behavioural and biochemical responses of two marine invertebrates *Scrobicularia plana* and *Hediste diversicolor* to copper oxide nanoparticles. *Chemosphere* 84, 166-174.
- Buffet, P.-E., Zalouk-Vergnoux, A., Châtel, A., Berthet, B., Métais, I., Perrein-Ettajani, H., Poirier, L., Luna-Acosta, A., Thomas-Guyon, H., Risso-de Faverney, C., Guibbolini, M., Gilliland, D., Valsami-Jones, E., Mouneyrac, C., 2013b. A marine mesocosm study on the environmental fate of silver nanoparticles and toxicity effects on two endobenthic species: The ragworm *Hediste diversicolor* and the bivalve mollusc *Scrobicularia plana*. *Science of the Total Environment* 470-471C, 1151-1159.
- Buffet, P.-E., Zalouk-Vergnoux, A., Poirier, L., Lopes, C., Risso-de-Faverney, C., Guibbolini, M., Gilliland, D., Perrein-Ettajani, H., Valsami-Jones, E., Mouneyrac, C., 2015. Cadmium sulfide quantum dots induce oxidative stress and behavioral impairments in the marine clam *Scrobicularia plana*. *Environmental Toxicology and Chemistry* 9999, 1-6.
- Burgeot, T., Woll, S., Galgani, F., 1996. Evaluation of the micronucleus test on *Mytilus galloprovincialis* for monitoring applications along French coasts. *Marine Pollution Bulletin*, 32 (1), 39-46.
- Cajaraville M.P., Díez, G., Marigómez, J.A., Angulo, E., 1990. Responses of basophilic cells of the digestive gland of mussels to petroleum hydrocarbon exposure. *Diseases of Aquatic Organisms* 9, 221-228.
- Cajaraville, M.P., Marigómez, J.A., Angulo, E., 1992. Comparative effects of the water accommodated fraction of three oils on mussels - 1. Survival, growth and gonad development. *Comparative Biochemistry and Physiology* 102C, 103-112.

- Calvin, S., Luo, S.X., Caragianis-Broadbridge, C., McGuinness, J.K., Anderson, E., Lehman, A., Wee, K.H., Morrison, S.A., Kurihara, L.K., 2005. Comparison of extended x-ray absorption fine structure and Scherrer analysis of x-ray diffraction as methods for determining mean sizes of polydisperse nanoparticles. *Applied Physics Letters* 87, 233102.
- Calvo-Ugarteburu, G., Saez, V., McQuaid, C.D., Angulo, E., 1995. Validation of a planimetric procedure to quantify stress in *Littorina littorea* (Gastropoda: Mollusca): is it independent of the reproductive cycle? *Hydrobiologia* 309, 37-44.
- Campana, O., Taylor, A.M., Blasco, J., Maher, W.A., Simpson, S.L., 2015. Importance of subcellular metal partitioning and kinetics to predicting sublethal effects of copper in two deposit-feeding organisms. *Environmental Science & Technology* 49, 1806-14.
- Campbell, P.G.C., Giguère, A., Bonneris, E., Hare, L., 2005. Cadmium-handling strategies in two chronically exposed indigenous freshwater organisms--the yellow perch (*Perca flavescens*) and the floater mollusc (*Pyganodon grandis*). *Aquatic Toxicology* 72, 83-97.
- Campos, A., Tedesco, S., Vasconcelos, V., Cristobal, S., 2012. Proteomic research in bivalves: Towards the identification of molecular markers of aquatic pollution. *Journal of Proteomics* 75, 4346-4359.
- Canesi, L., Ciacci, C., Betti, M., Fabbri, R., Canonico, B., Fantinati, A., Marcomini, A., Pojana, G., 2008. Immunotoxicity of carbon black nanoparticles to blue mussel hemocytes. *Environment International* 34, 1114-1119.
- Canesi, L., Corsi, I., 2016. Effects of nanomaterials on marine invertebrates. *Science of the Total Environment*. 1-8. doi:10.1016/j.scitotenv.2016.01.085.
- Canesi, L., Ciacci, C., Fabbri, R., Marcomini, A., Pojana, G., Gallo, G., 2012. Bivalve molluscs as a unique target group for nanoparticle toxicity. *Marine Environment Research* 76, 16-21.
- Canesi, L., Ciacci, C., Vallotto, D., Gallo, G., Marcomini, A., Pojana, G., 2010a. *In vitro* effects of suspensions of selected nanoparticles (C₆₀ fullerene, TiO₂, SiO₂) on *Mytilus* hemocytes. *Aquatic Toxicology* 96, 151-158.
- Canesi, L., Fabbri, R., Gallo, G., Vallotto, D., Marcomini, A., Pojana, G., 2010b. Biomarkers in *Mytilus galloprovincialis* exposed to suspensions of selected nanoparticles (Nano carbon black, C₆₀ fullerene, Nano-TiO₂, Nano-SiO₂). *Aquatic Toxicology* 100, 168-177.
- Canesi, L., Frenzilli, G., Balbi, T., Bernardeschi, M., Ciacci, C., Corsolini, S., Della Torre, C., Fabbri, R., Faleri, C., Focardi, S., Guidi, P., Kočan, A., Marcomini, A., Mariottini, M., Nigro, M., Pozo-Gallardo, K., Rocco, L., Scarcelli, V., Smerilli, A., Corsi, I., 2014. Interactive effects of n-TiO₂ and 2,3,7,8-TCDD on the marine bivalve *Mytilus galloprovincialis*. *Aquatic Toxicology* 153, 53-65.
- Canesi, L., Procházková, P., 2014. The invertebrate immune system as a model for investigating the environmental impact of nanoparticles. *Nanoparticles and the Immune System: Safety and Effects*, 1-21.
- Canesi, L., Viarengo, A., Leonzio, C., Filippelli, M., Gallo, G., 1999. Heavy metals and glutathione metabolism in mussel tissues. *Aquatic Toxicology* 46, 67-76.
- Carella, F., Feist, S.W., Bignell, J.P., De Vico, G., 2015. Comparative pathology in bivalves: Aetiological agents and disease processes. *Journal of Invertebrate Pathology* 131, 107-120.
- Casals, E., Vázquez-Campos, S., Bastús, N.G., Puentes, V., 2008. Distribution and potential toxicity of engineered inorganic nanoparticles and carbon nanostructures in biological systems. *TrAC Trends in Analytical Chemistry* 27, 672-683.

- CEN, 2016. Available from <http://www.cen.eu/work/areas/Nanotech/Pages/default.aspx>
- Chae, Y.J., Pham, C.H., Lee, J., Bae, E., Yi, J., Gu, M.B., 2009. Evaluation of the toxic impact of silver nanoparticles on Japanese medaka (*Oryzias latipes*). *Aquatic Toxicology* 94, 320-7.
- Chalew, A.T.E., Galloway, J.F., Graczyk, T.K., 2012. Pilot study on effects of nanoparticle exposure on *Crassostrea virginica* hemocyte phagocytosis. *Marine Pollution Bulletin* 64, 2251-2253.
- Chalmers, N.I., Palmer, R.J., Du-Thumm, L., Sullivan, R., Shi, W., Kolenbrander, P.E., 2007. Use of quantum dot luminescent probes to achieve single-cell resolution of human oral bacteria in biofilms. *Applied and Environmental Microbiology* 73, 630-636.
- Chandurvelan, R., Marsden, I.D., Gaw, S., Glover, C.N., 2013. Biochemical biomarker responses of green-lipped mussel, *Perna canaliculus*, to acute and subchronic waterborne cadmium toxicity. *Aquatic Toxicology*, 140-141, 303-13.
- Chen, K.L., Elimelech, M., 2007. Influence of humic acid on the aggregation kinetics of fullerene (C₆₀) nanoparticles in monovalent and divalent electrolyte solutions. *Journal of Colloid and Interface Science* 309, 126-34.
- Cho, E.J., Holback, H., Liu, K.C., Abouelmagd, S.A., Park, J., Yeo, Y., 2013. Nanoparticle characterization: state of the art, challenges, and emerging technologies. *Molecular Pharmacology* 10, 2093-2110.
- Chora, S., Bebianno, M.J., Roméo, M. Analysis of proteins from marine molluscs. In: Sheehan, D., Tyther, R. (Eds). *Two-dimensional Electrophoresis Protocols*, 519, pp.197-204.
- Ciacchi, C., Canonico, B., Bilaničová, D., Fabbri, R., Cortese, K., Gallo, G., Marcomini, A., Pojana, G., Canesi, L., 2012. Immunomodulation by different types of N-oxides in the hemocytes of the marine bivalve *Mytilus galloprovincialis*. *PLoS One* 7, e36937.
- Cleveland, D., Long, S.E., Pennington, P.L., Cooper, E., Fulton, M.H., Scott, G.I., Brewer, T., Davis, J., Petersen, E.J., Wood, L., 2012. Pilot estuarine mesocosm study on the environmental fate of silver nanomaterials leached from consumer products. *Science of the Total Environment* 421-422, 267-272.
- Contreras, E.Q., Cho, M., Zhu, H., Puppala, H.L., Escalera, G., Zhong, W., Colvin, V.L., 2013. Toxicity of quantum dots and cadmium salt to *Caenorhabditis elegans* after multigenerational exposure. *Environmental Science & Technology* 47, 1148-54.
- Conway, J.R., Hanna, S.K., Lenihan, H.S., Keller, A.A., 2014. Effects and Implications of Trophic Transfer and Accumulation of CeO₂ Nanoparticles in a Marine Mussel. *Environmental Science & Technology* 48, 1517-1524.
- Corsi, I., Cherr, G.N., Lenihan, H.S., Labille, J., Hasselov, M., Canesi, L., Dondero, F., Frenzilli, G., Hristozov, D., Puentes, Â.V., Torre, C. Della, Pinsino, A., Libralato, G., Marcomini, A., Sabbioni, Â.E., Matranga, V., 2014. Common Strategies and Technologies for the Ecosafety Assessment and Design of Nanomaterials Entering the Marine Environment. *ACS Nano* 8, 9694-9709.
- Costa, P.M., Carreira, S., Costa, M.H., Caeiro, S., 2013. Development of histopathological indices in a commercial marine bivalve (*Ruditapes decussatus*) to determine environmental quality. *Aquatic Toxicology* 126, 442-54.
- Costa, P.M., Diniz, M.S., Caeiro, S., Lobo, J., Martins, M., Ferreira, A.M., Caetano, M., Vale, C., DelValls, T.Á., Costa, M.H., 2009. Histological biomarkers in liver and gills of juvenile *Solea senegalensis* exposed to contaminated estuarine sediments: A weighted indices approach. *Aquatic Toxicology* 92, 202-212.

- Couleau, N., Techer, D., Pagnout, C., Jomini, S., Foucaud, L., Laval-Gilly, P., Falla, J., Bennasroune, A., 2012. Hemocyte responses of *Dreissena polymorpha* following a short-term *in vivo* exposure to titanium dioxide nanoparticles: preliminary investigations. *Science of the Total Environment* 438, 490-497.
- Coulon, J., Thouvenin, I., Aldeek, F., Balan, L., Schneider, R., 2010. Glycosylated quantum dots for the selective labelling of *Kluyveromyces bulgaricus* and *Saccharomyces cerevisiae* yeast strains. *Journal of Fluorescence* 20, 591-597.
- Cravo, A., Lopes, B., Serafim, A., Company, R., Barreira, L., Gomes, T., Bebianno, M.J., 2009. A multibiomarker approach in *Mytilus galloprovincialis* to assess environmental quality. *Journal of Environmental Monitoring* 11, 1673-1686.
- Cuevas, N., Zorita, I., Costa, P.M., Franco, J., Larreta, J., 2015. Development of histopathological indices in the digestive gland and gonad of mussels: integration with contamination levels and effects of confounding factors. *Aquatic Toxicology* 162, 152-164.
- Cupaioli, F.A., Zucca, F.A., Boraschi, D., Zecca, L., 2014. Engineered nanoparticles. How brain friendly is this new guest? *Progress in Neurobiology* 119-120C, 20-38.
- D'Agata, A., Fasulo, S., Dallas, L.J., Fisher, A.S., Maisano, M., Readman, J.W., Jha, A.N., 2013. Enhanced toxicity of "bulk" titanium dioxide compared to "fresh" and "aged" nano-TiO₂ in marine mussels (*Mytilus galloprovincialis*). *Nanotoxicology* 8, 549-558.
- Da Ros, L., Nasci, C., Campesan, G., Sartorello, P., Stocco, G., Menetto, A., 1995. Effects of Linear Alkylbenzene Sulphonate (LAS) and cadmium in the digestive gland of mussel, *Mytilus sp.* *Marine Environment Research* 39, 321-324.
- Dagnino, A.; Allen, J.I.; Moore, M.N.; Broeg, K.; Canesi, L.; Viarengo, A. (2007). Development of an expert system for the integration of biomarker responses in mussels into an animal health index. *Biomarkers* 12, 155-172.
- Dai, L., Syberg, K., Banta, G.T., Selck, H., Forbes, V.E., 2013. Effects, Uptake, and Depuration Kinetics of Silver Oxide and Copper Oxide Nanoparticles in a Marine Deposit Feeder, *Macoma balthica*. *ACS Sustainable Chemistry & Engineering* 1, 760-767.
- De Vico, G., Carella, F., 2012. Morphological features of the inflammatory response in molluscs. *Research in Veterinary Science* 93, 1109-1115.
- Dellali, M., Barelli, M.G., Romeo, M., Aissa, P., 2001. The use of acetylcholinesterase activity in *Ruditapes decussatus* and *Mytilus galloprovincialis* in the biomonitoring of Bizerta lagoon. *Comparative Biochemistry and Physiology Part C* 130, 227-235.
- Dimitriadis, V.K., Domouhtsidou, G.P., Cajaraville, M.P., 2004. Cytochemical and histochemical aspects of the digestive gland cells of the mussel *Mytilus galloprovincialis* (L.) in relation to function. *Journal of Molecular Histology* 35, 501-509.
- Directive 2001/22/EC of the European Parliament and of the council of 8 March 2001. *Official Journal of the European Union* 2001,14-21.
- Directive 2008/105/EC of the European Parliament and of the council of 16 December 2008. *Official Journal of the European Union*, 348, 84-97.
- Domingos, R.F., Simon, D.F., Hauser, C., Wilkinson, K.J., 2011. Bioaccumulation and effects of CdTe/CdS quantum dots on *Chlamydomonas reinhardtii* - nanoparticles or the free ions? *Environmental Science & Technology* 45, 7664-7669.
- Duan, J., Yu, Y., Li, Y., Yu, Y., Li, Y., Huang, P., Zhou, X., Peng, S., Sun, Z., 2013. Developmental toxicity of CdTe QDs in zebrafish embryos and larvae. *Journal of Nanoparticle Research* 15.

- Dumas, E., Gao, C., Suffern, D., Bradforth, S.E., Dimitrijevic, N.M., Nadeau, J.L., 2010. Interfacial charge transfer between CdTe quantum dots and gram negative vs gram positive bacteria. *Environmental Science & Technology* 44, 1464-1470.
- Dwarakanath, S., Bruno, J.G., Shastry, A., Phillips, T., John, A., Kumar, A., Stephenson, L.D., 2004. Quantum dot-antibody and aptamer conjugates shift fluorescence upon binding bacteria. *Biochemical and Biophysical Research Communications* 325, 739-743.
- Eisler, R., 2007. *Eisler's Encyclopedia of Environmentally Hazardous Priority Chemicals*. Chemicals. Elsevier Science Ltd, Oxford.
- Emmanouil, C., Sheehan, T.M.T., Chipman, J.K., 2007. Macromolecule oxidation and DNA repair in mussel (*Mytilus edulis* L.) gill following exposure to Cd and Cr(VI). *Aquatic Toxicology*, 82, 27-35.
- Erdelmeier, I., Ge, D., Yadan, J., Chaudie, J., 1998. Reactions of N -Methyl-2-phenylindole with Malondialdehyde and 4-Hydroxyalkenals. *Mechanistic Aspects of the Colorimetric Assay of Lipid Peroxidation* 2, 1184-1194.
- Fabrega, J., Luoma, S.N., Tyler, C.R., Galloway, T.S., Lead, J.R., 2011. Silver nanoparticles: behaviour and effects in the aquatic environment. *Environment International* 37, 517-31.
- Fadeel, B., Garcia-Bennett, A.E., 2010. Better safe than sorry: Understanding the toxicological properties of inorganic nanoparticles manufactured for biomedical applications. *Advanced Drug Delivery Reviews* 62, 362-374.
- Falfushynska, H., Gnatyshyna, L., Stoliar, O., Mitina, N., Skorokhoda, T., Filyak, Y., Zaichenko, A., Stoika, R., 2012. Evaluation of biotargeting and ecotoxicity of Co²⁺-containing nanoscale polymeric complex by applying multi-marker approach in bivalve mollusk *Anodonta cygnea*. *Chemosphere* 88, 925-936.
- Fan, W., Li, Q., Yang, X., Zhang, L., 2013. Zn subcellular distribution in liver of goldfish (*Carassius auratus*) with exposure to zinc oxide nanoparticles and mechanism of hepatic detoxification. *PLoS One* 8, 1-6.
- Fang, T.-T., Li, X., Wang, Q.-S., Zhang, Z.-J., Liu, P., Zhang, C.-C., 2012. Toxicity evaluation of CdTe quantum dots with different size on *Escherichia coli*. *Toxicology In Vitro* 26, 1233-1239.
- FAO, 2016. Cultured Aquatic Species Information Programme *Mytilus galloprovincialis* (Lamarck, 1819) Available from http://www.fao.org/fishery/culturedspecies/Mytilus_galloprovincialis/en#tcNA008C
- Farrell, P., Nelson, K., 2013. Trophic level transfer of microplastic: *Mytilus edulis* (L.) to *Carcinus maenas* (L.). *Environmental Pollution* 177C, 1-3.
- Ferry, J.L., Craig, P., Hexel, C., Sisco, P., Frey, R., Pennington, P.L., Fulton, M.H., Scott, I.G., Decho, A.W., Kashiwada, S., Murphy, C.J., Shaw, T.J., 2009. Transfer of gold nanoparticles from the water column to the estuarine food web. *NNano* 4, 441-444.
- Feswick, A., Griffitt, R.J., Siebein, K., Barber, D.S., 2013. Uptake, retention and internalization of quantum dots in *Daphnia* is influenced by particle surface functionalization. *Aquatic Toxicology*, 130-131, 210-218.
- Flohe, L., Gunzler, W.A., 1984. Assays of glutathione peroxidase. *Methods in Enzymology* 105, 114-121.
- Freitas, R., Pires, A., Quintino, V., Rodrigues, A.M., Figueira, E., 2012. Subcellular partitioning of elements and availability for trophic transfer: Comparison between the Bivalve *Cerastoderma edule* and the Polychaete *Diopatra neapolitana*. *Estuarine, Coastal and Shelf Science* 99, 21-30.

- Gagné, F., André, C., Blaise, C., 2008b. The Dual Nature of Metallothioneins in the Metabolism of Heavy Metals and Reactive Oxygen Species in Aquatic Organisms : Implications of Use as a Biomarker of Heavy-Metal Effects in Field Investigations. *Biochemistry Insights* 1, 31-41.
- Gagné, F., Auclair, J., Turcotte, P., Fournier, M., Gagnon, C., Sauvé, S., Blaise, C., 2008. Ecotoxicity of CdTe quantum dots to freshwater mussels: impacts on immune system, oxidative stress and genotoxicity. *Aquatic Toxicology* 86, 333-340.
- Gagné, F., Auclair, J., Turcotte, P., Gagnon, C., 2013a. Sublethal effects of silver nanoparticles and dissolved silver in freshwater mussels. *Journal of Toxicology and Environmental Health, Part A* 76, 479-490.
- Gagné, F., Fortier, M., Yu, L., Osachoff, H.L., Skirrow, R.C., van Aggelen, G., Gagnon, C., Fournier, M., 2010. Immunocompetence and alterations in hepatic gene expression in rainbow trout exposed to CdS/CdTe quantum dots. *Journal of Environmental Monitoring* 12, 1556-1565.
- Gagné, F., Maysinger, D., André, C., Blaise, C., 2008b. Cytotoxicity of aged cadmium-telluride quantum dots to rainbow trout hepatocytes. *Nanotoxicology* 2, 113-120.
- Gagné, F., Turcotte, P., Auclair, J., Gagnon, C., 2013b. The effects of zinc oxide nanoparticles on the metallome in freshwater mussels. *Comparative Biochemistry and Physiology Part C: Toxicology & Pharmacology* 158, 22-28.
- García-Negrete, C.A., Blasco, J., Volland, M., Rojas, T.C., Hampel, M., Lapresta-Fernández, A., Jiménez de Haro, M.C., Soto, M., Fernández, A., 2013. Behaviour of Au-citrate nanoparticles in seawater and accumulation in bivalves at environmentally relevant concentrations. *Environmental Pollution* 174, 134-141.
- Garmendia, L., Soto, M., Ortiz-Zarragoitia, M., Orbea, A., Cajarville, M.P., Marigómez, I., 2011. Application of a battery of biomarkers in mussel digestive gland to assess long-term effects of the Prestige oil spill in Galicia and Bay of Biscay: correlation and multivariate analysis. *Journal of Environmental Monitoring* 13, 933-942.
- Geret, F., Serafim, A., Bebianno, M.J., 2003. Antioxidant enzyme activities, metallothioneins and lipid peroxidation as biomarkers in *Ruditapes decussatus*? *Ecotoxicology* 12, 417-426.
- GISD. 2012. Global Invasive Species Database. Available from <http://www.issg.org/database/species/ecology.asp?si=102&fr=1&sts=sss&lang=EN>
- Gomes, T., Araújo, O., Pereira, R., Almeida, A.C., Cravo, A., Bebianno, M.J., 2013a. Genotoxicity of copper oxide and silver nanoparticles in the mussel *Mytilus galloprovincialis*. *Marine Environment Research* 84, 51-59.
- Gomes, T., Chora, S., Pereira, C.G., Cardoso, C., Bebianno, M.J., 2014a. Proteomic response of mussels *Mytilus galloprovincialis* exposed to CuO NPs and Cu²⁺: An exploratory biomarker discovery. *Aquatic Toxicology* 155, 327-336.
- Gomes, T., Pereira, C.G., Cardoso, C., Bebianno, M.J., 2013b. Differential protein expression in mussels *Mytilus galloprovincialis* exposed to nano and ionic Ag. *Aquatic Toxicology* 136-137, 79-90.
- Gomes, T., Pereira, C.G., Cardoso, C., Pinheiro, J.P., Cancio, I., Bebianno, M.J., 2012. Accumulation and toxicity of copper oxide nanoparticles in the digestive gland of *Mytilus galloprovincialis*. *Aquatic Toxicology* 118-119, 72-79.
- Gomes, T., Pereira, C.G., Cardoso, C., Sousa, V.S., Teixeira, M.R., Pinheiro, J.P., Bebianno, M.J., 2014b. Effects of silver nanoparticles exposure in the mussel *Mytilus galloprovincialis*. *Marine Environment Research* 101, 208-214.

- Gomes, T., Pinheiro, J.P., Cancio, I., Pereira, C.G., Cardoso, C., Bebianno, M.J., 2011. Effects of copper nanoparticles exposure in the mussel *Mytilus galloprovincialis*. *Environmental Science & Technology* 45, 9356-9362.
- Greenwald, R.A., 1985. *Handbook of Methods for Oxygen Radical Research*; CRC Press: Boca Raton, FL.
- Grillo, R., Rosa, A.H., Fraceto, L.F., 2015. Engineered nanoparticles and organic matter: A review of the state-of-the-art. *Chemosphere* 119C, 608-619.
- Habig, W.H., Pabst, M.J., Jakoby, W.B., 1974. Glutathione S-transferases. The first enzymatic step in mercapturic acid formation. *Journal of Biological Chemistry* 25, 7130-7139.
- Han, X., Lai, L., Tian, F., Jiang, F.-L., Xiao, Q., Li, Y., Yu, Q., Li, D., Wang, J., Zhang, Q., Zhu, B., Li, R., Liu, Y., 2012. Toxicity of CdTe quantum dots on yeast *Saccharomyces cerevisiae*. *Small* 8, 2680-9.
- Handy, R.D., Cornelis, G., Fernandes, T., Tsyusko, O., Decho, A., Sabo-Attwood, T., Metcalfe, C., Steevens, J.A., Klaine, S.J., Koelmans, A.A., Horn, N., 2012. Ecotoxicity test methods for engineered nanomaterials: Practical experiences and recommendations from the bench. *Environmental Toxicology and Chemistry* 31, 15-31.
- Hanna, S.K., Miller, R.J., Lenihan, H.S., 2014. Deposition of carbon nanotubes by a marine suspension feeder revealed by chemical and isotopic tracers. *Journal of Hazardous Materials* 279, 32-7.
- Hanna, S.K., Miller, R.J., Muller, E.B., Nisbet, R.M., Lenihan, H.S., 2013. Impact of engineered zinc oxide nanoparticles on the individual performance of *Mytilus galloprovincialis*. *PLoS One* 8, e61800.
- Hardman, R., 2006. A Toxicologic Review of Quantum dots: Toxicity Depends on Physicochemical and Environmental Factors. *Environmental Health Perspectives* 114, 165-172.
- Hervé-Fernández, P., Houlbrèque, F., Boisson, F., Mulsow, S., Teyssié, J.-L., Oberhänsli, F., Azemard, S., Jeffree, R., 2010. Cadmium bioaccumulation and retention kinetics in the Chilean blue mussel *Mytilus chilensis*: seawater and food exposure pathways. *Aquatic Toxicology* 99, 448-456.
- Hine, P.M., 1999. The inter-relationships of bivalve haemocytes. *Fish & Shellfish Immunology* 9, 367-385.
- Hirschey, M.D., Han, Y.J., Stucky, G.D., Butler, A., 2006. Imaging *Escherichia coli* using functionalized core/shell CdSe/CdS quantum dots. *Journal of Biological Inorganic Chemistry* 11, 663-669.
- Hoo, C.M., Starostin, N., West, P., McCartney, M.L., 2008. A comparison of atomic force microscopy (AFM) and dynamic light scattering (DLS) methods to characterize nanoparticle size distributions. *Journal of Nanoparticle Research* 10, 89-96.
- Hsu, P.-C.L., O'Callaghan, M., Al-Salim, N., Hurst, M.R.H., 2012. Quantum dot nanoparticles affect the reproductive system of *Caenorhabditis elegans*. *Environmental Toxicology and Chemistry* 31, 2366-74.
- Hu, W., Culloty, S., Darmody, G., Lynch, S., Davenport, J., Ramirez-Garcia, S., Dawson, K.A., Lynch, I., Blasco, J., Sheehan, D., 2014. Toxicity of copper oxide nanoparticles in the blue mussel, *Mytilus edulis*: a redox proteomic investigation. *Chemosphere* 108, 289-99.
- Hu, W., Culloty, S., Darmody, G., Lynch, S., Davenport, J., Ramirez-Garcia, S., Dawson, K., Lynch, I., Doyle, H., Sheehan, D., 2015. Neutral red retention time

- assay in determination of toxicity of nanoparticles. *Marine Environment Research* 5-8.
- Hui-lian, M., Chun-lei, W., Han-zhi, L., Wei, L., Shu-kun, Z., Li-ping, W. 2006. NHS Mediated CdTe Quantum dots/ Albumin Conjugates and Labeling *C. elegans*, *Journal Chemical Research in Chinese Universities* 2, 181-184.
- Hull, M.S., Chaurand, P., Rose, J., Auffan, M., Bottero, J.-Y., Jones, J.C., Schultz, I.R., Vikesland, P.J., 2011. Filter-feeding bivalves store and biodeposit colloiddally stable gold nanoparticles. *Environmental Science & Technology* 45, 6592-6599.
- Hull, M.S., Vikesland, P.J., Schultz, I.R., 2013. Uptake and retention of metallic nanoparticles in the Mediterranean mussel (*Mytilus galloprovincialis*). *Aquatic Toxicology* 140-141C, 89-97.
- IARC, 1993. Monographs on the Evaluation of Carcinogenic Risks to Humans, vol. 58, Beryllium, Cadmium, Mercury, and Exposures in the Glass Manufacturing Industry. IARC, Lyon.
- Ipe, B.I., Lehnig, M., Niemeyer, C.M., 2005. On the generation of free radical species from quantum dots. *Small* 1, 706-709.
- Jackson, B.P., Bugge, D., Ranville, J.F., Chen, C.Y., 2012. Bioavailability, toxicity, and bioaccumulation of quantum dot nanoparticles to the amphipod *Leptocheirus plumulosus*. *Environmental Science & Technology* 46 (10), 5550-5556.
- Joubert, Y., Pan, J.-F., Buffet, P.-E., Pilet, P., Gilliland, D., Valsami-Jones, E., Mouneyrac, C., Amiard-Triquet, C., 2013. Subcellular localization of gold nanoparticles in the estuarine bivalve *Scrobicularia plana* after exposure through the water. *Gold Bulletin* 46, 47-56.
- Ju-Nam, Y., Lead, J.R., 2008. Manufactured nanoparticles: an overview of their chemistry, interactions and potential environmental implications. *Science of the Total Environment* 400, 396-414.
- Kádár, E., Lowe, D.M., Solé, M., Fisher, A.S., Jha, A.N., Readman, J.W., Hutchinson, T.H., 2010. Uptake and biological responses to nano-Fe versus soluble FeCl₃ in excised mussel gills. *Analytical and Bioanalytical Chemistry* 396, 657-666.
- Kadar, E., Tarran, G. A, Jha, A.N., Al-Subiai, S.N., 2011. Stabilization of engineered zero-valent nanoiron with Na-acrylic copolymer enhances spermotoxicity. *Environmental Science & Technology* 45, 3245-51.
- Kahru, A., Dubourguier, H.-C., 2010. From ecotoxicology to nanoecotoxicology. *Toxicology* 269 (2-3), 105-119.
- Kahru, A., Ivask, A., 2013. Mapping the dawn of nanoecotoxicological research. *Accounts of Chemical Research* 46, 823-833.
- Karlsson, H.L., Gustafsson, J., Cronholm, P., Möller, L., 2009. Size-dependent toxicity of metal oxide particles - a comparison between nano- and micrometer size. *Toxicology Letters* 188, 112-118.
- Katsumiti, A., Berhanu, D., Howard, K.T., Arostegui, I., Oron, M., Valsami-jones, E., Cajaraville, M.P., 2014b. Cytotoxicity of TiO₂ nanoparticles to mussel hemocytes and gill cells *in vitro*: Influence of synthesis method, crystalline structure, size and additive. *Nanotoxicology* 4, 1-11.
- Katsumiti, A., Gilliland, D., Arostegui, I., Cajaraville, M.P., 2014a. Cytotoxicity and cellular mechanisms involved in the toxicity of CdS quantum dots in hemocytes and gill cells of the mussel *Mytilus galloprovincialis*. *Aquatic Toxicology* 153, 39-52.
- Keller, A.A., Wang, H., Zhou, D., Lenihan, H.S., Cherr, G., Cardinale, B.J., Miller, R., Ji, Z., 2010. Stability and aggregation of metal oxide nanoparticles in natural aqueous matrices. *Environmental Science & Technology* 44, 1962-1967.

- Kimbrough, K.L., Johnson, W.E., Lauenstein, G.G., Christensen, J.D., Apeti, D.A., 2008. An assessment of two decades of contamination monitoring in the nation's coastal zone. Silver Spring, MD. NOAA Technical Memorandum NOS NCCOS 44. 105pp.
- King-Heiden, T.C., Wiecinski, P.N., Mangham, A.N., Metz, K.M., Nesbit, D., Pedersen, J.A., Hamers, R.J., Heideman, W., Peterson, R.E., 2009. Quantum dot nanotoxicity assessment using the zebrafish embryo. *Environmental Science & Technology* 43, 1605-11.
- Kloepfer, J., Mielke, R., 2003. Quantum dots as strain-and metabolism-specific microbiological labels. *Applied and Environmental Microbiology* 69, 4205-4213.
- Koehler, A., Marx, U., Broeg, K., Bahns, S., Bressling, J., 2008. Effects of nanoparticles in *Mytilus edulis* gills and hepatopancreas - a new threat to marine life? *Marine Environmental Research* 66, 12-4.
- Koopal, L.K., Saito, T., Pinheiro, J.P., van Riemsdijk, W.H., 2005. Ion binding to natural organic matter: General considerations and the NICA-Donnan model. *Colloids and Surfaces A: Physicochemical and Engineering Aspects* 265, 40-54.
- Kruzynski, G.M., 2004. Cadmium in oysters and scallops: The BC experience. *Toxicology Letters* 148, 159-169.
- De Jong, L., Moreau, X., Bestel, I., Beaudoin, E., Aimé, A., Dolain, C., Saeza, G., Tonetto, A., Barthélémy, P., Thiéry, A., 2013. Uptake of quantum dots into a freshwater flatworm: Intracellular accumulation and transmission from parents to offspring. *Journal of nanoscience letters* 3, 28.
- Lai, L., Lin, C., Xu, Z.-Q., Han, X.-L., Tian, F.-F., Mei, P., Li, D.-W., Ge, Y.-S., Jiang, F.-L., Zhang, Y.-Z., Liu, Y., 2012. Spectroscopic studies on the interactions between CdTe quantum dots coated with different ligands and human serum albumin. *Spectrochimica Acta Part A: Molecular and Biomolecular Spectroscopy* 97, 366-76.
- Lapresta-Fernández, A., Fernández, A., Blasco, J., 2012. Nanoecotoxicity effects of engineered silver and gold nanoparticles in aquatic organisms. *Trends in Analytical Chemistry* 32, 40-59.
- Le Foll, F., Rioult, D., Boussa, S., Pasquier, J., Dagher, Z., Leboulenger, F., 2010. Characterisation of *Mytilus edulis* hemocyte subpopulations by single cell time-lapse motility imaging. *Fish and Shellfish Immunology* 28, 372-386.
- Lee, W.-M., An, Y.-J., 2014. Evidence of three-level trophic transfer of quantum dots in an aquatic food chain by using bioimaging. *Nanotoxicology* 9, 407-412.
- Lewinski, N.A., Zhu, H., Ouyang, C.R., Conner, G.P., Wagner, D.S., Colvin, V.L., Drezek, R.A., 2011. Trophic transfer of amphiphilic polymer coated CdSe/ZnS quantum dots to *Danio rerio*. *Nanoscale* 3, 3080-3083.
- Li, H., Luo, W., Tao, Y., Wu, Y., Lv, X., Zhou, Q., Jiang, G., 2009. Effects of nanoscale quantum dots in male Chinese loaches (*Misgurnus anguillicaudatus*): Estrogenic interference action, toxicokinetics and oxidative stress. *Science China Chemistry* 52, 1683-1690.
- Li, J., Zhang, Y., Xiao, Q., Tian, F., Liu, X., Li, R., Zhao, G., Jiang, F., Liu, Y., 2011. Mitochondria as target of quantum dots toxicity. *J. Hazard. Mater.* 194, 440-444.
- Li, W., Xie, H., Xie, Z., Lu, Z., Ou, J., Chen, X., Shen, P., 2004. Exploring the mechanism of competence development in *Escherichia coli* using quantum dots as fluorescent probes. *Journal of Biochemical and Biophysical Methods* 58, 59-66.
- Liang, J., Cheng, Y., Han, H., 2008. Study on the interaction between bovine serum albumin and CdTe quantum dots with spectroscopic techniques. *Journal of Molecular Structure* 892, 116-120.

- Libralato, G., Minetto, D., Totaro, S., Mičetić, I., Pigozzo, A., Sabbioni, E., Marcomini, A., Volpi Ghirardini, A., 2013. Embryotoxicity of TiO₂ nanoparticles to *Mytilus galloprovincialis* (Lmk). *Marine Environment Research* 92, 71-78.
- Lin, C.-H., Chang, L.W., Wei, Y.-H., Wu, S.-B., Yang, C.-S., Chang, W.-H., Chen, Y.-C., Lin, P.-P., 2012. Electronic microscopy evidence for mitochondria as targets for Cd/Se/Te-based quantum dot 705 toxicity *in vivo*. *Kaohsiung Journal of Medical Sciences* 28, S53-62.
- Lin, S., Bhattacharya, P., Rajapakse, N.C., Brune, D.E., Ke, P.C., 2009. Effects of quantum dots adsorption on algal photosynthesis. *The Journal of Physical Chemistry C* 113, 10962-10966.
- Liu, F., Wang, W.X., 2011. Metallothionein-like proteins turnover, Cd and Zn biokinetics in the dietary Cd-exposed scallop *Chlamys nobilis*. *Aquatic Toxicology* 105, 361-368.
- Livingstone, D.R., 1993. Biotechnology and pollution monitoring: Use of molecular biomarkers in the aquatic environment. *Journal of Chemical Technology and Biotechnology* 57, 195-211.
- López-Serrano, A., Olivas, R.M., Landaluze, J.S., Cámara, C., 2014. Nanoparticles: a global vision. Characterization, separation, and quantification methods. Potential environmental and health impact. *Analytical Methods* 6, 38-56.
- Lovrić, J., Cho, S.J., Winnik, F.M., Maysinger, D., 2005. Unmodified cadmium telluride quantum dots induce reactive oxygen species formation leading to multiple organelle damage and cell death. *Chemistry & Biology* 12, 1227-1234.
- Lowry, G. V., Gregory, K.B., Apte, S.C., Lead, J.R., 2012. Transformations of nanomaterials in the environment. *Environmental Science & Technology* 46, 6893-6899.
- Lu, Z., Li, C.M., Bao, H., Qiao, Y., Toh, Y., Yang, X., 2008. Mechanism of antimicrobial activity of CdTe quantum dots. *Langmuir* 24, 5445-52.
- Ma, S., Lin, D., 2013. The biophysicochemical interactions at the interfaces between nanoparticles and aquatic organisms: adsorption and internalization. *Environmental Science: Processes & Impacts* 15, 145.
- Macías-mayorga, D., Laiz, I., Moreno-garrido, I., Blasco, J., 2015. Is oxidative stress related to cadmium accumulation in the Mollusc *Crassostrea angulata*? *Aquatic Toxicology* 161, 231-241.
- Mahendra, S., Zhu, H., Colvin, V.L., Alvarez, P.J., 2008. Quantum dot weathering results in microbial toxicity. *Environmental Science & Technology* 42, 9424-9430.
- Mahl, D., Diendorf, J., Meyer-Zaika, W., Epple, M., 2011. Possibilities and limitations of different analytical methods for the size determination of a bimodal dispersion of metallic nanoparticles. *Colloids and Surfaces A: Physicochemical and Engineering Aspects* 377, 386-392.
- Manikandan, M., Wu, H.F., 2013. Probing the fungicidal property of CdS quantum dots on *Saccharomyces cerevisiae* and *Candida utilis* using MALDI-MS. *Journal of Nanoparticle Research* 15, 1728.
- Macías-mayorga, D., Laiz, I., Moreno-garrido, I., Blasco, J., 2015. Is oxidative stress related to cadmium accumulation in the Mollusc *Crassostrea angulata*? *Aquatic Toxicology* 161, 231-241.
- Marigómez, I., Garmendia, L., Soto, M., Orbea, A., Izagirre, U., Cajaraville, M.P., 2013. Marine ecosystem health status assessment through integrative biomarker indices: A comparative study after the Prestige oil spill “mussel Watch.” *Ecotoxicology* 22, 486-505.

- Marigómez, I., Lekube, X., Cancio, I., 1999. Immunochemical localisation of proliferating cells in mussel digestive gland tissue. *Histochemical Journal* 31, 781-788.
- Marigómez, I., Sáez, V., Cajaraville, M.P., Angulo, E., 1990. A planimetric study of the mean epithelial thickness (MET) of the molluscan digestive gland over the tidal cycle and under environmental stress conditions. *Helgoländer Meeresuntersuchungen* 44, 81-94.
- Marigómez, I., Soto, M., Cajaraville, M.P., Angulo, E., Giamberini, L., 2002. Cellular and subcellular distribution of metals in molluscs. *Microscopy Research and Technique* 56, 358-392.
- Markets Ra. 2011. The world market for nanoparticle titanium dioxide (TiO₂).
- Marmioli, M., Pagano, L., Pasquali, F., Zappettini, A., Tosato, V., Bruschi, C.V., Marmioli, N., 2015. A genome-wide nanotoxicology screen of *Saccharomyces cerevisiae* mutants reveals the basis for cadmium sulphide quantum dot tolerance and sensitivity. *Nanotoxicology* 1-10.
- Mashayekhi, H., Ghosh, S., Du, P., Xing, B., 2012. Effect of natural organic matter on aggregation behavior of C₆₀ fullerene in water. *Journal of Colloid and Interface Science* 374, 111-117.
- Matranga, V., Corsi, I., 2012. Toxic effects of engineered nanoparticles in the marine environment: model organisms and molecular approaches. *Marine Environment Research* 76, 32-40.
- Maurer-Jones, M.A., Gunsolus, I.L., Murphy, C.J., Haynes, C.L., 2013. Toxicity of engineered nanoparticles in the environment. *Analytical Chemistry* 85, 3036-3049.
- McCarthy, M.P., Carroll, D.L., Ringwood, A.H., 2013. Tissue specific responses of oysters, *Crassostrea virginica*, to silver nanoparticles. *Aquatic Toxicology* 138-139, 123-128.
- McCord, J. M., Fridovich, I., 1969. Superoxide dismutase: An enzymatic function for erythrocuprein (hemocuprein). *Journal of Biological Chemistry* 244, 6049-6955.
- McFarland, V.A., Inouye, L.S., Lutz, C.H., Jarvis, A.S., Clarke, J.U., McCant, D.D., 1999. Biomarkers of oxidative stress and genotoxicity in livers of field-collected brown bullhead *Ameiurus nebulosus*. *Archives of Environmental Contamination and Toxicology* 37, 236-241.
- Mei, J., Yang, L.Y., Lai, L., Xu, Z.Q., Wang, C., Zhao, J., Jin, J.C., Jiang, F.L., Liu, Y., 2014. The interactions between CdSe quantum dots and yeast *Saccharomyces cerevisiae*: Adhesion of quantum dots to the cell surface and the protection effect of ZnS shell. *Chemosphere* 112, 92-99.
- Miao, A.-J., Schwehr, K.A., Xu, C., Zhang, S.-J., Luo, Z., Quigg, A., Santschi, P.H., 2009. The algal toxicity of silver engineered nanoparticles and detoxification by exopolymeric substances. *Environmental Pollution* 157, 3034-3041.
- Michalet, X., Pinaud, F.F., Bentolila, L.A., Tsay, J.M., Doose, S., Li, J.J., Sundaresan, A.M., Wu, S.S., Gambhir, S., Weiss, 2005. Quantum dots for live cells, *in vivo* imaging, and diagnostics. *Science*, 307, 538-544.
- Minetto, D., Libralato, G., Volpi Ghirardini, A., 2014. Ecotoxicity of engineered TiO₂ nanoparticles to saltwater organisms: an overview. *Environment International* 66, 18-27.
- Misra, S.K., Dybowska, A., Berhanu, D., Luoma, S.N., Valsami-Jones, E., 2012. The complexity of nanoparticle dissolution and its importance in nanotoxicological studies. *Science of the Total Environment* 438, 225-232.

- Mohd Omar, F., Abdul Aziz, H., Stoll, S., 2014. Aggregation and disaggregation of ZnO nanoparticles: influence of pH and adsorption of Suwannee River humic acid. *Science of the Total Environment* 468-469, 195-201.
- Montes, M.O., Hanna, S.K., Lenihan, H.S., Keller, A. A., 2012. Uptake, accumulation, and biotransformation of metal oxide nanoparticles by a marine suspension-feeder. *Journal of Hazardous Materials* 225-226, 139-145.
- Moore, M.N., 2006. Do nanoparticles present ecotoxicological risks for the health of the aquatic environment? *Environment International* 32, 967-976.
- Moore, M.N., Readman, J.A.J., Readman, J.W., Lowe, D.M., Frickers, P.E., Beesley, A., 2009. Lysosomal cytotoxicity of carbon nanoparticles in cells of the molluscan immune system: An *in vitro* study. *Nanotoxicology* 3, 40-45.
- Morelli, E., Cioni, P., Posarelli, M., Gabellieri, E., 2012. Chemical stability of CdSe quantum dots in seawater and their effects on a marine microalga. *Aquatic toxicology* 122-123, 153-162.
- Morelli, E., Salvadori, E., Basso, B., Tognotti, D., Cioni, P., Gabellieri, E., 2015. The response of *Phaeodactylum tricornutum* to quantum dot exposure: Acclimation and changes in protein expression. *Marine Environment Research* 1-9.
- Morelli, E., Salvadori, E., Bizzarri, R., Cioni, P., Gabellieri, E., 2013. Interaction of CdSe/ZnS quantum dots with the marine diatom *Phaeodactylum tricornutum* and the green alga *Dunaliella tertiolecta*: A biophysical approach. *Biophysical Chemistry* 182, 4-10.
- Mortimer, M., Kahru, A., Slaveykova, V.I., 2014. Uptake, localization and clearance of quantum dots in ciliated protozoa *Tetrahymena thermophila*. *Environmental Pollution* 190, 58-64.
- Mouneyrac, C., Buffet, P.-E., Poirier, L., Zalouk-Vergnoux, A., Guibbolini, M., Faverney, C.R., Gilliland, D., Berhanu, D., Dybowska, A., Châtel, A., Perrein-Ettajni, H., Pan, J.-F., Thomas-Guyon, H., Reip, P., Valsami-Jones, E., 2014. Fate and effects of metal-based nanoparticles in two marine invertebrates, the bivalve mollusc *Scrobicularia plana* and the annelid polychaete *Hediste diversicolor*. *Environmental Science and Pollution Research* 21, 7899-7912.
- Muller, E.B., Hanna, S.K., Lenihan, H.S., Miller, R.J., Nisbet, R.M., 2014. Impact of engineered zinc oxide nanoparticles on the energy budgets of *Mytilus galloprovincialis*. *Journal of Sea Research* 94, 29-36.
- Munari, M., Sturve, J., Frenzilli, G., Sanders, M.B., Christian, P., Nigro, M., Lyons, B.P., 2014. Genotoxic effects of Ag₂S and CdS nanoparticles in blue mussel (*Mytilus edulis*) haemocytes. *Journal of Chemical Ecology* 1-7.
- Murdock, R.C., Braydich-Stolle, L., Schrand, A.M., Schlager, J.J., Hussain, S.M., 2008. Characterization of nanomaterial dispersion in solution prior to *in vitro* exposure using dynamic light scattering technique. *Toxicological Sciences* 101, 239-53.
- Mwangi, J.N., Wang, N., Ingersoll, C.G., Hardesty, D.K., Brunson, E.L., Li, H., Deng, B., 2012. Toxicity of carbon nanotubes to freshwater aquatic invertebrates. *Environmental Toxicology and Chemistry* 31, 1823-1830.
- Nair, P.S., Robinson, W.E., 2001. Histidine-rich glycoprotein in the blood of the bivalve *Mytilus edulis*: role in cadmium speciation and cadmium transfer to the kidney. *Aquatic Toxicology* 52 (2), 133-142.
- Ng, T.Y.T., Wang, W.-X., 2005. Dynamics of metal subcellular distribution and its relationship with metal uptake in marine mussels. *Environmental Toxicology and Chemistry* 24, 2365-2372.

- OECD. 2010. List of Manufactured Nanomaterials and List of Endpoint for phase One of the Sponsorship Programme for the Testing of Manufactured Nanomaterials: Revision. ENV/JM/MONO(2010)46. OECD, Paris.
- Owen, G., 1972. Lysosomes, peroxisomes and bivalves. *Science Progress* 60, 299-318.
- Owen, G., 1996. Feeding. In: Wilburn, K.M., Yonge, C.M. (Eds.), *Physiology of Mollusca*, vol. 2. Academic Press, New York, pp. 1-5.
- Palmiter, R.D., 1998. The elusive function of metallothioneins. *Proc Natl Acad Sci U S A* 95, 8428-8430.
- Pan, J.-F., Buffet, P.-E., Poirier, L., Amiard-Triquet, C., Gilliland, D., Joubert, Y., Pilet, P., Guibolini, M., Risso de Faverney, C., Roméo, M., Valsami-Jones, E., Mouneyrac, C., 2012. Size dependent bioaccumulation and ecotoxicity of gold nanoparticles in an endobenthic invertebrate: the Tellinid clam *Scrobicularia plana*. *Environmental Pollution* 168, 37-43.
- Pelley, A.J., Tufenkji, N., 2008. Effect of particle size and natural organic matter on the migration of nano- and microscale latex particles in saturated porous media. *Journal of Colloid and Interface Science* 321, 74-83.
- Peralta-Videa, J.R., Zhao, L., Lopez-Moreno, M.L., de la Rosa, G., Hong, J., Gardea-Torresdey, J.L., 2011. Nanomaterials and the environment: a review for the biennium 2008-2010. *Journal of Hazardous Materials* 186, 1-15.
- Pérez, S., Farré, M. I., Barceló, D., 2009. Analysis, behavior and ecotoxicity of carbon-based nanomaterials in the aquatic environment. *Trends in Analytical Chemistry* 28, 820-832.
- Petushkova, N.A., Kuznetsova, G.P., Larina, O.V, Kisrieva, Y.S., Samenkova, N.F., Trifonova, O.P., Miroshnichenko, Y.V, Zolotarev, K.V, Karuzina, I.I., Ipatova, O.M., Lisitsa, A.V, 2015. One-dimensional proteomic profiling of *Danio rerio* embryo vitellogenin to estimate quantum dot toxicity. *Proteome Science* 13, 1-12.
- Peyrot, C., Gagnon, C., Gagné, F., Willkinson, K.J., Turcotte, P., Sauvé, S., 2009. Effects of cadmium telluride quantum dots on cadmium bioaccumulation and metallothionein production to the freshwater mussel, *Elliptio complanata*. *Comparative Biochemistry and Physiology Part C* 150, 246-251.
- Piccinno, F., Gottschalk, F., Seeger, S., Nowack, B., 2012. Industrial production quantities and uses of ten engineered nanomaterials in Europe and the world. *Journal of Nanoparticle Research* 14, 1109.
- Pipe, R.K., Coles, J.A., 1995. Environmental contaminants influencing immune function in marine bivalve molluscs. *Fish and Shellfish Immunology* 5, 581-595.
- Putnam, M.C., Filler, M.A., Kayes, B.M., Kelzenberg, M.D., Guan, Y., Lewis, N.S., Eiler, J.M., Atwater, H.A., 2008. Secondary Ion Mass Spectrometry of Vapor - Liquid - Solid Grown , Au-Catalyzed , Si Wires. *Nano Letters* 8, 3109-3113.
- Qu, Y., Li, W., Zhou, Y., Liu, X., Zhang, L., Wang, L., Li, Y.F., Iida, A., Tang, Z., Zhao, Y., Chai, Z., Chen, C., 2011. Full assessment of fate and physiological behavior of quantum dots utilizing *Caenorhabditis elegans* as a model organism. *Nano Letters* 11, 3174-3183.
- Rainbow, P.S., Smith, B.D., 2010. Trophic transfer of trace metals: Subcellular compartmentalization in bivalve prey and comparative assimilation efficiencies of two invertebrate predators. *Journal of Experimental Marine Biology and Ecology* 390, 143-148.
- Rebello, V., Shaikh, S., Desai, P.V., 2010. Toxicity of Cobalt Oxide Nanoparticles Toxicity of Cobalt Oxide Nanoparticles on Microalgae (*Navicula* sp. and *Chetoceros* sp.) and Bivalve (*Meritrix meritrix*) Cells. *International Conference on Environmental Engineering and Applications* 195-199.

- Regoli, F., Principato, G., 1995. Glutathione, glutathione-dependent and antioxidant enzymes in mussel, *Mytilus galloprovincialis* exposed to metals under field and laboratory conditions: Implications for the use of biochemical biomarkers. *Aquatic Toxicology* 31, 143-164.
- Renault, S., Baudrimont, M., Mesmer-Dudons, N., Mornet, S., Brisson, A., 2008. Impact of nanoparticle exposure on two freshwater species: a phytoplanktonic alga (*Scenedesmus subspicatus*) and a benthic bivalve (*Corbicula fluminea*). *Gold Bulletin* 41, 116-126.
- Ribeiro, D.S.M., Frigerio, C., Santos, J.L.M., Prior, J. A.V., 2012. Photoactivation by visible light of CdTe quantum dots for inline generation of reactive oxygen species in an automated multipumping flow system. *Analytica Chimica Acta* 735, 69-75.
- Ringwood, A.H., Levi-Polyachenko, N., Carroll, D.L., 2009. Fullerene exposures with oysters: embryonic, adult, and cellular responses. *Environmental Science & Technology* 43, 7136-7141.
- Ringwood, A.H., McCarthy, M., Levi-Polyachenko, N., Carroll, D.L., 2010. Nanoparticles in Natural Aquatic Systems and Cellular Toxicity. *Comparative Biochemistry and Physiology - Part A Molecular & Integrative Physiology* 157, S53.
- Rizvi, S., Ghaderi, S., Keshtgar, M., Seifalian, A., 2010. Semiconductor quantum dots as fluorescent probes for *in vitro* and *in vivo* bio-molecular and cellular imaging. *Nano Reviews*, 1, 1-15.
- Rocha, L.S., Pinheiro, J.P., Carapuça, H.M., 2007. Evaluation of nanometer thick mercury film electrodes for stripping chronopotentiometry. *Journal of Electroanalytical Chemistry* 610, 37-45.
- Rocha, T.L., Gomes, T., Cardoso, C., Letendre, J., Pinheiro, J.P., Sousa, V.S., Teixeira, M.R., Bebianno, M.J., 2014. Immunocytotoxicity, cytogenotoxicity and genotoxicity of cadmium-based quantum dots in the marine mussel *Mytilus galloprovincialis*. *Marine Environment Research* 101C, 29-37.
- Rocha, T.L., Gomes, T., Mestre, N.C., Cardoso, C., Bebianno, M.J., 2015c. Tissue specific toxicity of cadmium-based quantum dots in the marine mussel *Mytilus galloprovincialis*. *Aquatic Toxicology* 169, 10-18.
- Rocha, T.L., Gomes, T., Pinheiro, J.P., Sousa, V.S., Nunes, L.M., Teixeira, M.R., Bebianno, M.J., 2015b. Toxicokinetics and tissue distribution of cadmium-based quantum dots in the marine mussel *Mytilus galloprovincialis*. *Environmental Pollution* 204, 207-214.
- Rocha, T.L., Gomes, T., Sousa, V.S., Mestre, N.C., Bebianno, M.J., 2015a. Ecotoxicological impact of engineered nanomaterials in bivalve molluscs: An overview. *Marine Environment Research* 111, 74-88.
- Rocha, T.L., Gomes, T., Giuliani, E., Bebianno, M.J., 2016. Subcellular partitioning kinetics, metallothionein response and oxidative damage in the marine mussel *Mytilus galloprovincialis* exposed to cadmium-based quantum dots. *Science of the Total Environment* 554-555, 130-141.
- Ruiz, P., Katsumiti, A., Nieto, J.A., Bori, J., Jimeno-Romero, A., Reip, P., Arostegui, I., Orbea, A., Cajarville, M.P., 2015. Short-term effects on antioxidant enzymes and long-term genotoxic and carcinogenic potential of CuO nanoparticles compared to bulk CuO and ionic copper in mussels *Mytilus galloprovincialis*. *Marine Environment Research* 111, 107-120.
- Saez, G., Aye, M., De Meo, M., Aimé, A., Bestel, I., Barthélémy, P., Di Giorgio, C., 2015. Genotoxic and oxidative responses in coelomocytes of *Eisenia fetida* and

- Hediste diversicolor* exposed to lipid-coated CdSe/ZnS quantum dots and CdCl₂. Environmental Toxicology 30, 918-926.
- Sanders, M.B., Sebire, M., Sturve, J., Christian, P., Katsiadaki, I., Lyons, B.P., Sheahan, D., Weeks, J.M., Feist, S.W., 2008. Exposure of sticklebacks (*Gasterosteus aculeatus*) to cadmium sulfide nanoparticles: biological effects and the importance of experimental design. Marine Environment Research 66, 161-3.
- Santana, R.M.M., Oliveira, T.D., Rodrigues, S.S.M., Frigerio, C., Santos, J.L.M., Korn, M., 2015. Enhancing reactive species generation upon photo-activation of CdTe quantum dots for the chemiluminometric determination of unreacted reagent in UV/S₂O₈²⁻ drug degradation process. Talanta 135, 27-33.
- Saveyn, H., De Baets, B., Thas, O., Hole, P., Smith, J., Van der Meeren, P., 2010. Accurate particle size distribution determination by nanoparticle tracking analysis based on 2-D Brownian dynamics simulation. Journal of Colloid and Interface Science 352, 593-600.
- Scebba, F., Tognotti, D., Presciuttini, G., Gabellieri, E., Cioni, P., Angeloni, D., Basso, B., Morelli, E., 2016. A SELDI-TOF approach to ecotoxicology: Comparative profiling of low molecular weight proteins from a marine diatom exposed to CdSe/ZnS quantum dots. Ecotoxicology and Environmental Safety 123, 45-52.
- Schneider, R., Wolpert, C., Guilloteau, H., Balan, L., Lambert, J., Merlin, C., 2009. The exposure of bacteria to CdTe-core quantum dots: the importance of surface chemistry on cytotoxicity. Nanotechnology 20, 225101.
- Serafim, A., Bebianno, M.J., 2007. Kinetic model of cadmium accumulation and elimination and metallothionein response in *Ruditapes decussatus*. Environmental Toxicology and Chemistry 26 (5), 960-969.
- Singh, N.P., McCoy, M.T., Tice, R.R., Schneider, E.L., 1988. A simple technique for quantitation of low levels of DNA damage in individual cells. Experimental Cell Research 175 (1), 184-191.
- Slaveykova, V.I., Startchev, K., 2009. Effect of natural organic matter and green microalga on carboxyl-polyethylene glycol coated CdSe/ZnS quantum dots stability and transformations under freshwater conditions. Environmental Pollution 157, 3445-3450.
- Soto, M., Cajaraville, M.P., Marigómez, I., 1996. Tissue and cell distribution of copper, zinc and cadmium in the mussel, *Mytilus galloprovincialis*, determined by autometallography. Tissue Cell 28, 557-568.
- Soto, M., Zaldibar, B., Cancio, I., Taylor, M.G., Turner, M., Morgan, A.J., Marigómez, I., 2003. Subcellular distribution of cadmium and its cellular ligands in mussel digestive gland cells as revealed by combined autometallography and X-ray microprobe analysis. Histochemical Journal 34, 273-80.
- Sousa, V.S., Teixeira, M.R., 2013. Aggregation kinetics and surface charge of CuO nanoparticles: The influence of pH, ionic strength and humic acids. Environmental Chemistry 10, 313-322.
- Stanca, L., Petrache, S.N., Radu, M., Serban, A.I., Munteanu, M.C., Teodorescu, D., Staicu, A.C., Sima, C., Costache, M., Grigoriu, C., Zarnescu, O., Dinischiotu, A., 2012. Impact of silicon-based quantum dots on the antioxidative system in white muscle of *Carassius auratus gibelio*. Fish Physiology and Biochemistry 38, 963-975.
- Stanca, L., Petrache, S.N., Serban, A.I., Staicu, A.C., Sima, C., Munteanu, M.C., Zărnescu, O., Dinu, D., Dinischiotu, A., 2013. Interaction of silicon-based quantum dots with gibel carp liver: oxidative and structural modifications. Nanoscale Research Letters 8, 254.

- Tang, S., Allagadda, V., Chibli, H., Nadeau, J.L., Mayer, G.D., 2013. Comparison of cytotoxicity and expression of metal regulatory genes in zebrafish (*Danio rerio*) liver cells exposed to cadmium sulfate, zinc sulfate and quantum dots. *Metallomics* 5, 1411.
- Tang, S., Cai, Q., Chibli, H., Allagadda, V., Nadeau, J.L., Mayer, G.D., 2013a. Cadmium sulfate and CdTe-quantum dots alter DNA repair in zebrafish (*Danio rerio*) liver cells. *Toxicology and Applied Pharmacology* 272 (2), 443-452.
- Tang, Y., Han, S., Liu, H., Chen, X., Huang, L., Li, X., Zhang, J., 2013b. The role of surface chemistry in determining *in vivo* biodistribution and toxicity of CdSe/ZnS core-shell quantum dots. *Biomaterials* 34, 8741-8755.
- Tedesco, S., Doyle, H., Blasco, J., Redmond, G., Sheehan, D., 2010a. Exposure of the blue mussel, *Mytilus edulis*, to gold nanoparticles and the pro-oxidant menadione. *Comparative Biochemistry and Physiology Part C* 151, 167-174.
- Tedesco, S., Doyle, H., Blasco, J., Redmond, G., Sheehan, D., 2010b. Oxidative stress and toxicity of gold nanoparticles in *Mytilus edulis*. *Aquatic Toxicology* 100, 178-186.
- Tedesco, S., Doyle, H., Redmond, G., Sheehan, D., 2008. Gold nanoparticles and oxidative stress in *Mytilus edulis*. *Marine Environment Research* 66, 131-133.
- Tian, S., Zhang, Y., Song, C., Zhu, X., Xing, B., 2014. Titanium dioxide nanoparticles as carrier facilitate bioaccumulation of phenanthrene in marine bivalve, ark shell (*Scapharca subcrenata*). *Environmental Pollution* 192, 59-64.
- Thit, A., Banta, G.T., Selck, H., 2015. Bioaccumulation, subcellular distribution and toxicity of sediment-associated copper in the ragworm *Nereis diversicolor*: The relative importance of aqueous copper, copper oxide nanoparticles and microparticles. *Environmental Pollution* 202, 50-57.
- Tmejova, K., Hynek, D., Kopel, P., Gumulec, J., Krizkova, S., Guran, R., Heger, Z., Kalina, M., Vaculovicova, M., Adam, V., Kizek, R., 2015. Structural effects and nanoparticle size are essential for quantum dots-metallothionein complex formation. *Colloids and Surfaces B: Biointerfaces* 134, 262-272.
- Tmejova, K., Hynek, D., Kopel, P., Krizkova, S., Blazkova, I., Trnkova, L., Adam, V., Kizek, R., 2014. Study of metallothionein-quantum dots interactions. *Colloids and Surfaces B: Biointerfaces* 117, 534-7.
- Trevisan, R., Delapedra, G., Mello, D.F., Arl, M., Schmidt, E.C., Meder, F., Monopoli, M., Cargnin-Ferreira, E., Bouzon, Z.L., Fisher, A.S., Sheehan, D., Dafre, A.L., 2014. Gills are an initial target of zinc oxide nanoparticles in oysters *Crassostrea gigas*, leading to mitochondrial disruption and oxidative stress. *Aquatic Toxicology* 153, 27-38.
- U.S. Environmental Protection Agency. 1999. Integrated Risk Information System (IRIS) on Cadmium. National Center for Environmental Assessment, Office of Research and Development, Washington, DC.
- Vale, G., Franco, C., Diniz, M.S., Santos, M.M.C. Dos, Domingos, R.F., 2014. Bioavailability of cadmium and biochemical responses on the freshwater bivalve *Corbicula fluminea* - the role of TiO₂ nanoparticles. *Ecotoxicology and Environmental Safety* 109, 161-168.
- Viarengo, A., Nott, J.A., 1993. Mechanisms of heavy metal cation homeostasis in marine invertebrates. *Comparative Biochemistry and Physiology Part C: Toxicology & Pharmacology* 104, 355-372.
- Viarengo, A.M., Canesi, L., 1991. Mussels as biological indicators of pollution. *Aquaculture* 94, 225-243.

- Villalba, A., Mourelle, S.G., Lopez, M.C., Carballal, M.J., 1993. Marteiliasis affecting cultured mussels *Mytilus galloprovincialis* of Glacia (NW Spain). I Etiology, phases of the infection, and temporal and spatial variability in prevalence. *Diseases of Aquatic Organisms* 16, 61-72.
- Vincent-Hubert, F., Arini, A., Gourlay-Francé, C., 2011. Early genotoxic effects in gill cells and haemocytes of *Dreissena polymorpha* exposed to cadmium, B[a]P and a combination of B[a]P and Cd. *Mutation Research* 723 (1), 26-35.
- Wallace, W.G., Lee, B.-G., Luoma, S.N., 2003. Subcellular compartmentalization of Cd and Zn in two bivalves. I. Significance of metal-sensitive fractions (MSF) and biologically detoxified metal (BDM). *Marine Ecology Progress Series* 249, 183-197.
- Wang, C., Zhao, J., Mu, C., Wang, Q., Wu, H., Wang, C., 2013. cDNA cloning and mRNA expression of four glutathione S-transferase (GST) genes from *Mytilus galloprovincialis*. *Fish and Shellfish Immunology* 34, 697-703.
- Wang, J., Zhang, X., Chen, Y., Sommerfeld, M., Hu, Q., 2008. Toxicity assessment of manufactured nanomaterials using the unicellular green alga *Chlamydomonas reinhardtii*. *Chemosphere* 73, 1121-1128.
- Ward, J.E., Kach, D.J., 2009. Marine aggregates facilitate ingestion of nanoparticles by suspension-feeding bivalves. *Marine Environment Research* 68, 137-142.
- Wegner, A., Besseling, E., Foekema, E.M., Kamermans, P., Koelmans, A.A., 2012. Effects of nanopolystyrene on the feeding behavior of the blue mussel (*Mytilus edulis* L.). *Environmental Toxicology and Chemistry* 31, 2490-2497.
- Werlin, R., Priester, J.H., Mielke, R.E., Krämer, S., Jackson, S., Stoimenov, P.K., Stucky, G.D., Cherr, G.N., Orias, E., Holden, P.A. 2011. Biomagnification of CdSe quantum dots in a simple experimental microbial food chain. *Nature Nanotechnology* 6, 65-71.
- Wiesner, M., Lowry, G. V., Jones, K., Hochella, M., Di Giulio, R., Casman, E., Bernhardt, E., 2009. Decreasing uncertainties in assessing environmental exposure, risk, and ecological implications of nanomaterials. *Environmental Science & Technology* 43, 6453-6457.
- Worms, I.A.M., Boltzman, J., Garcia, M., Slaveykova, V.I., 2012. Cell-wall-dependent effect of carboxyl-CdSe/ZnS quantum dots on lead and copper availability to green microalgae. *Environmental Pollution* 167, 27-33.
- Wu, X., Jia, Y., Zhu, H., 2012. Bioaccumulation of cadmium bound to ferric hydroxide and particulate organic matter by the bivalve *M. meretrix*. *Environmental Pollution* 165, 133-139.
- Xiao, Q., Huang, S., Su, W., Li, P., Liu, Y., 2013. Evaluate the potential toxicity of quantum dots on bacterial metabolism by microcalorimetry. *Thermochimica Acta* 552, 98-105.
- Yang, L., Li, Y., 2006. Simultaneous detection of *Escherichia coli* O157:H7 and *Salmonella Typhimurium* using quantum dots as fluorescence labels. *Analyst* 131, 394-401.
- Yang, S.P., Bar-ilan, O., Peterson, R.E., Heideman, W., Hamers, R.J., Pedersen, J.A., 2013. Influence of Humic Acid on Titanium Dioxide Nanoparticle Toxicity to Developing Zebrafish. *Environmental Science & Technology* 47, 4718-4725.
- Zaldibar, B., Cancio, I., Marigómez, I., 2008. Epithelial cell renewal in the digestive gland and stomach of mussels: season, age and tidal regime related variations. *Histology and histopathology* 23, 281-90.
- Zhang, S., Jiang, Y., Chen, C.-S., Creeley, D., Schwehr, K.A., Quigg, A., Chin, W.-C., Santschi, P.H., 2013. Ameliorating effects of extracellular polymeric substances

- excreted by *Thalassiosira pseudonana* on algal toxicity of CdSe quantum dots. *Aquatic Toxicology* 126, 214-223.
- Zhang, W., Lin, K., Miao, Y., Dong, Q., Huang, C., Wang, H., Guo, M., Cui, X., 2012. Toxicity assessment of zebrafish following exposure to CdTe QDs. *Journal of Hazardous Materials* 213-214, 413-20.
- Zhang, W., Lin, K., Sun, X., Dong, Q., Huang, C., Wang, H., Guo, M., Cui, X., 2012. Toxicological effect of MPA-CdSe QDs exposure on zebrafish embryo and larvae. *Chemosphere* 89, 52-9.
- Zhang, W., Miao, Y., Lin, K., Chen, L., Dong, Q., Huang, C., 2013. Toxic effects of copper ion in zebrafish in the joint presence of CdTe QDs. *Environmental Pollution* 176C, 158-164.
- Zhang, X.-Q., Xu, X., Bertrand, N., Pridgen, E., Swami, A., Farokhzad, O.C., 2012. Interactions of nanomaterials and biological systems: Implications to personalized nanomedicine. *Advanced Drug Delivery Reviews* 64 (13), 1363-1384.
- Zhao, Y., Wang, X., Wu, Q., Li, Y., Wang, D., 2015. Translocation and neurotoxicity of CdTe quantum dots in RMEs motor neurons in nematode *Caenorhabditis elegans*. *Journal of Hazardous Materials* 283, 480-489.
- Zhou, Y., Wang, Q., Song, B., Wu, S., Su, Y., Zhang, H., He, Y., 2015. A real-time documentation and mechanistic investigation of quantum dots-induced autophagy in live *Caenorhabditis elegans*. *Biomaterials* 72, 38-48.
- Zhu, X., Zhou, J., Cai, Z., 2011. The toxicity and oxidative stress of TiO₂ nanoparticles in marine abalone (*Haliotis diversicolor supertexta*). *Marine Pollution Bulletin* 63, 334-338.
- Zolotarev, K.V., Kashirtseva, V.N., Mishin, A.V., Belyaeva, N.F., Medvedeva, N.V., Ipatova, O.M., 2012. Assessment of Toxicity of Cdse/Cds/Zns/S,S-Dihydrolipoic Acid/Polyacrylic Acid Quantum dots at *Danio rerio* Embryos and Larvae. *ISRN Nanotechnology*, 1-5.
- Zorita, I., Bilbao, E., Schad, A., Cancio, I., Soto, M., Cajaraville, M.P., 2007. Tissue- and cell-specific expression of metallothionein genes in cadmium- and copper-exposed mussels analyzed by *in situ* hybridization and RT-PCR. *Toxicology and Applied Pharmacology* 220, 186-196.
- Zuykov, M., Pelletier, E., Belzile, C., Demers, S., 2011a. Alteration of shell nacre micromorphology in blue mussel *Mytilus edulis* after exposure to free-ionic silver and silver nanoparticles. *Chemosphere* 84, 701-706.
- Zuykov, M., Pelletier, E., Demers, S., 2011b. Colloidal complexed silver and silver nanoparticles in extrapallial fluid of *Mytilus edulis*. *Marine Environment Research* 71, 17-21.